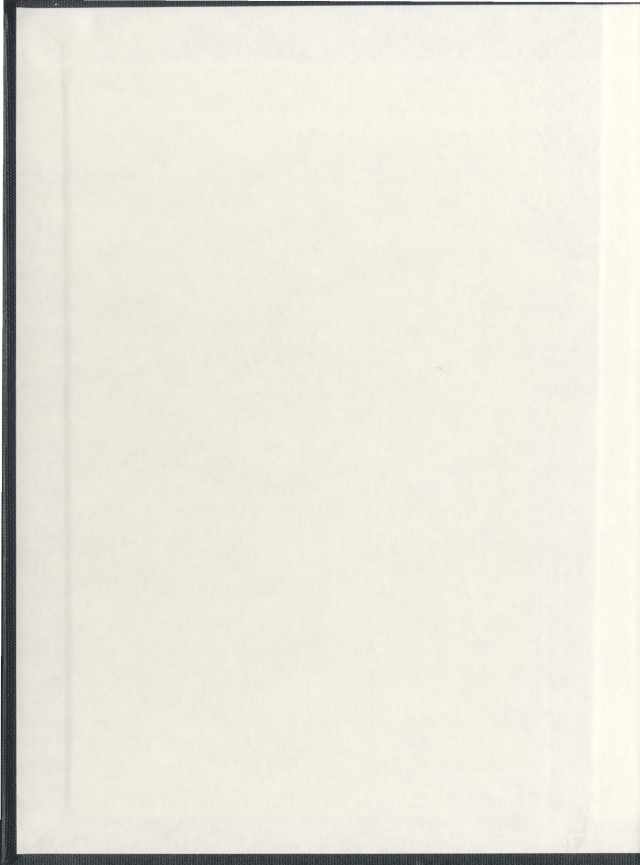


SYNTHESIS AND CHARACTERIZATION OF
MACROCYCLIC NAPHTHALENE RING-BASED
CALIX[n]ARENES, LACTONES AND AMIDES

TAYEL AL HUJAN



**Synthesis and Characterization of Macrocyclic Naphthalene
Ring-Based Calix[*n*]arenes, Lactones and Amides**

By

© **Tayel Al Hujran**

A thesis submitted to the School of Graduate Studies
in partial fulfillment of the requirements for the degree of
Doctor of Philosophy

Department of Chemistry

Memorial University Newfoundland and Labrador

2012

St. John's

Newfoundland and Labrador

Dedication

To the memory of my late Father

And to the memory of my late Uncle Abdul Lataif

To my Mother

And to all members of my family

Abstract

The work described in this thesis is concerned mainly with the synthesis of some new molecular receptors which are naphthalene ring-based calixarenes, lactones and amide macrocycles. Their complexation properties with fullerenes C_{60} and/or cationic guests such as tetramethylammonium acetate and/or alkali metal cations were studied.

In Chapter 2, the syntheses of the macrocycle lactones and their clathrates are described. The structures of these macrocycles were determined by X-ray analysis which revealed that they formed either *cage* or *channel-type* clathrates when crystallized from different solvents.

The work described in the Chapter 3 concerns the synthesis of a series of new di- and tetraamide macrocycles, respectively, from the [1+1] and [2+2] fragment cyclocondensation reactions of 4,4'-methylenebis(3-methoxy-2-naphthoyl chloride) and its derivatives with 1,8-diamino-3,6-dioxaoctane or with 1,10-diamino-4,7-dioxadecane.

In Chapter 4, synthetic studies are described toward unprecedented acenaphthene, ring-based calixarene analogues, which could serve as wider and deeper bowl-shaped cavity-containing molecular receptors. The syntheses of homooxacalix[4]acenaphthene was achieved using a [2+2] fragment condensation strategy. Its X-ray structure showed the macrocycle in an 1,3-alternate conformation. As determined by $^1\text{H-NMR}$ spectroscopy, homooxacalix[4]acenaphthene was found to be a moderately good host for complexation with C_{60} in toluene- d_6 solution.

In Chapter 5 a series of new mixed naphthalene ring-based homooxacalix[4]arenes were synthesized also by employing a [2+2]-type fragment condensation reaction. X-ray structures of octahomotetraoxacalix[2]naphthalene[2]pyridine crystals grown from two different solvent systems revealed that the structures adopted *1,3-alternate* and *cone* conformations. ¹H-NMR titration studies for this macrocycle revealed it to be a good host for binding TMAA in CDCl₃ solution in 1:1 ratio.

Acknowledgments

I would like to extend my sincere admiration and immeasurable thanks to my supervisor, Professor Paris E. Georghiou, for his guidance, encouragement and valuable advice during the course of my research project and the writing of this thesis.

I am also grateful to Dr. Louise Dawe for all of her X-ray crystal structure determinations. My appreciation is also extended to my supervisory committee, Dr. Francesca Kerton, and Dr. Ray Poirier, for proofreading and valuable comment and suggestions. I also would also like to thank Ms. Linda Winsor, for training and support with mass spectroscopy and Dr. Celine Schneider for training and support with NMR spectroscopy Ms. Julie Collins is also thanked for training and support with NMR spectroscopy and X-ray crystal structure determination.

Thanks are also due to Professors Graham Bodwell, Sunil Pansare, and Yuming Zhao for helpful discussions and encouragements. To the members of the Georghiou group, both past and present, it has been a great joy to me to work together with you all.

Special thanks are also extended to my father, my mother, my sisters, my brothers, and the staff in the Chemistry Department for their support, help and friendship. The financial support from Memorial University of Newfoundland, the Dean of Science and the Chemistry Department is gratefully acknowledged.

Table of Contents

Title	i
Dedication	ii
Abstract.....	iii
Acknowledgments	v
Table of Contents	vi
List of Figures	xii
List of Schemes	xvi
List of Tables	xx
List of Abbreviations	xxi
List of Appendixes	xxiv

Chapter 1 Introduction

1.1 Supramolecular chemistry.....	1
1.2 Calixarenes	4
1.2.1 Nomenclature of calixarenes	5
1.2.2 Conformational properties of <i>p-tert</i> -butylcalixarenes.....	7
1.2.3 Synthesis of calix[4]naphthalenes.....	11
1.3 Homocalix[<i>n</i>]naphthalenes.....	17
1.4 Heterocalixarenes.....	21
1.5 Macrocyclic amide receptor molecules.....	24
1.6 Clathrates.....	26
1.6.1 Calixarene clathrates.....	26
1.6.2 Cyclodextrin clathrates	27
1.7 Objectives and results.....	30
1.8 References	32

Chapter 2 Synthesis and clathrates of unprecedented oligomeric 7-*tert*-butyl-2-naphthoide macrocycles

2.1 Introduction	38
2.1.1 Tri- <i>O</i> -thymotide ("TOT").....	38
2.1.2 One-pot synthesis of TOT	39
2.1.3 Multi-step mixed synthesis.....	44
2.1.4 Resolution of chiral compounds.....	46

2.2 Synthesis of the tetra-, tri- and hexamacrocyclic lactones 27-28	50
2.2.1 Results and discussion	50
2.3 Conclusions	56
2.4 Experimental section.....	57
2.4.1 Materials	57
2.4.2 General methods.....	57
2.4.3 Instrumentation.....	57
2.4.4 Experimental.....	59
2.5 References	63
Chapter 3 Amide-based macrocycles derived from 4,4'-methylenebis(3-methoxy-2-naphthoyl chloride).	
3.1 Introduction	65
3.1.1 Properties of anion receptors	65
3.1.2 Application of anion receptors	66
3.1.3 Acyclic amide and sulfonamide-based receptors	67
3.1.4 Macrocyclic amide receptors.....	69
3.2 Design and retrosynthetic analysis of di- and tetraamide macrocycles	78
3.2.1 Retrosynthetic analysis	78
3.3 Results and discussion	79
3.3.1 Synthesis of di- and tetraamide macrocycles	79

3.3.2 Synthesis of diamide macrocycle 32 from reaction of bis(3-aminomethyl-2-methoxy-1-naphthyl)methane (35) with 4,4'-methylenebis(3-methoxy-2-naphthoyl chloride) (31a).....	85
3.3.2.1 Retrosynthetic analysis and synthesis.....	85
3.4 Attempts to synthesize Schiff macrocycles 36a-b	86
3.4.1 Retrosynthetic analysis	86
3.4.2 Results and discussion	87
3.4.3 Attempted synthesis of Schiff macrocycles 36a-b	88
3.5 Conclusions	91
3.6 Experimental section.....	92
3.6.1 Experimental.....	92
3.7 References	111

Chapter 4 Attempts at the synthesis of calix[4]acenaphthenes and the synthesis of octahomotetraoxacalix[4]acenaphthenes

4.1 Introduction	114
4.1.1 Homooxacalix[<i>n</i>]arenes	114
4.1.2 Homooxacalixnaphthalenes.....	117
4.2 Synthesis of calix[<i>n</i>]acenaphthenes.....	121
4.2.1 Design of a target structures	121
4.2.2 Retrosynthetic analysis	124
4.3 Results and discussion	125

4.3.1	Synthesis of functionalized acenaphthenes	125
4.3.2	Attempted synthesis of calix[4]acenaphthene	131
4.4	Synthesis of homooxacalix[4]acenaphthenes.....	134
4.4.1	Design of the target structure	134
4.4.2	Retrosynthetic analysis	135
4.5	Results and discussions	136
4.5.1	Functionalized 5,6-dialkoxyacenaphthene synthesis	136
4.5.2	Synthesis of homooxacalix[4]acenaphthene	140
4.5.2	Complexation study	142
4.6	Conclusions	145
4.7	Experimental section.....	147
4.7.1	Experimental.....	147
4.8	References	167

Chapter 5 Naphthalene ring-based homooxacalix[4]arenes

5.1	Introduction	171
5.1.1	Heterocalixarenes	171
5.2	Synthesis of the octahomotetraoxacalix[2]acenaphthene[2]naphthalene (18a) and octahomotetraoxacalix[2]naphthalene[2]pyridine (18b).....	176
5.2.1	Retrosynthetic analysis	176
5.2.2	Results and discussions.....	177
5.2.3	NMR spectra of 18a.....	179

5.3 Synthesis of the octahomotetraoxacalix[2]naphthalene[2]pyridine (18b).....	180
5.3.1 Results and discussion.....	180
5.3.2 NMR spectra of 18b	181
5.3.3 X-Ray crystallography of 18b	181
5.4 Attempts at the synthesis of octahomotetrathiacalix[2]naphthalene[2]pyridine (18c).....	182
5.4.1 Results and discussion.....	182
5.5 Synthesis of tetrahomodioxacalix[4]naphthalene (26).....	184
5.5.1 Retrosynthetic analysis.....	184
5.5.2 Results and discussion.....	185
5.6 Complexation studies.....	187
5.6.1 Complexation with metal salts.....	192
5.6.2 Protonation of the macrocycle.....	194
5.7 Conclusions.....	195
5.8 Experimental section.....	196
5.8.1 Experimental.....	196
5.9 References.....	203
Appendix A.....	205
Appendix B.....	214
Appendix C.....	261
Appendix D.....	306
Appendix E.....	322

List of Figures

Figure 1.1. Cyclodextrin (1a-c) and valinomycin (2) macrocycles	2
Figure 1.2. Examples of supramolecular complexes 6 , 7 and 8	4
Figure 1.3. Nomenclature system used for calixarenes.	6
Figure 1.4. Rims defined in calixarenes.	7
Figure 1.5. The four major types of conformers of <i>p-tert</i> -butylcalix[4]arene.	9
Figure 1.6. ¹ H- and ¹³ C-NMR spectral patterns of the methylene groups in the four calix[4]arene conformational isomers.	10
Figure 1.7. The three regioisomeric calix[4]naphthalenes and their numbering system.	11
Figure 1.8. Structures of acyclic amide receptors 80-83	25
Figure 1.9. The structure of tricyclic amide receptor 84	26
Figure 1.10. <i>p-Tert</i> -butylcalix[4]arene forms a clathrate with toluene.	27
Figure 1.11. Structures of α -, β - and γ -cyclodextrins respectively.....	28
Figure 1.12. Structures of heptakis(2,6- <i>O</i> -dimethyl)- β -CD and of hydroxypropyl- β -CD.	29
Figure 1.13. Cyclodextrin and <i>p</i> -xylene complex in water.....	29
Figure 2.1. Tri- <i>O</i> -thymotide (TOT), (1) structure.....	39
Figure 2.2. <i>Tetra</i> -1-naphthoide structure 14	43
Figure 2.3. Separation of a racemic mixture using TOT as chiral resolution agent.....	49
Figure 2.4. Structures of macrocycle lactones 27-29	50

Figure 2.5. (a) X-ray structure of the tetra-2- <i>O</i> -naphthoide (27) (dichloromethane molecules omitted for clarity), and (b) Space-filling representation showing the close π - π stacking between a pair of molecules of the tetramer and the dichloromethane molecules.	54
Figure 2.6. X-ray structure (ORTEP 30 % thermal ellipsoids) of tri-2- <i>O</i> -naphthoide (28) containing a water molecule (hydrogen atoms omitted for clarity).	55
Figure 2.7. X-ray structure (a) space-filling and (b) packing diagram viewed along the <i>c</i> axis of hexa-2- <i>O</i> -naphthoide 29 showing the inclusion of four molecules of chloroform.	56
Figure 3.1. Structures of trisamides 1a-d and trissulfonamides 2a-b	67
Figure 3.2. Isophthalamide structures 3a-b and X-ray structure of 3a:Br ⁻ complex.	68
Figure 3.3. The structure of compound 4	69
Figure 3.4. Cyclic triamide compounds 5a-b and acyclic triamide compound 6	70
Figure 3.5. Changes in the amide ¹ H-NMR chemical shift of macrocycle 5b with increasing iodide anion concentration.	72
Figure 3.6. Structure of diamide macrocycles 14 and 15	76
Figure 3.7. X-ray structures of macrocyclic amides 20a , 21a and 22a	83
Figure 3.8. The structures of the tetra- 19b and diamide macrocycles 20b and 21b	84
Figure 3.9. X-ray structure of tetramide macrocycle 19b	84
Figure 4.1. Hexahomotrioxacalix[3]naphthalenes 18a-b and 19 and their precursors ...	119
Figure 4.2. X-ray stereoview of 22b showing its <i>flattened partial-cone</i> conformation.	121

Figure 4.3. Computer-generated structure of 34 : (<i>Left: Top view</i>) and (<i>Right: Side view</i>) respectively, showing the flattened 1,3-alternate-type shallow cavity conformation	122
Figure 4.4. Computer-generated structures of calix[4]acenaphthene (36a left-top view) and of its 1:1 C ₆₀ complex (<i>right-side view</i>) respectively.	123
Figure 4.5. ¹ H-NMR spectrum of the crude product from the dehydrating reaction of 4-hydroxymethyl-5,6-dimethoxyacenaphthene	133
Figure 4.6. Computer-generated structures of calix[4]acenaphthene (47a left) and of a 1:1 47a : C ₆₀ complex (<i>right</i>)	134
Figure 4.7. X-ray structure of 4,7-bis(bromomethyl)-5,6-dimethoxyacenaphthene (48b).	137
Figure 4.8. X-ray structure of 47b (side view) showing its 1,3-alternate conformation.	141
Figure 4.9. X-ray structure of the unit cell packing of 47b (<i>c-axis view</i>).....	142
Figure 4.10. Plot of chemical shift changes ($\Delta\delta$) for protons on 47b in toluene- <i>d</i> ₆ solution vs added C ₆₀	143
Figure 4.11. 1:1 Binding isotherm for the titration of 47b with C ₆₀	144
Figure 5.1. Heterocyclic ring-based calixarenes 1-5	172
Figure 5.2. Mixed heterocalix[4]arenes 6 , 7 and 8	173
Figure 5.3. Heterocyclic-based calixarenes 9 and 10	174
Figure 5.4. X-ray structure showing the inclusion complex of 10 with acetone and CH ₂ Cl ₂	174

Figure 5.5. The X-ray structures of macrocycle 18b in (a): a "1,3- <i>alternate</i> " (left), and (b): " <i>cone</i> " conformation (right).....	182
Figure 5.6. Partial ¹ H-NMR spectra (500 MHz) of TMAA upon addition to the macrocycle 18b in CDCl ₃ solution at 298K.	189
Figure 5.7. ¹ H-NMR titration curves for TMAA complexation with 18b , titration curves for TMA cation (<i>left</i>) and methyl group of acetate anion (<i>right</i>).	189
Figure 5.8. ¹ H-NMR titration curves for 18b with 1,3-dihydroxybenzene (<i>left</i>), and 1,3- dihydroxynaphthalene (<i>right</i>).	190
Figure 5.9. Expanded section of the ¹ H-NMR spectra (in 1m L, CDCl ₃ , 298 K) of 1,3- dihydroxybenzene (<i>top</i>) and 1,3-dihydroxynaphthalene (<i>bottom</i>) in the presence of increasing amounts of macrocycle 18b	191
Figure 5.10. Expanded section of the ¹ H-NMR spectra (CDCl ₃ /5% DMSO- <i>d</i> ₆ , 298 K) of macrocycle 18b in the presence of different metal nitrate salts	193
Figure 5.11. Expanded section of the ¹ H-NMR spectra of macrocycle 18b in CDCl ₃ at 298 K, in the presence of different concentrations of CF ₃ CO ₂ D	194
Figure 5.12. A computer-generated model of a 1:1 C ₆₀ : 18b complex	195

List of schemes

Scheme 1.1. Synthesis of the first crown ether by Pedersen.....	3
Scheme 1.2. Synthesis of calixarenes ($n = 9, 10, 11$).....	6
Scheme 1.3. Synthesis of calix[4]naphthalenes 17 using a [2+2] approach.....	12
Scheme 1.4. Synthesis of calix[4]naphthalenes 14 and 22 using a [1+3] approach.....	12
Scheme 1.5. Synthesis of calix[4]naphthalenes 23a-b via self-condensation approach.....	13
Scheme 1.6. Synthesis of calix[4]naphthalenes 25a-b via Suzuki-Miyaura coupling.....	14
Scheme 1.7. Synthesis of 29 derived from chromotropic acid, disodium salt (30).....	15
Scheme 1.8. Synthesis of tetrasulfonatocalix[4]naphthalene (31).....	15
Scheme 1.9. Synthesis of "3,5- and 3,6-linked" calix[n]naphthalenes (33) and (34).....	16
Scheme 1.10. Synthesis of "3,6-linked" calix[4]naphthalene (37).....	16
Scheme 1.11. Some examples of homocalix[n]arenes 40a-c and 41-42	17
Scheme 1.12. Synthesis of dihomocalix[4]naphthalenes 51 and 52	18
Scheme 1.13. Synthesis of dihomocalix[4]naphthalene 52	19
Scheme 1.14. Synthesis of tetrahomocalix[4]naphthalene 53	19
Scheme 1.15. Synthesis of hexaester 64 and octaester 65 macrocycles.....	20
Scheme 1.16. Synthesis of 1,2-bis(3-hydroxy-2-naphthyl)ethane (60).....	21
Scheme 1.17. Synthesis of pyridine-based calixarenes 66a-e	22
Scheme 1.18. Synthesis of mixed heterocalix[3]arene 68	23
Scheme 1.19. Synthesis of mixed heterocalix[3]arene 76 and heterocalix[3]arene 77	24
Scheme 2.1. Synthesis of the chiral TOT analogue 5	40
Scheme 2.2. Synthesis of halogenated TOT analogues 8a-d	41

Scheme 2.3. Synthesis of <i>hexa</i> - and <i>tetramacrocylic</i> lactones 10a-e and 11a-b	42
Scheme 2.4. Synthesis of mixed macrocyclic trimers 12 and 13	42
Scheme 2.5. (a) Decarboxylation of <i>O</i> -thymotic acid under cyclization conditions. (b) Synthesis of TOT (1), DOT (18), and other acyclic products 16a-c	44
Scheme 2.6. Multi-step synthesis of mixed TOT analogues.....	46
Scheme 2.7. Synthesis of tetramacrocycle lactone 27	51
Scheme 2.8. Synthesis of the tri- and hexamacrocycle lactones 28 and 29 respectively.....	53
Scheme 3.1. Synthesis of tetra-, hexa- and octamide macrocycles using Method A or Method B	73
Scheme 3.2. Breakage in the intramolecular hydrogen bonds of tetraamide macrocycle 11b upon addition of anions.....	74
Scheme 3.3. Synthesis of macrocycle 18	77
Scheme 3.4. Retrosynthetic analysis of di- and tetraamide macrocycles 19a-b	78
Scheme 3.5. Synthesis of methyl-3-hydroxy-2-naphthoate and its derivatives 25a-b	80
Scheme 3.6. Synthesis of compounds 30a-c	81
Scheme 3.7. Synthesis of tetra- and diamide macrocycles 19a , 20a , 20a and 22a	82
Scheme 3.8. Synthesis of macrocycle 32	86
Scheme 3.9. Retrosynthetic analysis for Schiff base macrocycles 36a-b	87
Scheme 3.10. Attempt to synthesize Schiff macrocycles 36a-b	88
Scheme 3.11. The Reinhoudt syntheses of calixsalenes 42a-c and 43	89
Scheme 3.12. Macrocycles 46-48 formed by Schiff base macrocyclizations.....	90
Scheme 4.1. Synthesis of the dihomoxacalix[4]arene 1 and calixarenes 3-5	115

Scheme 4.2. Synthesis of oxacalixarenes 1 , 9 and 10 via thermal dehydration.....	115
Scheme 4.3. Synthesis of octahomotetraoxacalix[4]arene 11	116
Scheme 4.4. Synthesis of homooxacalix[<i>n</i>]arenes 9 (<i>n</i> = 3) and 11 (<i>n</i> = 4).....	117
Scheme 4.5. Synthesis of homooxacalix[<i>n</i>]arenes 14 (<i>n</i> = 3) and 15 (<i>n</i> = 4).....	117
Scheme 4.6. Synthesis of tetrahomodioxacalix[4]naphthalenes 20a-b	119
Scheme 4.7. Synthesis of hexahomodioxacalix[4]naphthalene 21	120
Scheme 4.8. Synthesis of homooxaisocalix[<i>n</i>]naphthalenes 22a-d , 23a and 23d	121
Scheme 4.9. Cyclotetrachromotropylenes (34) derived from chromotropic acid (35).....	122
Scheme 4.10. Calix[4]acenaphthene (36a) derived from 5,6-dihydroxyacenaphthene (37a).....	123
Scheme 4.11. Retrosynthetic analysis of calix[4]acenaphthenes 36a-d	124
Scheme 4.12. Synthesis of 5,6-dibromoacenaphthene (39).....	125
Scheme 4.13. Attempted synthesis of 5,6-dihydroxyacenaphthene (37a).....	126
Scheme 4.14. Synthesis of 5,6-diiodo- and 5,6-dimethoxyacenaphthene 42 and 37b	127
Scheme 4.15. General reaction scheme experiments summarized in Table 1	128
Scheme 4.16. Synthesis of 5,6-dialkoxycenaphthenes 37b-d	130
Scheme 4.17. Synthesis of 4-formyl-5,6-dialkoxycenaphthenes (41a-c).....	131
Scheme 4.18. Synthesis of 4-hydroxymethyl-5,6-dialkoxycenaphthenes (40a-c).....	131
Scheme 4.19. Attempts at the synthesis of calix[4]acenaphthene 36b from 37b	132
Scheme 4.20. Attempts at the synthesis of calix[4]acenaphthene (36b) from 4-hydroxy- methyl-5,6-dimethoxyacenaphthene (40a).....	133

Scheme 4.21. Retrosynthetic analysis for octahomotetraoxacalix[4]acenaphthenes 47a-c .	135
Scheme 4.22. Synthesis of the 4,7-bis(bromomethyl)-5,6-dialkoxyacenaphthenes (38b-d).	136
Scheme 4.23. Attempted <i>in situ</i> synthesis of 49a (R = H).	137
Scheme 4.24. Attempted <i>ortho</i> -metalation approach to 49b .	138
Scheme 4.25. Duff method syntheses of 50a and 50b .	138
Scheme 4.26. Kornblum oxidation synthesis of 50a-c .	139
Scheme 4.27. Synthesis of 4,7-bis(dihydroxymethyl)-5,6-dialkoxyacenaphthenes 49b-c .	139
Scheme 4.28. Synthesis of octahomotetraoxacalix[4]acenaphthene (47b).	140
Scheme 5.1. Mixed thiophene-octahomotetraoxacalixarene 11 .	175
Scheme 5.2. Tetrahomotetraoxacalix[2]arene[2]triazine (14).	176
Scheme 5.3. Retrosynthetic analysis of macrocycles 18a-c .	177
Scheme 5.4. Synthesis of octahomotetraoxacalix[2]acenaphthene[2]naphthalene (18a).	178
Scheme 5.5. Synthesis of the octahomotetraoxacalix[2]naphthalene[2]pyridine (18b).	180
Scheme 5.6. Synthesis of 1,4-bis(mercaptomethyl)-2,3-dimethoxynaphthalene (20b).	183
Scheme 5.7. Attempted synthesis of octahomotetraoxacalix[2]pyridine[2]naphthalene (18c).	184
Scheme 5.8. Retrosynthetic analysis of tetrahomodioxacalix[4]naphthalene (26).	185
Scheme 5.9. Synthesis of tetrahomodioxacalix[4]naphthalene (26).	187

List of tables

Table 3.1. Radii of some cations and anions in Å.....	66
Table 4.1. Cu-catalyzed coupling of 5,6-dibromoacenaphthene (39) with NaOMe to form 37b	129
Table 4.2. ¹ H-NMR titration data of 47b with C ₆₀ in toluene- <i>d</i> ₈ at 298 K. ($\Delta\delta$ values are absolute values).....	144

List of Abbreviations

ACS	American Chemical Society
Å	angstrom
Aq	aqueous
APCI-MS	Atmospheric Pressure Chemical Ionization Mass Spectrometry
Bn	benzyl
br.	broad (in NMR)
Bu	butyl
<i>n</i> -BuLi	<i>n</i> -butyllithium
CPK	Corey-Pauling-Koltun
δ	chemical shift in ppm down-field from tetramethylsilane
DMF	<i>N,N</i> -dimethylformamide
DMSO	dimethyl sulfoxide
Dec.	decomposed
Et	ethyl
h	hour (s)
HRMS	High-Resolution Mass Spectrum
Hz	hertz
<i>J</i>	coupling constant (Hz)

K	Kelvin (degree)
K_{assoc}	association constant
kJ	kilojoule
LC	liquid chromatography
Lit.	literature
M	multiplet (in NMR)
M^+	molecular ion
MALDI-TOF	Matrix-Assisted Laser Desorption Ionization-Time of Flight
Me	methyl
mol equiv	molar equivalent
mp	melting point
MS	mass spectrometry
Min	minute(s)
MW	microwave
NBS	<i>N</i> -bromosuccinimide
NMR	nuclear magnetic resonance
NR	no reaction
<i>p</i>	para
Ph	phenyl
PLC	preparative layer chromatography

PCC	pyridinium chlorochromate
ppm	parts per million
ⁿ Pr	<i>n</i> -propyl
ⁱ Pr	isopropyl
PTFE	polytetrafluoroethylene
q	quartet (in NMR)
quant	quantitative
rt	room temperature
s	singlet (in NMR)
t	triplet (in NMR)
<i>tert</i>	tertiary
THF	tetrahydrofuran
TLC	thin-layer chromatography
TMS	tetramethylsilane (in NMR)
TMAA	tetramethylammonium acetate
TMEDA	<i>N, N, N', N'</i> -tetramethylethylenediamine
TOT	<i>tri-O</i> -thymotide

List of Appendixes

Appendix A	^1H and ^{13}C NMR spectra for compounds described in Chapter 2.....	205
Appendix B	^1H and ^{13}C NMR spectra for compounds described in Chapter 3.....	214
Appendix C	Complexation data and ^1H and ^{13}C NMR spectra for compounds described in Chapter 4.....	261
Appendix D	Complexation data and ^1H and ^{13}C NMR spectra for compounds described in Chapter 5.....	306
Appendix E	^1H and ^{13}C NMR spectra for compounds described in Chapter 2-5.....	322

Chapter1

Introduction

1.1 Supramolecular chemistry

Chemists have been continually synthesizing new molecules in order to study their chemical and physical properties. Although a vast amount of research has focused on forming covalent bonds, which form the basis of much of synthetic chemistry, studies focused on supramolecular chemistry have also emerged in recent years. This branch of chemistry focuses on the assembly of two or more molecules via intermolecular forces only, and is prevalent in many biological systems and processes. Therefore, a major driving force behind studying supramolecular chemistry is to mimic biological systems.¹

In biological systems there are many receptors which can selectively bind to a specific type of molecule. This process is called "molecular recognition".² Molecular recognition forms the cornerstone for supramolecular chemistry. It was introduced for the first time by Emil Fischer³ in 1894, who proposed the "Lock and Key" principle to explain how enzymes function in living cells. Based on this principle, Emil Fisher devised the fundamental foundation for identifying and devising target molecules in supramolecular chemistry. There are many different types of molecular interactions that occur during molecular recognition processes such as electrostatic, hydrogen-bonding, π - π stacking and dispersion and/or induction forces.^{2,3}

Among the most common type of macrocycles formed in nature are the cyclodextrins.⁴ Cyclodextrins (**1a-c**) (Figure 1.1) are formed from 6, 7 or 8 glucopyranose units and are produced enzymatically from starch and are also now produced in quantities of more than 1000 tons per year for industrial purposes. The valinomycin macrocycle (**2**)⁵ (Figure 1.1) is another example of a naturally-occurring macrocycle, and is a dodecadepsipeptide formed from repeated D-hydroxyisovaleric acid, L-lactic acid and L- and D-valine (Figure 1.1). During the process of transferring potassium cations through the mitochondrial membranes, valinomycin selectively forms a complex with a potassium cation in the presence of a sodium cation.

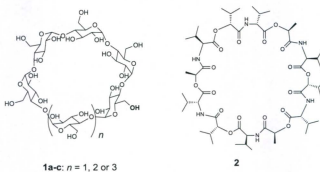
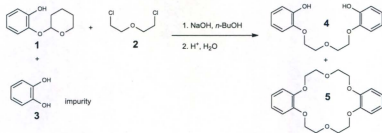


Figure 1.1. Cyclodextrins (**1a-c**) and valinomycin (**2**) macrocycles.

The first artificial molecular receptor was discovered in 1967, by Pedersen.⁶ While he was attempting to synthesize bisphenol (**4**), a by-product dibenzo[18]crown-6 (**5**) was formed from the catechol (1,2-dihydroxybenzene, **3**) which was an impurity in the starting material for that reaction (Scheme 1.1).



Scheme 1.1. Synthesis of the first crown ether by Pedersen.

Pedersen⁶ observed that the cyclic ether **5** enhanced the solubility of potassium permanganate in benzene or chloroform and the solubility of **5** in methanol was increased by the addition of sodium cation to form "Complex **6**" (Figure 1.2). Based on these observations Pedersen suggested that the cyclic ether formed complexes with cations in general, and called the macrocycle a *crown ether*, because it encircled the metal ion like a crown. In 1969, Lehn and co-workers⁷ reported the synthesis of a new class of crown ether receptors which they called "*cryptands*". These types of receptors have been shown to be more highly selective than the analogous crown ethers when they formed complexes with cations *e.g.* "Complex **7**" (Figure 1.2). Also, Cram⁸ designed and synthesized preorganized macrocycles which have rigid structures and fixed binding sites. They called those types of macrocycles "*spherands*" which showed higher selectivity toward some cations than others. For example, the spherand in "Complex **8**" (Figure 1.2) binds with sodium and lithium but not with potassium ions at all. In 1987, the Nobel Prize was awarded jointly to Charles J. Pedersen, Donald Cram and Jean-Marie Lehn for their efforts in introducing a new specialized field in chemistry.

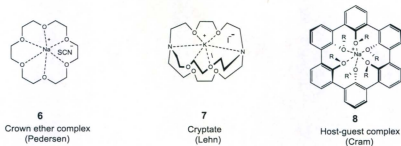


Figure 1.2. Examples of supramolecular complexes 6, 7 and 8.

1.2 Calixarenes

In 1872, a resinous tar was observed by Adolph von Beayer⁹ as a product of the reaction between *p*-*tert*-butylphenol and formaldehyde under basic conditions. Similarly, Zinke and Ziegler in the 1940s noticed the formation¹⁰ of a “resinous tar” which produced a solid product that decomposed above 300 °C. After several years’ work on this “resinous tar”, Ziegler and co-workers concluded that products from that reaction were “cyclic oligomers”. In the early 1950’s,^{10c} Cornforth and co-workers¹¹ reinvestigated the “resinous tar” product and they found that “the resinous tar” was composed of a mixture of cyclic oligomers.

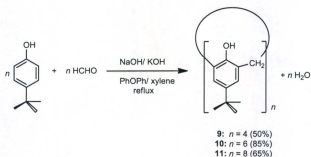
In the mid 1970’s Gutsche and co-workers¹² also reinvestigated Zinke’s compounds while they were looking for biomimetic receptors as part of their studies of enzyme catalysts. Gutsche and co-workers characterized the cyclic oligomers which were produced from condensation of *p*-*tert*-butylphenol and paraformaldehyde in the presence of a catalytic amount of base, as being a cyclic tetramer, a cyclic hexamer and a cyclic

octamer. As a result, Gutsche and co-workers developed efficient methods to synthesize each of these macrocycles in scales ranging from less than one gram up to many kilograms, using a one-pot procedure, starting from cheap starting materials.¹²

1.2.1 Nomenclature of calixarenes

Macrocycle oligomers **9-11** (Scheme 1.2) are classified as “[1*n*] metacyclophenes” according to the Cram and Steinberg nomenclature system.¹³ The systematic name given to the basic macrocycle **9** by Chemical Abstracts is “[19.3.1.1^{3,7}1^{9,13}1^{15,19}]octacosal(25),3,5,7(28), 9,11,13(27),15,17,19(26)21,23-dodecaene.”¹⁴ As a result, the systematic names for these types of macrocycles are complicated and are not suitable for facile writing and communication purposes.

Gutsche classified these types of macrocycles simply as “calix(*n*)arenes”^{12a} a simpler and easier name with which to write and communicate. This naming system was chosen based on the fact that these macrocycles have a bowl shape, similar to the Greek vase which is called a “calix krater”.¹⁵ As the “calix” refers to the shape of the macrocycle, the number of the aromatic units in the macrocycle is indicated by a bracketed number “*n*” and “arene” refers to the incorporated aromatic rings.¹⁶ For example, compound **9** takes the systematic name, according to Gutsche’s naming system, as follows: 5,11,17,23-tetra-*tert*-butyl-25,26,27,28-tetrahydroxycalix[4]arene (**9**), shortened simply also as *p-tert*-butylcalix[4]arene,¹⁵ a name which appears in the text of many publications and is the systematic one used in the experiment parts of this thesis (Figure 1.3).



Scheme 1.2. Synthesis of calixarenes ($n = 9, 10, 11$).

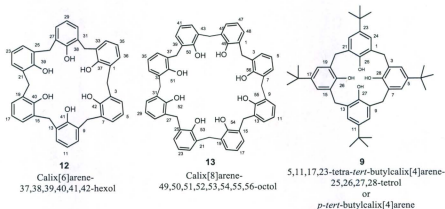


Figure 1.3. Nomenclature system used for calixarenes.

The bowl-shaped cyclooligomer calixarene can be designated as having two distinct regions. One is referred to as the “lower- or narrow-rim” and is that which carries the hydroxyl groups. The second region is called the “upper- or wide-rim” and is that which

carries various substituents on the *para*-positions to the hydroxyl groups of the aromatic rings (Figure 1.4).¹⁵

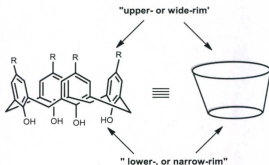


Figure 1.4. Rims defined in calixarenes.

1.2.2 Conformational properties of *p*-*tert*-butylcalixarenes

One of the most useful properties of calixarenes is their flexibility which allows them to adopt various conformers (Figure 1.5). This high flexibility is produced as a result of the free rotation of the phenolic units around the σ -bonds of the bridging $-\text{CH}_2-$ groups.¹⁶ There are two possible pathways for the aromatic rings to rotate around the σ -bonds in calixarenes. The first possibility is that one or more of the *para*-substituent groups rotate through the calixarene cavity (annulus) but in the case of the *p*-*tert*-butylcalix[4]arenes this motion is not possible, even if there are no *para*-substituents at all. The second possibility is that one or more of the hydroxyl groups instead rotate through the calixarene annulus.¹⁷

The *p*-*tert*-butylcalix[4]arenes have the possibility to exist in four distinctly different conformers which were first recognized by Cornforth. These main four conformers are characterized by the orientation of the aryl groups being upward ("u") or downward ("d") as compared to the average plane defined by the methylene bridges. Furthermore, Gutsche proposed new names for these four conformers, as follows: *cone* or *crown*, *partial-cone* or *partial-crown* or "*paco*"; *1,2-alternate* and *1,3-alternate* for the (u,u,u,u); (u,u,u,d); (u,u,d,d); and (u,d,u,d) Gutsche¹⁵ and Cornforth¹¹ conformers, respectively (Figure 1.5). In the case of the *p*-*tert*-butylcalix[4]arenes (**9**), it was found that the *cone* conformer is the most thermodynamically-stable conformer. The stability of the *cone* conformer can be explained by the fact that the intramolecular hydrogen bonding between the phenol groups in the narrow rim inhibits the rotation of the phenol group through the calixarene cavity. It has been found that the *O*-alkylation of the phenolic groups of the *p*-*tert*-butylcalix[4]arenes (**9**) conformers is strongly affected by *O*-substituents and the metal template. For example, attaching propyl groups to the phenolic groups using different bases with their different metal templating effects will inhibit the rotation of the phenolic groups through the calixarene cavity, allowing for the isolation and characterization of these type(s) of atropisomeric conformers.¹⁸

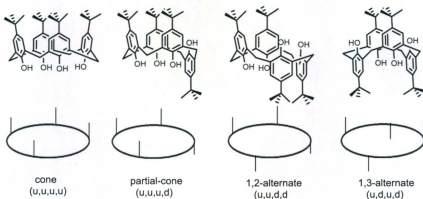


Figure 1.5. The four major types of conformers of *p*-*tert*-butylcalix[4]arene.

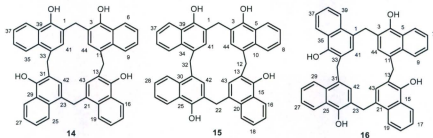
These four calixarene conformers now can be easily distinguished due to the simple “de Mendoza rules” introduced by de Mendoza and co-workers.¹⁹ These rules help to differentiate between the conformers via the ¹H- and ¹³C-NMR correlation spectra of the methylene bridges of the calixarenes. Also, the conformations of the calix[5]arenes and calix[6]arenes in solution can be identified by applying the same “de Mendoza rules”.

According to these rules the ¹H-NMR spectra for the *cone* conformer shows an AB pair of doublets, and the *1,3-alternate* conformer show one singlet (Figure 1.6), for the methylene bridges. The *partial-cone* and *1,2-alternate* conformations, each shows a singlet and a pair of doublets (Figure 1.6).¹⁹

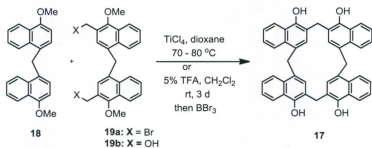
1.2.3 Synthesis of calix[4]naphthalenes

During the past decades, there has been a growing interest in the supramolecular chemistry of calixarenes. A new class of supramolecular hosts having deeper, wider and electron-rich cavities was reported in 1993 by Georghiou and Li.^{22,23} In those types of calixarenes the phenol units were replaced by naphthol units to form what were named "calix[4]naphthalenes".

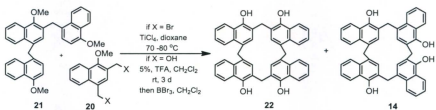
Georghiou and Li²³ synthesized three isomeric calix[4]naphthalenes, **14-16**, (Figure 1.7) in a "one-pot" procedure via self-condensation of the 1-naphthol with paraformaldehyde in the presence of K_2CO_3 in DMF. In principle, a fourth possible tetrameric isomer could be produced from that reaction, but it was not detected. Since the self-condensation of 1-naphthol produces a mixture of *exo*-calix[4]naphthalenes in only modest yields and required careful chromatographic purification, alternate routes were developed to synthesize all four of those *exo*-calix[4]naphthalenes individually including the previously unknown **17**.



Convergent syntheses for all four regioisomeric *exo*-calix[4]naphthalenes using [2+2] and [3+1] condensation approaches were reported by Georghiou and Ashram.²⁴ The [2+2] approach involved the condensation of **18** with bis(bromomethyl) **19a** or bis(hydroxymethyl) **19b** using TiCl₄ or 5% TFA in chloroform respectively, to produce calix[4]naphthalene **17**. On the other hand, the [3+1] condensation method involved reaction of the bis(hydroxymethyl) **20** with trimer **21** using TiCl₄ or 5% TFA in chloroform, to produce calix[4]naphthalenes **14** and **22** after de-methylation.

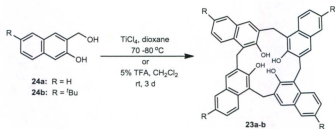


Scheme 1.3. Synthesis of calix[4]naphthalenes **17** using a [2+2] approach.



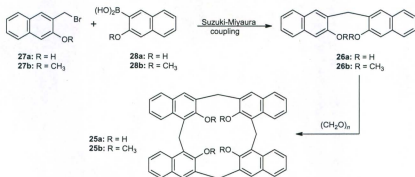
Scheme 1.4. Synthesis of calix[4]naphthalenes **14** and **22** using a [1+3] approach.

Endo-calix[4]naphthalenes are those naphthalene-based calixarenes in which the hydroxyl groups are situated *inside* the calixarene cavity. In 1993, Böhmer and co-workers²⁵ reported the synthesis of the *endo*-calix[4]arene **23a** (Scheme 1.5) in a relatively poor yield, *via* the self-condensation of 3-hydroxymethyl-2-naphthol (**24a**) using TiCl₄ in refluxing anhydrous dioxane. Georghiou et al.²⁶ reported improved yields of **23a** and the synthesis of the *tert*-butylated *endo*-calix[4]naphthalene **23b** in yields of 30% (Scheme 1.5) from 6-*tert*-butyl-3-hydroxymethyl-2-naphthol (**24b**) using TiCl₄ in dioxane by modifying Böhmer's previously reported method.



Scheme 1.5. Synthesis of calix[4]naphthalenes **23a-b** *via* self-condensation approach.

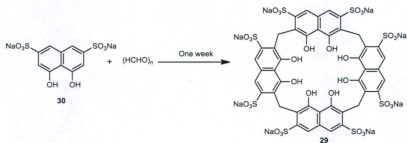
The C_2 -symmetrical *endo*-calix[4]naphthalenes **25a-b** were also synthesized by Georghiou and co-workers, using the [2+2] condensation approach (Scheme 1.6). The key intermediates **26a-b** were constructed from bromomethylnaphthyl **27a-b** and naphthylboronic acid **28a-b** using a modified Suzuki-Miyaura cross-coupling reaction.²⁷ Exposure of the Suzuki-Miyaura cross-coupling products **26a-b** to the [2+2]-type cyclocondensation reaction conditions in the presence of paraformaldehyde produced the *endo*-calix[4]naphthalenes **25a-b**.



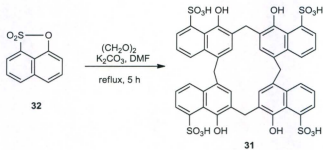
Scheme 1.6. Synthesis of calix[4]naphthalenes **25a-b** via Suzuki-Miyaura coupling.

In 1989, Poh's group²⁸ described the synthesis of a highly water-soluble "chromotropylene" which can be considered to be an *endo*-sulfonatocalix[4]naphthalene (**29**), from the cyclocondensation of the disodium salt of 1,8-dihydroxy-3,6-naphthalenedisulfonic acid or "chromotropic acid" (**30**), with an excess of paraformaldehyde in aqueous solution (Scheme 1.7). Also, Poh and co-workers²⁹ conducted several complexation studies of **29** in aqueous solution with different metal ions. The precise structure of **29** however, to this date, remains ambiguous.

A different example of a (less) water-soluble sulfonatocalix[4]naphthalene (**31**) was synthesized via condensation of 1,8-naphthalenesultone (**32**) and paraformaldehyde (Scheme 1.8) by the Georghiou group.³⁰



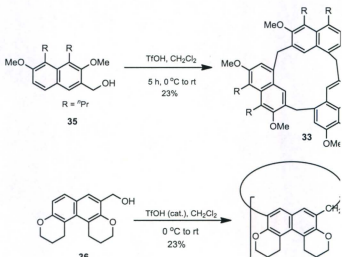
Scheme 1.7. Synthesis of **29** derived from chromotropic acid, disodium salt (**30**).



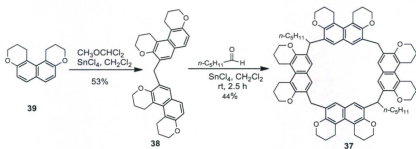
Scheme 1.8. Synthesis of tetrasulfonatocalix[4]naphthalene (**31**).

Glass et al.³¹ reported the synthesis of the “3,5-linked” calix[3]naphthalene (**33**) and “3,6-linked” calix[*n*]naphthalenes (**34**) (*n* = 3-6), (Scheme 1.9), which were obtained via Friedel-Crafts alkylation of the hydroxymethyl derivatives **35** and **36** respectively, using trifluoromethanesulfonic acid as catalyst. The Glass group³¹ also reported the synthesis of a mixture of *cis/trans* isomers of the 3,6-linked-calix[4]naphthalene (**37**). The reaction sequence involves a [2+2] SnCl₄-catalyzed cyclocondensation of the key intermediate dinaphthyl **38** with hexanal in dichloromethane in 44% yield (Scheme 1.10). The key

intermediate **39** was synthesized from condensation of the compound with dichloromethyl methyl ether.



Scheme 1.9. Synthesis of “3,5- and 3,6-linked” calix[*n*]naphthalenes (**33**) and (**34**).



Scheme 1.10. Synthesis of “3,6-linked” calix[4]naphthalene (**37**).

1.3 Homocalix[*n*]naphthalenes

Homocalixarenes are a class of calixarenes in which one or more of the methylene bridges are replaced by ethylene bridges, or larger bridges,^{15,32-34} such as **40-42** (Figure 1.8). As a result, these modifications increase the size of the annulus of the calixarenes. Many complexation studies have shown that homocalixarenes and their derivatives have the potential to host several different cationic guests, such as transition metal ions,^{15,32-36} uranyl ion,³⁷ alkali metal ions^{38,39} and alkaline earth metal ions.³⁹

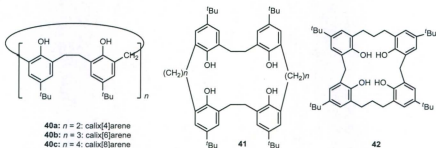
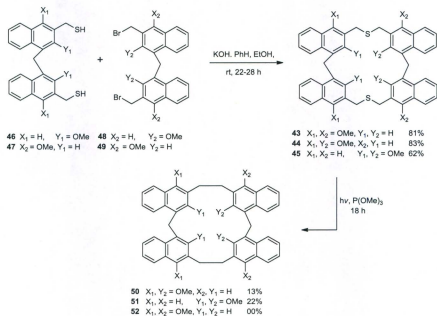


Figure 1.8. Some examples of homocalix[*n*]arenes **40a-c** and **41-42**.

Several new homocalix[*n*]naphthalenes in which one or more of the methylene bridges are replaced by ethylene bridges, such as dihomocalixarenes, tetrahomocalix[4]-arenes and *n*-homocalixnaphthalenes have been synthesized by the Georghiu group.^{22,40,41} The strategy used to synthesize the dihomocalix[4]naphthalenes involves synthesis of the tetrahomodithiacalix[4]naphthalenes **43-45** via [1+1] coupling reactions between bis(mercaptomethyl) compounds **46** or **47** and bis(bromomethyl) compounds **48**

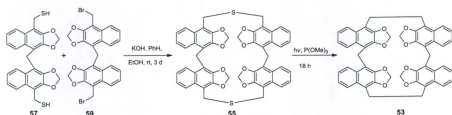
or **49**, respectively, (Scheme 1.11) under high-dilution conditions using potassium hydroxide as base to mediate the coupling reactions. Extrusion of the sulfur atoms from the resulting coupling products by photochemical methods formed dihomocalix[4]naphthalenes **50** and **51** in yields of 13 and 22% respectively (Scheme 1.11)



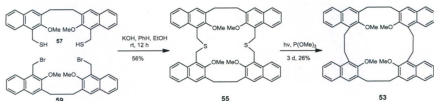
Scheme 1.11. Synthesis of dihomocalix[4]naphthalenes **50** and **51**.

In addition, dihomocalix[4]naphthalene **53**⁴² (Scheme 1.12) and tetrahomocalix[4]-naphthalene **54**^{40,41} (Scheme 1.13) were obtained from tetrahomodithiacalix[4]-naphthalenes **55** and dithiatetrahomocalix[4]naphthalenes **56**, respectively. These di- and tetrahomocalix[4]naphthalenes **53** and **54** were produced by employing the same

methodologies used before by the Georghiou group to synthesize macrocycles **50** and **51**, starting from bis(mercaptomethyl) compounds **57** or **58** and bis(bromomethyl) compounds **59** or **60**, respectively. No complexation properties of these compounds were studied.



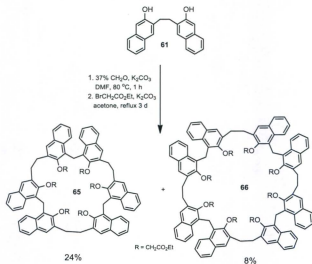
Scheme 1.12. Synthesis of dihomocalix[4]naphthalene **53**.⁴²



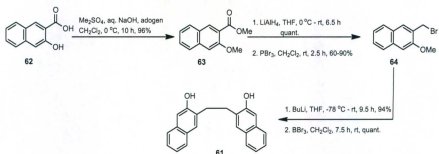
Scheme 1.13. Synthesis of tetrahomocalix[4]naphthalene **54**.⁴¹

The Georghiou group⁴³ also synthesized *n*-homocalixnaphthalenes from the intermediate 1,2-bis(3-hydroxy-2-naphthyl)ethane (**61**), (Scheme 1.14). This key intermediate was derived from 3-hydroxy-2-naphthoic acid (**62**) which reacts smoothly with dimethyl sulfate in the presence of sodium hydroxide to form ester **63** which was

then reduced with lithium aluminum hydride and brominated with PBr_3 to produce 3-(bromomethyl)-2-methoxynaphthalene (**64**) (Scheme 1.15). Treatment of **64** with *n*-butyllithium resulted in homocoupling to produce **61**, after BBr_3 de-methylation. Cyclocondensation of **61** with formaldehyde, in DMF, in the presence of potassium carbonate, produces a mixture of homocalix[*n*]naphthalenes. Due to the low solubility of those macrocycles in most organic solvents, they were directly converted into their ester derivatives **64** and **66** to enhance their solubility, and as a result, could be purified by column chromatography. Two-phase solvent extraction experiments of the alkaline metal picrates from aqueous solution by esters **65** and **66** in chloroform at 25 °C indicated that **65** showed relatively high selectivity toward potassium cation.



Scheme 1.14. Synthesis of hexaester **65** and octaester **66** macrocycles.



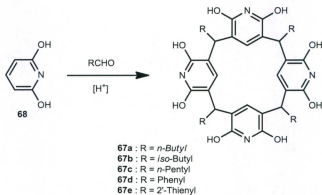
Scheme 1.15. Synthesis of 1,2-bis(3-hydroxy-2-naphthyl)ethane (61).

1.4 Heterocalixarenes

While the effort to improve the properties of calixarenes by introducing new functional groups onto the calixarene scaffold is ongoing, the construction and design of new types of calixarenes are being studied by several research groups. One of those developments involves introducing heterocalixarenes which are constructed by replacing one or more of the phenolic units in calixarenes with one or more heterocyclic units such as pyrrole, pyridine, or thiophene, etc. For example, the pyridine ring-based calixarenes **67a-e** have been synthesized from the condensation reactions of 2,6-dihydropyridine (**68**) with aromatic and aliphatic aldehydes under acidic conditions, as shown in Scheme 1.16.⁴⁴

Black and co-workers⁴⁵ reported the synthesis of mixed heterocalixarenes containing benzofuran and indole units. They synthesized two types of heterocalix[3]arenes by different approaches (Scheme 1.17). For example, heterocalix[3]arene **69** was

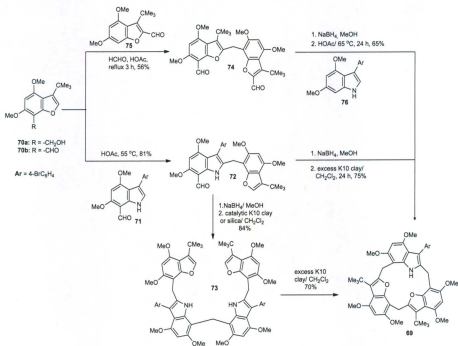
synthesized starting from **72**, the condensation product of **70a** and **71**. Reduction of **72**, followed by treatment with a catalytic amount of Montmorillonite K10 clay, or with silica gel, produced the linear oligomer **73**. Upon further treatment with excess K10 in dichloromethane, the heterocalix[3]arene **69**, was afforded in 70% yield. A direct approach involved treatment of the resulting product from the reduction of **72** with an excess of K10 clay in dichloromethane. A third approach involved treatment of the condensation product **74** of two benzofuran aldehyde units **70b** and **75** with sodium borohydride, followed by addition of compound **76** to the reduction product in acetic acid.



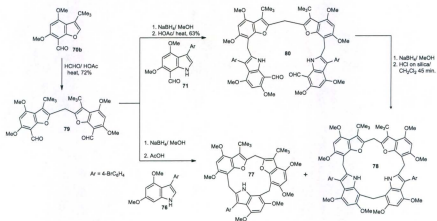
Scheme 1.16. Synthesis of pyridine-based calixarenes **67a-e**.

Black et al.⁴⁵ constructed the benzofuran/indole-mixed heterocalix[3]arene **77** and heterocalix[4]arene **78**, starting from benzofurancarbaldehyde (**70b**) which is condensed with paraformaldehyde. Reduction of the resulting dialdehyde **79** followed by treatment with compound **71** produced a linear-oligomer **80** (Scheme 1.18). After reduction of **80**

to the corresponding dialcohol, cyclocondensation using dry HCl on silica produced heterocalix[3]arene **77** and heterocalix[4]arene **78**. They also, synthesized heterocalix[3]-arene **77** from the reaction of **76** with the dialcohol obtained from the reduction of **79**.



Scheme 1.17. Synthesis of mixed heterocalix[3]arene **69**.



Scheme 1.18. Synthesis of mixed heterocalix[3]arene **77** and heterocalix[4]arene **78**.

1.5 Macrocyclic amide receptor molecules

Since the first example of anion receptors reported by Jean-Marie Lehn,⁴⁶ and due to the important roles anions play in various aspects of everyday life such as in health, in industry and in the environment, research in the supramolecular chemistry of anions has grown very rapidly. Much of this research has been aimed to develop new types of receptors that have the ability for the recognition and sensing of anions in various solvent media. As a result, new methods have been used to achieve this purpose. In spite of the many special demands or features which must be considered in designing anion receptors, such as the limited pH range, in which to function and the sizes and shapes of the particular anions, much research has been devoted to design of new anion receptors.⁴⁷

There are many receptors which have different types of functional groups^{48,49} such as: amides, thioamides, pyrroles, indoles, urea, thiourea, guanidinium or hydroxyl groups that have the ability to bind anions via hydrogen bonding. Since the first examples of synthetic anion receptors containing secondary amide groups reported by Pascal and co-workers in 1986,⁵⁰ different kinds of anion amide-containing receptors and sensors have been synthesized. For example, Sessler and co-workers⁵¹ synthesized some acyclic amide-containing anion receptors, (**81-84**, Figure 1.9) from the condensation of anthracene diamine, or carbazole diamine with benzoyl chloride and pyrroly-2-carboxyl chloride acid. ¹H-NMR titration of these amide receptors with various tetrabutylammonium salts in DMSO-*d*₆ revealed selective binding of dihydrogen phosphate over benzoate and chloride, and also that the binding constants increased as the number of the hydrogen-bonding possibilities increased.

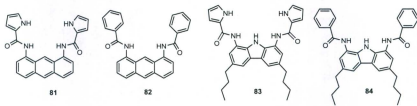


Figure 1.9. Structures of acyclic amide receptors **80-83**.

Bowman-James and co-workers⁵² synthesized the tricyclic amide **85**, (Figure 1.10), via condensation of pyridine-2,6-dicarbonyl chloride with diethylenetriamine in dichloromethane, in the presence of Et₃N by using selective protection and deprotection

techniques. The $^1\text{H-NMR}$ titration studies of **85** with tetrabutylammonium salts in $\text{DMSO-}d_6$ revealed that **85** forms stable complexes with hydrogen bifluoride (FHF^-) and azide (N_3^-) linear anions selectively over the spherical Cl^- , Br^- or I^- anions.

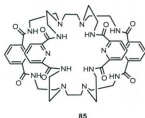


Figure 1.10. The structure of tricyclic amide receptor **85**.

1.6 Clathrates

1.6.1 Calixarene clathrates

Calix[4]arenes such as *p-tert*-butylcalix[4]arene have the ability to form *cage*-type clathrates with different types of neutral aromatic guests such as benzene, *p*-xylene, anisole⁵³ and toluene,⁵⁴ and also *channel*-type clathrates with acetic acid.⁵⁵ The crystal structure of the calix[4]arene clathrate with toluene revealed that the toluene molecules interacted with *p-tert*-butylcalix[4]arene cavity *via* π - π interactions, (Figure 1.11).⁵⁶ A solution complexation study showed only weak binding approximately $K_{\text{assoc}} = 1.1 \text{ M}^{-1}$ between toluene and *p-tert*-butylcalix[4]arene in chloroform.

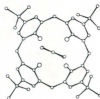


Figure 1.11. *p*-*Tert*-butylcalix[4]arene forms a clathrate with toluene.

Calix[*n*]arenes have the ability to bind different-sized guests depending on the size of the calix[*n*]arenes. For example, Atwood and co-workers⁵⁷ and later Shinkai et al.⁵⁸ independently reported that *p*-*tert*-butylcalix[8]arene had the ability to separate [60]fullerene (C_{60}) selectively from a mixture containing C_{60} and [70]fullerene (C_{70}). The spherical C_{60} molecules fit inside the *p*-*tert*-butylcalix[8]arene cavity to form complexes which precipitated from the toluene solution. This precipitate was separated from the rest of the toluene solution by filtration after which the solid precipitate was stirred in chloroform. The *p*-*tert*-butylcalix[8]arene dissolved in the chloroform but the C_{60} was insoluble and was isolated by filtration.⁵⁹

1.6.2. Cyclodextrin clathrates

Cyclodextrins are well-known macrocycles and have been used as hosts on an industrial level, in drug, food and cosmetic products, in the thousand-tons scale because they are easily synthesized from starch using environmentally-friendly enzymes. The most important cyclodextrin macrocycles are α -, β - and γ -cyclodextrins which are composed of six, seven and eight D-glucopyranose units, respectively, linked *via* α -1,4-

glycosidic bonds, as shown in Figure 1.12. Cyclodextrin rings have conical cylindrical shapes. Their rings have wide-diameter rims lined with $2n$ secondary hydroxyl groups, and their smaller-diameter rims lined with n primary hydroxyl groups.⁶⁰

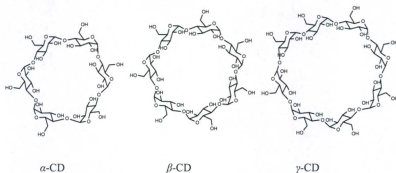


Figure 1.12. Structures of α -, β - and γ -cyclodextrins respectively.

The most important β -cyclodextrin (β -CD) derivatives are methylated β -CD and 2-hydroxypropylated β -CD (Figure 1.13). Because these types of cyclodextrins have higher-water solubilities, these cyclodextrins cannot be crystallized from water. This physical property makes them very important for drug formulations in which drugs in liquid form can be produced. Methylated β -CD and 2-hydroxypropylated β -CD both formed soluble complex with cholesterol; on the other hand, unmodified β -CD formed insoluble cholesterol complex crystals. Methylated β -CD has also been used to extract cholesterol from blood.⁴

Another modified β -CD is *heptakis*-sulfobutyl- β -CD. This type of cyclodextrin is very soluble in water even at high concentrations and showed no toxicity. Thus, much

research has been undertaken to develop it as a drug carrier for water-insoluble drugs. Also, this cyclodextrin could be used as a chiral separating agent. When cyclodextrins dissolve in water the cavity of the macrocycle is filled with water molecules. The addition of non-polar molecules like *p*-xylene to that solution increases the solubility of *p*-xylene in the water due to the complexation formed between cyclodextrin and *p*-xylene. The driving force for that interaction is that the slightly non-polar cavity of the cyclodextrin prefers binding of the non-polar *p*-xylene over the polar water molecules, as shown in Figure 1.14.⁴

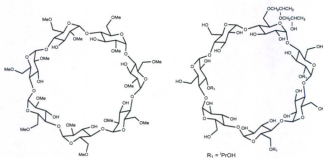


Figure 1.13. Structures of heptakis(2,6-*O*-dimethyl)- β -CD and of hydroxypropyl β -CD.

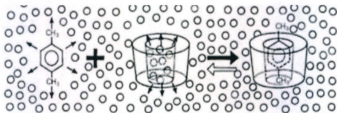


Figure 1.14. Cyclodextrin and *p*-xylene complex in water, reproduced with permission from IUPAC.⁴

1.7. Objectives and results

The synthesis of several macrocycle lactones and their clathrates are reported in Chapter 2 of this thesis. The structures of these macrocycles have been determined by X-ray analysis which revealed formation of either *cage* or *channel-type* clathrates when crystallized from different solvents.

The synthesis of a series of new di- and tetraamide macrocycles from the condensation of 4,4'-methylenebis(3-methoxy-2-naphthoyl chloride) and its derivatives with 1,8-diamino-3,6-dioxaoctane or with 1,10-diamino-4,7-dioxadecane, are described in Chapter 3.

A major part of the objectives of the work described in this thesis was also to synthesize new calixacenaphthene, which could serve as larger, wider and deeper bowl-shaped cavity-containing molecular receptors. Computer-based molecular modeling was used to design and evaluate the potential of this type of compound to form supramolecular complexes. The molecular modeling⁶¹ showed that these acenaphthene-based calixarenes had the ability to bind C₆₀ fullerene and also other guests such as alkylammonium and metal salts. The syntheses of homooxacalix[4]acenaphthene by employing a [2+2] fragment condensation, and attempts to synthesize calix[n]acenaphthenes *via* condensation with paraformaldehyde and self-condensation of hydroxymethylacenaphthene are reported in Chapter 4. The binding constants of homooxacalix[4]acenaphthene in solution were calculated using ¹H-NMR spectroscopy.

The X-ray structure for the octahomotetraoxacalix[4]acenaphthene revealed that it adopted a *1,3-alternate* conformation.

In Chapter 5 a series of new mixed naphthalene ring-based homooxacalix[4]arenes were also synthesized by employing a [2+2]-type fragment condensation reaction. A single crystal X-ray crystallographic analysis of octahomotetraoxacalix[2]naphthalene[2]-pyridine were grown in two different solvent systems which revealed that the structures adopted *1,3-alternate* and *cone* conformations. Computer molecular modeling was used to evaluate the potential of octahomotetraoxacalix[2]naphthalene[2]pyridine to form supramolecular complexes. A limited binding study of this new host in solution was investigated using ¹H-NMR spectroscopy.

1.8 References

1. Atwood, J. L.; Davies, J. E. D.; MacNicol, D. D.; Vogtle, F.; Lehn, J.-M., *Comprehensive Supramolecular Chemistry*, Oxford, U. K., 1996.
2. (a) Lehn, J.-M., *Supramolecular Chemistry*, 1st ed.; VCH, Weinheim, 1995. (b) Lehn, J.-M. *Pure & Appl. Chem.* **1987**, *50*, 871. (c) Lehn, J.-M. *Acc. Chem. Res.* **1978**, *11*, 49.
3. (a) Ariga, K. Kunitake T., *Supramolecular Chemistry Fundamentals and Applications*, 1st ed.; Springer-Verlag, Berlin, Heidelberg, Germany, 2006. (b) Fischer, E. Ber. *Deutsch. Chem. Ges.* **1894**, *27*, 2985. (c) Koshland, D. E. *Angew. Chem. Int. Ed. Engl.* **1994**, *33*, 2375.
4. Szejtli, J. *Pure & Appl. Chem.* **2004**, *76*, 1825.
5. (a) Steed, J. W.; Atwood, J. L. *Supramolecular Chemistry*; Wiley VCH: Weinheim, Germany, 2009. (b) Frish, L. Sanson, F.; Casnati, A.; Ungaro, R.; Cohen, Y. *J. Org. Chem.* **2000**, *65*, 5026.
6. (a) Pedersen, C. J. (Nobel Lecture) *Angew. Chem. Int. Ed.* **1988**, *27*, 1021. (b) Pedersen, C. J. *J. Am. Chem. Soc.* **1967**, *89*, 153. (c) Pedersen, C. J. *J. Am. Chem. Soc.* **1967**, *89*, 7017.
7. (a) Lehn, J.-M. . (Nobel Lecture) *Angew. Chem. Int. Ed.* **1988**, *27*, 89. (b) Lehn, J.-M. *Angew. Chem. Int. Ed.* **1990**, *29*, 1304.
8. (a) Cram, D. J. (Nobel Lecture) *Angew. Chem. Int. Ed.* **1988**, *27*, 1009. (b) Cram, D. J.; R. Carmack, A.; deGrandpre, M, P.; Lein, G. M. Goldberg, I.; C.; Konbler, B.; Maverick, E. F.; Trueblood, K. N. *J. Am. Chem. Soc.* **1987**, *109*, 7068.

9. Baeyer, A. *Ber. Dtsch. Chem. Ges.* **1872**, *5*, 280, 1904.
10. (a) Zinke, A.; Ziegler, E. *Ber. Dtsch. Chem. Ges.* **1944**, *77*, 264. (b) Zinke, A.; Ziegler, E. *Ber. Dtsch. Chem. Ges.* **1944**, B74, 1729. (c) Zinke, A.; Kretz, R.; Leggewie, E.; Hössinger, K. *Monatsh*, **1952**, *83*, 1213.
11. (a) Cornforth, J. W.; D'Arcy Hart, P.; Nicholls, G. A.; Rees, R. J. W.; Stock, J. A. Br. *J. Pharmacol.* **1955**, *10*, 73. (b) Cornforth, J. W.; Morgan, E. D.; Potts, K. T.; Rees, R. J. W. *Tetrahedron* **1973**, *29*, 1659.
12. (a) Gutsche, C. D.; Muthukrishnan, R. *J. Org. Chem.* **1978**, *43*, 4905. (b) Muthukrishnan, R.; Gutsche, C. D. *J. Org. Chem.* **1979**, *44*, 3962. (c) Gutsche, C. D.; Dhawan, B.; No, K. H.; Muthukrishnan, R. *J. Am. Chem. Soc.* **1981**, *103*, 3782. (d) Gutsche, C. D.; Iqbal, M.; Stewart, D. *J. Org. Chem.* **1986**, *51*, 742. (e) Gutsche, C. D.; Iqbal, M. *Org. Synth.* **1990**, *68*, 234. (f) Gutsche, C. D.; Dhawan, B.; Leonis, M.; Stewart, D. *Org. Synth.* **1990**, *68*, 238. (g) Munch, J. H.; Gutsche, C. D. *Org. Synth.* **1990**, *68*, 243.
13. (a) Cram, D. J.; Steinberg, H. *J. Am. Chem. Soc.* **1951**, *73*, 5691. (b) IUPAC Tentative Rules for Nomenclature of Organic Chemistry, Section E. Fundamental Stereochemistry *J. Org. Chem.* **1970**, *35*, 284.
14. Patterson, A. M.; Capell, L. T.; Walker, D. F. *The Ring Index*, 2nd ed.; American Chemical Society, Washington D. C., 1960, Ring index No. 6485.
15. Gutsche, C. D. *Calixarenes, Monographs in Supramolecular Chemistry*, Stoddart, J. F.; Ed.; The Royal Society of Chemistry 1989 and references cited therein.

16. Dodziuk, H. *Introduction to Supramolecular Chemistry*. Hingham, MA, USA; Kluwer Academic Publishers, **2001**, 102.
17. Gutsch, C. D.; Dhawan, B.; Levine, J. A.; No, K. H.; Bauer, L. J. *Tetrahedron* **1983**, *39*, 409.
18. Stewart, D. R.; Krawiec, M.; Kashyap, R. P.; Watson, W. H.; Gutsche, C. D. *J. Am. Chem. Soc.* **1995**, *117*, 586.
19. Iwamoto, K.; Araki, K.; Shinkai, S. *J. Org. Chem.* **1991**, *56*, 4955.
20. Jaime, C.; de Mendoza, J.; Prados, P.; D.; Sanchez, C. *J. Org. Chem.* **1991**, *56*, 3372.
21. Mandolini, L.; Ungaro, R. *Calixarenes in Action*, Imperial College Press, London, 2000.
22. Georghiou, P. E.; Li, Z.; Ashram, M.; Chowdhury, S.; Mizyed, S.; Tran, H. A.; Al-Saraierh, H.; Miller, D. O. *Synlett* **2005**, 879.
23. (a) Georghiou, P. E.; Li, Z. *Tetrahedron Lett.* **1993**, *34*, 2887. (b) Georghiou, P. E.; Li, Z. *J. Incl. phenom. Mol. Recogni. Chem.* **1994**, *19*, 55. (c) Li, Z. Ph. D. Dissertation, Memorial University of Newfoundland, 1996.
24. Georghiou, P. E.; Ashram, M.; Li, Z.; Chaulk, S.; G. *J. Org. Chem.* **1995**, *60*, 7284.
25. Andreet, G. D.; Böhmer, V.; Jordon, J. G.; Tabatabai, M.; Ugozzoli, F.; Vogt, W.; Wolff, W. *J. Org. Chem.* **1993**, *58*, 4023.
26. Georghiou, P. E.; Ashram, M.; Clase, H. J.; Bridson, J. N. *J. Org. Chem.* **1998**, *63*, 1819.
27. (a) Chowdhury, S.; Georghiou, P. E. *J. Org. Chem.* **2002**, *67*, 6808. (b) Chowdhury, S. Ph. D. Dissertation. Memorial University of Newfoundland, 2001.

28. (a) Poh, B.-L.; Lim, C. S.; Khoo, K. S. *Tetrahedron Lett.* **1989**, *30*, 1005. (b) For a different interpretation of the structures of the products obtained from the reaction of formaldehyde with chromotropic acid (4,5-dihydroxy-2,7-naphthalenedisulfonic acid) under similar conditions, see Georghiou, P. E.; Ho, C. K. *Can. J. Chem.* **1989**, *67*, 871.
29. (a) Poh, B.-L.; Team. C. M. *Tetrahedron* **2005**, *61*, 5123. (b) Poh, B.-L.; Tan. C.-M. *J. Incl. phenom. Macro. Chem.* **2000**, *38*, 69. (c) Poh, B.-L.; Tan. C.-M. *Tetrahedron* **1995**, *51*, 953. (d) Poh, B.-L.; Tan. C.-M. *Tetrahedron* **1994**, *50*, 3453. (f) Poh, B.-L.; Tan. C.-M.; Wong, W. M. *Tetrahedron* **1993**, *49*, 7259. (g) Poh, B.-L.; Tan. C.-M.; Loh, C. L. *Tetrahedron* **1993**, *49*, 3849. (h) Poh, B.-L.; Lim, C. S.; Koay, L. S. *Tetrahedron* **1990**, *46*, 6155. (i) Poh, B.-L.; Lim, C. S.; Koay, L. S. *Tetrahedron* **1990**, *46*, 3651. (j) Poh, B.-L.; Seah, L. H.; Lim, C. S.; *Tetrahedron* **1990**, *46*, 4379. (k) Poh, B.-L.; Koay, L. S. *Tetrahedron Lett.* **1990**, *31*, 1911.
30. Georghiou, P. E.; Ashram, M.; Li, Z. *J. Org. Chem.* **1998**, *63*, 3748
31. (a) Shorthill, B. J.; Granucci, R. G.; Powell, D. R.; Glass, T. E. *J. Org. Chem.* **2002**, *67*, 904. (b) Shorthill, B. J.; Glass, T. E. *Org. Lett.* **2001**, *3*, 577.
32. Asfari, Z; Böhmer, V.; Harrowfield, J. Vicens, J.; Eds., Calixarenes 2001, Kluwer Academic Publishers, Dordrecht The Netherlands, 2001, pp 219-234 and references therein.
33. (a) Brodesser, G.; Vögtle, F. *J. Incl. Phenom. Mol. Recogni. Chem.* **1994**, *19*, 1111. (b) Schmitz J.; Vögtle, F.; Nieger M.; Gloe, K.; Stephen, H.; Heitzsch, O.; Buschmann, H.-J.; Hass, W. K.; *Cammann. Chem. Ber.* **1993**, *126*, 2483.

34. Ibach, S.; Prautzsch, V.; Vögtle, F. *Acc. Chem. Res.* **1999**, *32*, 729.
35. Yamato, T.; Kohno, K.; Tsuchichashi, K. *J. Incl. Phenom. Macro. Chem.* **2002**, *43*, 137.
36. Yamato, T. *J. Incl. Phenom. Mol. Recogni. Chem.* **1998**, *32*, 195.
37. (a) Thuery, P.; Jeong, T. G.; Yamato, T. *Supramol. Chem.* **2003**, *15*, 359. (b) Salmon, L.; Thuery, P.; Miyamoto, S.; Yamato, T.; Ephritikhine, M. *Polyhedron* **2006**, *62*, 1250.
38. Yamato, T.; Iwasa, T.; Zhang, F. *J. Incl. Phenom. Macro. Chem.* **2001**, *39*, 285.
39. Yamato, T.; Saruwatari, Y.; Yasumatsu, M.; Tsuzuki, H. *New. J. Chem.* **1998**, 1351.
40. Ashram, M. Ph. D. Dissertation. Memorial University of Newfoundland, 1997.
41. Georghiou, P. E.; Ashram, M.; Miller, D. O. *J. Org. Chem.* **1996**, *61*, 3865.
42. Li, Z. Ph. D. Dissertation. Memorial University of Newfoundland, 1996.
43. Tran, H.A.; Ashram, M.; Mizyed, M.; Thompson, D.W. and Georghiou, P. E. *J. Incl. Phenom. Macrocycl.* **2008**, *60*, 43.
44. Gerkenmeier, T.; Mattay, J.; Näther, C. *Chem. Eur. J.* **2001**, *7*, 729.
45. Black, D. S.; Craig, D. C.; Rezaie, R. *Chem. Commun.* **2002**, 810.
46. Lehn, J.-M.; Sonveaux, E. Willared, A.K. *J. Am. Chem. Soc.* **1978**, *100*, 4914.
47. (a) Dietrich, D. *Pure & Appl. Chem.* **1993**, *65*, 1457.
48. *Structure and Bonding: Recognition of Anions*, 129. Mingos, D. M. P.; Ed.; Springer-Verlag; Berlin, 2008.
49. (a) Caltagirone, C.; Gale, P. A. *Chem. Soc. Rev.* **2009**, *38*, 520..
50. Pascal, R. A.; Spergel, J.; van Engen, D. *Tetrahedron Lett.* **1986**, *27*, 4099.

51. Gross, D. E.; Mikkilineni, V.; Lynch, V. M.; Sessler, J. L. *Supramol. Chem.* **2010**, *22*, 135.
52. Kang, S. O.; Powell, D.; Day, V. W.; Bowman-James, K. *Angew. Chem. Int. Ed.* **2006**, *45*, 1921.
53. Coruzzi, M.; Andreetti, G. D.; Pochini, A.; Ungaro, R. *J. Chem. Soc. Perkin Trans II*, **1982**, 1133.
54. Andreetti, G. D.; Ungaro, R.; Pochini, A. *J. Chem. Soc. Chem. Commun.* **1979**, 1006.
55. Rizzoli, C.; Andreetti, G. D.; Ungaro, R.; Pochini, A. *J. Mol. Struct.* **1982**, *82*, 133.
56. Andreetti, G. D.; Ungaro, R.; Pochini, A. *J. Chem. Soc. Chem. Commun.* **1979**, 1005.
57. Atwood, J. L.; Koutsantonis, G. A.; Raston, C. L. *Nature (London)*, **1994**, *368*, 229.
58. Suzuki, T.; Nakashima, K.; Shinkai, S. *Chem. Lett.* **1994**, 699.
59. (a) MacGillivray, L. R.; Atwood, J. L. *Nature (London)*, **1997**, *389*, 469. (b) Atwood, J. L.; Barbour, L. J.; Raston, C. L.; Sudria, I. B. *Angew. Chem. Int. Ed.* **1998**, *37*, 981.
60. (a) Connors, A. K. *Chem. Rev.* **1997**, *97*, 1325. (b) Chen, G.; Jiang, M. *Chem. Soc. Rev.* **2011**, *40*, 2254.
61. Molecular modeling was conducted using the MMFF force field with Spartan¹⁰ software by Wavefunction Inc., Irvine, CA.

Chapter 2

Synthesis and clathrates of unprecedented oligomeric 7-*tert*-butyl-2-naphthoide macrocycles

2.1 Introduction

Host-guest inclusion phenomena have been extensively investigated in many applications¹ such as for the optical resolution of enantiomers,^{2,3} as reaction media for included molecules;⁴ for chirality transfer to reactants;^{5,4b} and for the separation of isomeric compounds.⁶ There are many molecules which have the ability as hosts, to form clathrates, the most important being water, *tri-O*-thymotide, (TOT), cyclodextrins, calix[*n*]arenes and cyclotriveratrylenes. Clathrates form as a result of van der Waals interactions between the "host" and the "guest" molecules in solution which can then form stable crystals containing both, as clathrates, from that solution.⁷

2.1.1 *Tri-O*-thymotide ("TOT")

Tri-O-thymotide ("TOT", **1**), is a trimeric lactone prepared from *O*-thymotic acid (Figure 2.1), and is one of the best-studied host compound that forms clathrates with different guest molecules.⁸ First synthesized in 1865, its correct structure was only established by Baker⁹ in 1952. TOT forms two types of clathrates with inclusion compounds: (a) *cage*-type clathrates, or (b) *channel*-type clathrates, when crystallized from various organic solvents. In its crystalline state *tri-O*-thymotide (**1**) exists in two helical chiral C_3 -symmetrical propeller-shaped conformations that are either *P* or *M*, and

which are rapidly interconverted at room temperature, because the low energy barrier to enantiomerization *M* to *P* or vice-versa *ca.* 88 kJ mol⁻¹ in solution. TOT, however, is capable of selective discrimination between enantiomers of a racemic guest upon crystallization.²

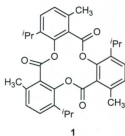
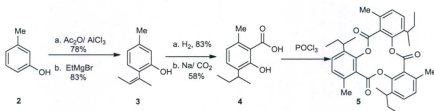


Figure 2.1. Tri-*O*-thymotide (TOT), (1) structure.

2.1.2 One-pot synthesis of TOT

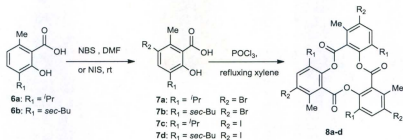
Due to the unique physical properties of TOT as a host, much research has been devoted to modifying its structure, or to improve the synthetic yield. Gnaim et al.¹⁰ reported new procedures to improve the synthesis of TOT and its analogues by varying the amounts and types of solvents, dehydrating agents and reaction times. They found that the concentration of the carboxylic acid plays an important role in the cyclization process. The most favorable condition was found using neat POCl₃ as a dehydrating agent in a 1:1.1 molar ratio of carboxylic acid to the POCl₃ respectively, and heating at 100 °C for 2 h.

On the other hand, Green and co-workers¹¹ modified the chemical structure of TOT by introducing a chiral *sec*-butyl group in the aromatic ring, (Scheme 2.1). They prepared compound **4** from *m*-cresol (**2**) which was reacted with acetic anhydride in the presence of anhydrous aluminum chloride, followed by the addition of magnesium ethyl bromide and then dehydration, to produce compound **3** in 83% yield. Hydrogenation of intermediate **3** followed by use of the Kolbe-Schmitt reaction with Na/CO₂ produced **4** in 58% yield as a racemic mixture. Following this, macrocycle **5** was synthesized by dehydration of racemic 3-(*sec*-butyl)-6-methylsalicylic acid (**4**) using POCl₃.



Scheme 2.1. Synthesis of the chiral TOT analogue **5**.

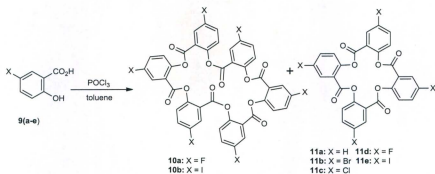
Gnaim et al.¹² also reported the synthesis of several halogenated TOT analogues **8a-d**, (Scheme 2.2). Their strategy involved synthesis of bromosalicylic acids (**7a-b**) and iodosalicylic acids (**7c-d**) using *N*-bromosuccinimide (NBS) or *N*-iodosuccinimide (NIS), respectively. Heating **7a-c** under reflux in xylene with the dehydrating agent POCl₃ produced the macrocycles **8a-d** in 10-28% yields.



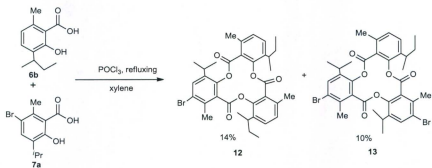
Scheme 2.2. Synthesis of halogenated TOT analogues **8a-d**.

Tanaka and co-workers¹³ reported the synthesis of several *tetra* and *hexa*salicylides **10a-b** and **11a-e** (Scheme 2.3), from halogenated salicylic acids **9a-e**, using POCl₃ in refluxing toluene. They discovered that these macrocyclic lactones had the ability to form clathrates. For example, crystallization of tetrasalicylide **11a** from CHCl₃ and DMSO formed a 1:2 host:guest clathrate. Tetrasalicylide macrocycles **11b-e** formed organogels with different organic solvents only, but, hexasalicylide macrocycles **10a-b** formed stable clathrates with different organic solvents.

Green and co-workers¹² also, reported the synthesis of mixed-macrocyclic trimers **12** and **13**, (Scheme 2.4). These two macrocyclic compounds were synthesized using Baker conditions by mixing the two different salicylic acids **6b** and **7a** in an equal mole ratio to produce **12** and **13** in 14 and 10% yields, respectively.



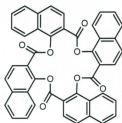
Scheme 2.3. Synthesis of *hexa*- and *tetra*macrocyclic lactones **10a-e** and **11a-b**.



Scheme 2.4. Synthesis of mixed macrocyclic trimers **12** and **13**.

Gerdil and Bernardinelli^{14b} reported the synthesis of the *tetra*-1-naphthoide (**14**), (Figure 2.2), by heating 1-hydroxy-2-naphthoic acid with phosphoric anhydride in xylene at reflux for 6 h. The *tetra*-1-naphthoide (**14**) formed different types of clathrates with various guests such as cyclohexanone, chlorocyclohexane, chloroform, 2-bromobutyric

acid, naphthalene, benzene and tetracyanoethylene as reported by Gerdil and Suwinska.^{14c}



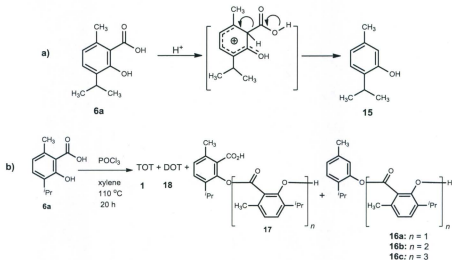
14

Figure 2.2. *Tetra*-1-naphthoide structure 14.

The synthesis of TOT and analogues using dehydrating agents such as POCl_3 or thionyl chloride (SOCl_2) suffer from different disadvantages. First, in addition to the formation of TOT, other acyclic and cyclic dimers, trimers and many other oligomers were produced which made the separation of TOT or TOT analogues very difficult. Second, the yield of the *triaryl*-macrocycle was very low under the reaction conditions, because the formed macrocycles are unstable and are easy to ring-open, which allowed *tetra*-, and *hexa*-macrocycles and also decarboxylated products to form. Third, using a one-pot dehydration method is only possible for synthesis of the *tri*-macrocycle from a single unit and not for mixed tricyclic trimers containing different aromatic units.¹⁰

As mentioned above, many side-products were formed during the dehydration reaction to form TOT and its analogues; for example, decarboxylation of the precursor

produced compound **15**, (Figure 2.5a), which also condensed with one or more of the carboxylic acids **6a** to produce the acyclic ester **16a**, acyclic diester **16b**, the triester **16c**, (Scheme 2.5b) and other acyclic oligomers **17**, as well as cyclic di-*O*-thymotide ("DOT", **18**).¹⁰



Scheme 2.5. (a) Decarboxylation of *O*-thymotic acid under cyclization conditions.

(b) Synthesis of TOT (**1**), DOT (**18**), and other acyclic products **16a-c**.

2.1.3 Multi-step mixed synthesis

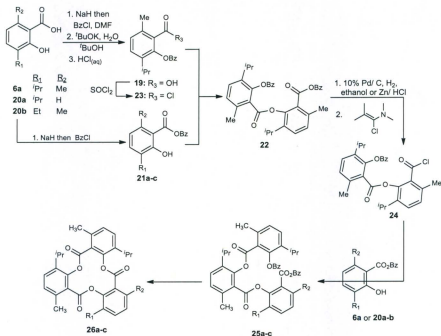
Harris et al.¹⁵ synthesized a series of TOT analogues using a multi-step convergent method (Scheme 2.6). In this strategy, either the phenol group or the carboxylic group of the salicylic acid was reacted with a different, or the same, protected salicylic unit, to form the diarylester(s) **22**. Selective deprotection of **22** was followed by

esterification with another protected salicylic unit to form the triarylesters **25a-c**. Deprotection of both the phenol and carboxylic groups was followed by the cyclization-lactonization reaction to give the specific lactones **26a-c**.

Selective protection of the phenolic group was achieved in two steps; the first step involved protection both of the phenolic and carboxylic acid groups of thymotic acid **6a**. Treatment of **6a** with more than two equivalents of both sodium hydride and benzyl chloride formed the bis-benzylated thymotic acid. The second step involved debenzylation of the carboxylic group using ^tBuOK, followed by acidification to produce compound **19**, (Scheme 2.6).¹⁵

The methodology used to selectively protect the carboxylic acid groups was accomplished by treating the carboxylic acids **6a** or **20a-b** with 1.3 equivalents of sodium hydride and one equivalent of benzyl chloride to afford the corresponding benzyl esters **21a-c**. Diaryl ester **22**, for example, was prepared by treating **21a** with sodium hydride and reacting the resulting carboxylate with the protected salicylic acid chloride, **23**. Selective deprotection of the carboxyl benzyl protecting group of **22** was carried out using 10% Pd/C and one mole of hydrogen, or Zn/HCl_(aq), to afford **24** after treatment with 1-chloro-*N,N*,2-trimethyl-1-propenylamine. The open-chain triaryl esters **25a-c** were prepared using the same sequence of reactions as that for **22**. Coupling **24** with **6a** or **20a-b** in diethyl ether using sodium hydride to generate the phenolic sodium salts gave the bisbenzyl-protected open-chain trimers **25a-c**. Debenzylation of the acyclic trimers,

followed by treatment with strong dehydrating agents such as POCl_3 under high dilution conditions, produced the corresponding lactones **26a-c**, (Scheme 2.6).¹⁵



Scheme 2.6. Multi-step synthesis of mixed TOT analogues.

2.1.4 Resolution of chiral compounds

TOT has C_3 -symmetry, and its propeller-shaped *P* or *M* conformers in solution exist as a racemic mixture, since they undergo rapid interconversion in solution. TOT

adopts only one conformation either *P* or *M*, upon forming a clathrate with a chiral compound.³

In order to separate *R* and *S* enantiomers for example, from a racemic mixture, both the resolving agent and the enantiomeric compounds must have active functional groups such as an amine, alcohol, or carboxylic acid group, in order to form covalent or ionic bonds thereby forming the corresponding diastereoisomers. The resolution depends on the fact that the diastereoisomers have different physical properties. Thus any separation or resolving method, like crystallization or using column chromatography, is able to separate the original enantiomers as diastereoisomers which can yield the pure *S* or *R* enantiomers after removing the resolving agent(s). However, some compounds have a chiral center whose absolute configuration cannot be determined correctly and/or difficult to separate as pure enantiomers because they lack the functional groups that can be used as described above. TOT has the ability to resolve a variety of racemic molecules that lack those kinds of functional groups.^{3,4,17} For example, haloalkane compounds such as CF_3CHBrCl (haloethane), $\text{CF}_3\text{CHClOCHF}_2$ (isoflurane), $\text{CF}_3\text{CHFOCHF}_2$ (desflurane) and $\text{CHFClCF}_2\text{OCHF}_2$ (enflurane) are used in inhalation anesthetics and all have a stereogenic center. Due to this reason a vast amount of research has been devoted to preparing these compounds in order to understand their behaviour as anesthetics and to evaluate potential problems which may be caused by their use as anesthetics, and also to study their chiroptical properties. The synthesis of each in its pure enantiomeric form is a challenging problem since using either an asymmetric synthesis approach or a chiral resolution method, cannot be used because these compounds lack a functional group that

usually can be used to form a covalent or ionic bond with chiral auxiliaries or other resolution compounds.¹⁷

The general procedure used in resolving a racemic mixture using TOT was first to dissolve the TOT in a large excess of the racemic compound in hot solution. After this, the solution is left to cool very slowly to room temperature. Single crystals of any of the clathrates that are formed are used as seeds for further crystallizations. Large single crystals (up to 0.5 g) can be obtained by re-dissolving the clathrate crystals in an excess of the same racemic mixture, followed by seeding this solution with the seed clathrate crystals previously obtained, and slowly cooling the solution. Large clathrate crystals that become resolved as their *P* or *M*-containing diastereomers can then be separated manually. The optical rotation of these resolved clathrates were measured at 2 °C, because the rate of racemization at 2 °C is very slow. Approximately 0.5-1.0 mg portions were taken from each of the larger formed clathrate crystal and were dissolved in chloroform at -10 °C. On the basis of their resulting optical rotations the diastereomers could then be bulk separated (Figure 2.3).³

TOT formed clathrates with enflurane upon mixing with enflurane in 2,2,4-trimethylpentane (TMP) was heated at reflux. After the TOT dissolved completely, the solution was then left to cool slowly to reach 0 °C over 24 h. This process produced cage-type clathrate inclusion complexes, which were then filtered and washed with cold methanol. Large crystals with masses around 80 mg, and as colorless cubic crystals, could be produced as 2:1 TOT to enflurane complexes.¹⁷

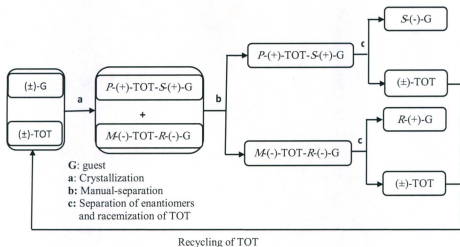


Figure 2.3. Separation of a racemic mixture using TOT as chiral resolution agent.

Powell² was first to use the TOT enclathration configuration to determine the absolute configuration of the guests which were hosted by the TOT macrocycles. Arad-Yellin et al.²⁶ studied the clathrates of many 2-haloalkanes and they established a "rule" which can be used to determine the type of 2-haloalkane enantiomer guest. If the *P*-(+)-TOT is the major enantiomer in the clathrate-crystal, the major guest has the *S* configuration; and if the *M*-(-)-TOT is the major enantiomer in it, the major guest has the *R* configuration. For example, all of the *S*-(+)-2-haloalkanes were either crystallized in *cage* or *channel* complex types, and both types of those complexes preferred to form clathrates with *P*-(+)-TOT rather than *M*-(-)-TOT.

In this Chapter the syntheses of three macrocyclic lactones **27-29**, (Figure 2.4), from the 3-hydroxy-2-naphthoic acid (**30**) are reported and their *channel-* or *cage-type* clathrates are described. Also, attempts to determine if the macrocyclic trimer **28** has the ability to work as a chiral resolution agent are reported. The major results obtained from this part of the study have been published in the Journal of Organic Chemistry.¹⁸

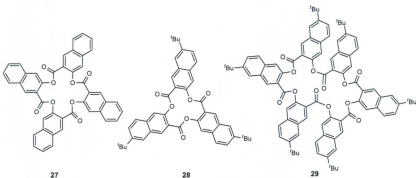


Figure 2.4. Structures of macrocycle lactones **27-29**.

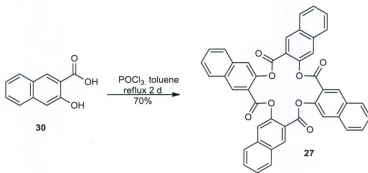
2.2 Synthesis of the *tetra-*, *tri-* and hexamacrocyclic lactones **27-28**

2.2.1 Results and discussion

As described above, *tri-O*-thymotide (TOT, **1**) has the ability to form a large number of *cage-type* and *channel-type* clathrates with different guest molecules. Due to the fact that TOT can crystallize with both *M* and *P* conformations in the solid state, it has the ability to carry out discrimination and resolution of various chiral guests. As a result,

much research has been devoted to synthesizing TOT (1) and TOT analogues in order to study the chemical and physical properties of its clathrate compounds.

The strategy used to synthesize some analogous naphthalene ring-based macrocycles such as **27**, (Scheme 2.7) involved using 3-hydroxy-2-naphthoic acid (**30**) and heating at reflux, in anhydrous toluene, in the presence of POCl_3 for two days. After TLC showed that all of the starting material was consumed, the solvent was removed under reduced pressure and the resulting crude product was purified by preparative thin layer chromatography using 1:1 ethyl acetate:hexane to furnish the macrocycle **27** in 70% yield.

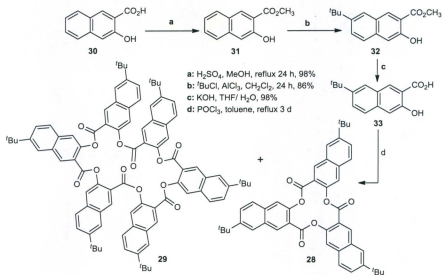


Scheme 2.7. Synthesis of tetramacrocycle lactone **27**.

Macrocycles **28** and **29** were synthesized from 7-*tert*-butyl-3-hydroxy-2-naphthoic acid (**33**). Esterification of **30** with methanol and using H_2SO_4 as a catalyst, afforded methyl-3-hydroxy-2-naphthoate (**31**) in 98% yield after refluxing the reaction mixture for 12 h. Methyl-7-*tert*-butyl-3-hydroxy-2-naphthoate (**32**) was then prepared using the

Friedel-Crafts reaction of *tert*-butylchloride with anhydrous AlCl_3 in anhydrous dichloromethane or 1,2-dichloroethane. After the reaction mixture was stirred at room temperature for two days compound **32** was obtained in 86% yield after column chromatographic purification using 0.5:9.5 ethyl acetate:hexanes as eluent (Scheme 2.8). Treatment of methyl-7-*tert*-butyl-3-hydroxy-2-naphthoate (**32**) with aqueous potassium hydroxide in THF, and stirring for 12 h at room temperature followed by acidification furnished **33** in 98% yield. When **33** was treated with POCl_3 in anhydrous toluene under reflux condition for three days, dehydration of **33** produced a mixture which included macrocycles **28** and **29**. The solvent toluene was removed under vacuum and the resulting crude product was purified using preparative thin layer chromatography to afford **28** and **29** in 10 and 15% yields, respectively (Scheme 2.8).

Single crystals of tetramer **27** were grown by dissolving the chromatographically-purified product in hot dichloromethane and left to slowly crystallize at room temperature. The X-ray structure of tetramer **27** revealed the formation of a *channel*-type clathrate containing two molecules of dichloromethane for each molecule of **27**. Its X-ray structure also showed the oxygen of the carbonyl group to be in a close contact distance of about 2.26 Å with one of the dichloromethane molecules. The conformation adopted by this macrocycle is the *1,3-alternate* type (Figure 2.5). This type of conformation has been seen in many different calix[4]arenes, and also with *tetra*-1-naphthoide **14** which was synthesized by Gerdil and Bernardinelli¹⁵ using 1-hydroxy-2-naphthoic acid under the same dehydration conditions, as well as, with some tetrasalicylides synthesized from 5-chlorosalicylic acid by Tanaka and co-workers¹⁴ under similar dehydration conditions.



Scheme 2.8. Synthesis of the *tri*- and *hexa*macrocycle lactones **28** and **29** respectively.

The X-ray structure analysis of the tetramer **27** (Figure 2.5), shows the packing structure has π - π stacking of the naphthyl rings between pairs of the macrocycles with close contact distances of 3.396 Å. This observation can possibly explain the difficulty encountered when trying to dissolve the purified recrystallized macrocyclic compounds in different solvents. Also, the X-ray structure revealed short contacts between the dichloromethane molecules and the macrocycle (**29**), including distances of 2.82, 2.94, and 3.37 Å.

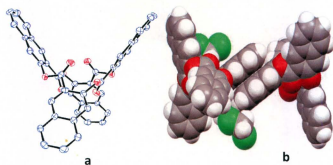


Figure 2.5. (a) X-ray structure of the *tetra-2-O-naphthoide* (**27**) (dichloromethane molecules omitted for clarity), and (b) Space-filling representation showing the close π - π stacking between a pair of molecules of the tetramer and the dichloromethane molecules.

Recrystallization of **28** from wet methanol/dichloromethane solution formed suitable single crystals for single-crystal X-ray crystallography. The X-ray structure showed the conformation of the macrocycle to be propeller-shaped with C_3 -symmetry, (Figure 2.6). The X-ray structure also revealed that a channel-type clathrate was formed with water, and that **28** existed as a racemic mixture of both *P* and *M* conformers. The X-ray structure revealed that the short contact distances are 2.62 and 2.62 Å between the oxygen of the carbonyl group and a hydrogen atom of the *tert*-butyl group.

As described previously, research focused on TOT has shown its ability to function as a chiral resolution agent for racemic mixtures, upon crystallization from solutions

containing racemic mixtures of the appropriate guest species. By analogy with TOT, it was hypothesized that **28** could also be expected to be a chiral resolution agent. Therefore, **28** was dissolved in a solution containing chiral compounds such as: (+)-1-(1-bromoethyl)-4-nitrobenzene, (+)-2-bromooctane and (-)-1-(3-methylphenyl)ethanol, by heating the solution and leaving the resulting solution to recrystallize at room temperature. Unfortunately, no chiral recognition properties for **28** were observed as previously seen by others using TOT with many chiral guests and racemic mixtures.

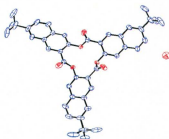


Figure 2.6. X-ray structure (ORTEP 30% thermal ellipsoids) of *tri-2-O-naphthoide* (**28**) containing a water molecule (hydrogen atoms omitted for clarity).

Crystallization of macrocycle hexamer **29** from methanol/chloroform also afforded suitable single crystals for X-ray crystallography. X-ray structure analysis revealed that the compound adopted a *1,3,5-alternate* conformation (Figure 2.7). Four chloroform molecules are contained within the cavities of the two alternate groups of naphthyl rings, as a *cage*-type clathrate. Also, important intermolecular short contacts of 3.39 and 3.17 Å are found between chlorine atoms of each pair of the “caged” chloroform molecules.¹⁸

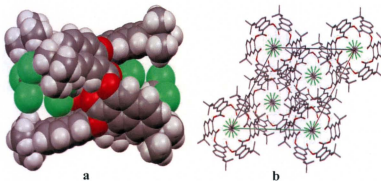


Figure 2.7. X-ray structure (a) space-filling and (b) packing diagram viewed along the *c* axis of *hexa-2-O-naphthoide* **29** showing the inclusion of four molecules of chloroform.

2.3 Conclusions

Macrocycles **27-28** were synthesized using 3-hydroxy-2-naphthoic acid (**32**) as a starting material, and POCl_3 as the dehydrating agent, under refluxing conditions. The $^1\text{H-NMR}$ spectra of these macrocycles revealed that they were all highly symmetrical in solution. Suitable crystals of all of the macrocycles **27-29** were also obtained and the single-crystal X-ray crystallography revealed macrocycles **27** and **29** to be in *1,3-* and *1,3,5-alternate* conformations, respectively, and that macrocycle **28** adopted a C_3 -symmetrical propeller-shaped conformation that is either *P* or *M*. The X-ray structure of **27** showed that it formed a *channel-type* clathrate with dichloromethane whereas that of **29** revealed it to have a *1,3,5-alternate* conformation and that it formed a *cage-type* clathrate containing four chloroform molecules.

2.4 Experimental section

2.4.1 Materials

All chemical reagents and solvents were purchased from Sigma-Aldrich or Fluka. ACS grade solvents purchased from Fisher were dried and distilled according to standard procedures.

2.4.2 General methods

All moisture- or air-sensitive reactions were conducted under argon (Ar), or nitrogen (N_2), in anhydrous solvents unless otherwise indicated. THF and toluene were dried over sodium hydroxide and then distilled over sodium metal. Dichloromethane was dried over phosphorus pentoxide and then distilled over calcium hydride. Organic solvents were evaporated under reduced pressure using a rotary evaporator. Flash chromatography was performed on Silicycle Silia-P Ultrapure Flash silica gel (40-63 μm), particle size 32-63 μm , pore size 60 Å. Preparative thin-layer chromatography plates (PLC) were made from SAI F-254 silica gel for TLC (particle size 5-15 μm). Thin-layer chromatography (TLC) was performed using percolated SAI F-254 silica gel plates layer thickness 200 μm .

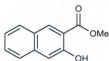
2.4.3 Instrumentation

Melting points (mp) were determined on a MEL-TEMP II apparatus and are uncorrected. Mass spectra of compounds were obtained using LCMS (HP series 1100) or GCMS (HP 5972 series II), MALDI-TOF MS (Voyager- DE PRO) instruments. MS data were presented as follows: m/z (relative intensity), assignment (when appropriate), and

calculated mass for the corresponding formulas. All ^1H - and ^{13}C NMR were recorded on a Bruker Avance 500 and 300 MHz spectrometers respectively, using CDCl_3 containing Me_4Si as an internal standard or otherwise noted. Chemical shifts for the ^1H NMR spectra are relative to the internal standard at 0.00 ppm. Data were reported as follows: chemical shift, multiplicity (s = singlet, d = doublet, dd = doublet of doublets, t = triplet, b = broad, h = heptet, m = multiplet), coupling constant (J , Hz), integration and assignment ($m\text{H-x}$, where m denotes the number of protons at position x in the molecule). ^1H - and ^{13}C NMR spectra were processed using "MestReNova" software. Chemical shifts for ^{13}C NMR spectra are relative to the solvent, 77.23 ppm for CDCl_3 . All of the X-ray structures were measured with a Rigaku Saturn CCD area detector equipped with a SHINE optic using $\text{Mo K}\alpha$ radiation, and were performed by Dr. L. N. Dawe, Dept. of Chemistry, Memorial University of Newfoundland.

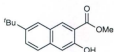
2.4.4 Experimental

Methyl-3-hydroxy-2-naphthoate (31).



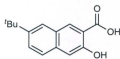
Methyl-3-hydroxy-2-naphthoate (31) was prepared as described by Ashram.¹⁹

Methyl-7-*tert*-butyl-3-hydroxy-2-naphthoate (32).



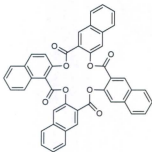
Methyl-7-*tert*-butyl-3-hydroxy-2-naphthoate (32) was prepared as described by Tran.²⁰

7-*Tert*-butyl-3-hydroxy-2-naphthoic acid (33).



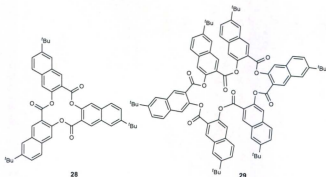
KOH (1.23 g, 22.0 mmol) was added to a solution of methyl-7-*tert*-butyl-3-hydroxy-2-naphthoate (32) (2.58 g, 10.0 mmol) in 4:1 THF:H₂O (60 mL). The reaction mixture was heated at reflux for 2 h. After that THF solvent was removed on a rotavap and the residue was acidified with 2M HCl_(aq) until the solution became acidic. The yellow precipitate was isolated by suction filtration, washed with distilled water (3 x 20 mL) and dried in an oven at 60 °C over night to give 33 (2.4 g, 98%) as a yellow solid: mp 226.2-227 °C; ¹H-NMR ((CD₃)₂CO): δ 1.38 (s, 9H), 7.28 (s, 1H), 7.72-7.74 (m, 2H), 7.90 (s, 1H), 8.61 (s, 1H), 10.72 (s, 1H, disappears upon D₂O addition); ¹³C-NMR (75.46 MHz, (CD₃)₂CO): δ 31.2, 35.2, 111.5, 114.9, 124.9, 126.8, 128.0, 129.3, 133.7, 137.3, 147.3, 157.5, 172.5.

Tetra-2-O-naphthoide (27).



POCl_3 (0.70 mL, 7.5 mmol) was added dropwise to a stirred solution of 3-hydroxy-2-naphthoic acid (**30**) (0.94 g, 5.0 mmol) in toluene. The reaction mixture was heated at reflux until the TLC showed that all of the starting material was consumed. The reaction mixture was cooled to room temperature and the off-white precipitate was filtered by suction filtration. The crude product was purified by preparative TLC, using a 40:10:50 dichloromethane:ethyl acetate:hexanes, solvent system to afford **27** (2.4 g, 70%), as a colorless solid: mp > 300 °C; $^1\text{H-NMR}$ (500 MHz, CDCl_3): δ 7.50-7.54 (m, 4H), 7.57-7.60 (m, 4H), 7.67 (s, 4H), 7.79 (d, $J = 8.0$ Hz, 4H), 8.07 (d, $J = 8.0$ Hz, 4H), 8.98 (s, 4H); $^{13}\text{C-NMR}$ (CD_2Cl_2): δ 121.7, 122.1, 127.4, 127.8, 129.8, 129.9, 131.4, 135.3, 136.6, 147.7, 163.9. HRMS (TOFEI) calcd. for $\text{C}_{44}\text{H}_{24}\text{O}_8$ 680.1471, found 680.1476. Crystal data for **27**: $\text{C}_{46}\text{H}_{28}\text{Cl}_4\text{O}_8$, $M = 850.48$, colorless prism (dichloromethane: methanol), space group $C2/c$ (no. 15), $a = 40.421(12)$ Å, $b = 11.179(3)$ Å, $c = 16.906(5)$ Å, $\beta = 95.979(6)^\circ$, $V = 7598(4)$ Å 3 , $Z = 8$, $D_c = 1.487$ g/cm 3 , $F_{000} = 3488.00$, $\mu(\text{Mo K}\alpha) = 3.699$ cm $^{-1}$, $T = 123(1)$ K, $2\theta_{\text{max}} = 61.8^\circ$, 62787 reflections collected, 7442 unique ($R_{\text{int}} = 0.0573$). Final GoF = 1.173, $R1$ ($I > 2.00\sigma(I)$) = 0.1071, $R(\text{all reflections}) = 0.1093$, $wR2(\text{all reflections}) = 0.3185$. The crystallographic data for compound **27** has been deposited with the Cambridge Crystallographic Data center, deposition no. 795679.

Tri- and hexa-2-O-naphthoide (28) and (29).



POCl_3 (0.7 mL, 7.5 mmol) was added dropwise to a stirred solution of 7-*tert*-butyl-3-hydroxy-2-naphthoic acid (**33**) (1.22 g, 5.0 mmol) in toluene. The reaction mixture was heated at reflux until all of the starting material, by TLC, was consumed. The reaction solvent was removed on a rotavap to give the crude product that was purified by preparative TLC, using a 50:50 hexanes:dichloromethane solvent system to afford **28** and **29** in yields 10 and 15%, respectively; **28**: mp >300 °C; $^1\text{H-NMR}$ (500 MHz, CDCl_3): δ 1.37 (s, 27H), 7.58 (s, 3H), 7.65 (dd, $J = 9.0, 1.5$ Hz, 3H), 7.71 (d, $J = 8.9$ Hz, 3H), 7.86 (d, $J = 1.5$ Hz, 3H), 8.93 (s, 3H); $^{13}\text{C-NMR}$ (CDCl_3): δ 31.1, 34.9, 120.8, 121.2, 124.3, 126.9, 128.2, 130.9, 134.3, 135.4, 146.5, 149.5, 164.1; HRMS (TOFEI) calcd for $\text{C}_{45}\text{H}_{42}\text{O}_6$ 678.2981, found 678.2991.

Crystal data for **28**: $\text{C}_{45}\text{H}_{42}\text{O}_6$ (H_2O), $M = 696.84$, colorless prism, space group $R\bar{3}$ (no. 148), $a = 15.849(5)$ Å, $c = 26.950(9)$ Å, $V = 5863(3)$ Å³, $Z = 6$, $D_c = 1.184$ g/cm³, $F_{000} = 2220$, $\mu(\text{Mo K}\alpha) = 0.79$ cm⁻¹, $T = 153(2)$ K, $2\theta_{\text{max}} = 61.8^\circ$, 25563 reflections collected, 2699 unique ($R_{\text{int}} = 0.0307$). Final GoF = 1.128, R_1 ($I > 2.00\sigma(I)$) = 0.0835, $R(\text{all})$

reflections) = 0.0839, $wR2(\text{all reflections}) = 0.2405$. The crystallographic data for compound **28** has been deposited with the Cambridge Crystallographic Data center, deposition no.795680.

29; mp >300 °C; $^1\text{H-NMR}$ (500 MHz, CD_2Cl_2): δ 1.26 (s, 54H), 7.34 (s, 6H), 7.47 (d, $J = 8.7$ Hz, 6H), 7.50 (dd, $J = 8.7, 1.4$ Hz, 6H), 7.76 (s, 6H), 8.78 (s, 6H); $^{13}\text{C-NMR}$ (CD_2Cl_2): δ 31.2, 35.1, 121.0, 121.6, 124.4, 127.0, 128.5, 131.0, 134., 135.4, 146.7, 149.9, 164.0. MS (MALDI-TOF) (m/z) 1395.54 $[\text{M} + \text{K}]^+$, 1379.56 $[\text{M} + \text{Na}]^+$.

Crystal data for **29**: $\text{C}_{90}\text{H}_{84}\text{O}_{12}$ (CHCl_3)₄, $M = 1835.04$, colorless prism, space group $R\bar{3}$ (no.148), $a = 16.6442(16)$ Å, $c = 27.928(3)$ Å, $V = 6700.3(12)$ Å³, $Z = 3$, $D_c = 1.364$ g/cm³, $F_{000} = 2856$, $\mu(\text{Mo K}\alpha) = 4.32$ cm⁻¹, $T = 153(1)$ K, $2\theta_{\text{max}} = 59.4^\circ$, 20958 reflections collected, 2622 unique ($R_{\text{int}} = 0.0291$). Final GoF = 1.908, $R1$ ($I > 2.00\sigma(I)$) = 0.1111, $R(\text{all reflections}) = 0.1113$, $wR2$ (all reflections) = 0.3914. The crystallographic data for compound **29** has been deposited with the Cambridge Crystallographic Data center, deposition no.795681.

Chiral resolution studies. The following chiral guests were examined with trimer **28** under ambient conditions with the solvent system(s) indicated: (+)-1-(1-bromoethyl)-4-nitrobenzene: (a) in a DCM/methanol/hexane solvent mixture, (b) in a CHCl_3 /methanol solvent mixture, and (c) in the neat chiral solvent; (+)-2-bromooctane: (a) in CS_2 , (b) in a DCM/methanol/*n*-hexane solvent mixture, and (c) in the neat chiral solvent; and (-)-1-(3-methylphenyl)ethanol: (a) in CS_2 , (b) in a DCM/ methanol/*n*-hexane solvent mixture, and (c) in a DCM/ hexane solvent mixture.

2.5. References:

1. (a) *Topics in Current Chemistry: Molecular Inclusion and Molecular recognition. Clathrates I, 140*; Weber, E.; Ed. Springer-Verlag; New York, 1987.
2. (a) Newman, A. C. D.; Powell, H. M. *J. Chem. Soc.* **1952**, 3747. (b) Lawton, D.; Powell, H. M. *J. Chem. Soc.* **1958**, 2339. (c) Arad-Yellin, R.; Green, B. S.; Knossow, M.; Tsoucaris, G. *J. Am. Chem. Soc.* **1983**, *105*, 4561.
3. Arad-Yellin, R.; Green, S. B.; Knossow, M. *J. Am. Chem. Soc.* **1980**, *102*, 1157.
4. (a) Gerdil, R.; Barchietto, G. *Tetrahedron Lett.* **1987**, *28*, 4685. (b) Gerdil, R.; Liu, H.; Bernardinelli, G. *Helv. Chem. Acta.* **1999**, *82*, 418. (c) Gerdil, R.; Liu, H.; Bernardinelli, G.; Jefford, C. W. *J. Am. Chem. Soc.* **1984**, *106*, 8004.
5. Gerdil, R.; Barchietto, G.; Jefford, W. C. *J. Am. Chem. Soc.* **1984**, *106*, 8004.
6. (a) Ripmeester, J. A.; Burlinson, N. W. *J. Am. Chem. Soc.* **1985**, *107*, 3713. (b) Gerdil, R.; Barchietto, G. *Helv. Chem. Acta.* **1994**, *77*, 691.
7. Steed, J. W., Atwood, J. L., Eds. *Supramolecular Chemistry*, 2nd ed. John Wiley and Sons, Ltd.; Chichester, UK, 2009.
8. Gerdil, R. *Top. Curr. Chem.* **1987**, *140*, 71.
9. Baker, W.; Gilbert, B.; Ollis, W. D. *J. Chem. Soc.* **1952**, 1443.
10. Gnami, M. J.; Barchietto, S. G.; Arad-Yellin, R.; Keehn, M. P. *J. Org. Chem.* **1991**, *56*, 4525 and references therein.
11. Gnami, M. J.; Green, B. S.; Arad-Yellin, R.; Vyas, K.; Levy, T. J.; Frolow, F. Keehn, P. M. *J. Am. Chem. Soc.* **1992**, *114*, 1915.
12. Gnami, M. J.; Keehn, M. P.; Green, B. S. *Tetrahedron Lett.* **1992**, *33*, 2883

13. Tanaka, K.; Hayashi, S.; Caira, M. R. *Org. Lett.* **2008**, *10*, 2119.
14. (a) Geridil, R.; Bernardinilli, G. *Acta Crystallogr.* **1985**, *C41*, 1523. (b) An incorrect structure for this compound is shown as "Figure 7.34" In *Supramolecular Chemistry*, 2nd ed.; Steed, J. W.; Atwood, J. L. Eds.; John Wiley & Sons, Ltd, Chichester, UK, 2009. (c) Suwinska, K.; Geridil, R. *Acta Crystallogr.* **1987**, *C43*, 898.
15. Harris, D. T.; Oruganti, S. R.; Davis, M. L.; Keehn, P. M.; Green, S. B. *Tetrahedron* **1987**, *43*, 1519.
16. Ollis, W. D.; Stoddart, J. F.; Sutherland, I. O. *Tetrahedron* **1974**, *30*, 1903.
17. Gnami, M. J.; Schurig, V.; Grosenick, H.; Green, B. S. *Tetrahedron Asymmetry* **1995**, *6*, 1499.
18. Al Hujran, T. A.; Dawe, L. N.; Collins, J.; Georghiou, P. E. *J. Org. Chem.* **2010**, *76*, 971.
19. Ashram, M. Ph.D. Dissertation, Memorial University of Newfoundland, 1997.
20. Tran, A. H. Ph.D. Dissertation, Memorial University of Newfoundland, 2006.

Chapter 3

Amide-based macrocycles derived from 4,4'-methylenebis(3-methoxy-2-naphthoyl chloride)

3.1 Introduction

3.1.1 Properties of anion receptors

Anions play many important roles in industry, in health and in the environment,^{1,2} and as a result, research devoted to designing efficient anion receptors is an ongoing process. The design of anion receptors however, is more complex than that of cation receptors since there are many prerequisites that have to be considered. For example, many anions are larger than their corresponding isoelectronic cations (Table 3.1), therefore the cavity size of any anion receptor must be large enough to accommodate the desired anion.^{1,2,3} Another factor that must be considered is that anions have a number of different geometries which makes the design of a general anion receptor challenging; for example, F⁻, Cl⁻, Br⁻ and I⁻ are spherical anions; N₃⁻, CN⁻ and SCN⁻ are linear anions; NO₃⁻, CO₃²⁻, R-CO₂⁻ are planar anions; as well, PO₄³⁻, SO₄²⁻, ClO₄⁻, are tetrahedral anions and (Fe(CN)₆)⁴⁻, Co(CN)₆³⁻ are octahedral anions. An additional consideration that must be taken is the pH of the medium since many anion species exist only in a narrow pH

range. For example, carboxylates, phosphates, and sulfates are all found as anions above pH 5-6 while below this pH range, these anions lose their negative charge.^{1,2}

Table 3.1. Radii of some cations and anions in Å.^{1b}

Cations	Radii (Å)	Anions	Radii (Å)
Na ⁺	0.95	F ⁻	1.36
K ⁺	1.33	Cl ⁻	1.81
Rb ⁺	1.48	Br ⁻	1.95
Cs ⁺	1.69	I ⁻	2.16

3.1.2 Application of anion receptors

Anion receptors play essential roles in many aspects of everyday life including environmental and medical application. They also have many different roles in chemical reactions since some act as catalysts, some as bases or some as nucleophiles. Using anion receptors to bind anions can increase the reactivity of those anions, and they may also be used to selectively separate anions from solutions containing different charged species.^{1,2,3}

From an environmental perspective, anion receptors can play important roles such as in the selective extraction and/or detection of nitrate anion in water which may be leaching into ground water and surface water from fertilizers used in agriculture. As another example, anion receptors may be used to extract the radioactive pertechnetate (TcO₄⁻) anion from nuclear wastes.^{1,2}

In the medical field, development and utilization of anion receptors which have the ability to bind and transport anions through cell membranes, can lead to advancements in medicine and provide better understanding and possible treatments to various medical conditions. An example of the role that anions can have is provided by cystic fibrosis which is a genetic disease caused when cells do not have the ability to control the transfer of chloride anions through cell membranes.^{4,3a}

3.1.3 Acyclic amide and sulfonamide-based receptors⁵

Synthetic secondary amides were first shown to be anion receptors by Pascal and co-workers in 1986.⁶ Since then, many other examples of secondary amides have been synthesized in order to study their anion receptor properties. In 1993, Reinhoudt and co-workers⁷ reported the synthesis of a series of triamides **1a-d** and trisulfonamides **2a-b** (Figure 3.1), in order to study their binding properties as receptors with different anion species. These receptors have shown selective binding to the phosphate anion in acetonitrile solution.

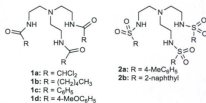


Figure 3.1. Structures of triamides **1a-d** and trisulfonamides **2a-b**.

In 1997, Crabtree⁸ synthesized the first simple anion receptor, **3a** that had the ability to bind chloride anion in deuterated dichloromethane (CD₂Cl₂) solutions. Due to the low solubility of **3a** in CD₂Cl₂, they also synthesized **3b** (Figure 3.2) from isophthaloyl dichloride and *p*-*n*-butylaniline. These anion receptors are simpler than Reinhoudt's and can be more easily prepared on a multigram scale. ¹H-NMR titration studies in CD₂Cl₂ revealed that receptors **3a** and **3b** have high affinities to selectively bind smaller halide anions and formed 1:1 host to guest complexes. ¹H-NMR titration studies of **3b** in CD₂Cl₂ with [PPh₄]X (X = halide) in CD₂Cl₂, showed stability constants of 6.1 × 10⁴ M⁻¹ for the chloride, 7.1 × 10³ M⁻¹ for the bromide and 4.6 × 10² M⁻¹ for the iodide salt.

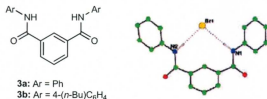


Figure 3.2. Isophthalamide structures **3a-b** and X-ray structure of **3a**:Br⁻ complex, reproduced with permission of ACS.⁸

Crystals of **3a** were grown by the addition of [PPh₄]Br to **3a** in dichloromethane solution. The X-ray crystal structure, (Figure 3.2), reveals the 1:1 complexation of the bromide anion with **3a**, with the receptor **3a** adopting a *syn-syn* conformation. The X-ray structure also showed that bromide ion coordinated above the plane of the centre of the two amide phenyl rings and formed hydrogen bonds with both amide groups. Br-H distances were found to be at 2.39 and 2.68 Å and the N-H angles were 166° and 172°.⁸

B. D. Smith and co-workers⁹ designed a new derivative of the isophthalamide receptor compound **4**, which adopted a *syn-syn* conformation. This new receptor was synthesized in two steps from 2-(aminophenyl)boronic acid and isophthaloyl dichloride. In this compound the two carbonyl groups interacted with the Lewis acidic boron atom which forced compound **4** to adopt the *syn-syn* conformation, as shown in Figure 3.3. This conformation is preferable for anion coordination due to the increasing of the amide group acidity. ¹H-NMR titration of **4** with tetrabutylammonium acetate in DMSO-*d*₆ revealed that the stability constant for acetate anion is $2.1 \times 10^3 \text{ M}^{-1}$ compared with $1.1 \times 10^2 \text{ M}^{-1}$ for the same solvent and salt, for compound **3a** which was synthesized by Crabtree and co-workers.⁸

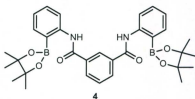


Figure 3.3. The structure of compound **4**.

3.1.4 Macrocyclic amide receptors

Hamilton and Choi¹⁰ synthesized the trisbiphenyl macrocyclic amides **5a-b**, (Figure 3.4). These compounds were synthesized in a stepwise protocol *via* Suzuki coupling of the appropriate 5-substituted-3-iodobenzoic acid with 3-nitrophenylboronic acid to give the corresponding 5-substituted-3'-nitro-3-biphenylcarboxylic acid, followed by reduction of the nitro group after first protecting the carboxylic acid group. The *C*₃-symmetric

macrocyclic receptor **5a** has three amide groups that can form hydrogen bonds with an anion. $^1\text{H-NMR}$ titration studies of macrocycles **5a** and **5b** with tetrabutylammonium tosylate in CDCl_3 containing 2% $\text{DMSO-}d_6$ revealed strong and selective binding of the tosylate anion in a 1:1 stoichiometric ratio and with association constants of $2.6 \times 10^5 \text{ M}^{-1}$ and $2.1 \times 10^5 \text{ M}^{-1}$ at 296 K, for **5a** and **5b**, respectively.

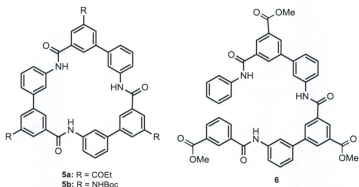


Figure 3.4. Cyclic triamide compounds **5a-b** and acyclic triamide compound **6**.

Hamilton¹⁰ compared the cyclic and acyclic trisamide receptors **5a** and **6** (Figure 3.4), respectively. The $^1\text{H-NMR}$ titration studies in 2% $\text{DMSO-}d_6/\text{CDCl}_3$, revealed that **5a** had a higher stability constant for anions when compared with the analogous acyclic receptor, **6**. The $^1\text{H-NMR}$ titration experiments at 296 K showed that the iodide and nitrate anions had stability constants of only 120 M^{-1} and 620 M^{-1} , respectively, for the acyclic triamide **6** whereas for the cyclic triamide **5a** the stability constants for both anions were $1.3 \times 10^5 \text{ M}^{-1}$ and $4.6 \times 10^5 \text{ M}^{-1}$ respectively. Similar results were found by

Jurczak and coworkers,¹¹ for many different anions, namely, that the cyclic receptors had higher stability constants than the acyclic ones, when comparison studies were done with several cyclic tetraamides and their acyclic tetraamide analogues.

Titration studies of receptor **5b** with tetrabutylammonium iodide in CDCl₃ containing 2% DMSO-*d*₆, showed that **5b** formed a 2:1 host to guest "sandwich"-type complex. The sandwich complex was formed when the number of equivalents of iodide anion was lower than, or equal to, 0.5 equivalents of compound **5b**. The ¹H-NMR spectra showed that the NH proton shifted up-field upon addition of the iodide anion until reached it *ca.* 0.5 equivalents. Thereafter, the chemical shifts changed to down-field indicating that the 2:1 complex switches to a 1:1 complex, as shown in Figure 3.5. In addition to the iodide anion, chloride and planar nitrate anions also formed 2:1 host to guest sandwich complexes at lower concentrations and 1:1 host to guest complexes at higher concentrations. The association constants for the formation of the iodide, chloride and nitrate complexes with cyclic amide **5a** were $1.1 \times 10^4 \text{ M}^{-1}$, $1.7 \times 10^2 \text{ M}^{-1}$ and $2.1 \times 10^3 \text{ M}^{-1}$, respectively, and the association constants for the iodide and chloride complexes with receptor **5b** were $9.0 \times 10^3 \text{ M}^{-1}$ and $1.9 \times 10^3 \text{ M}^{-1}$, respectively.¹⁰

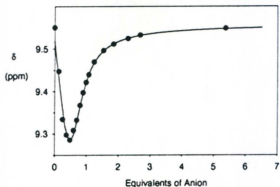
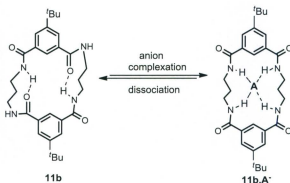


Figure 3.5. Changes in the amide ^1H -NMR chemical shift of macrocycle **5b** with increasing iodide anion concentration, reproduced with permission of ACS.¹⁰

Jurczak and co-workers^{11,12} synthesized a series of macrocyclic octa- (**7a-c** and **8a-c**), hexa- (**9a-b** and **10 a-c**), and tetraamides (**11a-d** and **12a-e**), using two methods. The first one, (Method A), was a high-dilution method which involved condensation of 5-*tert*-butylisophthalic acid dichloride (**13a**) with the appropriate diamine(s) under high dilution conditions in the presence of triethylamine in dichloromethane at room temperature, (Scheme 3.6). The second method, (Method B), involved the condensation of dimethyl-2,6-pyridinedicarboxylate (**13b**) using different diamines in methanol, at room temperature (Scheme 3.1). These macrocyclic amides have rigid cavities due to the intramolecular hydrogen bonds which exist between the nitrogen atoms of the pyridine rings and the hydrogen atoms on the amide groups.

are soluble in organic solvents in the presence of anions like fluoride, chloride, acetate, and dihydrogen phosphate as their tertbutylammonium salts. The X-ray structures of the free tetraamide macrocycles **11b-d** could explain the reasons why these types of compounds behaved in that way. In the solid-state, the macrocycles adopt a highly twisted conformation which is stabilized by two intramolecular NH--O hydrogen bonds (Scheme 3.2). Thus, when these tetramacrocycles **11a-d** dissolved in various organic solvents containing the tetrabutylammonium salts, it is likely due to the fact that these intramolecular hydrogen bonds are broken to form complexes with the anions, as shown in Scheme 3.2.¹¹



Scheme 3.2. Breakage in the intramolecular hydrogen bonds of tetraamide macrocycle **11b** upon addition of anions.

¹H-NMR titration studies of the pyridine receptor **12b** and the isophthalamide receptor **11b** revealed that the binding constant values of **12b** at the same temperature, 298K, and solvent are higher than those of **11b**, despite the fact that the pyridine lone pair

would have been expected to compete with the anion for hydrogen bonding with the NH groups of the amide groups.^{11d} For example, the binding constants for the pyridine receptor **12b** in DMSO-*d*₆ for chloride, acetate and bromide anions as the tertbutylammonium salts are 1930 M⁻¹, 3240 M⁻¹ and 150 M⁻¹, respectively, compared with the binding constants for the benzene receptor **11b** in DMSO-*d*₆ for the same anions which are 385 M⁻¹, 3066 M⁻¹ and 19 M⁻¹, respectively. Also, both of the receptors formed complexes with 1:1 host to guest stoichiometry.¹¹

Chmielewski and co-workers¹¹ also studied the effect of the sizes of the tetraamide macrocycles **12a-b** and **12d** in anion binding using ¹H-NMR spectroscopy. They found that the increase of the ring size from the 18-membered ring to the 20-membered ring, as in receptors **12a** and **12b**, respectively, showed a 30-fold increase in the binding constant of the anions. On the other hand, increasing the macrocycle receptor's size further reduced the binding constant toward anions. This result could be explained by the fact that the 24-membered macrocycle **12d** has greater flexibility and would suffer an "entropic penalty" for complexation.¹¹

Since the first reported synthetic cation receptor, a crown ether which was synthesized by Pedersen,¹³ there has been great interest in cation receptors due to the many roles that cations play. One of these cation receptors is a macrocyclic amide which showed the ability to bind various cations, as well as neutral molecules *via* hydrogen bonding.¹ Janusz Jurczak and co-workers¹⁴ reported the synthesis of the macrocyclic secondary amide-ether based receptors **14** and **15**, (Figure 3.6) in order to investigate

their complexation properties. The $^1\text{H-NMR}$ titration data obtained in CD_3CN revealed that **14** and **15** have the potential to form complexes with $\text{Ca}(\text{ClO}_4)_2$ in 1:1 and 2:1 ratios respectively. The X-ray structures of the complexes of **14** and **15** with Ca^{2+} showed that the calcium cation was located inside and outside respectively, of the cavities of the two macrocycles. This observation can be explained based on the fact that macrocycle **14** has a larger sized cavity than macrocycle **15**.

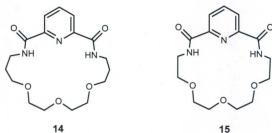
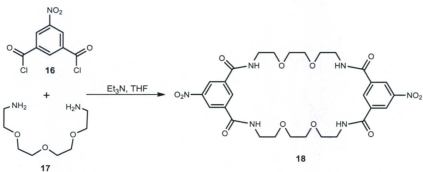


Figure 3.6. Structure of diamide macrocycles **14** and **15**.

A neutral macrocycle was synthesized by Ulrich Lünig,¹⁵ from an amidation reaction of 5-nitrosophthaloyl dichloride (**16**) with 1,8-diamino-3,6-dioxaoctane (**17**) in the presence of triethylamine in anhydrous THF to furnish the [2+2] macrocycle **18**, (Scheme 3.3). This compound contains three binding sites, namely, two amide groups and two diethylene glycol linkages on each of the opposite sides of the macrocycle. These have the ability to bind anions via hydrogen bonding, and cations via the ether oxygen atoms, respectively. The technique used to study the complexation properties of

macrocycle **18** is as follows: a solution of **18** in CDCl_3 containing 5% of $\text{DMSO-}d_6$ was added to NMR tubes each of which contained an excess of different individual powdered alkali and alkaline earth metal salts, and after mixing were left to stand for 12 h. Their $^1\text{H-NMR}$ spectra were then recorded and analyzed, based on the differences in chemical shifts between the $^1\text{H-NMR}$ spectra for the free macrocycle and for the macrocycle with the added alkali or alkaline earth salts. The $^1\text{H-NMR}$ spectra revealed that **18** selectively binds lithium chloride and calcium chloride over the other metal chlorides examined. Also, the authors speculated that the mass analyses of the NMR solutions of macrocycle **18** containing calcium chloride using electrospray ionization mass spectrometry (ESI-MS) suggested that **18** formed a "ternary" complex with CaCl_2 , although only the mass of the macrocycle plus CaCl^+ could be detected in the positive ion mode.

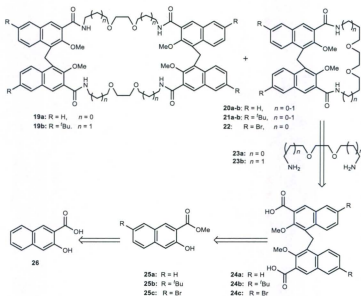


Scheme 3.3. Synthesis of macrocycle **18**.

3.2 Design and retrosynthetic analysis of di- and tetraamide macrocycles

3.2.1 Retrosynthetic analysis

A retrosynthetic analysis, as outlined in Scheme 3.4, suggested that tetraamide macrocycles **19a** and **19b** and diamide macrocycles **20a-b**, **21a-b** and **22** could be produced from the condensation of 1,8-diamino-3,6-dioxaoctane ("Jeffamine 148", **23a**) or 1,10-diamino-4,7-dioxadecane ("Jeffamine 176", **23b**) with 4,4'-methylenebis(3-methoxy-2-naphthoyl chloride) and their derivatives **24a-c** using Ulrich Lünig's procedure.¹⁵



Scheme 3.4. Retrosynthetic analysis of di- **20a-b**, **21a-b** and **22** and tetraamide macrocycles **19a-b**.

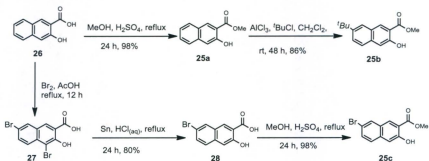
The intermediate **25a** was prepared as before, *via* esterification of 3-hydroxy-2-naphthoic acid (**26**) with methanol in the presence of a catalytic amount of H₂SO₄. Also, the corresponding intermediate **25b** was synthesized using a Friedel-Crafts reaction¹⁶ with *tert*-butylchloride on intermediate **25a**. Intermediate **25c** was prepared by bromination of compound **26** and then converting the resulting product to the ester. Bisnaphthylmethanes **24a-c** were synthesized by a direct condensation reaction of **25a-c** with paraformaldehyde.

3.3 Results and discussion

3.3.1 Synthesis of di- and tetraamide macrocycles

Treatment of 3-hydroxy-2-naphthoic acid (**26**), (Scheme 3.5), with methanol in the presence of a catalytic amounts of concentrated sulfuric acid and heating at reflux for 12 h furnished methyl-3-hydroxy-2-naphthoate (**25a**) in 98% yield as described in Chapter 2. Also described in Chapter 2, was the Friedel-Crafts alkylation¹⁶ of **25a** with *tert*-butylchloride, in the presence of anhydrous AlCl₃ in dichloromethane at ambient temperature formed **25b** in 86% yield after chromatographic purification. 3-Hydroxy-2-naphthoic acid (**26**) (Scheme 3.5), was also treated with bromine in acetic acid and then heated at reflux for 12 h to afford 4,7-dibromo-3-hydroxy-2-naphthoic acid (**27**) as an intermediate which was used in the next step without further purification. Selective removal of the C-4 bromine atom using tin and concentrated hydrochloric acid in acetic acid produced 7-bromo-2-hydroxy-3-naphthoic acid (**28**)¹⁷ in 80% yield. Subsequently,

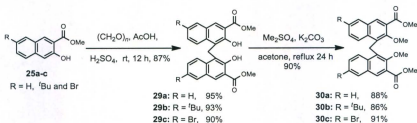
esterification of **26** with methanol and a catalytic amount of concentrated sulfuric acid provided compound **25c** in 98% yield.



Scheme 3.5. Synthesis of methyl-3-hydroxy-2-naphthoate and its derivatives **25a-b**.

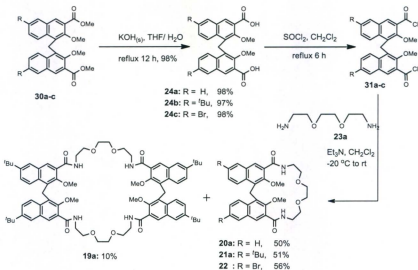
Compounds **30a-c** are the key intermediates for the synthesis of the tetraamide macrocycles **19a-b** and diamides **20a-b**, **21a-b** and **22a-c**. Therefore precursors **29a-c**, (Scheme 3.6), were synthesized from the corresponding previously synthesized methyl-3-hydroxy-2-naphthoate (**25a**) and their derivatives **25b-c**. When esters **25a-c** were treated with solid paraformaldehyde in acetic acid and a catalytic amount of sulfuric acid, compounds **29a-c** were produced in 95, 93 and 90% yields, respectively. Protection of the phenolic groups of **29a-c** was accomplished using potassium carbonate and four equivalents of dimethyl sulfate, to obtain **30a-c** in 88, 86 and 91% yields, respectively. Hydrolysis of the ester groups was achieved using three equivalents of potassium hydroxide in 1:1 THF/water under refluxing conditions, followed by acidification of the

reaction mixtures using 2M HCl_(aq) to form the corresponding compounds **24a-c** (Scheme 3.7).



Scheme 3.6. Synthesis of compounds **30a-c**.

Acid dichloride compounds **31a-c**, (Scheme 3.7), were prepared from the reactions of thionyl chloride with the corresponding acids **24a-c** in refluxing dichloromethane for 6 h. These products were then used directly without further purifications in the next step after the solvent was removed under reduced pressure. Tetraamide macrocycle **19a** and diamide macrocycles **20a**, **21a** and **22a**, (Scheme 3.7), were prepared by the reaction of 4,4'-methylenebis(3-methoxy-2-naphthoyl chloride) (**31a**) and their derivatives **31b-c** with a diamine (1,8-diamino-3,6-dioxaoctane, **23a**) at -20 °C, and also at room temperature in dichloromethane. These reactions were carried out in the presence of three equivalents of triethylamine to give [1+1] cyclocondensation products diamide macrocycles **20a**, **21a** and **22a** as the major products in 50, 51 and 56% yields, respectively. The tetraamide macrocycle **19a** was also produced in 10% yield by a [2+2] cyclocondensation also occurred, when compound **31b** reacted with 1,8-diamino-3,6-dioxaoctane (**23a**) under the same conditions.



Scheme 3.7. Synthesis of tetra- and diamide macrocycles **19a**, **20a**, **20a** and **22**.

The X-ray structures for diamide macrocycles **20a**, **21a** and **22** were successfully determined (Figure 3.7). The single crystal X-ray structure of **20a** shows it to be a “channel-type” clathrate,¹⁸ in which the methanol “bridges” the pair of molecules in the unit cell with short contact distances of 2.47 and 2.50 Å between a carbonyl oxygen and the methyl protons of the methanol, and the oxygen atom of the same methanol and the methyl protons of a methoxy group of the partner macrocycle. The structure of **21b** however, is not a channel-type clathrate and close contacts are only found between the *tert*-butyl groups of adjacent molecules. The structure of **22** does not form a clathrate with no close contact distances of note between the two molecules in the unit cell.

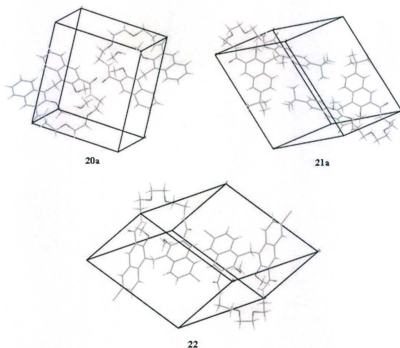


Figure 3.7. X-ray structures of macrocyclic amides **20a**, **21a** and **22**.

The [1+1] condensation of 4,4'-methylenebis(3-methoxy-2-naphthoyl chloride) (**31a**) and their derivatives **31b** with 1,10-diamino-4,7-dioxadecane (**23b**) at room temperature, or at $-20\text{ }^{\circ}\text{C}$ in the presence of triethylamine in dichloromethane, produces macrocyclic amides **20b** and **21b** (Figure 3.8); in 43 and 52% yields, respectively. Only the [2+2] condensation product **19b** (Figure 3.8), was observed when **31a** reacted with 1,10-diamino-4,7-dioxadecane (**23b**) in the presence of triethylamine at $-20\text{ }^{\circ}\text{C}$ and its X-ray structure was determined, as shown, in Figure 3.9. The macrocycle crystallizes as a *channel-type* clathrate with methanol in a 1:2 ratio. The unit cell consists of two

molecules of the macrocycle and four molecules methanol. H-bond distances of 1.85-1.88

Å between the H atoms of methanol and oxygen of carbonyl groups can be seen.

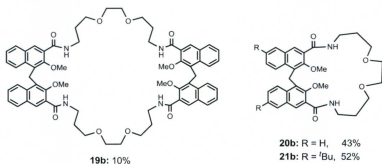


Figure 3.8. The structures of the tetra- **19b** and diamide macrocycles **20b** and **21b**.

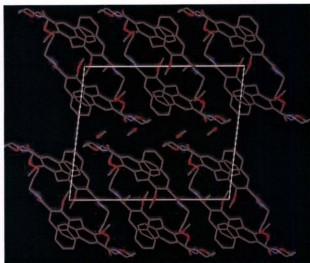
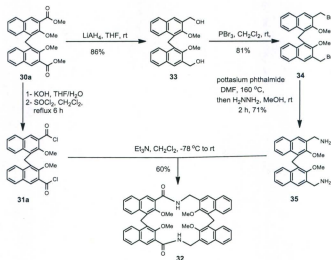


Figure 3.9. X-ray structure of tetraamide macrocycle **19b**.

3.3.2 Synthesis of diamide macrocycle 32 from reaction of bis(3-aminomethyl-2-methoxy-1-naphthyl)methane (35) with 4,4'-methylenebis(3-methoxy-2-naphthoyl chloride) (31a).

3.3.2.1 Retrosynthetic analysis and synthesis

The precursor 4,4'-methylenebis(methyl-3-methoxy-2-naphthoate) (**30a**), which was previously described, was used as a starting point to synthesize diamide macrocycle **32** (Scheme 3.8). Reduction of the ester groups of **30a** to the corresponding primary alcohol with LiAlH_4 in anhydrous THF at room temperature afforded bis(hydroxymethyl) **33** in 86% yield. Treatment of **33** with phosphorous tribromide in CH_2Cl_2 gave bis(3-bromo-methyl-2-methoxy-1-naphthyl)methane (**34**) in 81% yield. The diamino compound **35** was synthesized from **34** using Gabriel methodology (Scheme 3.8),¹⁹ which took place in two steps. The first step involved treatment of **35** with potassium phthalimide in DMF. After heating the reaction mixture for 5 h at reflux, the resulting product was used without further purification in the next step which involved the reaction with NH_2NH_2 in refluxing methanol for 12 h to produce the desired diamine **35** in 71% yield. The condensation reaction between diamine **35** and 4,4'-methylenebis(3-methoxy-2-naphthoyl chloride) (**31a**) in the presence of triethylamine as the acid scavenger in dichloromethane, furnished the bisamide macrocycle **32** in 60% yield after purification by column chromatography.

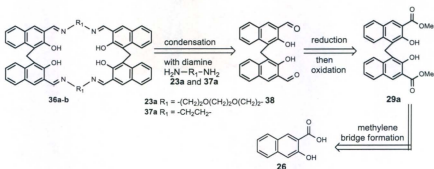


Scheme 3.8. Synthesis of macrocycle 32.

3.4 Attempts to synthesize Schiff macrocycles (36a-b).

3.4.1 Retrosynthetic analysis

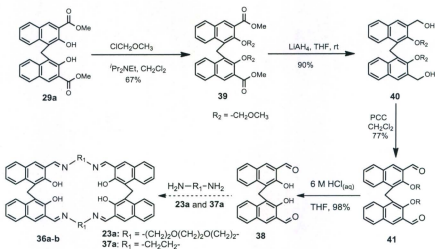
A retrosynthetic analysis as outlined in Scheme 3.9, indicates that cyclic Schiff base macrocycles **36a-b** could be synthesized from the condensation of diamine **23a** and **37a** and 4,4'-methylenebis(3-hydroxy-2-naphthaldehyde) (**38**). Intermediate **38** (Scheme 3.9) was obtained directly from **29a** previously closed (Scheme 3.6) via *O*-alkylation of the naphthol groups followed by reduction of the ester groups and subsequent mild oxidation of bis(hydroxymethyl) precursor (**40**).



Scheme 3.9. Retrosynthetic analysis for Schiff base macrocycles **36a-b**.

3.4.2 Results and discussion

The strategy used for the construction of the Schiff base macrocycles **36a-b** from dialdehyde **38** and diamines **23a** or **37a**, is shown in Scheme 3.10. The synthesis of intermediate **39** first involved protection of the naphthol groups of the compound **29a** using chloromethyl methyl ether (MOM-Cl) in anhydrous dichloromethane in the presence of Hünig's base (Pr_2NEt) and heating at reflux for 2 h to produce **39** in 67 % yield. Reduction of the ester groups of **39** was carried out using $LiAlH_4$ in anhydrous THF at room temperature, and the resulting bis(hydroxymethyl) **40** was oxidized with PPC in dichloromethane to give dialdehyde **41** in 71% yield. Finally, treatment of the chloromethyl methyl ether (MOM-Cl) protected dialdehyde **41** with four equivalents of 6 $M HCl_{(aq)}$ in THF furnished of the key intermediate **38** in 98% yield.



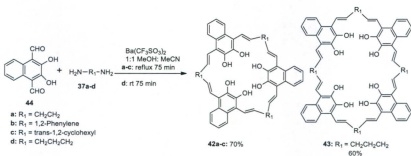
Scheme 3.10. Attempt to synthesize Schiff macrocycles 36a-b.

3.4.3 Attempted synthesis of Schiff macrocycles (36a-b).

The condensation reaction of 4,4'-methylenebis(3-hydroxy-2-naphthaldehyde) (**38**), and ethylenediamine (**37a**) and 1,8-diamino-3,6-dioxaoctane ("Jeffamine 148", **23a**) was carried out in high dilution conditions. In order to find the most suitable solvent system, several solvents were tried, such as: MeOH, CH₂Cl₂,²⁰ CH₃CN,²¹ 1:1 MeOH:THF, 2:1 CH₃CN:CHCl₃,²² and 1:1 MeOH:CH₂Cl₂. To keep the concentrations of the intermediate **38** low, solutions of diamines (**23a**) and (**37a**) were added dropwise slowly using a syringe pump to the solution of the dialdehyde (**38**) in the same solvent system, or vice-versa (Scheme 3.11). The reaction mixtures were stirred at room temperature for 2-4 d, or were heated at reflux temperature for 6-12 h. After TLC showed that the starting

materials were completely consumed under the conditions employed, the reactions were worked-up. The reactions, however, produced intractable and unidentified products which were not soluble in most of the common organic solvents. Oligomers or polymeric products were formed instead of the desired Schiff base macrocycles **36a-b**.

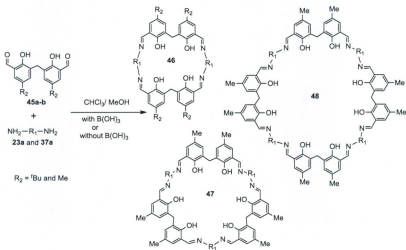
Reinhoudt and co-workers²³ reported using metal ions as templates for several macrocycle syntheses. They reported using Ba^{2+} to synthesize calixsalenes **42a-c** and **43** in yields 60-70%, *via* condensation of 1,4-diformyl-2,3-dimethoxynaphthalene (**44**) with diamines **37a-d**, (Scheme 3.11).



Scheme 3.11. The Reinhoudt syntheses of calixsalenes **42a-c** and **43**.

Based on the Reinhoudt procedures, the condensation reactions of 4,4'-methylenebis(3-hydroxy-2-naphthaldehyde) (**38**) and diamines **23a** or **37a** were reinvestigated using $Ba(ClO_4)_2$ as a source of the Ba^{2+} template, in several solvents (1:1 $CH_2Cl_2:CH_3CN$; 1:1 $CH_3CN:CHCl_3$ and/or 1:1 $MeOH:CH_3CN$). The reactions were conducted either at room temperature for 2-4 d, or heated at reflux temperatures for 4-12 h. After the TLC showed that the starting materials were completely consumed the

reaction mixtures were worked-up to give light brown precipitates which could not be identified because they were insoluble in most common organic solvents. Hisaeda and co-workers²⁴ reported the synthesis of other large macrocycles, *via* cyclocondensation of methylenebis(4,4'-alkyl-6,6'-salicylaldehyde) (**45a-b**) in the presence of boric acid²¹ as a template. Only, macrocycle **46** was formed without any template.²⁵ Macrocycles **46-48** (Scheme 3.11) were produced in MeOH/CHCl₃.



Scheme 3.12. Macrocycles **46-48** formed by Schiff base macrocyclizations.

When the same Hisaeda methodology was used for the reaction of **38** with diamines **23a** or **37a**, and stirring for 3 d at room temperature, a yellow precipitate was formed which could not be characterized due to the difficulty in purifying any compound from

the reaction mixture using column chromatography or preparative thin layer chromatography. No further attempts were carried out using this approach

3.5 Conclusions

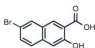
Several new diamide macrocycles **20a-b**, **21a-b** and **22** and tetraamide macrocycles **19a** and **19b** have been synthesized from reactions 4,4'-methylenebis(3-methoxy-2-naphthoyl chloride (**31a-c**) with 1,8-diamino-3,6-dioxaoctane (**23a**), or 1,10-diamino-4,7-dioxadecane (**23b**), and their structures were characterized. Suitable crystals of diamide macrocycles **20a**, **21a** and **22a** and tetraamide macrocycles **19a**, for a single-crystal X-ray crystallography were obtained and their structures were determined. The structure of macrocycle **20a** shows a "channel-type" clathrate, in which the methanol "bridges" the pair of molecules in the unit cell. The X-ray structure of **21a**, however, does not appear to be a clathrate at all and close contact distances are only found between the *tert*-butyl groups of adjacent molecules in the unit cell. The structure of **22** does not form a clathrate either with no close contact distances of note between the two molecules in the unit cell. All of these compounds however remain to be evaluated for their complexation potential since these had not been studied at the time of the writing of this thesis.

3.6 Experimental section

General methods, materials, and instrumentation used are identical to those described in Chapter 2. Huntsman Petrochemical Corporation was acknowledged for the generous gift of 1,8-diamino-3,6-dioxaoctane "Jeffamine® EDR 148" and 1,10-diamino-4,7-dioxadecane "Jeffamine® EDR 176".

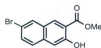
3.6.1 Experimental

7-Bromo-3-hydroxy-2-naphthoic acid (**28**).



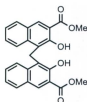
7-Bromo-3-hydroxy-2-naphthoic acid (**28**) was prepared as described by Murphy et al.¹⁷

Methyl-7-bromo-3-hydroxy-2-naphthoate (**25c**).



Methyl-7-bromo-3-hydroxy-2-naphthoate (**25c**) was prepared from **28** as described by Al Saraierh.²⁶

Bis(methyl-3-hydroxy-2-naphthoyl)methane (**29a**).

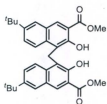


General procedure: A solution of **25a** (2.02 g, 10.0 mmol), paraformaldehyde (0.450 g, 15.0 mmol) and H₂SO₄ (0.5 mL) in glacial acetic acid (40 mL) was stirred at room temperature for 12 h.

After the reaction mixture was quenched by addition of water (80 mL), the resulting yellow precipitate was filtered by suction filtration, washed with brine

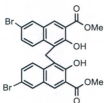
solution (2×20 mL) and then with water (2×15 mL). The product was dried under vacuum and was crystallized from methanol to give **29a** (1.98 g, 95%), as a light yellow solid: mp 247.1 °C; $^1\text{H-NMR}$ (500 MHz, CDCl_3): δ 4.04 (s, 6H), 4.95 (s, 2H), 7.17-7.20 (m, 2H), 7.33-7.37 (m, 2H), 7.68 (dd, $J = 8.8, 1.5$ Hz, 2H), 8.23(d, $J = 8.8$ Hz, 2H), 8.40 (s, 2H), 11.21 (s, br, 2H); $^{13}\text{C-NMR}$ (75.46 MHz, CDCl_3): δ 20.6, 52.7, 113.4, 121.9, 123.4, 124.3, 127.1, 129.0, 129.9, 131.5, 137.2, 153.3, 171.0; (+)-APCI MS m/z (relative intensity) 514.2 (M^+ , 33), 215.1(100).

Bis(methyl-7-*tert*-butyl-3-hydroxy-2-naphthoyl)methane (29b).



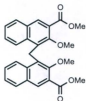
Using the general procedure for **29a**: A mixture of **25b** (5.16 g, 20.0 mmol), paraformaldehyde (0.900 g, 30.0 mmol) and H_2SO_4 (1.0 mL) in glacial acetic acid (60 mL) was stirred at room temperature for 12 h. The reaction mixture was then worked-up in a similar manner as in the general procedure used for compound **29a** to give the crude product which was purified by column chromatography (3:7 ethyl acetate:hexanes) to produce **29b** (4.91 g, 93%) as a yellow solid: mp 267.3-268.0 °C; $^1\text{H-NMR}$ (500 MHz, CDCl_3): δ 1.33 (s, 18H), 4.03 (s, 6H), 4.99 (s, 2H), 7.57 (d, $J = 9.0$ Hz, 2H), 7.79 (s, 2H), 8.08 (d, $J = 9.0$ Hz, 2H), 8.61(s, 2H); $^{13}\text{C-NMR}$ (75.46 MHz, CDCl_3): δ 20.5, 31.0, 34.4, 52.6, 113.3, 121.7, 124.2, 124.6, 127.1, 128.2, 131.4, 135.6, 145.8, 152.9, 171.2; (-)-APCI MS m/z (relative intensity) 528.3 (60), 527.3 (M^+ , 100), 271.1 (75).

Bis(methyl-7-bromo-3-hydroxy-2-naphthoyl)methane (29c).



Using the general procedure for the compound **29a**: The mixture reaction of **25c** (2.81 g, 10.0 mmol), paraformaldehyde (0.45 g, 15.0 mmol) and H_2SO_4 (0.5 mL) in glacial acetic acid (50 mL) was stirred at room temperature for 12 h. The reaction mixture was then worked-up in a similar manner as in the general procedure used for compound **29a** to give a crude product which was purified by washing the solid, with hot methanol. Compound **29c** (2.34 g, 90%) was a light yellow solid: mp 282.0-283.2 °C. Due to its low solubility in most of the organic solvents tested which prevented obtaining NMR spectroscopic data, **29c** was used directly in the next step.

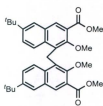
4,4'-Methylenebis(methyl-3-methoxy-2-naphthoate) (30a).



General procedure: Dimethyl sulfate (2.7 mL, 29 mmol) was added dropwise over a period of 30 min at room temperature to a mixture of **29a** (3.00 g, 7.21 mmol) and K_2CO_3 (5.97 g, 43.3 mmol) in anhydrous acetone (60 mL). The reaction mixture was heated at reflux for an additional 10 h. The reaction mixture was cooled to room temperature then the solvent was removed on a rotavap. The resulting product was dissolved in ether (40 mL) mixed with 10 mL of water and followed by addition of 2 M $\text{HCl}_{(\text{aq})}$ (10 mL). The ether layer was separated and then washed with aqueous 2 M NH_4OH (2×10 mL) in order to remove the excess dimethyl sulfate. The ether layer was washed with saturated NaCl (2×20 mL), water (2×20 mL) and dried over anhydrous MgSO_4 , filtered and the

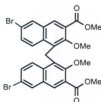
solvent removed on a rotavap. The resulting product was dried under vacuum, then purified by column chromatography (2:8 ethyl acetate:hexane) to give compound **30a** (1.94 g, 88%) as a cream-coloured solid: mp 133.5 °C (lit.²⁷ mp 117 °C); ¹H-NMR (500 MHz, CDCl₃): δ 3.79 (s, 6H), 3.98 (s, 6H), 5.00 (s, 2H), 7.30–7.33 (m, 2H), 7.73–7.40 (m, 2H), 7.75 (d, *J* = 8.5 Hz, 2H), 8.16 (d, *J* = 8.5 Hz, 2H), 8.2 (s, 2H); ¹³C-NMR (75.46 MHz, CDCl₃): δ 22.7, 52.4, 62.7, 123.9, 124.8, 125.3, 128.3, 129.4, 129.9, 130.2, 132.3, 135.3, 153.7, 166.9; (-)-APCI MS *m/z* (relative intensity) 443.1 (M⁺, 53), 212.1(100).

4,4'-Methylenebis(methyl-7-*tert*-butyl-3-methoxy-2-naphthoate) (**30b**).



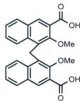
Using the general procedure for the compound **30a**: Dimethyl sulfate (2.7 mL, 28.0 mmol) was added dropwise over a period of 30 min at room temperature to a mixture of **29b** (4.00 g, 7.00 mmol) and K₂CO₃ (5.79 g, 42.0 mmol) in anhydrous acetone (60 mL). The reaction mixture was heated at reflux for an additional 10 h then the reaction mixture was worked-up as described in the general procedure used for **30a** to give the crude product which was purified by column chromatography (2:8 ethyl acetate:hexanes) to give **30b** (2.5 g, 86%) as a light yellow solid: mp. 193.3-194.0 °C; ¹H-NMR (500 MHz, CDCl₃): δ 1.31 (s, 18H), 3.87 (s, 6H), 4.00 (s, 6H), 4.98 (s, 2H), 7.51 (dd, *J* = 9.0, 2.0 Hz, 2H), 7.78 (d, *J* = 2.0 Hz, 2H), 8.15 (d, *J* = 9.0 Hz, 2.0 Hz, 2H), 8.27 (s, 2H); ¹³C-NMR (75.46 MHz, CDCl₃): δ 22.5, 31.0, 34.6, 52.3, 62.8, 123.6, 124.3, 124.6, 127.5, 129.8, 129.9, 132.5, 133.6, 147.9, 153.3, 167.0; (-)-APCI MS *m/z* (relative intensity) 555.3 (M⁺, 100).

4,4'-Methylenebis(methyl-7-bromo-3-methoxy-2-naphthoate) (30c).



Using the general procedure for the compound **30a**: Dimethyl sulfate (2.7 mL, 28.0 mmol) to a mixture of **29c** (4.00 g, 7.00 mmol) and K_2CO_3 (5.79 g, 42.0 mmol) in anhydrous acetone (60 mL), was added dropwise over a period of 30 min at room temperature. The reaction mixture was heated at reflux for an additional 8 h then the reaction mixture was worked-up as in the general procedure used for **30a** to give the crude product which was purified by column chromatography (15:85 ethyl acetate:hexanes) to give **30c** (2.2 g, 90%) as a light yellow solid: mp 216.5-217.6 °C; 1H -NMR (500 MHz, $CDCl_3$): δ 3.85 (s, 6H), 4.00 (s, 6H), 4.94 (s, 2H), 7.45 (dd, J = 10.0, 5.0 Hz, 2H), 7.89 (d, J = 5.0 Hz, 2H), 8.10 (d, J = 10.0 Hz, 2H), 8.14 (s, 2H); ^{13}C -NMR (75.46 MHz, $CDCl_3$): δ 22.5, 52.6, 62.9, 119.4, 125.0, 126.5, 130.3, 131.1, 131.1, 131.3, 1131.6, 133.5, 153.8, 166.4; (+)-APCI MS m/z (relative intensity) 605.1 (M^+ , ^{81}Br , ^{81}Br , 12), 603.1 (M^+ , ^{81}Br , ^{79}Br ; 24), 601.1 (M^+ , ^{79}Br , ^{79}Br , 14), 309.0 (100).

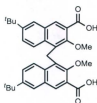
4,4'-Methylenebis(3-methoxy-2-naphthoic acid) (24a).



General procedure: Solid KOH (1.51 g, 27.0 mmol) was added to solution of **30a** (3.00 g, 6.76 mmol) in 4:1 THF:H₂O (60 mL). The reaction mixture was heated at reflux with stirring for 2 h. After THF solvent was removed on a rotavap, the residue was acidified with 2M HCl_(aq) until the solution became acidic (pH = 4). The yellow precipitate was isolated by suction filtration, washed several times with distilled water (3 x 10 mL) and methanol,

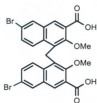
then dried in an oven at 60 °C overnight to give **24a** (2.75 g, 98%) as a yellow solid: mp 259.8-260.1 °C; ¹H-NMR (500 MHz, DMSO-*d*₆): δ 3.74 (s, 6H), 4.95 (s, 2H), 7.41-7.45 (m, 4H), 7.96 (d, *J* = 5.0 Hz, 2H), 7.18 (d, *J* = 5.0 Hz, 2H), 8.25 (s, 2H), 13.12 (s, br., 2H, disappears upon addition of D₂O); ¹³C-NMR (75.46 MHz, DMSO-*d*₆): δ 22.4, 62.3, 124.2, 125.2, 125.8, 127.8, 129.5, 129.6, 130.8, 134.3, 153.4, 167.6; (-)-APCI MS *m/z* (relative intensity) 515.1 (M⁺, 100), 215.1(25).

4,4'-Methylenebis(7-*tert*-butyl-3-methoxy-2-naphthoic acid) (**24b**).



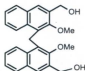
Using the general procedure of the compound **24a**: Solid KOH (1.12 g, 20.0 mmol) was added to the mixture containing **30b** (2.78 g, 5.00 mmol) in 4:1 THF:H₂O (60 mL). The reaction mixture was heated at reflux, with stirring, for 2 h, and then was worked-up as in the general procedure used for compound **24a** to give **24b** (2.56 g, 97%) as a yellow solid: mp 269.2-270.1 °C; ¹H-NMR (500 MHz, DMSO-*d*₆): δ 1.24 (s, 9H; H), 3.33 (s, br., OH disappears upon D₂O addition), 3.77 (s, 6H, CH₃), 4.85 (s, 2H), 7.48 (d, *J* = 10.0 Hz, 2H), 7.80 (s, 2H), 8.02 (d, *J* = 10.0 Hz, 2H), 8.19 (s, 2H); ¹³C-NMR (75.46 MHz, CDCl₃): δ 22.1, 30.8, 34.3, 62.4, 123.9, 124.2, 125.5, 126.6, 129.1, 129.4, 130.9, 132.4, 147.4, 152.8, 167.6; (-)-APCI MS *m/z* (relative intensity) 527.3 (M⁺, 100).

4,4'-Methylenebis(7-bromo-3-methoxy-2-naphthoic acid) (24c).



Using the general procedure for the compound **24a**: Solid of KOH (1.12 g, 20.0 mmol) was added to mixture of **30c** (3.00 g, 0.500 mmol) in 4:1 THF:H₂O (60 mL), then the reaction mixture was heated at reflux 2 h, and then was worked-up in similar way as in the general procedure used for **24a** to give a compound **24c** (2.8 g, 98%) as a yellow solid: mp 267.6-268.5 °C; ¹H-NMR (500 MHz, DMSO-*d*₆): δ 3.63 (s, 6H), 4.88 (s, 2H), 7.58 (dd, *J* = 9.5, 2.0 Hz, 2H), 8.11 (d, *J* = 9.5 Hz, 2H), 8.23 (s, 2H), 8.26 (d, *J* = 2.0 Hz, 2H), 13.22 (s, br., 2H, disappears upon D₂O addition); ¹³C-NMR (75.46 MHz, DMSO-*d*₆): δ 22.4, 62.1, 118.3, 126.4, 126.9, 129.8, 130.5, 130.8, 131.0, 132.6, 153.7, 167.3; (+)-APCI MS *m/z* (relative intensity) 592.0 ([M+H₂O]⁺, 38), 293.0 (100).

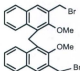
Bis(3-hydroxymethyl-2-methoxy-1-naphthyl)methane (33).



General procedure: To a mixture of LiAlH₄ (0.642 g, 16.9 mmol) in anhydrous THF (30 mL) under Ar at -20 °C was added dropwise, a solution of **30a** (5.00 g, 11.3 mmol) in THF (40 mL) over a period of 30 min. After the addition was complete, the cooling bath was removed and the reaction mixture was allowed to warm to room temperature. The mixture was stirred for an additional 4 h at room temperature and was worked-up by adding water dropwise until excess hydride decomposed, followed by the addition of 40 mL of aqueous 10% HCl. The organic layer was separated and washed with aqueous 5% NaHCO₃, followed by two 20 mL portions of aqueous saturated NaCl. After the solution

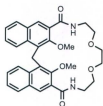
was dried over anhydrous MgSO_4 and filtered, the solvent was removed under reduced pressure to give a crude product which was purified by crystallization from diethyl ether and water to afford **33** (3.8 g, 86%), mp 90-91 °C (lit.²⁷ mp. 89-90 °C); $^1\text{H-NMR}$ (500 MHz, $\text{DMSO-}d_6$): δ 3.87 (s, 6H), 4.84 (d, $J = 5.0\text{Hz}$, 4H), 4.89 (s, br, 2H), 5.35 (s, 2H), 7.22–7.28 (m, 4H), 7.77 (d, $J = 5.0\text{ Hz}$, 2H), 7.83 (s, 2H), 8.11 (d, $J = 5.0\text{ Hz}$, 2H); $^{13}\text{C-NMR}$ (75.46 MHz, $\text{DMSO-}d_6$): δ 22.0, 58.7, 61.9, 124.2, 124.4, 125.2, 125.5, 127.8, 128.1, 130.7, 132.1, 135.3, 153.2.

Bis(3-bromomethyl-2-methoxy-1-naphthyl)methane (34).



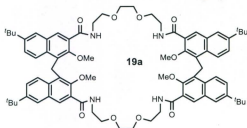
General procedure: To a solution of **33** (0.50 g, 1.3 mmol) in CH_2Cl_2 (30 mL), PBr_3 (0.40 mL, 4.1 mmol) KOH (1.12 g, 20.0 mmol) was added dropwise, via a syringe. The reaction mixture was stirred at room temperature for 4 h, and then worked-up by diluting the mixture with an additional 20 mL of CH_2Cl_2 and washing with water ($3 \times 15\text{ mL}$). After the solution was dried over MgSO_4 and filtered, the solvent was removed on a rotavap, the resulting crude crystallized from diethyl ether to give **34** (0.49 g, 74%) as a colourless solid: mp 186.7-187.2 °C, (lit.²⁷ mp.191-193°C); $^1\text{H-NMR}$ (500 MHz, CDCl_3): δ 4.05 (s, 6H), 4.80 (s, 4H), 4.95 (s, 2H), 7.25–7.27 (m, 4H), 7.63 (d, $J = 7.0\text{ Hz}$, 2H), 7.75 (s, 2H), 8.11 (d, $J = 7.0\text{ Hz}$, 2H); $^{13}\text{C-NMR}$ (75.46 MHz, CDCl_3): δ 23.1, 29.5, 63.00, 124.8, 125.1, 126.8, 128.3, 129.2, 130.4, 130.6, 131.0, 133.8, 153.7.

Macrocyclic diamide **20a**.

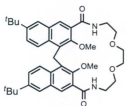


General procedure: To a mixture of **24a** (0.220 g, 0.529 mmol) in anhydrous dichloromethane (50 mL), thionyl chloride (SOCl₂) (4.0 mL, 53 mmol), was added dropwise, and the reaction mixture was heated at reflux for 6 h. The solvent was then removed on a rotavap, and the resulting product dried under vacuum for 30 min, dissolved in dry dichloromethane (60 mL) and cooled at -10 °C, under N₂. A solution of 1,8-diamino-3,6-dioxaoctane (0.080 mL, 0.53 mmol) and triethylamine (0.22 mL, 1.6 mmol) in dry dichloromethane (20 mL) was then added dropwise over a period of 30 min. After the addition was complete, the cooling bath was removed and the reaction mixture was allowed to warm to room temperature. The mixture was stirred for an additional 8 h at room temperature, then worked-up by adding water, followed by the addition of 15 mL of 10% HCl_(aq). The separated organic layer was washed with aqueous 5% NaHCO₃, aqueous saturated NaCl (2 × 20 mL) and water (2 × 20 mL). Then the organic layer was dried over anhydrous MgSO₄, filtered, and the solvent was removed on a rotavap. The crude product was purified by column chromatography (40:40:10:10 hexanes:-dichloromethane:methanol:ethyl acetate) to afford **20a** (49 mg, 50%) as a colorless solid: mp 286.8-287.3 °C; ¹H-NMR (500 MHz, CDCl₃): δ 3.59 (s, 6H), 3.61 (m, 8H), 3.72 (m, 4H), 7.42-7.49 (m, 4H), 7.91 (dd, *J* = 8.0, 1.6 Hz, 2H), 7.94 (s, br., 2H), 8.13 (d, *J* = 8.0 Hz, 2H), 8.43 (s, 2H); ¹³C-NMR (75.46 MHz, CDCl₃): δ 22.83, 39.70, 62.85, 70.32, 71.20, 123.68, 125.32, 126.71, 128.27, 128.68, 130.25, 130.57, 131.72, 134.30, 154.24, 168.82; (+)-APCI MS *m/z* (relative intensity) 529.3 (M⁺, 100).

Macrocyclic tetraamide **19a** and diamide **21a**.

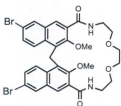


Using the general procedure for the macrocycle **20a**: SOCl_2 (3.2 mL, 44 mmol) was added to the mixture of **24b** (0.230 g, 0.436 mmol) in anhydrous dichloro-methane (50 mL) under N_2 at -10°C . After the reaction heated at reflux for 4 h the solvent was removed on a rotavap and the resulting product dried under vacuum for 30 min and dissolved in dichloromethane (60 mL). After that, a solution of 1,8-diamino-3,6-dioxaoctane (0.074 mL, 0.50 mmol) and triethylamine (0.21 mL, 1.5 mmol) in dry dichloromethane (10 mL) was added dropwise via a syringe pump, at -10°C over 30 min. The reaction mixture was stirred at room temperature for 8 h, then was worked-up in a similar way as was used in the general procedure for **20a** to give **19a** (37 mg, 10%) as a colorless solid: mp $> 300^\circ\text{C}$; $^1\text{H-NMR}$ (500 MHz, CDCl_3): δ 1.35 (s, 18H), 3.48 (s, 6H), 3.59 (s, 4H), 3.64 (m, br., 8H), 7.47 (dd, $J = 9.0, 1.8$ Hz, 2H), 7.77 (d, $J = 1.8$ Hz, 2H), 7.89 (d, $J = 9.0$ Hz, 2H), 8.02 (t, br., $J = 5.0$ 2H), 8.38 (s, 2H); $^{13}\text{C-NMR}$ (75.46 MHz, CDCl_3): δ 22.8, 31.1, 34.6, 39.6, 62.2, 69.8, 70.2, 123.7, 125.0, 125.9, 127.1, 128.7, 130.5, 132.6, 148.0, 152.7, 166.0; (+)-APCI MS m/z (relative intensity) 1281.8 (M^+ , 90), 971.7 (20), 671.5 (100), 641.5 (78), 346.3 (75); and give also **21a** (47 mg, 51%) as a colorless solid: mp $278.4\text{--}279.0^\circ\text{C}$; $^1\text{H-NMR}$ (500 MHz, CDCl_3): δ 1.39 (s, 18H), 3.57



(s, 6H), 3.59-3.61 (m, 8H), 3.71-3.73 (m, 4H), 7.57 (dd, $J = 9.0, 1.9$ Hz, 2H), 7.84 (d, $J = 1.9$ Hz, 2H), 7.98 (t, br., 2H), 8.07 (d, $J = 9.0$ Hz, 2H), 8.41 (s, 2H); $^{13}\text{C-NMR}$ (75.46 MHz, CDCl_3): δ 22.8, 31.2, 34.7, 39.7, 62.8, 70.4, 71.2, 123.5, 125.2, 126.5, 127.3, 128.4, 130.5, 131.6, 132.5, 148.0, 153.9, 165.9; (+)-APCI MS m/z (relative intensity) 641.5 (M^+ , 100).

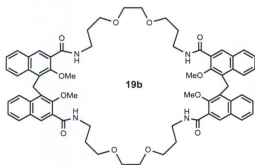
Macrocyclic diamide **22**.



Using the general procedure for the macrocycle **20a**: SOCl_2 (0.40 mL, 5.0 mmol) was added dropwise to the solution of **24c** (0.286 g, 0.500 mmol) in anhydrous dichloromethane (50 mL) under N_2 at -10 °C. After the reaction heated at reflux for 4 h, solvent was removed on a rotavap and the resulting product dried on vacuum for 30 min, dissolved in anhydrous dichloromethane (60 mL). After that, a solution of 1,8-diamino-3,6-dioxaoctane (0.074 mL, 0.50 mmol) and triethylamine (0.21 mL, 1.5 mmol) in dry dichloromethane (10 mL) was added dropwise via a syringe pump, at -10 °C over 30 min. The reaction was worked-up after the reaction mixture stirred at room temperature 8 h, in similar manner as in general procedure for **20a** to give **22** (0.192 g, 56%) as a colorless solid: mp 290-291 °C; $^1\text{H-NMR}$ (500 MHz, CDCl_3): δ 3.59-3.62 (m, 14H), 3.72 (m, 4H), 7.55 (dd, $J = 9.0, 1.8$ Hz, 2H), 7.84 (t, br., $J = 5.3$ Hz, 2H), 7.93 (d, $J = 9.0$ Hz, 2H), 8.05 (d, $J = 1.8$ Hz, 2H), 8.32 (s, 2H); $^{13}\text{C-NMR}$ (75.46 MHz, CDCl_3): δ 23.1, 39.9, 63.2, 70.5, 71.4, 119.6, 125.5, 128.2, 129.0, 131.0, 131.9, 132.0, 132.3, 132.8, 154.7, 165.5; (+)-APCI

MS m/z (relative intensity) 689.2 (M^+ , ^{81}Br , ^{81}Br , 68), 687 (M^+ , ^{81}Br , ^{79}Br , 100), 685.0 (M^+ , ^{79}Br , ^{79}Br , 65).

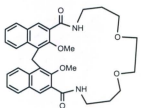
Macrocyclic tetraamide 19b and diamide 20b.



General procedure:

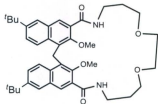
Thionyl chloride (SOCl_2) (4.0 ml, 53 mmol), was added dropwise to the mixture of **24a** (0.220 g, 0.528 mmol) in anhydrous dichloromethane (50 mL), the reaction mixture was heated at reflux for 6 h, then the solvent was removed on a rotavap, and the resulting product dried on vacuum for 30 min, dissolved in dry dichloromethane (60 mL) and cooled at $-10\text{ }^\circ\text{C}$ under N_2 atmosphere, then a solution of 1,10-diamino-4,7-dioxadecane (0.09 mL, 0.5 mmol) and triethylamine (0.21 mL, 1.5 mmol) in anhydrous dichloromethane (10 mL) was added dropwise via a syringe pump over period 30 min. After the addition was completed, the cooling bath was removed and the reaction mixture was allowed to warm to room temperature with stirring for 8 h. The reaction mixture was then worked-up by addition aqueous 10% HCl (15 mL). The reaction mixture was extracted, washed with aqueous 5% NaHCO_3 (15 mL), aqueous saturated NaCl (2×20 mL) and water (2×20), dried over anhydrous MgSO_4 , filtered and the solvent was removed on a rotavap to afford crude product which was purified by column

chromatography using (40:40:10:10 hexanes:dichloromethane:ethyl acetate:methanol) to afforded **19b** (51 mg, 13%) as a colorless solid: mp >300 °C; ¹H-NMR (500 MHz, CDCl₃): δ 1.72-1.77 (p, *J* = 6.0 Hz, 8H), 3.42-3.47 (m, 16H), 3.49 (s, 8H), 3.52 (s, 12H), 4.89 (s, 4H), 7.31 (t, *J* = 8.0 Hz, 4H), 7.36 (t, *J* = 8.0 Hz, 4H), 7.74 (d, *J* = 8.0 Hz, 4H), 7.77(t, *J* = 5.5 Hz, 4H), 8.05 (d, *J* = 8.5 Hz, 4H), 8.30 (s, 4H); ¹³C-NMR (75.46 MHz, CDCl₃): δ 23.1, 29.3, 37.9, 62.3, 69.7, 70.1, 124.0, 125.3, 126.9, 127.8, 129.0, 129.8, 130.5, 131.4, 134.7, 152.9, 165.9; MALDI-TOF *m/z* 1135.5 [M + Na]⁺.



Macrocycle **20b** (49 mg, 43%), was also obtained as a colorless solid: mp 276-277 °C; ¹H-NMR (500 MHz, CDCl₃): δ 1.88 (m, 4H), 3.37 (s, 6H), 3.65-3.70 (m, 12H), 4.95 (s, 2H), 7.42 (m, 4H), 7.91 (dd, *J* = 9.0, 5.0 Hz, 2H), 8.07 (dd, *J* = 9.0, 5.0 Hz, 2H), 8.47 (s, 2H), 8.51 (t, br., *J* = 5.0 Hz, 2H); ¹³C-NMR (75.46 MHz, CDCl₃): δ 23.1, 28.3, 40.0, 62.0, 69.2, 71.4, 123.8, 125.2, 127.0, 128.0, 129.1, 130.2, 130.6, 131.8, 134.3, 153.9, 165.5; MALDI-TOF *m/z* 579.2 [M + Na]⁺.

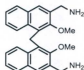
Macrocyclic diamide **21b**.



Using the general procedure for the compound **20b**: (SOCl₂) (4.0 ml, 53 mmol), was added dropwise to the mixture of **24b** (0.264 g, 0.500 mmol) in anhydrous dichloromethane (50 mL),

the reaction mixture was heated at reflux for 6 h, then the solvent was removed under reduced pressure, and the resulting product dried on vacuum for 30 min, dissolved in dry dichloromethane (60 mL) and cooled at $-10\text{ }^{\circ}\text{C}$ under N_2 atmosphere, then a solution of 1,10-diamino-4,7-dioxadecane (0.09 mL, 0.5 mmol) and triethylamine (0.21 mL, 1.5 mmol) in dry dichloromethane (10 mL) were added dropwise over period 30 min via a syringe pump. The reaction mixture was stirred at room temperature 8 h. And worked-up as the procedure compound to give compound **21b** (58 mg, 52%) as colorless solid: mp $268.2\text{--}269.0\text{ }^{\circ}\text{C}$; $^1\text{H-NMR}$ (500 MHz, CDCl_3): δ 1.38 (s, 18H), 1.88 (m, 4H), 3.37 (s, 6H), 3.65–3.70 (m, 12H), 4.90 (s, 2H), 7.52 (dd, $J = 9.0, 2.0$ Hz, 2H), 7.84 (d, $J = 2.0$ Hz, 2H), 8.02 (d, $J = 9.0$ Hz, 2H), 8.45 (t, $J = 5.0$ Hz, 2H), 8.53 (s, br., 2H); $^{13}\text{C-NMR}$ (75.46 MHz, CDCl_3): δ 23.1, 28.3, 31.1, 34.7, 39.9, 62.00, 69.2, 71.3, 123.7, 125.1, 126.7, 127.1, 128.8, 130.6, 131.8, 132.6, 147.8, 153.5, 165.7; (+)-APCI MS m/z (relative intensity) 669.6 (M^+ , 100).

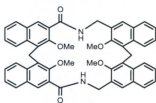
Bis(3-aminomethyl-2-methoxy-1-naphthyl)methane (35).



To a solution of compound **34** (2.56 g, 5.00 mmol) in DMF (100 ml), was added potassium phthalimide (2.33 g, 12.5 mmol). The reaction mixture was heated at reflux to $160\text{ }^{\circ}\text{C}$, with stirring for 6 h, and then the reaction mixture cooled to the room temperature and poured into cold water (200 mL). The resulting precipitate was filtered and dried by air to afford crude product (2.4 g, 83%) as a colourless solid, which was used in the next step without further purification. The suspension of crude product from the first step (2.43g,) and hydrate hydrazine (2.5 ml, 0.050 mol) in MeOH (30 mL) was heated at reflux with

stirring for 4 h after that, solvent was removed on a rotavap, the residue was dissolved in distilled water (50 mL) and extracted with CH_2Cl_2 (3×20 mL). The combined organic layers were washed with distilled water (2×20), brine (15 mL), water (20 mL), dried over anhydrous MgSO_4 and filtered. The solvent was removed on a rotavap, the residue was dried overnight on vacuum pump, then dissolved in ether and 6 M HCl was added, the aqueous layer washed with ether (3×10 mL), triethylamine (1.0 mL) was added with ether (20 mL), the organic layer dried over MgSO_4 , filtered, the solvent removed on a rotavap to afford **35** (1.4 g, 71%) as a brown solid: mp 138.4 °C; $^1\text{H-NMR}$ (500 MHz, CDCl_3): δ 1.77 (s, br., 4H), 3.88 (s, 6H), 4.07 (s, 4H), 4.94 (s, 2H), 7.21-7.27 (m, 4H), 7.61(s, 2H), 7.66 (d, $J = 8.0$ Hz, 2H), 8.17 (d, $J = 8.0$ Hz, 2H); $^{13}\text{C-NMR}$ (75.46 MHz, CDCl_3): δ 22.8, 43.0, 62.1, 124.6, 124.7, 125.5, 126.4, 128.0, 128.8, 131.3, 132.8, 136.1, 154.2; (+)-APCI MS m/z (relative intensity) 387.3 (M^+ , 100).

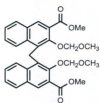
Macrocyclic diamide **32**.



To a mixture of **31a** (0.220 g, 0.529 mmol) in anhydrous dichloromethane (50 mL) was added dropwise SOCl_2 (0.40 mL, 5.3 mmol), the reaction mixture was heated at reflux for 6 h, then the solvent was removed on a rotavap, the resulting product dried under vacuum for 30 min, dissolved in dry dichloromethane (50 mL) under N_2 atmosphere at room temperature, then a solution of **35** (0.204 g, 0.529 mmol) in anhydrous dichloromethane (20 mL) was added dropwise over period 20 min. The mixture was stirred for an additional 4 h at

room temperature, after that, was worked up by addition water (10 mL); followed by addition aqueous 10% HCl (10 mL). Separated organic layer was washed with aqueous 5% NaHCO₃, aqueous saturated NaCl (2 × 10 mL) and water (20 mL). Then the organic layer dried over anhydrous MgSO₄, filtered and the solvent was removed on a rotavp to afford crude. The crude product was purified by column chromatography (hexanes:dichloromethane:methanol:ethyl acetate 40:40:10:10) to afforded **32** (0.24 g, 60%) as a colorless solid: mp 254.2°C; ¹H-NMR (500 MHz, CDCl₃): δ 2.18 (s, 4H), 3.17 (s, 6H), 3.82 (s, 6H), 4.93 (s, 2H), 4.94 (s, 2H), 7.40-7.44 (m, 2H), 7.80 (s, 2H), 7.83-7.85 (m, 2H), 7.91 (d, *J* = 8.0 Hz, 2H), 8.07-8.11 (m, 4H), 8.55 (s, 2H), 9.17 (s, 2H); ¹³C-NMR (75.46 MHz, CDCl₃): δ 22.62, 23.68, 41.61, 59.82, 63.10, 123.53, 123.74, 124.96, 125.1, 125.7, 126.7, 128.1, 128.8, 128.9, 129.0, 129.2, 130.3, 130.5, 131.0, 131.1, 132.0, 132.9, 134.5, 154.6, 155.6, 164.7; (+)-APCI MS *m/z* (relative intensity) 767.6 (M⁺, 100).

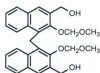
4,4'-Methylenebis(methyl-3-methoxymethoxy-2-naphthoate) (39).



To solution of **29a** (0.420 g, 1.01 mmol) in anhydrous CH₂Cl₂ (10 mL) at room temperature was added chloromethyl methyl ether (0.40 mL, 5.0 mmol) and diisopropylethylamine (0.38 mL, 5.0 mmol). The mixture was heated at reflux for 2 h. After that, the reaction mixture was worked-up by addition aqueous 1% HCl until the aqueous layer become acidic, separated organic layer was dried over Na₂SO₄, filtered and the solvent was removed on a rotavap to the resulting crude product was purified by recrystallized from methanol to afford compound **39** (0.34 g, 67%) as a light yellow solid: mp 139.4-

140.3 °C; ¹H-NMR (500 MHz, CDCl₃): δ 3.67(s, 6H), 4.00 (s, 6H), 5.14 (s, 2H), 5.20 (s, 4H), 7.28 (t, *J* = 8.0 Hz, 2H), 7.37 (t, *J* = 8.0 Hz, 2H), 7.72 (d, *J* = 8.0 Hz, 2H), 8.02 (d, *J* = 8.0 Hz, 2H), 8.27 (s, 2H); ¹³C-NMR (75.46 MHz, CDCl₃): δ 24.0, 52.4, 58.0, 101.9, 124.0, 125.0, 125.4, 128.4, 129.3, 130.0, 131.0, 132.3, 135.1, 150.7, 166.8; (+)-APCI MS *m/z* (relative intensity) 522.2 ([M+ H₂O]⁺, 15), 215.1 (25), 215 (100).

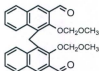
Bis(3-hydroxymethyl-2-methoxymethoxy-1-naphthyl)methane (40).



To the suspension of LiAlH₄ (0.254 g, 6.68 mmol) in anhydrous THF (30 mL) under Ar at -20 °C, a solution of **39** (0.843 g, 1.67 mmol) in THF (40 mL) was added dropwise over period 20 min.

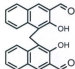
The reaction mixture was allowed to warm to room temperature and stirred for an additional 2 h. The reaction mixture was then worked-up by addition water dropwise, the organic layer was separated and washed with aqueous 5% NaHCO₃, aqueous saturated NaCl (2 × 20 mL), dried over anhydrous Na₂SO₄ and filtered, the solvent was removed under reduced pressure to give crude product which was purified by crystallized from diethyl ether to afford compound **40** (0.67 g, 90%), mp 82.1-83.3 °C; ¹H-NMR (500 MHz, CDCl₃): δ 3.21 (t, *J* = 6.0Hz, 2H), 3.64 (s, 6H), 4.85 (d, *J* = 5.6 Hz, 4H), 5.06 (s, 4H), 7.26-7.31 (m, 4H), 7.77(d, *J* = 8.0 Hz, 2H), 7.73 (s, 2H), 8.02 (d, *J* = 8.0 Hz, 2H); ¹³C-NMR (75.46 MHz, CDCl₃): δ 24.5, 57.7, 62.1, 100.8, 124.4, 125.0, 126.2, 128.4, 128.5, 128.7, 131.4, 133.0, 133.8, 152.5; (-)-APCI MS *m/z* (relative intensity) 447.3 (M⁺, 60), 403.1 (100).

4,4'-Methylenebis(3-methoxymethoxy-2-naphthaldehyde) (41).



To a stirred suspension of PCC (0.550 g, 2.55 mmol) in dichloromethane (30 mL) at room temperature was added a solution of **40** (0.520 g, 1.16 mmol) in dichloromethane (100 mL). The reaction mixture was stirred for a further 3 h, after that, was filtered through celite pad, washed with water (2×10 mL), dried over anhydrous Na_2SO_4 and filtered. After the solvent was removed on a rotavap, the crude product was purified by column chromatography (ethyl acetate:hexanes, 1:9) to afford **41** (0.40 g, 77%) as a yellow solid: mp 130.5-131.3 °C, (Lit.²⁸ mp 117-119 °C); $^1\text{H-NMR}$ (500 MHz, CDCl_3): δ 3.64 (s, 6H), 5.09 (s, 2H), 5.23 (s, 4H), 7.36 (t, $J = 8.0\text{Hz}$, 2H), 7.43 (t, $J = 8.0$ Hz, 2H), 7.85 (d, $J = 8.0$, 2H), 8.17 (d, $J = 8.0$ Hz, 2H), 8.30 (s, 2H); $^{13}\text{C-NMR}$ (75.46 MHz, CDCl_3): δ 23.4, 58.3, 102.1, 124.8, 125.8, 128.5, 129.3, 129.8, 130.4, 130.5, 132.2, 136.2, 152.6, 191.0; (-)-APCI MS m/z (relative intensity) 443.1 (M^+ , 100), 429.1 (75).

4,4'-Methylenebis(3-hydroxy-2-naphthaldehyde) (38).



To solution of compound **41** (0.232 g, 5.22 mmol) in THF (20 mL) was added dropwise aqueous 6 M HCl (1.0 mL), the reaction mixture stirred at room temperature 30 min. After that the reaction mixture was extracted with dichloromethane (2×20 mL), the organic layer washed with water (2×10 mL), dried over MgSO_4 , filtered and the solvent was removed on a rotavap the resulting crude product purified by crystallized from methanol to afford compound **38** (0.18 g,

98%) as a yellow solid: mp 141.5-142.8 °C; ¹H-NMR (500 MHz, DMSO-*d*₆): δ 4.79 (s, 2H), 7.31 (t, *J* = 7.5 Hz, 2H), 7.46 (t, *J* = 7.5 Hz, 2H), 7.96 (d, *J* = 7.5, 2H), 8.13 (d, *J* = 7.5 Hz, 2H), 8.43 (s, 2H), 10.24 (s, 2H), 11.12 (s, 2H); ¹³C-NMR (75.46 MHz, DMSO-*d*₆): δ 19.3, 120.8, 122.0, 123.4, 124.0, 127.4, 130.0, 130.5, 136.3, 136.8, 152.2, 198.0; (-)- APCI-MS *m/z* (relative intensity) 355.2 (M⁺, 100), 339.2 (55).

3.7. References:

1. (a) Steed, J. W.; Atwood, J. L. *Supramolecular Chemistry*; Wiley VCH: Weinheim, Germany, 2009. (b) Beer, P. D.; Gale, P. A.; Smith, D. K. *Supramolecular Chemistry*; Oxford University Press: Oxford, UK, 1999.
2. (a) Dietrich, B.; *Pure & Appl. Chem.* **1993**, *65*, 1457. (b) Bowman-James, K. *Acc Chem. Res.* **2005**, *38*, 671.
3. (a) Gale, P. A. *Chem. Soc. Rev.* **2010**, *39*, 3746. (b) Wenzel, M.; Hiscock, J. R.; Gale, P. A. *Chem. Soc. Rev.* **2012**, *41*, 480.
4. Gale, P. A. *Acc Chem. Res.* **2011**, *44*, 226.
5. *Structure and Bonding: Recognition of Anions, 129*. Mingos, D. M. P.; Ed.; Springer-Verlag: Berlin, 2008.
6. Pascal, R. A.; Spergel, Jr. J.; van Engen, D. *Tetrahedron Lett.* **1989**, *27*, 4099.
7. Valiyaveetil, S.; Engbersen, J. F. J.; Verboom, W.; Reinhoudt, D. *Angew Chem. Int. Ed.* **1993**, *32*, 900.
8. Kavalieratos, K.; de Gala, S. R.; Austin, D. J.; Crabtree, H. R. *J. Am. Chem. Soc.* **1997**, *119*, 2325.
9. Hughes, M. P.; Smith, B. D. *J. Org. Chem.* **1997**, *62*, 4492.
10. Choi, K.; Hamilton, A. D. *J. Am. Chem. Soc.* **2001**, *123*, 2456.
11. (a) Chmielewski, M. J.; Zielinski, T.; Jurczak, J. *Pure & Appl. Chem.* **2007**, *79*, 1087. (b) Chmielewski, M. J.; Jurczak, J. *Chem. Eur. J.* **2006**, *12*, 76052. (c) Chmielewski, M. J.; Jurczak, J. *Chem. Eur. J.* **2005**, *11*, 6080. (d) Chmielewski, M.; Szumna, A.;

- Jurczak, J. *Tetrahedron Lett.* **2004**, *45*, 8699. (e) Szumna, A.; Jurczak, J. *Eur. J. Org. Chem.* **2001**, 4031.
12. (a) Chmielewski, M.; Jurczak, J. *Tetrahedron Lett.* **2004**, *45*, 6007.
(b) Chmielewski, M. J.; Jurczak, J. *Tetrahedron Lett.* **2005**, *46*, 3085.
13. Pedersen, C. J. *J. Am. Chem. Soc.* **1967**, *89*, 153. (b) Pedersen, C. J. *J. Am. Chem. Soc.* **1967**, *89*, 7017.
14. (a) Gryko, D. T.; Piętek, P.; Pecak, A. Palys, M. Jurczak, J. *Tetrahedron* **1998**, *54*, 7505. (b) Szumna, A.; Gryko, D. T.; Jurczak, J. *J. Chem. Soc., Perkin Trans 2*, **2000**, 1553.
15. Eckelmann, J. Saggiomo, V.; Sönnichsen, F. D.; Lüning, U. *New J. Chem.* **2010**, *34*, 1247.
16. Tran, A. H. Ph.D. Dissertation, Memorial University of Newfoundland, 2007.
17. Murphy, A. R.; Kung, F. H.; Kung, M.-P.; Billings, J. *J. Med. Chem.* **1990**, *33*, 171.
18. Al Hujran, T. A.; Dawe, L. N.; Collins, J.; Georghiou, P. E. *J. Org. Chem.* **2010**, *76*, 971.
19. Campaigne, E.; Bosin, T. R. *J. Med. Chem.* **1968**, *11*, 178.
20. Kuhert, N.; Rossignolo, G. M.; Lopez-Periago, A. *Org. Biomol. Chem.* **2003**, *1*, 1157.
21. Akine, S.; Tanighuchi, T.; Nabeshima, T. *Tetrahedron Lett.* **2001**, *42*, 8861.
22. (a) Gallant, A. J.; Yun, M.; Sauer, M.; Yeung, C. S.; MacLachlan, M. J. *Org. Lett.* **2005**, *7*, 4827. (b) Gallant, A. J.; MacLachlan, M. J. *Angew. Chem. Int. Ed.* **2003**,

- 42, 5307. (c). Gallant, A. J.; Patrick, B. O.; MacLachlan, M. J. *J. Org. Chem.* **2004**, *69*, 8739.
23. Huck, W. T. S.; van Veggel, F. C. J. M.; Reinhoudt, D. N. *Recl. Trav. Chim. Pays-Bas* **1995**, *114*, 273.
24. Shimakoshi, H.; Takemoto, H.; Aritome, I.; Hisaeda, Y. *Tetrahedron Lett.* **2002**, *43*, 4809.
25. Shimakoshi, H.; Takayuki, K.; Aritome, I.; Hisaeda, Y. *Tetrahedron Lett.* **2002**, *43*, 8261.
26. Al Saraierh, H. Ph.D. Dissertation, Memorial University of Newfoundland, 2007.
27. Georghiou, P. E.; Li, Z.; Ashram, M.; Miller, D. O. *J. Org. Chem.* **1996**, *61*, 3865.
28. Chowdhury, S. Ph.D. Dissertation, Memorial University of Newfoundland, 2001.

Chapter 4

Attempts at the synthesis of calix[4]acenaphthenes and the synthesis of homooxalix[4]acenaphthenes

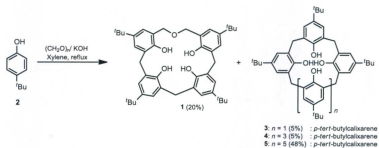
4.1 Introduction

4.1.1 Homooxalix[*n*]arenes

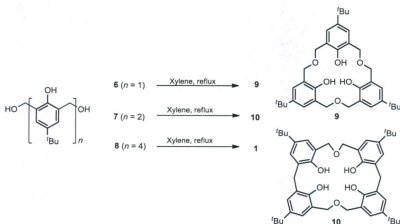
Homooxalixarenes in which the methylene bridges are partly or completely replaced by (-CH₂-O-CH₂-) bridges form an important sub-class of the calixarene family of cavity-containing macrocycles. The presence of the ether linkages in homooxalixarenes increases the ring size which, in turn, enhances the flexibility of macrocycles and therefore their conformations, and their molecular receptor binding properties.^{1,2} These macrocycles have been shown to have the ability to accommodate various types of cations and neutral molecules. The first example of an homooxalixarene, dihomooxalix[4]arene (**1**) was reported in 1979 by Gutsche and co-workers.³ The base-catalyzed condensation of *p*-*tert*-butylphenol (**2**) with paraformaldehyde in xylene under refluxing conditions was designed to synthesize calixarenes **3-5** (Scheme 4.1), and it produced **1** as a by-product.

Dhawan and Gutsche⁴ reported that thermal dehydration of the 2,6-bis(hydroxymethyl)-*p*-*tert*-butylphenol (**6**), the linear dimer **7** and the linear tetramer **8** of the 2,6-bis(hydroxymethyl)-*p*-*tert*-butylphenol in boiling xylene produced

homooxalixarenes **2**, **9** and **10**, respectively (Scheme 4.2). Hampton and co-workers⁵ reported the syntheses of a series of hexahomooxalix[3]arenes like **9** but having different *p*-substituents, using perchloric acid as a dehydrating agent, under high dilution conditions.

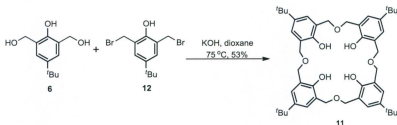


Scheme 4.1. Synthesis of the dihomoxalix[4]arene **1** and calixarenes **3-5**.



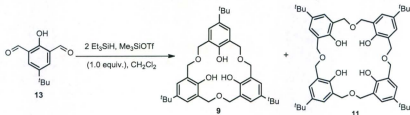
Scheme 4.2. Synthesis of oxalixarenes **1**, **9** and **10** via thermal dehydration.

Masci et al.⁶ reported a new way to synthesize homooxalixarenes via a Williamson ether coupling reaction. For example, the synthesis of octahomotetraoxalix[4]arene **11** was accomplished by reacting 2,6-bis(bromomethyl)-*p*-*tert*-butylphenol (**12**) with 2,6-bis(hydroxymethyl)-*p*-*tert*-butylphenol (**6**) in anhydrous dioxane under high dilution conditions in the presence of KOH as shown in Scheme 4.3.

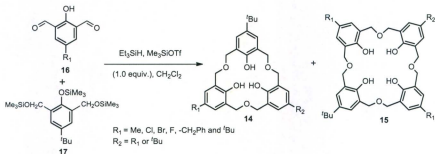


Scheme 4.3. Synthesis of octahomotetraoxalix[4]arene **11**.

A different method was developed by Komatsu's group to synthesize homooxalix[n]arenes **9** and **11** using the *one-pot* reductive homocoupling reaction of *p*-*tert*-butyl-2,6-diformylphenol (**13**) with triethylsilane in the presence of Me₃SiOTf in dry dichloromethane, (Scheme 4.4).⁷ Homooxalix[n]arenes **14** and **15** having different *p*-alkyl substituents were also synthesized by Komatsu's group *via* reductive heterocoupling reaction of the *p*-substituted-2,6-diformylphenol (**16**) with the tris(trimethylsilyl)ether of the *p*-substituted-2,6-bis(hydroxymethyl)phenol (**17**), in the presence of trimethylsilyltriflate (Me₃SiOTf) in dry dichloromethane (Scheme 4.5).⁷



Scheme 4.4. Synthesis of homooxalix[n]arenes **9** ($n=3$) and **11** ($n=4$).



Scheme 4.5. Synthesis of homooxalix[n]arenes **14** ($n=3$) and **15** ($n=4$).

4.1.2 Homooxalixnaphthalenes⁸

Georgiou and co-workers reported the synthesis of several new hexahomotrioxalix[3]naphthalenes⁹ (**18a-b** and **19**, Figure 4.1), tetrahomodioxalix[4]naphthalenes (**20a-b**, Scheme 4.6)¹⁰, hexahomodioxalix[4]naphthalene (**21**, Scheme 4.7)¹¹ from 3-hydroxy-2-naphthoic acid, and 1-naphthol. Also reported by the same group were the “homooxaisocalix[n]naphthalenes”, octahomotetraoxalix[4]naphthalenes¹² **22a-d** and

23a, **23d** (Scheme 4.8) or, and the macrocycle they named as "Zorbarene", all of which employed 2,3-dihydroxynaphthalene as the starting material.

Hexahomotrioxacalix[3]naphthalenes⁹ **18a-b** and **19**, (Figure 4.1), were synthesized using Fuji's wet $\text{CHCl}_3/\text{HClO}_3$ conditions by two different approaches. The first approach is a convergent route which involved the condensation cyclization reactions of the linear trimers **24a** and **24b** with **25a** and **25b**, respectively, to produce hexahomotrioxacalix[3]naphthalenes **18a** and **18b** and **19** (from **24a** and **25a**) in yields of 5 and 3% respectively. The second approach is a *one-pot* route which involved cyclocondensation of compounds **25a** and **25b** using Fuji's conditions to afford hexahomotrioxacalix[3]-naphthalenes **18a** and **18b** respectively, in yields of 5 and 6% respectively. ¹H-NMR titration experiments revealed that both hexahomotrioxacalix[3]naphthalenes **18a** and **18b** could accommodate C_{60} in benzene- d_6 or toluene- d_8 solutions. The single-crystal X-ray structure of ruby-red crystals isolated from these titration experiments revealed that **18b** formed a stable 2:1 supramolecular complex with C_{60} .¹³

Ashram et al.¹⁰ reported the synthesis of *endo*- and *exo*-tetrahomodioxacalix[4]-naphthalenes **20a** and **20b** starting from 2-naphthol and 3-hydroxy-2-naphthoic acid via Williamson ether-type reactions between intermediates, bis(hydroxymethyl)naphthalenes **26a** and **26b** and bis(bromomethyl)naphthalenes **27a** and **27b**, respectively (Scheme 4.6). The corresponding products, tetrahomodioxacalix[4]naphthalenes, **20a** and **20b**, were produced in 34 and 23% yields, respectively.

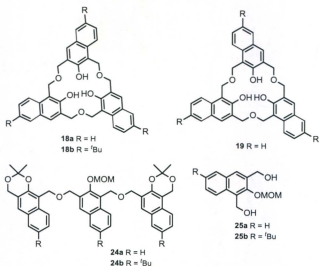
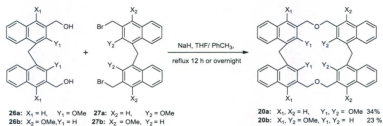
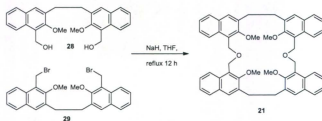


Figure 4.1. Hexahomotrioxacalix[3]naphthalenes **18a-b** and **19** and their precursors.



Scheme 4.6. Synthesis of tetrahomodioxacalix[4]naphthalenes **20a-b**.

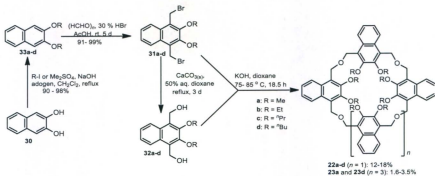
Using a similar method, hexahomodioxacalix[4]naphthalene **21** was synthesized in 15% yield via the base-mediated coupling reaction between the bis(hydroxymethyl)- and bis(bromomethyl)naphthalene intermediates **28** and **29** (Scheme 4.7).¹¹



Scheme 4.7. Synthesis of hexahomodioxacalix[4]naphthalene **21**.

The synthesis of the homooxaisocalix[*n*]naphthalenes **22a-d**, **23a** and **23d** reported by Georgiou and coworkers¹² started from 2,3-dihydroxynaphthalene (**30**). The two sets of intermediates, 1,4-bis(bromomethyl)-2,3-dialkoxy naphthalenes **31a-d** and 1,4-bis-(hydroxymethyl)-2,3-dialkoxy naphthalenes **32a-d** were prepared in excellent yields, via the corresponding 2,3-dialkoxy naphthalenes **33a-d**. Reaction of 1,4-bis(bromomethyl)-2,3-dialkoxy naphthalenes **31a-d** with 1,4-bis(hydroxymethyl)-2,3-dialkoxy naphthalenes **32a-d** in anhydrous dioxane in the presence of KOH, under refluxing conditions, afforded homooxaisocalix[4]naphthalenes **22a-d** and homooxaisocalix[6]naphthalenes **23a** and **23d** (Scheme 4.8).

¹H-NMR titration complexation experiments in CDCl₃ at 298 K revealed that **22a** and **22b** bound tetramethylammonium chloride (TMCl) in 1:1 ratios, and with association constants (K_{assoc}) of 1320 and 724, respectively. The X-ray structure of **22b** is shown in Figure 4.2 revealing that it adopted a “flattened partial-cone” conformation. The X-ray structure resembled four “anthromorphic dancers” holding hands and dancing in a ring formation so the compound was named “Zorbarene”.¹²



Scheme 4.8. Synthesis of homooxaisocalix[n]naphthalenes **22a-d**, **23a** and **23d**.

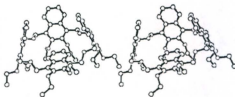


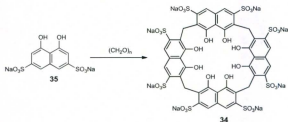
Figure 4.2. X-ray stereoview of **22b** showing its *flattened partial-cone* conformation, reproduced by permission of ACS.¹²

4.2 Synthesis of calix[n]acenaphthenes

4.2.1 Design of target structures

Since 1993, Georghiou and co-workers⁸ have been exploring the potential of using naphthalene-ring units to form naphthalene-based macrocyclic or calixarene-like compounds. Previously, only one example of a naphthalene ring-based calixarene which is linked by the 2- and 7- positions (i.e. *ortho* to the *peri*-positions) on each of the rings of the naphthalene units had been reported. Poh¹⁴ reported the highly water-soluble

“cyclotetrachromotropylenes” (**34**), (Scheme 4.9), formed from four chromotropic acid (“CTA” or 4,5-dihydroxy-2,7-naphthalenedisulfonic acid) units (**35**). Poh’s group published several host-guest complexation studies¹⁵ using **34**, although the structure of **35** has yet to be unequivocally established. Molecular modeling¹⁶ shows that **34** (Figure 4.3), to have a wider, but rather more shallow cavity than calix[4]naphthalenes synthesized from the 1- and 2-naphthol^{8,17} units studied by the Georghiou group. A potentially deeper-cavity calixnaphthalene was envisioned using 5,6-dihydroxyacenaphthene (**37**) as the subunit to form an analogous “calix[4]acenaphthene” **36**, (Scheme 4.10). The synthetic efforts towards such acenaphthene-ring targets form the main subject of this Chapter.



Scheme 4.9. Cyclotetrachromotropylenes (**34**) derived from chromotropic acid (**35**).

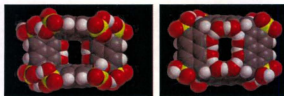
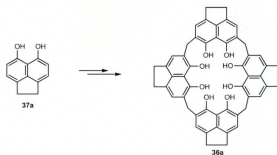


Figure 4.3. Computer-generated structure of **34**: (Left: Top view) and (Right: Side view) respectively, showing the flattened 1,3-alternate-type shallow cavity conformation.¹⁶



Scheme 4.10. Calix[4]acenaphthene (**36a**) derived from 5,6-dihydroxyacenaphthene (**37a**).

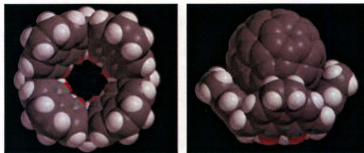
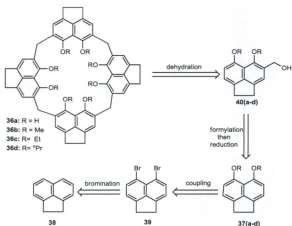


Figure 4.4. Computer-generated structures of calix[4]acenaphthene (**36a** *Left- top view*) and of its 1:1 C₆₀ complex (*Right-side view*) respectively.¹⁶

Computer-assisted molecular modeling study using the Spartan'10 program¹⁶ showed that a calix[4]acenaphthene (**36a**) can adopt a bowl ("calix") shape, as shown in Figure 4.4. The modeling also showed **36a** to be an attractive candidate as a receptor to accommodate fullerenes C₆₀ (Figure 4.4) and/or C₇₀ via π - π van der Waals supramolecular interactions between the electron-rich acenaphthene unit and the electron-poor fullerenes.

4.2.2 Retrosynthetic analysis

For the synthesis of calix[*n*]acenaphthenes composed from *n*=3-6 acenaphthene subunits linked by methylene bridges, two strategies were considered. The key steps are outlined in retrosynthetic Scheme 4.11. The first approach is a “one-pot” strategy using various Lewis¹⁸ or Bronsted acids to catalyze the direct cyclocondensation of 5,6-dihydroxy- or dialkoxyacenaphthenes (with paraformaldehyde, or 1,3,5-trioxane, to form the corresponding calix[4]acenaphthene (**36a-d**, R = H or alkyl). The second strategy involves the self-cyclocondensation¹⁹ of 4-hydroxymethyl-5,6-dialkoxyacenaphthenes **37b-d**, using various Lewis acids. Acenaphthene (**38**) itself was chosen as the starting compound for the synthesis *via* 5,6-dibromoacenaphthene (**39**) and 5,6-dialkoxyacenaphthenes, **37b-d**, of the key intermediates 4-hydroxymethyl-5,6-dialkoxyacenaphthenes **40b-d**.



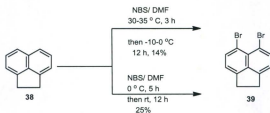
Scheme 4.11. Retrosynthetic analysis of calix[4]acenaphthenes **36a-d**.

Synthesis of **39** from acenaphthene using Kasai's²⁰ procedure, followed by its conversion to 5,6-dialkoxyacenaphthenes **37a-d** utilizing a modified Ullman coupling²¹ procedure, could afford **37a-d**. After formylation using TiCl_4 and dichloromethylmethyl ether²² **37a-d** could give the corresponding 4-formyl-5,6-dialkoxy-acenaphthenes **41a-c**, which are reduced to alcohols **40b-d**.

4.3 Results and discussion

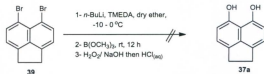
4.3.1 Synthesis of functionalized acenaphthenes

Using Tanaka's²⁰ procedure, acenaphthene was treated with *N*-bromosuccinimide (NBS) which was added as a solution in DMF over 3 h at 30-35 °C. The resulting mixture was then cooled to 0 °C and allowed to stand for 12 h to afford 5,6-dibromoacenaphthene (**39**) in yields of 14% as a yellow solid. Using a modified procedure,²³ in which the solution of acenaphthene in DMF was first cooled to 0 °C and then the NBS added in DMF solution over a 5 h period, followed by stirring at room temperature for 12 h, **39** could be consistently produced in higher yields (25%) than those reported by Tanaka (Scheme 4.12).



Scheme 4.12. Synthesis of 5,6-dibromoacenaphthene (**39**).

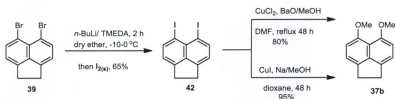
Attempts to synthesize 5,6-dihydroxyacenaphthene (**37a**) are shown in Scheme 4.13. Treatment of **39** with three equivalents of *n*-butyllithium (*n*-BuLi) and three equivalents of tetramethylethylenediamine (TMEDA) in anhydrous diethyl ether at -10-0 °C, was followed by addition of trimethylborate at 0-10 °C, hydrogen peroxide, and then acidification with aqueous 6 M HCl. A dark intractable product was obtained only, which could not be purified or characterized. An alternative route therefore was necessary since the direct hydroxylation could not be effected under various conditions tried.



Scheme 4.13. Attempted synthesis of 5,6-dihydroxyacenaphthene (**37a**).

When the same procedure described above for the formation of the 5,6-dilithioacenaphthene intermediate in dry ethyl ether was used, but was instead quenched with three equivalents of solid iodine, 5,6-diiodoacenaphthene (**42**)²⁰ could be obtained in 60% yield (Scheme 4.14). After much experimentation, 5,6-dimethoxyacenaphthene (**37b**) was successfully obtained using a modified Ullmann methodology,²¹ in which **42** was reacted with copper (I) iodide, and sodium methoxide, freshly prepared from sodium metal and methanol, in a solvent mixture of methanol and 1,4-dioxane. The mixture was heated at reflux for 24 h and then the methanol was distilled off, followed by heating the resulting mixture at reflux for a further two days. Using this protocol, **37b** was obtained

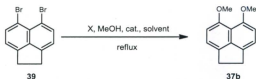
in 95% yield (Scheme 4.14). Another approach to the synthesis of **37b** was conducted using copper (II) chloride and barium oxide²⁴ as the base instead of sodium metal, to generate the methoxide from the methanol in a mixed DMF-methanol solvent with heating at reflux over 48 h. In this way, **37b** was produced in 80% yields (Scheme 4.14).



Scheme 4.14. Synthesis of 5,6-diiodo- and 5,6-dimethoxyacenaphthene **42** and **37b**.

This second method had several shortcomings: firstly, a large amount of DMF was needed to dissolve both the copper (II) chloride and the 5,6-dibromoacenaphthene; secondly, a large amount of foaming was produced during the heating of the reaction mixture at reflux. These two problems therefore required a large reaction flask in order to prepare **37b** on a multigram scale making this method unsatisfactory. The synthesis of **37b** from **42** also suffered from several other drawbacks; among these, a large amount of the dry ether solvent, a large amount of *n*-BuLi and iodine, as well as long reaction times were all needed to prepare **42** in only a moderate yield. As a result of the difficulties encountered for synthesizing synthetically-useful quantities of 5,6-dimethoxyacenaphthene, a re-investigation was undertaken for the use of 5,6-dibromoacenaphthene (**39**), instead of **42**, as the starting material in a modified Ullmann coupling and these experiments (Scheme 4.15) are shown in Table 4.1.

Different copper halides such as CuBr, CuCl, CuI, and CuCl₂ have all been used in many instances to synthesize alkylaryl ether compounds using solvents such as DMF, NMP, dioxane, DMSO, collidine and toluene.²⁵ In our hands, when CuI and sodium methoxide in DMF or in collidine as solvents (Table 4.1, Entries 3 and 4) were used under reflux heating conditions **37b** could be produced in yields 61 and 64% respectively. The yields could be improved to 84 and 80% respectively, using CuCl instead, and DMF or collidine as solvents (Entries 9 and 10, Table 4.1). Under microwave condition (Entry 5, Table 4.1) without solvent produce **37b** in yield 64%. With dioxane as solvent with CuI only the starting material was recovered after heating at reflux for 3 d (Table 4.1, Entry 2). When dioxane was used with CuCl under the same reaction conditions however, **37b** was obtained in 95% yield (Entry 8, Table 4.1). With pyridine as solvent with either CuI or CuCl under the same reaction conditions, only unreacted starting material and acenaphthene itself, presumably the reductive product of **39** was recovered (Entries 1 and 11, Table 4.1). A possible explanation²⁵ is that the pyridine forms a strong complex with the copper thus decreasing the reactivity of the copper reagent in the reaction.

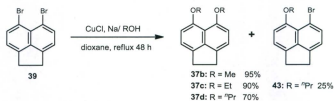


Scheme 4.15. General reaction scheme experiments summarized in Table 1.

Table 1. Cu-catalyzed coupling of **39** with NaOMe to form **37b**.

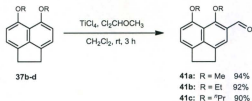
Entry	X/ MeOH	Catalyst	MeOH/ Solvent	Time (h)	Yield (%)
1	Na	CuI	pyridine	72	NR
2	Na	CuI	dioxane	72	NR
3	Na	CuI	DMF	48	61
4	Na	CuI	2,4,6-collidine	48	64
5	Na	CuI	microwave no solvent	4	60
6	CaO	CuCl ₂	DMF	48	NR
7	BaO	CuCl ₂	DMF	48	35
8	Na	CuCl	dioxane	48	95
9	Na	CuCl	2,4,6-collidine	48	80
10	Na	CuCl	DMF	72	84
11	Na	CuCl	pyridine	48	NR

The use of CuCl and dioxane under the same reaction conditions was therefore found to be the best choice of reagent and reaction conditions, and was used with *in situ*-generated sodium methoxide, sodium ethoxide and sodium *n*-propoxide to form the corresponding 5,6-dialkoxyacenaphthenes **37b-d** in good to excellent yields of 95, 90 and 70%, respectively, as summarized in Scheme 4.16. With *n*-propoxide, 5-bromo-6-*n*-propoxy-acenaphthene (**43**) was also formed, possibly as a result of steric hindrance toward displacement of the second bromide by another propoxide nucleophile by the bulky peri-substituent propoxy group.



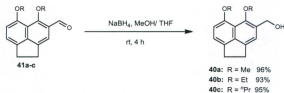
Scheme 4.16. Synthesis of 5,6-dialkoxyacenaphthenes **37b-d**.

The target intermediates, 4-formyl-5,6-dialkoxyacenaphthenes **41a-c** were afforded from the corresponding 5,6-dialkoxyacenaphthenes **37b-d** via Reiche formylation reactions.²² Treatment of each of the 5,6-dialkoxyacenaphthenes **37b-d** with 1.5 equivalents of titanium(IV) chloride and one equivalent of dichloromethyl methyl ether in dry dichloromethane with stirring at room temperature for 3 h gave the corresponding 4-formyl-5,6-dialkoxyacenaphthenes **41a-c** in 90-95% yields (Scheme 4.17).



Scheme 4.17. Synthesis of 4-formyl-5,6-dialkoxyacenaphthenes (**41a-c**).

Reduction of each of the precursors **41a-c** in the presence of sodium borohydride in 1:1 methanol/THF, with stirring for 4 h, yielded the corresponding products 4-hydroxymethyl-5,6-dialkoxyacenaphthenes **40a-c** in yields of 91-96% (Scheme 4.18).

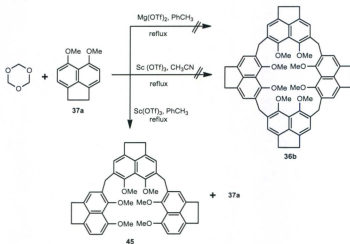


Scheme 4.18. Synthesis of 4-hydroxymethyl-5,6-dialkoxyacenaphthenes (**40a-c**).

4.3.2 Attempted synthesis of calix[4]acenaphthene

With synthetically useful amounts of **37b** in hand, the synthesis of the target macrocyclic compound **36b** using different Lewis acid-mediated¹⁸ cyclocondensation reactions with 1,3,5-trioxane were explored (Scheme 4.19). Reaction of **37b** with 1,3,5-trioxane and magnesium triflate in toluene solution under refluxing conditions failed to produce any of the desired cyclic product, and only unreacted **37b** was recovered from the reaction mixture. When scandium triflate [$\text{Sc}(\text{OTf})_3$] was used in acetonitrile¹⁹ under similar conditions, the reaction of **37b** with 1,3,5-trioxane also failed to produce the

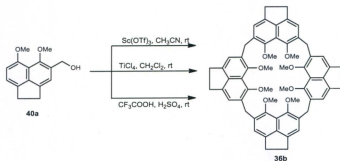
desired product and only unreacted starting material was recovered. However, when toluene was used as the solvent, with $\text{Sc}(\text{OTf})_3$, mass spectrometric analysis of the reaction mixture suggested the presence of only uncyclized linear trimer **45** without any desired **36b**.



Scheme 4.19. Attempts at the synthesis of calix[4]acenaphthene **36b** from **37b**.

The second approach (Scheme 4.12) to synthesize calix[4]acenaphthene **36a** *via* its octamethoxy ether **36b** was investigated by attempting the direct cyclocondensation of 4-hydroxymethyl-5,6-dimethoxyacenaphthene (**40a**) with $\text{Sc}(\text{OTf})_3$ ¹⁹ in acetonitrile, or with titanium (IV) chloride²⁷ in dichloromethane, or with trifluoroacetic acid.²⁹ Unfortunately, all of these approaches, including using varied reaction temperatures and times offered only hints of trace amounts of the octamethoxycalix[4]acenaphthene (**36b**) as indicated by mass spectrometry. When $\text{Sc}(\text{OTf})_3$ was used as the catalyst the ¹H-NMR spectra of

the crude product revealed that an intractable mixture was formed (Figure 4.5). TLC revealed more than six spots which could not be separated, purified or identified.



Scheme 4.20. Attempts at the synthesis of calix[4]acenaphthene (**36b**) from 4-hydroxymethyl-5,6-dimethoxyacenaphthene (**40a**).

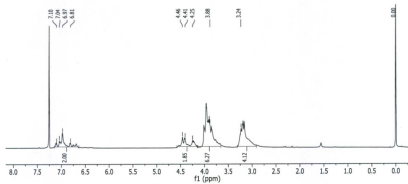


Figure 4.5. $^1\text{H-NMR}$ spectrum of the crude product from the dehydrating reaction of 4-hydroxymethyl-5,6-dimethoxyacenaphthene (**40a**).

4.4 Synthesis of homooxacalix[4]acenaphthenes

4.4.1 Design of the target structure

A computer-assisted molecular modeling study¹⁶ (Figure 4.6) was undertaken to evaluate whether the interaction between the macrocyclic ring-expanded octahomotetra-oxacalix[4]acenaphthene (**47a**) and fullerene C_{60} would be feasible. Molecular modeling¹⁶ suggested that **47a** could indeed form such a supramolecular complex by analogy with the similar prediction for a C_{60} : **36a** complex previously described.

This new class of homooxacalix[4]acenaphthenes (**47a-d**), which forms the subject of the research reported in this section, has deeper and wider cavities in comparison with Poh's cyclotetrachromotropyene whose structure is shown in Figure 4.3. This is due to both the $-CH_2OCH_2-$ bridges which result in macrocycles with larger diameters, and due to the CH_2CH_2- groups of the acenaphthene units which impart deeper cavities than Poh's macrocycle.¹⁴

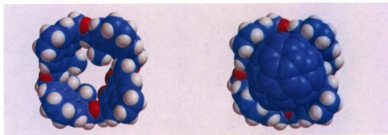
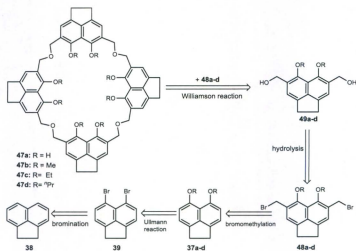


Figure 4.6. Computer-generated structures of calix[4]acenaphthene (**47a**, *left*) and of a 1:1 **47a**: C_{60} complex (*right*).¹⁶

4.4.2 Retrosynthetic analysis

The analysis outlined in Scheme 4.21 shows that the first retrosynthetic cut of octahomotetraoxacalix[4]acenaphthenes (**47a-d**) leads to **48a-d** and **49a-d** as potential synthetic precursors which could be coupled via Williamson-type ether cross-coupling.



Scheme 4.21. Retrosynthetic analysis for octahomotetraoxacalix[4]acenaphthenes

47a-d.

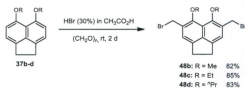
4,7-Bis(hydroxymethyl)-5,6-dialkoxyacenaphthenes **49a-d** are derived by the hydrolysis of 4,7-bis(bromomethyl)-5,6-dialkoxyacenaphthenes **48a-d** which are derived from 5,6-dialkoxyacenaphthenes **37a-d**. Since the *ortho*-positions of the **37a-d** are activated by the electron-donating alkoxy groups, bis(bromomethylation) should selectively and smoothly take place to furnish 4,7-bis(bromomethyl)-5,6-dialkoxyacenaphthenes **48a-d**. Starting from readily-available acenaphthene, 5,6-dibromo-

acenaphthene (**39**) could be synthesized *via* the modified Tanaka bromination methodology,²³ and 5,6-dialkoxyacenaphthenes **37a-d** could be synthesized as described previously in this chapter *via* the Ullman coupling.²¹

4.5 Results and discussions

4.5.1 Functionalized 5,6-dialkoxyacenaphthenes

The actual synthesis of the desired target homooxacalix[4]acenaphthenes **47a-d** required both the efficient synthesis of and the Williamson-type coupling between intermediates **48a-c** with **49a-c**. 5,6-Dialkoxyacenaphthenes **37b-d** which were synthesized as described previously, could easily be converted to the corresponding 4,7-bis(bromomethyl) derivatives **48b-d** by the reaction of alkoxyacenaphthenes **37b-d** with paraformaldehyde in glacial acetic acid, and 30% hydrogen bromide solution in acetic acid. The desired products **48b-d** were obtained in 82, 85 and 83% yields respectively (Scheme 4.22). ¹H- and ¹³C-NMR spectra of these products were in agreement with the desired and proposed structures but to unequivocally confirm the structure of **48b** a single-crystal X-ray diffraction analysis of crystals of **48b** obtained from dichloromethane: hexane was undertaken. The structure is shown in Figure 4.7.



Scheme 4.22. Synthesis of the 4,7-bis(bromomethyl)-5,6-dialkoxyacenaphthenes (**38b-d**).

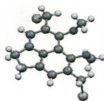
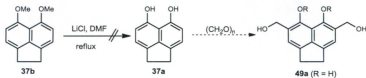


Figure 4.7. X-ray structure of 4,7-bis(bromomethyl)-5,6-dimethoxyacenaphthene (**48b**), red = oxygen; brown = bromine atoms.

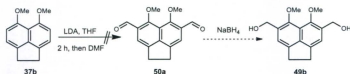
Synthesis of the corresponding hydroxymethyl derivatives **49b-d** was explored using several methodologies. The first attempt involved trying to trap pre-formed 5,6-dihydroxyacenaphthene (**37a**) *in situ* with paraformaldehyde, to form **49a** (R = H) directly. Exploratory attempts to deprotect 5,6-dimethoxyacenaphthene (**37b**), however, failed to give the desired product, while only starting material was recovered from the reaction mixture (Scheme 4.23).



Scheme 4.23. Attempted *in situ* synthesis of **49a** (R = H).

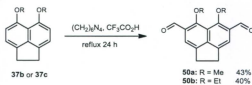
The second approach was to use a double *ortho*-metalation (Scheme 4.24) of 5,6-dimethoxyacenaphthene (**37b**) using *tert*-butyllithium, or LDA, in THF, at $-78\text{ }^{\circ}\text{C}$ to form intermediate diformyl **50a** which could in turn be reduced to **49b**. The resulting reaction

mixture was stirred for 2 h at the same temperature, and then was quenched with dry DMF at $-78\text{ }^{\circ}\text{C}$. This approach also failed to give the desired product **50a** (Scheme 4.24).



Scheme 4.24. Attempted *ortho*-metalation approach to **49b**.

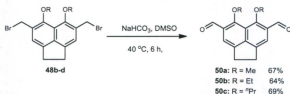
The third approach employed the Duff methodology²⁹ which involved formylation of the 5,6-dialkoxyacenaphthenes **37b-c** with hexamethylenetetraamine in trifluoroacetic acid as solvent, and heating at reflux for 24 h. This method afforded **50a** and **50b** in 43 and 40% yields, respectively (Scheme 4.25).



Scheme 4.25. Duff method syntheses of **50a** and **50b**.

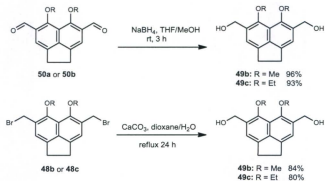
The fourth approach employed the Kornblum oxidation methodology³⁰ which involves oxidizing benzylbromide analogue precursors to the corresponding aldehydes by dissolving the halide precursors in dimethyl sulfoxide (DMSO) in the presence of a base. Applying this methodology with 4,7-bis(bromomethyl)-5,6-dimethoxy-, 4,7-bis(bromomethyl)-5,6-diethoxy- and 4,7-bis(bromomethyl)-5,6-dipropoxyacenaphthene **48b-d**, each of which was dissolved in DMSO and stirred for 6 h at $40\text{ }^{\circ}\text{C}$ in the presence

of sodium bicarbonate. The desired 4,7-diformyl-5,6-dialkoxyacenaphthenes **50a-c** were isolated in yields of 67, 64 and 69%, respectively (Scheme 4.26).



Scheme 4.26. Kornblum oxidation synthesis of **50a-c**.

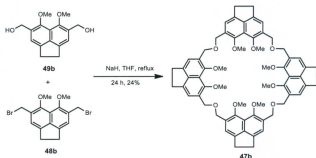
The desired 4,7-bis(hydroxymethyl)-5,6-dialkoxyacenaphthenes **49b** and **49c** could now be produced in high yields by NaBH_4 reduction in 1:1 methanol:THF, of the diformyl compounds **50a** and **50b**, respectively. Another approach involved hydrolysis of **48b** and **48c** with CaCO_3 in aqueous dioxane¹² to furnish **49b** and **49c** in 84 and 80% yields, respectively (Scheme 4.27).



Scheme 4.27. Synthesis of 4,7-bis(dihydroxymethyl)-5,6-dialkoxyacenaphthenes **49b-c**.

4.5.2 Synthesis of homooxalix[4]acenaphthene

Many attempts to effect the cyclization of **48b** with **49b** under different conditions failed. The desired macrocycle could not be obtained using conditions including the use of NaH with solvents such as DMF and dioxane; or using KOH in either dioxane or THF. Ultimately however, optimal conditions were found which were based on Masci's methodology.⁶ The best conditions to effect the macrocyclization of **48b** and **49b** via a Williamson ether reaction was found to be the use of NaH in dry THF. Thus, **49b** was dissolved in anhydrous THF and the bis(bromomethyl)acenaphthene **48b** in THF was added slowly over 2 h, using a syringe pump, and after the addition was completed, the reaction mixture was heated at reflux for 48 h. After work-up and chromatographic purification, gratifyingly, the desired octahomotetraoxalix[4]acenaphthene ("tetraoxa[3.3.3.3](4,7)acenaphthenophane") macrocycle **47b** was obtained in an unoptimized yield of 24%, (Scheme 4.28).



Scheme 4.28. Synthesis of octahomotetraoxalix[4]acenaphthene (**47b**).

This new macrocycle has a simple $^1\text{H-NMR}$ spectrum at temperature 298 K which indicates that the macrocycle was highly symmetrical. The $^1\text{H-NMR}$ spectrum showed only one sharp signal for all methylene bridges, which confirms the fast conformational equilibration in solution at ambient temperature. The position of the CH_3 signal of the methoxy group in the macrocycle appears at δ 3.61 ppm which is shifted upfield from the positions of the corresponding signals in the starting materials which appear at δ 3.99 and 3.84 ppm for the 4,7-bis(bromomethyl)- and 4,7-bis(hydroxymethyl)-5,6-dimethoxy-acenaphthenes, **48b** and **49b**, respectively. This suggests that the methoxy groups in **47b** in CDCl_3 could be partially shielded by the “partial cavity” created by the three other acenaphthene rings.

Again, gratifyingly, single crystals suitable for X-ray diffraction analysis were obtained from slow evaporation of the NMR CDCl_3 with hexane solution. This X-ray structure which was collected and solved by Dr. L. N. Dawe (C-CART, MUN) revealed that **47b** adopted a calixarene-like *1,3-alternate* conformation having C_{2v} symmetry (Figure 4.8) all H-atoms omitted for clarity).

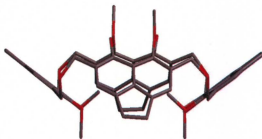


Figure 4.8. X-ray structure of **47b** (*side view*) showing its *1,3-alternate* conformation.

As well, as Figure 4.9 shows, the unit cell packing looking down the “c-axis” showed four significant-sized voids. L. Dawe’s report on this compound³¹ states:

“The Platon Squeeze procedure was applied to recover 228 electrons per unit cell in four voids that were sufficiently large to contain a small molecule (total volume 5143 Å³); with Z = 16, that is, 14.25 electrons per formula unit. Discrete lattice solvent could not be located from difference maps, however, each void electron count (57 electrons) is consistent with the presence of one hexane molecule (50 electrons). The formula was therefore adjusted by 0.25 hexane to reflect this electron contribution to the calculation of the intensive properties”

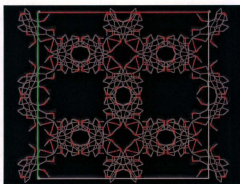


Figure 4.9. X-ray structure of the unit cell packing of **47b** (c-axis view).

4.5.3 Complexation study

Since **22a** and “Zorbarene” (**22b**) had previously been shown to bind significantly with tetramethylammonium chloride (TMACl) it was decided to undertake a similar complexation study with **47b**. ¹H-NMR titration experiments with the new host failed to

reveal any similar binding. A primary objective for undertaking the synthesis of this macrocyclic host had been to determine if the molecular modeling prediction of binding to C_{60} as a guest molecule could be realized experimentally. Equimolar amounts of the host and guest compounds were mixed in several separate solvents. Dark microcrystalline materials separated from the toluene solution but were too small and thus unsuitable for X-ray analysis. However, when the residue obtained after all of the solvent had evaporated was re-dissolved in toluene- d_8 and its 1H NMR spectrum was measured, significant chemical shift changes could be noted. A titration experiment was therefore undertaken with a fresh amount of **47b**, (Table 4.2). In these titration experiments, the chemical shifts of the methoxy and the acenaphthene bridging (CH_2CH_2) groups, and the aromatic singlet proton signals of **47b** were affected by complexation with C_{60} , as Figure 4.10 shows.

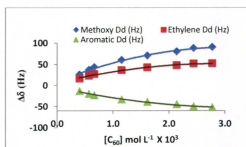


Figure 4.10. Plot of chemical shift changes ($\Delta\delta$) for protons on **47b** in toluene- d_8 solution vs added C_{60} .

The 1:1 binding isotherm was determined as shown in Figure 4.11 to reveal a modest K_{assoc} values of 614 ± 28 based upon the methoxy group shifts; 718 ± 54 based upon the

acenaphthene $-\text{CH}_2\text{CH}_2-$ group shifts and 513 ± 88 based upon the aromatic singlet shifts. These different binding constants presumably reflecting the fact that the different chemical shift changes due to the “nesting” of the C_{60} into the host has, as would be expected, spatially different contacts with these three sets of protons.

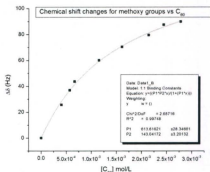


Figure 4.11. 1:1 Binding isotherm for the titration of **47a** with C_{60} .

Table 4.2. $^1\text{H-NMR}$ titration data of **47b** (conc. 3.42×10^{-3} M), with C_{60} in toluene- d_8 at 298 K. ($\Delta\delta$ values are absolute values).

Entry	Wt. C_{60} (mg)	$\text{C}_{60} \times 10^6$ mol	$[\text{C}_{60}]$ $\times 10^3 \text{M}$	Δ Ar (ppm)	$\Delta\delta$ Ar (Hz)	Δ $-\text{CH}_2\text{CH}_2-$ (ppm)	$\Delta\delta$ $-\text{CH}_2\text{CH}_2-$ (Hz)	Δ OCH_3 (ppm)	$\Delta\delta$ OCH_3 (Hz)
1	0	0	0	7.41	0	2.97	0	3.57	0
2	0.29	4.03	4.03	7.39	13.62	3.00	16.1	3.62	25.7
3	0.41	5.69	5.69	7.38	20.12	3.01	23.0	3.64	37.1
4	0.48	6.67	6.67	7.37	23.72	3.02	26.9	3.66	43.7
5	0.83	11.5	11.5	7.35	33.34	3.04	36.2	3.69	60.1
6	1.16	16.1	16.1	7.34	39.49	3.05	42.5	3.71	70.4
7	1.54	21.4	21.4	7.33	44.88	3.06	47.4	3.73	79.5
8	1.76	24.4	24.4	7.32	50.14	3.07	51.6	3.74	87.5
9	2.00	27.8	27.8	7.31	51.94	3.07	52.2	3.75	89.9

4.6 Conclusions

As part of the Georghiou group's on-going studies concerned with naphthalene-based calix[*n*]arenes, this project aimed to synthesize analogues of acenaphthene-based calix[*n*]arenes which would have larger and deeper cavities than the corresponding calix[*n*]arenes in order to study the binding properties with neutral guest molecules such as fullerenes and other guests.

A series of new derivatives for acenaphthene were therefore synthesized, for the first time. Acenaphthene was functionalized at positions 5 and 6 by introducing different alkoxy groups to produce 5,6-dimethoxy-, 5,6-diethoxy- and 5,6-dipropoxyacenaphthene **37b-d**, respectively. Methylbromination of these 5,6-dialkoxyacenaphthenes using paraformaldehyde and HBr in glacial acetic acid successfully introduced bromomethyl groups to the acenaphthene ring to afford the corresponding 4,7-bis(bromomethyl)-5,6-dialkoxyacenaphthenes **48b-d**. Also the mono formyl and diformyl of these acenaphthenes were synthesized using different methods. These new compounds in the acenaphthene family were the 4-formyl **41a-c**, and the 4,7-diformyl-5,6-dialkoxyacenaphthenes **50a-c**. The 4-hydroxymethyl **40a-c** and 4,7-bis(hydroxymethyl)-5,6-dialkoxyacenaphthenes **49b-c** were also synthesized via reduction of 4-formyl- **41a-c** and 4,7-diformyl-5,6-dialkoxy-acenaphthenes **50a-b**, respectively. The 4,7-bis(hydroxymethyl) compounds **49b-c** were also obtained by CaCO₃-mediated hydrolysis of **48b-c**.

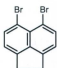
The use of the Williamson-ether type coupling between 4,6-bis(hydroxymethyl)-5,6-dimethoxyacenaphthene (**49b**) and 4,6-bis(bromomethyl)-5,6-dimethoxyacenaphthene (**48b**) successfully afforded macrocycle **47b** in 24% yield. This is the first acenaphthene ring-based macrocycle to be reported and can be considered as an octahomotetraoxacalix[4]acenaphthene. Single-crystal X-ray crystallography revealed that this macrocycle has a "1,3-alternate" conformation. The solution complexation experiments showed that the macrocycle formed a 1:1 complex with C₆₀-fullerene in toluene-*d*₈ as determined by ¹H-NMR. On-going studies with this new bowl-shaped macrocycle will be conducted by the Georghiou group.

4.6 Experimental section:

General methods, materials, and instrumentation used are identical to those described in Chapter 2.

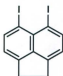
4.6.1 Experimental:

5,6-Dibromoacenaphthene (39).



A suspension of *N*-bromosuccinimide (NBS) (125 g, 0.702 mol) in DMF (250 mL) was added dropwise over 5 h to the solution of acenaphthene (**38**) (50.0 g, 0.324 mol) in DMF (100 mL) cooled to 0 °C in an ice-bath. The solution was maintained at 10 °C for 12 h and then was allowed to warm to room temperature. The resulting precipitate was filtered with suction, washed with ethanol (3 × 50 mL), and purified by heating at reflux in ethanol (150 mL) overnight and then cooling to room temperature and filtered. The precipitate was washed with ethanol and then dried under vacuum to afford a beige solid which was crystallized from ethanol to give **39** (25 g, 25% yield); mp 170-171 °C; (lit.²⁰ 174.0-176.0 °C); ¹H-NMR (CDCl₃, 500 MHz): δ 3.28 (s, 4H), 7.07 (d, *J* = 7.50 Hz, 2H), 7.78 (d, *J* = 7.50 Hz, 2H); ¹³C-NMR (75.46 MHz, CDCl₃): δ 30.1, 114.4, 120.9, 127.8, 135.8, 141.9, 147.0; GC-MS *m/z* (relative intensity) 314 (M⁺, ⁸¹Br,⁸¹Br; 33), 312 (M⁺, ⁸¹Br,⁷⁹Br, 100) 310 (M⁺, ⁷⁹Br,⁷⁹Br; 40), 232 (60), 150 (100), 115 (27).

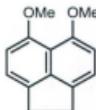
5,6-Diiodoacenaphthene (**42**).



5,6-Dibromoacenaphthene (**39**) (4.00 g, 12.8 mmol) in 1.0 L anhydrous ether in a 2.0-L three-necked flask fitted with an addition funnel and under dry N_2 , was cooled to $-10\text{ }^\circ\text{C}$ in an ice-ethanol bath. *n*-BuLi (1.6 M in hexane, 24 mL, 39 mmol) was injected into the addition funnel containing TMEDA (5.76 mL, 38.5 mmol). The resulting solution was added dropwise into the ethereal solution with rapid stirring. After the addition was finished, the resulting solution was stirred for 30 min at the same temperature and then solid iodine (4.00 g, 32.1 mmol) was added and the solution was stirred at $-10\text{ }^\circ\text{C}$ for 2 h. The solution was then allowed to warm to room temperature and stirred for 3 h. To that solution aqueous 5% sodium thiosulfate (100 mL) was added, with vigorous stirring. The organic layer was separated, washed with aqueous sodium thiosulfate (20 mL) and then water (20 mL), dried over anhydrous $MgSO_4$, filtered and the solvent removed on a rotavap. The residue was crystallized from ethanol to afford **42** (3.4 g, 65%), as a brown solid: mp $169.6\text{--}170\text{ }^\circ\text{C}$, (lit.²⁰ $159.0\text{--}160.0\text{ }^\circ\text{C}$); $^1\text{H-NMR}$ (500 MHz, $CDCl_3$): δ 3.26 (s, 4H), 6.091 (d, $J = 7.0$ Hz, 2H), 8.23 (d, $J = 7.00$ Hz, 2H); $^{13}\text{C-NMR}$ (75.46 MHz, $CDCl_3$): δ 29.9, 89.4, 12.8, 130.8, 140.2, 144.6, 148.9; GC-MS m/z (relative intensity) 406 (M^+ , 100), 279 ($[M-I]^+$, 50), 152 ($[M-2I]^+$, 100).

5,6-Dimethoxyacenaphthene (37b).

(a) Method A: Using CuCl or CuI as catalyst.



General procedure: To 100 mL of anhydrous methanol, sodium (6.00 g, 0.261 mol) was added portion-wise until all of the sodium was converted to sodium methoxide; solid CuCl (2.54 g, 13.4 mmol) was then added in one portion to the reaction mixture, followed by addition of dioxane (50 mL). The reaction mixture was then heated at reflux for 30 min. To the suspension was added **39** (8.00 g, 25.6 mmol), and the reaction mixture heated at reflux for 4 h. The methanol was distilled off, and then the reaction mixture was heated at reflux for 48 h. The reaction mixture was cooled to room temperature, and extracted with ether (5 x 100 mL). The combined organic extract was filtered by simple filtration and the solvent was removed on a rotavap. The resulting product was purified by column chromatography (2:8 ethyl acetate:hexanes) to give **37b** (5.1 g, 85-93%), as a light yellow solid: mp 107.5-108.5 °C, (from methanol); ¹H-NMR (500 MHz, CDCl₃): δ 3.30 (s, 4H), 3.96 (s, 6H), 6.78 (d, *J* = 7.50 Hz, 2H), 7.14 (d, *J* = 7.50 Hz); ¹³C-NMR (75.46 MHz, CDCl₃): δ 29.9, 57.2, 107.4, 115.6, 119.7, 137.6, 142.7, 153.9; GC-MS *m/z* (relative intensity) 214 (M⁺, 100), 199 (35), 171 (100), 155(48), 141(67), 115 (40).

(b) Method B: Using BaO.

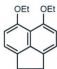
In a two-necked 250-mL round-bottomed flask, under Ar, a mixture of **39** (2.00 g, 6.41 mmole) and CuCl₂ (0.862 g, 6.41 mmol) in DMF (100 mL) was heated at reflux for 2 h. Using a cannula, this mixture was transferred to another 500-mL flask containing a

suspension of BaO (15.7 g, 103 mmol) in methanol (100 mL) also under Ar. The resulting mixture was stirred for 12 h at 115 °C. After cooling to room temperature most of the solvents were removed under reduced pressure. Water (100 mL) and concentrated hydrochloric acid (10 mL) were added to the residue. The mixture was extracted with ethyl acetate (3 x 50 mL), and the combined organic layers were dried over anhydrous MgSO₄ and then filtered. The solvent was removed on a rotovap and the residue was purified by column chromatography (2:8 ethyl acetate:hexanes) to give **37b** (0.50 g, 35%) as a light yellow solid having identical characterization data to that obtained from Method A.

(c) Method C: Using microwave-assisted conditions.

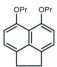
To 50 mL of anhydrous methanol sodium metal (0.631 g, 0.261 mol) was added portion-wise until all of the sodium was converted to sodium methoxide; solid CuI (0.500 g, 2.63 mmol) and **39** (0.820 g, 2.63 mmol) were added in one portion to the reaction mixture which was then heated at reflux for 30 min. The methanol was distilled off and the residue transferred under N₂ atmosphere into a microwave vial of 2.0-5.0 mL capacity. After, sealing with an aluminum crimp cap with a PTFE-lined rubber seal the heterogeneous mixture was heated in a microwave synthesizer at 140 °C for 4 h. The reaction mixture cooled to room temperature and was worked-up in the same manner as in Method A to afford **37b** (0.34 g, 60%) as a light yellow solid having identical characterization data to that obtained from the Method A.

5,6-Diethoxyacenaphthene (37c).



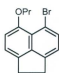
Using the general procedure for Method A: To 100 mL of absolute ethanol was added sodium (6.00 g, 0.261 mol) portion-wise until all of the sodium was converted to sodium ethoxide. Solid CuCl (2.54 g, 13.4 mmol) was added in one portion to the reaction mixture, followed by the addition of dioxane (50 mL), and the reaction mixture was then heated at reflux for 30 min. To the reaction mixture **39** (8.00 g, 25.6 mmol) was added, and heated at reflux for 4 h. The methanol was distilled off from the reaction mixture and the mixture was heated at reflux for another 48 h. After that, the reaction was worked-up as in Method A to give a colourless ether solution which was evaporated using a rotavap and the resulting product purified by column chromatography (1:9 ethyl acetate:hexanes) to give **37c** (5.1 g, 92%), as a light brown solid: mp 106.3-107.5°C, (from methanol); ¹H-NMR (500 MHz, CDCl₃): δ 1.51(t, *J* = 7.00Hz, 6H), 3.28 (s, 4H), 4.10 (q, *J* = 14.00Hz, *J* = 7.00 Hz 4H), 6.77 (d, *J* = 7.50 Hz), 7.90 (d, *J* = 7.50 Hz); ¹³C-NMR (75.46 MHz, CDCl₃): δ 15.0, 29.9, 65.5, 109.6, 116.6, 119.5, 137.7, 142.7, 153.2; GC-MS *m/z* (relative intensity) 243 (M⁺, 100), 213 (100), 186 (100), 157(100), 141(100), 128(100).

5,6-Dipropoxyacenaphthene (37d).



To 100 mL of *n*-propanol was added sodium (6.00 g, 0.261 mol) portion-wise until all of the sodium was converted to sodium propoxide. Then solid CuCl (2.54 g, 13.4 mmol) was added to the reaction mixture in one portion, followed by the addition of dioxane (50 mL) after which the mixture was

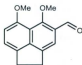
heated at reflux for 30 min. After cooling to room temperature **39** (8.00 g, 25.6 mmol) was added to the reaction mixture and after being heated at reflux for 4 h, the *n*-propanol was distilled off. After heating at reflux for 48 h, the reaction mixture was worked-up as in Method A and after the ether was removed on rotavap, the residue was purified by column chromatography (hexanes) to give **37d** (2.4 g, 70%), as a light brown solid: mp 73.1-74°C, (from methanol); ¹H-NMR (500 MHz, CDCl₃): δ 1.11(t, *J* = 7.5 Hz, 6H), 1.89-1.96 (m, 4H), 3.28 (s, 4H), 4.00 (t, *J* = 7.0 Hz, 4H), 6.74 (d, *J* = 7.5 Hz, 2H), 7.90 (d, *J* = 7.5 Hz, 2H); ¹³C-NMR (75.46 MHz, CDCl₃): δ 10.8, 22.9, 30.0, 71.2, 108.7, 116.3, 119.6, 137.3, 142.7, 153.6; GC-MS *m/z* (relative intensity) 270 (M⁺, 100), 228



(80), 186 (100), 168 (100), 128(100). A second product: **5-bromo-6-propoxyacenaphthene (43)** (0.93 g, 25 %), as a yellow solid: mp 83.6-84.7 °C; was also isolated from the reaction mixture: ¹H-NMR (500 MHz, CDCl₃): δ 1.15 (t, *J* = 5.0 Hz, 6H), 1.99-1.96 (m, 4H), 3.29 (s, 4H), 4.02 (t, *J* = 7.0, 4H), 6.83 (d, *J* = 7.5 Hz, 1H), 7.03 (d, *J* = 7.4 Hz, 1H), 7.15 (d, *J* = 7.5 Hz, 1H), 7.61 (d, *J* = 7.4 Hz, 1H); ¹³C-NMR (75.46 MHz, CDCl₃): δ 11.1, 22.7, 29.6, 30.4, 71.4, 109.4, 112.0, 119.9, 120.5, 122.3, 133.1, 137.8, 142.2, 145.4; GC-MS *m/z* (relative intensity) 290 (M⁺, ⁸¹Br, 100), 290 (M⁺, ⁷⁹Br, 100), 250 (100), 168 (100), 139(100), 115(10).

4-Formyl-5,6-dimethoxyacenaphthene (41a).

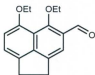
General procedure:



To a solution of 5,6-dimethoxyacenaphthene (**37b**) (0.214 g, 1.00 mmol) in anhydrous dichloromethane (50 mL) was added

titanium tetrachloride (TiCl₄) (0.16 mL, 1.5 mmol). Then, dichloromethyl methyl ether (0.10 mL, 1.1 mmol) was added dropwise to the reaction mixture. The ice-bath was then removed and the reaction mixture was stirred at room temperature for 2 h. Cold water (20 mL) was added to the reaction mixture which was then extracted with dichloromethane (3 × 20 mL), the combined organic layers were dried over anhydrous MgSO₄, filtered and the solvent removed on a rotavap. The crude product was purified by column chromatography (2:8 ethyl acetate:hexanes) to afford **41a** (0.23 g, 94%) as a yellow solid; mp 105.5 °C; ¹H-NMR (500 MHz, CDCl₃): δ 3.31 (s, 4H), 4.00 (s, 3H), 4.03 (s, 3H), 6.86 (d, *J* = 7.7 Hz, 1H), 7.31 (d, *J* = 7.7 Hz, 1H), 7.62 (s, 1H); ¹³C-NMR (75.46 MHz, CDCl₃): δ 29.7, 30.1, 56.4, 65.3, 108.1, 116.3, 117.6, 123.3, 127.4, 137.9, 141.9, 145.8, 154.2, 160.9, 190.8; GC-MS *m/z* (relative intensity) 242 (M⁺, 100), 127 (60), 212 (55), 185(30), 169 (42), 141 (46), 115 (30).

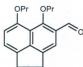
4-Formyl-5,6-diethoxyacenaphthene (**41b**).



Using the general procedure used for **41a**: To a solution of 5,6-diethoxyacenaphthene (**37c**) (0.242 g, 1.00 mmol) in dry dichloromethane (50 mL) was added titanium tetrachloride (TiCl₄) (0.17 mL, 1.5 mmol), and then, dichloromethyl methyl ether (0.10 mL, 1.1 mmol) was added dropwise. After the addition was completed, the ice-bath was removed and the reaction mixture was stirred at room temperature for 2 h. Cold water (20 mL) was added to the reaction mixture which was then extracted with dichloromethane (2 × 20 mL). The combined organic layers were dried over anhydrous MgSO₄, filtered and the solvent

removed on a rotavap to give a crude product which was purified by column chromatography (2:8 ethyl acetate:hexanes) to give **41b** (0.25 g, 92%) as a yellow solid: mp 82.0 °C; ¹H-NMR (500 MHz, CDCl₃): δ 1.50 (t, *J* = 7.0, 3H), 1.58 (t, *J* = 7.0 Hz, 3H), 3.31 (s, 4H), 4.16 (q, *J* = 14.0 Hz, 7.0 Hz, 2H), 4.20 (q, *J* = 14.0 Hz, 7.0 Hz, 2H), 6.84 (d, *J* = 8.0 Hz, 1H), 7.27 (d, *J* = 8.0 Hz, 1H), 7.62 (s, 1H), 10.57 (s, 1H); ¹³C-NMR (75.46 MHz, CDCl₃): δ 15.1, 15.1, 29.7, 30.1, 64.7, 73.9, 108.9, 116.2, 118.0, 123.3, 127.7, 137.7, 141.7, 145.8, 153.7, 159.7, 191.1; GC-MS *m/z* (relative intensity) 270 (M⁺, 100), 241(30), 214 (100), 185 (20), 157(40), 128 (35).

4-Formyl-5,6-dipropoxyacenaphthene (**41c**).

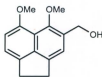


Using the general procedure used for the compound **41a**: To a solution of 5,6-dipropoxyacenaphthene (**37d**) (0.300 g, 1.11 mmol) in dry dichloromethane (50 mL) was added titanium tetrachloride TiCl₄ (0.18 mL, 1.7 mmol). Dichloromethyl methyl ether (0.10 mL, 1.1 mmol) was then added. After the addition was completed, the ice-bath was removed and the reaction mixture was stirred for 2 h at room temperature. The reaction mixture was chilled with cold water (20 mL) and after the usual work-up, the product was purified by column chromatography (2:8 ethyl acetate:hexanes) to give **41c** (0.28 g, 90%) as a yellow solid: mp 63.5-64.3 °C; ¹H-NMR (500 MHz, CDCl₃): δ 1.06-1.14 (m, 6H), 1.92-2.00 (m, 4H), 3.30 (s, 4H), 4.03-4.09 (m, 4H), 6.84 (d, *J* = 8.0 Hz, 1H), 7.27 (d, *J* = 8.0 Hz, 1H), 7.61 (s, 1H), 10.58 (s, 1H); ¹³C-NMR (75.46 MHz, CDCl₃): δ 10.4, 10.7, 22.7, 23.0, 29.7, 30.0, 70.9, 80.0, 108.8, 116.18, 118.0, 123.2, 127.5, 137.5, 141.6,

145.7, 153.8, 160.0, 191.1; GC-MS m/z (relative intensity) 298 (M^+ , 100), 256 (56), 213 (100), 185 (50), 157(85), 139 (65).

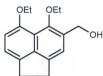
4-Hydroxymethyl-5,6-dimethoxyacenaphthene (40a).

General procedure:



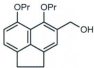
To a solution of 4-formyl-5,6-dimethoxyacenaphthene (**41a**) (0.500 g, 2.06 mmol) in 1:4 THF:methanol (20 mL) was added NaBH_4 (78 mg, 2.1 mmol) portion-wise. The reaction mixture was stirred at room temperature for 3 h. After that, the reaction mixture was chilled by cold water (15 mL) and acidified with aqueous 2M HCl (10 mL). The reaction mixture was extracted with dichloromethane (3×30 mL) and the combined organic layers were dried over anhydrous MgSO_4 , filtered and the solvent removed on a rotavap. The crude product was purified by column chromatography (3:7 ethyl acetate:hexanes) to give compound **40a** (0.48 g, 96%), as a colorless solid; mp 107.7 °C; $^1\text{H-NMR}$ (500 MHz, CDCl_3): δ 2.34 (s, br., 1H, disappeared up on addition D_2O), 3.31 (s, 4H), 3.91 (s, 3H), 3.99 (s, 3H), 4.84 (s, 2H), 6.81 (d, $J = 7.5$ Hz, 1H), 7.14 (d, $J = 7.5$ Hz, 1H), 7.25 (s, 1H); $^{13}\text{C-NMR}$ (75.46 MHz, CDCl_3): δ 29.6, 30.2, 56.2, 62.0, 62.8, 107.3, 117.8, 119.2, 120.8, 131.6, 137.8, 141.6, 142.5, 151.0, 152.7; GC-MS m/z 244 (M^+ , 100), 228 (11), 201 (100), 186 (98), 170(35), 152 (35), 115 (25).

4-Hydroxymethyl-5,6-diethoxyacenaphthene (40b).



Using the general procedure used for **40a**: To a solution of 4-formyl-5,6-diethoxyacenaphthene (**41b**) (0.270 g, 1.00 mmol) in 1:4 THF:methanol (20 mL), NaBH₄ (38 mg, 1.0 mmol) was added portion-wise. The reaction mixture was stirred at room temperature for 4 h. The reaction mixture was then worked-up in a similar way to the general procedure. The crude product was purified by column chromatography (3:7 ethyl acetate:hexanes) to give **40b** (0.25 g, 93%), as a colorless solid: mp 101.5-102.1 °C; ¹H-NMR (500 MHz, CDCl₃): δ 1.49 (t, *J* = 7.0, 3H), 1.56 (t, *J* = 7.0 Hz, 3H), 2.40 (s, br, 1H, disappeared up on addition D₂O), 3.30 (s, 4H), 4.07 (q, *J* = 7.0 Hz, 2H), 4.16 (q, *J* = 7.0 Hz, 2H), 4.83 (s, 2H), 6.80 (d, *J* = 7.5 Hz, 1H), 7.11 (d, *J* = 7.5 Hz, 1H), 7.23 (s, 1H); ¹³C-NMR (75.46 MHz, CDCl₃): δ 15.1, 15.7, 29.7, 30.3, 62.2, 64.5, 108.4, 118.4, 119.3, 120.8, 131.8, 137.8, 141.4, 142.5, 149.9, 152.2; GC-MS *m/z* (relative intensity) 272 (M⁺, 100), 242 (20), 226 (70), 211 (100), 187(100), 169 (98), 139 (73), 115 (65).

4-Hydroxymethyl-5,6-dipropoxyacenaphthene (40c).

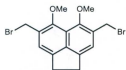


Using the general procedure used for **40a**: To a solution of 4-formyl-5,6-dipropoxyacenaphthene (**41c**) (0.200 g, 0.704 mmol) in 1:4 THF:methanol (20 mL) was added NaBH₄ (27 mg, 0.70 mmol) portion-wise. The reaction mixture was stirred at room temperature for 3 h after which it was worked-up in a similar way to the general procedure, to give a product which was purified by column chromatography (2:7 ethyl acetate:hexanes) to afford compound **40c**

(0.19 g, 95%), as a colorless solid: mp 103.0-103.8 °C; $^1\text{H-NMR}$ (CDCl_3 , 500 MHz): δ 1.06-1.11 (m, 6H), 1.86-1.99 (m, 4H), 3.27 (s, 4H), 3.95 (t, $J = 7.0$ Hz, 2H), 4.04 (t, $J = 7.0$ Hz, 2H), 4.82 (s, 2H), 6.78 (d, $J = 7.6$ Hz, 1H), 7.09 (d, $J = 7.6$ Hz, 1H), 7.22 (s, 1H); $^{13}\text{C-NMR}$ (75.46 MHz, CDCl_3): δ 10.6, 10.7, 22.8, 23.4, 29.7, 30.3, 62.1, 70.9, 108.4, 118.4, 119.3, 120.8, 131.8, 137.7, 141.4, 142.5, 150.0, 152.4; GC-MS m/z (relative intensity) 298 (M^+ , 100), 256 (56), 213 (100), 185 (50), 157 (85), 139 (65).

4,7-Bis(bromomethyl)-5,6-dimethoxyacenaphthene (**48b**).

General procedure:

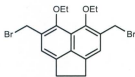


To a mixture of 5,6-dimethoxyacenaphthene (**37b**) (4.28 g, 20.0 mmol) and 95% paraformaldehyde (3.60 g, 0.120 mol) in glacial acetic acid (70 mL) was added a solution of HBr in glacial acetic acid (30%, 25.3 mL, 0.120 mol). After stirring at room temperature for 3 d, the reaction mixture was poured into ice-cold water (200 mL). The resulting precipitate was filtered, washed with distilled water (2×50 mL), aqueous 5% NaHCO_3 (2×50 mL) and distilled water until the washings were neutral to pH paper. The remaining solid was dissolved in ethyl acetate (200 mL), dried over anhydrous MgSO_4 and filtered. After the solvent was removed under reduced pressure, the product was crystallized from acetone to afford **48b** (6.6 g, 82%) as a brown solid: mp 149.6 °C; $^1\text{H-NMR}$ (500 MHz, CDCl_3): δ 3.31 (s, 4H), 3.99 (s, 6H), 4.77 (s, 4H), 7.27 (s, 2H); $^{13}\text{C-NMR}$ (75.46 MHz, CDCl_3): δ 29.4, 30.1, 63.1, 120.5, 122.5, 129.9, 142.3, 143.4, 151.1; GC-MS m/z (relative intensity)

402 (M^+ , ^{81}Br , ^{81}Br , 10), 400 (M^+ , ^{81}Br , ^{79}Br , 20), 398 (M^+ , ^{79}Br , ^{79}Br , 10), 319 (60), 225 (100), 152 (20), 120 (9).

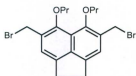
Crystal data for **48b**: $\text{C}_{16}\text{H}_{16}\text{Br}_2\text{O}_2$, $M = 400.11$, colorless prism, space group P-1 (no. 2), $a = 7.946(2)$ Å, $b = 9.482(3)$ Å, $c = 9.955(3)$ Å, $V = 737.0(4)$ Å³, $Z = 2$, $D_c = 1.803$ g/cm³, $F_{000} = 396.00$, $\mu(\text{Mo K}\alpha) = 55.141$ cm⁻¹, $T = 113(1)$ K, $2\theta_{\text{max}} = 61.6^\circ$, 6186 reflections collected, 3012 unique ($R_{\text{int}} = 0.016$). Final GoF = 1.099, R_1 ($I > 2.00\sigma(I)$) = 0.0257, $R(\text{all reflections}) = 0.0271$, $wR_2(\text{all reflections}) = 0.0625$.

4,7-Bis(bromomethyl)-5,6-diethoxyacenaphthene (**48c**).



Using the general procedure used for **48b**: To a mixture of 5,6-diethoxyacenaphthene (2.42 g, 10.0 mmol) and 95% paraformaldehyde (1.9 g, 60 mmol) in glacial acetic acid (50 mL) was added a solution of HBr in glacial acetic acid (30%, 12.7 mL, 60 mmol). The reaction mixture was stirred at room temperature for 24 h, after which the reaction mixture was worked-up in a similar manner to the general procedure used for **48b**, to give a crude product (3.94 g) which was purified by recrystallization from acetone to afford **48c** (3.6 g, 85%); mp 152.8-153.5 °C; ¹H-NMR (500 MHz, CDCl₃): δ 3.31 (t, $J = 6.5$, 6H), 3.30 (s, 4H), 4.13 (q, $J = 7.0$, 4H), 7.7 (s, 4H), 7.28 (s, 2H); ¹³C-NMR (75.46 MHz, CDCl₃): δ 15.9, 30.0, 30.3, 71.8, 120.8, 122.7, 130.1, 142.3, 143.5, 150.5; GC-MS m/z (relative intensity) 430 (M^+ , ^{81}Br , ^{81}Br , 10), 428 (M^+ , ^{81}Br , ^{79}Br , 20), 426 (M^+ , ^{79}Br , ^{79}Br , 10), 347 (45), 239 (79), 211 (100), 152 (15), 115 (5).

4,7-Bis(bromomethyl)-5,6-dipropoxyacenaphthene (48d).

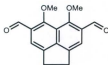


Using the general procedure used for **48b**: To a mixture of 5,6-dipropoxyacenaphthene (**37d**) (3.00 g, 11.1 mmol) and 95% paraformaldehyde (2.10 g, 66.6 mmol) in glacial acetic acid (50 mL) was added a solution of HBr in glacial acetic acid (30%, 13.3 mL, 66.6 mmol), and the reaction mixture was stirred at room temperature for 24 h. The reaction mixture was worked-up in similar way to the general procedure for **48b**, to give a crude product (7.80 g) which was crystallized from acetone to afford **48d** (4.2 g, 83%); mp 122.9 °C; ¹H-NMR (500 MHz, CDCl₃): δ 1.10 (t, *J* = 7.0, 6H), 1.90-1.98 (m, 4H), 3.31 (s, 4H), 4.02 (t, *J* = 7.0, 4H), 4.80 (s, 4H), 7.28 (s, 2H); ¹³C-NMR (75.46 MHz, CDCl₃): δ 10.5, 23.53, 29.9, 30.0, 120.7, 122.6, 129.7, 142.0, 143.3, 150.5; GC-MS *m/z* (relative intensity) 458 (M⁺, ⁸¹Br, ⁸¹Br, 10), 456 (M⁺, ⁸¹Br, ⁷⁹Br, 20), 454 (M⁺, ⁷⁹Br, ⁷⁹Br, 10), 377 (32), 333 (18), 253 (37), 211 (100), 115 (5).

4,7-Diformyl-5,6-dimethoxyacenaphthene (50a).

(a) Method A: Diformylation using the Kornblum oxidation method.

General procedure: To a suspension of NaHCO₃ (6.72 g, 80.0 mmol) in DMSO (50 mL) at 40 °C, 4,7-bis(bromomethyl)-5,6-dimethoxyacenaphthene



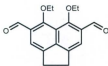
(**48b**) (4.00 g, 10.0 mmol) was added, with stirring. The heating was removed, and the reaction mixture was stirred for 1 h at room temperature, and then it was poured into a mixture of ice-water (200 mL) and aqueous 6 M HCl (15 mL) and stirred for an additional 15 min. The reaction mixture was

extracted using dichloromethane (3 × 30 mL), the combined organic layers were washed with water (3 × 20 mL), dried over anhydrous Na₂SO₄, filtered and the solvent removed on a rotavap. The resulting solid residue was purified by column chromatography (3:7 ethyl acetate:hexane) to give **50a** (1.8 g, 67%) as a yellow solid: mp 213-214 °C; ¹H-NMR (500 MHz, CDCl₃): δ 3.38 (s, 4H), 4.08 (s, 6H), 7.81 (s, 2H), 10.60 (s, 2H); ¹³C-NMR (75.46 MHz, CDCl₃): δ 29.4, 30.1, 63.1, 120.5, 122.5, 129.9, 142.3, 143.4, 151.1; GC-MS *m/z* (relative intensity) 270 (M⁺, 100), 255 (25), 212 (30), 152 (10), 115 (10).

(b) Method B: Diformylation using the Duff method.

General procedure: 5,6-Dimethoxyacenaphthene (0.214 g, 1.00 mmol) and hexamethylenetetramine (0.308 g, 2.20 mmol) were dissolved in anhydrous trifluoroacetic acid (15 mL), under N₂. The reaction mixture was heated at reflux with stirring for 12 h and the resulting dark-brown solution was quenched by the addition of 2 M HCl_(aq) (10 mL) with stirring at room temperature for 15 min. The reaction mixture was extracted with dichloromethane (3 × 20 mL), the combined organic layers were washed with 4 M HCl_(aq) (10 mL), water (20 mL) and brine (10 mL), then dried over MgSO₄, filtered and the solvent removed on a rotavap. The crude product (0.25 g) was purified by column chromatography (3:7 ethyl acetate:hexanes) to give compound **50a** (0.12 g, 43%) as a yellow solid having identical characterization data to those obtained from Method A.

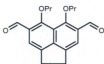
4,7-Diformyl-5,6-diethoxyacenaphthene (50b).



Using the general Kornblum procedure used for **50a**: To a suspension of NaHCO_3 (6.72 g, 80.0 mmol) in DMSO (50 mL) at 40 °C was added 4,7-bis(bromomethyl)-5,6-diethoxyacenaphthene (**48c**) (4.28 g, 10.0 mmol) and the mixture stirred at room temperature for 2 h. The reaction mixture was worked-up in a similar manner to the general procedure used for **50a**. The crude product obtained was purified by column chromatography (2:8 ethyl acetate:hexane) to give **50b** (1.9 g, 64%) as a yellow solid: mp 105.3 °C; $^1\text{H-NMR}$ (500 MHz, CDCl_3): δ 1.52 (t, $J = 5$, 6H) 3.3 (s, 4H), 4.24 (q, 4H), 7.80 (s, 2H), 10.61 (s, 2H); $^{13}\text{C-NMR}$ (75.46 MHz, CDCl_3): δ 15.2, 30.0, 74.7, 119.8, 120.6, 128.7, 142, 3, 148.8, 159.5, 190.5; GC-MS m/z (relative intensity) 298 (M^+ , 100), 269 (10), 241 (50), 214 (80), 196 (16), 157 (24), 139 (24).

Using the general Duff procedure used for **50a**: 5,6-Diethoxyacenaphthene (**37c**) (0.500 g, 2.07 mmol) and hexamethylenetetramine (0.636 g, 4.54 mmol) were dissolved in anhydrous trifluoroacetic acid (15 mL) under N_2 atmosphere. The reaction mixture was heated at reflux, with stirring, for 12 h and then worked-up in a similar manner to the general procedure used for **50a**, to afford a product (0.375 g) which was purified by column chromatography (3:7 ethyl acetate:hexanes) to give **50b** (0.25 g, 40%) as a yellow solid having identical characterization data to that obtained from the procedure used in Method A.

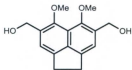
4,7-Diformyl-5,6-dipropoxyacenaphthene (50c).



Using the general Kornblum procedure used for **50a**: To a suspension of NaHCO_3 (2.95 g, 35.1 mmol) in dry DMSO (20 mL) at 40 °C was added 4,7-bis(bromomethyl)-5,6-dipropoxyacenaphthene (**48d**) (2.00 g, 4.40 mmol). The heating was removed, and the mixture was stirred for 2 h at room temperature, and then worked-up in a similar way to the general procedure used in Method A for **50a**, to give a crude product which was purified by chromatography (1:9 ethyl acetate:hexanes) to give **50c** (0.99 g, 69%) a yellow solid; 117-118 °C; $^1\text{H-NMR}$ (500 MHz, CDCl_3): δ 1.05 (t, $J = 7.5$ Hz, 6H), 1.94 (m, 4H), 3.35 (s, 4H), 4.09 (t, $J = 7.1$ Hz, 4H), 7.78 (s, 2H), 10.60 (s, 2H). $^{13}\text{C-NMR}$ (75.46 MHz, CDCl_3): δ 10.3, 23.0, 30.0, 80.7, 119.9, 120.6, 128.6, 142.7, 148.9, 159.8, 190.5; GC-MS m/z (relative intensity) 326 (M^+ , 100), 284 (8), 242 (98), 214 (100), 196 (25), 157 (25), 139 (27).

4,7-Bis(hydroxymethyl)-5,6-dimethoxyacenaphthene (49b).

(a) Method A: NaBH_4 reduction.



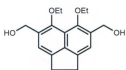
General procedure: To a solution of 4,7-diformyl-5,6-dimethoxyacenaphthene (**50a**) (1.00 g, 3.7 mmol) in 1:4 methanol:THF (50 mL), was added portion-wise sodium borohydride (0.14 g, 3.7 mmol) at room temperature, and the mixture stirred for 2 h. The reaction mixture was quenched with cold water (20 mL), followed by the addition of 2 M $\text{HCl}_{(\text{aq})}$ (5 mL). The mixture was extracted with ethyl

acetate (3 × 20 mL) and the combined organic layers were dried over anhydrous MgSO₄ and filtered. The solvent was removed on a rotavap and the resulting crude product purified by column chromatography (4:6 ethyl acetate:hexanes) to give **49b** (0.97 g, 96%) as a colorless solid: mp 158.2 °C; ¹H-NMR (500 MHz, (CD₃)₂CO): δ 3.32 (s, 4H), 3.84 (s, 6H), 4.1 (s, br. 2H), 4.85 (s, 4H), 7.40 (s, 2H); ¹³C-NMR (75.46 MHz, (CD₃)₂CO): δ 30.2, 61.8, 63.1, 120.1, 120.5, 132.4, 142.2, 142.6, 150.2; GC-MS *m/z* (relative intensity) 274 (M⁺, 100), 213 (60), 183 (40), 152 (15), 115 (10).

(b) Method B: hydrolysis using CaCO₃.

General procedure: A mixture of compound **48b** (2.00 g, 5.00 mmol) and CaCO₃ (5.00 g, 50.0 mmol) in aqueous 50% dioxane (120 mL) was heated at reflux, with stirring, for 24 h. The solvent was reduced to the half its volume on a rotavap and to the residue was added 6M HCl_(aq) (15 mL) and ethyl acetate (20 mL). The mixture was stirred for 15 min and then was extracted with ethyl acetate (3 × 20 mL). The combined organic layers were washed with water (2 × 20 mL), dried over anhydrous MgSO₄, and filtered. The solvent was removed on a rotavap and the crude product purified by column chromatography (4:6 ethyl acetate:hexanes) to give compound **49b** (1.2 g, 84%) as a colorless solid having identical characterization data to that obtained from Method A.

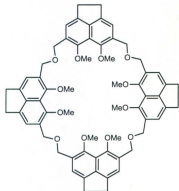
4,7-Bis(hydroxymethyl)-5,6-diethoxyacenaphthene (**49c**).



Using the general procedure of Method A used for compound **49b**: To a solution of 4,7-diformyl-5,6-diethoxyacenaphthene (**50b**) (0.993 g, 3.33 mmol) in 1:4 methanol:THF, (30 mL), sodium borohydride (0.127 g, 3.33 mmol) was added portion-wise at room temperature. The reaction mixture was stirred for 2 h at room temperature, and then the reaction mixture was worked-up in a similar manner to the general procedure used in Method A for **59b**, to give a crude product which was purified by chromatography using (4:6 ethyl acetate:hexanes) to give **49c** (0.94 g, 93%) as a colorless solid; mp 125 °C; $^1\text{H-NMR}$ (500 MHz, CDCl_3): δ 1.47 (t, $J = \text{Hz}$, 6H), 2.50 (s, br., 2H), 3.32 (s, 4H), 4.06 (q, $J = 7.0 \text{ Hz}$, 6H), 4.86 (s, 4H), 7.25 (s, 2H); $^{13}\text{C-NMR}$ (75.46 MHz, CDCl_3): δ 15.8, 30.2, 62.2, 71.7, 120.4, 120.5, 132.5, 142.0, 142.4, 149.2; GC-MS m/z (relative intensity) 302 (M^+ , 100), 227 (40), 211 (100), 171 (40), 152 (20), 141 (20), 115 (15).

Using the general procedure of Method B used for compound **49b**: A mixture of 4,7-bis(bromomethyl)-5,6-diethoxyacenaphthene (**48c**) (0.993 g, 3.33 mmol) and CaCO_3 (3.33 g, 33.3 mmol) in 50% aqueous dioxane (60 mL) was heated at reflux, with stirring, for 24 h. The reaction mixture was then worked-up in similar manner to the general procedure used in Method B for **59b**, to give, a crude product which was purified by chromatography (4:6 ethyl acetate: hexanes) to give **49c** (0.80 g, 80%) as a colorless solid having identical characterization data to that obtained from Method A.

Octahomotetraoxacalix[4]acenaphthene (**47b**).



To a mixture of NaH (0.083 g, 3.5 mmol) in anhydrous THF (130 mL) **49b** (0.236 g, 0.868 mmol) stirred at room temperature under Ar, a solution of **48b** (0.347 g, 0.868 mmol) in THF was added over a 2 h period using a syringe-pump. The reaction mixture was heated at reflux for 24 h. After the reaction mixture was cooled to room temperature and was quenched with water (50 mL),

the solvent was reduced to half its volume on a rotavap. The resulting mixture was extracted with ethyl acetate (3 × 30 mL). The combined organic layers washed with 2M HCl_(aq) (10 mL), dried over anhydrous MgSO₄ and filtered. The solvent was removed on a rotavap and the residue purified by column chromatography (2:3 ethyl acetate:hexanes) to afford **47b** (0.11 g, 24%) as a colorless solid; mp 220 °C (dec.); ¹H-NMR (500 MHz, CDCl₃): δ 3.27 (s, 4H), 3.62 (s, 6H), 4.76 (s, 4H), 7.32 (s, 2H); ¹³C-NMR (75.46 MHz, CDCl₃): δ 30.1, 62.9, 67.0, 120.0, 121.6, 129.6, 141.5, 142.7, 150.9; (+)-MALDI-TOF MS *m/z* (relative intensity) 1025.4622 (*M*⁺, 70), 1024.4579 (100).

Crystal data for **47b**: C_{65.50}H_{67.50}O₁₂, *M* = 1046.75, colorless prism, space group I4₁/acd (no.142), *a* = 27.6050(9) Å, *c* = 32.4280(13) Å, *V* = 24711.3(15) Å³, *Z* = 16, *D*_c = 1.125 g/cm³, *F*₀₀₀ = 8904, μ(Mo Kα) = 0.77 cm⁻¹, *T* = 295(1) K, 2θ_{max} = 59.8°, 5752 reflections collected, 5752 unique (*R*_{int} = 0.000). Final GoF = 1.160, *R*1 (*I* > 2.00σ(*I*)) = 0.0904, *R*(all reflections) = 0.1274, w*R*2 (all reflections) = 0.2371.

Association constant determinations.

Association constant (K_{assoc}) **47b** studies in toluene- d_6 solutions between **47b** with C_{60} were determined by ^1H NMR spectroscopy from the changes in the chemical shifts of the respective proton signals. For the determination of K_{assoc} values, the non-linear curve fitting plots^{32b} from 1:1 binding isotherms as described by Connors^{32a} were employed.

In a typical experiment, aliquots of the stock solutions of host **47b** (1.00 mL, 3.42×10^{-3} M solutions) were added to NMR tubes, and weighed amounts of solid C_{60} were then added in small portions directly to the host solutions in the NMR tubes. The resulting solutions were sonicated for approx. 10 min before NMR measurements were recorded at 298 K at 500 MHz.

References

1. Asfari, Z.; Böhmer, V.; Harrowfield, J.; Vicens, J.; Eds., *Calixarenes 2001*, Kluwer Academic Publishers, Dordrecht, The Netherlands 2001, pp 236-248, and references cited therein.
2. Araki, K.; Hashimoto, N.; Otsuka, H.; Shinkai, S. *J. Org. Chem.* **1993**, *58*, 5958.
3. Gutsche, C. D.; Muthukrishnan, R.; No, K. H. *Tetrahedron Lett.* **1979**, 2213.
4. Dhawan, B.; Gutsche, C. D. *J. Org. Chem.* **1983**, *48*, 1536.
5. (a) Hampton, P. D.; Tong, W.; Bencze, Z.; Daitch, C. E. *J. Org. Chem.* **1994**, *59*, 4838.
(b) Hampton, P. D.; Daitch, C. E.; Alam, T. M.; Bencze, Z.; Rosay, M. *Inorg. Chem.* **1994**, *33*, 4750. (c) Daitch, C. E.; Hampton, P. D.; Duesler, E. N. *Inorg. Chem.* **1995**, *34*, 5641. (d) Daitch, C. E.; Hampton, P. D.; Duesler, E. N. Alam, T. M. *J. Am. Chem. Soc.* **1996**, *118*, 7769. (e) Hampton, P. D.; Daitch, C. E.; Alam, T. M.; Pruss, E. *A. Inorg. Chem.* **1997**, *36*, 2879.
6. (a) Masci, B. *Tetrahedron* **1995**, *51*, 5459. (b) Masci, B.; Finelli, M.; Varrone, M. *Chem. Eur. J.* **1998**, *4*, 2018. (c) Masci, B. *Tetrahedron* **2001**, *57*, 2841. (d) Masci, B. *J. Org. Chem.* **2001**, *66*, 1497. Masci, B. In *Calixarenes 2001*; Asfari, Z.; Böhmer, V.; Harrowfield, J.; Vicens, J.; Eds., Kluwer Academic Publishers, Dordrecht, The Netherlands, 2001.
7. (a) Komatsu, N. *Tetrahedron Lett.* **2001**, *42*, 1733. (b) Komatsu, N. *Org. Biomol. Chem.* **2003**, *1*, 204.
8. Georghiou, P. E.; Li, Z.; Ashram, M.; Chowdhary, S.; Mizyed, S.; Tran, A. H.; Al-Saraierh, H.; Miller, D. O. *Synlett* **2005**, 879.

9. Ashram, M.; Mizyed, S.; Georghiou, P. E. *J. Org. Chem.* **2001**, *66*, 1473.
10. Ashram, M. Ph.D. Dissertation, Memorial University of Newfoundland, 1997.
11. Al-Saraierh, H. Ph.D. Dissertation, Memorial University of Newfoundland, 2007.
12. Tran, A. H.; Miller, D. O.; Georghiou, P. E. *J. Org. Chem.* **2005**, *70*, 1115.
13. Mizyed, S.; Ashram, M.; Miller, D. O.; Georghiou, P. E. *J. Chem. Soc. Perkin Trans. 2*, **2001**, 1916.
14. Poh, B.-L.; Lim, C. S.; Khoo, K. S. *Tetrahedron Lett.* **1989**, *30*, 1005.
15. (a) Poh, B.-L.; Team, C. M. *Tetrahedron* **2005**, *61*, 5123. (b) Poh, B.-L.; Tan, C.-M. *J. Incl. Phenom. Macro. Chem.* **2000**, *38*, 69. (c) Poh, B.-L.; Tan, C.-M. *Tetrahedron* **1995**, *51*, 953. (d) Poh, B.-L.; Tan, C.-M. *Tetrahedron* **1994**, *50*, 3453. (f) Poh, B.-L.; Tan, C.-M.; Wong, W. M. *Tetrahedron* **1993**, *49*, 7259. (g) Poh, B.-L.; Tan, C.-M.; Loh, C. L. *Tetrahedron* **1993**, *49*, 3849. (h) Poh, B.-L.; Lim, C. S.; Koay, L. S. *Tetrahedron* **1990**, *46*, 6155. (i) Poh, B.-L.; Lim, C. S.; Koay, L. S. *Tetrahedron* **1990**, *46*, 3651. (j) Poh, B.-L.; Seah, L. H.; Lim, C. S.; *Tetrahedron* **1990**, *46*, 4379. (k) Poh, B.-L.; Koay, L. S. *Tetrahedron Lett.* **1990**, *31*, 1911.
16. Molecular modeling was conducted using the MMFF force field with Spartan'10 software by Wavefunction Inc., Irvine, CA.
17. (a) Georghiou, P. E.; Li, Z. *Tetrahedron Lett.* **1993**, *34*, 2887. (b) Georghiou, P. E.; Li, Z. *J. Incl. Phenom. Mol. Recogn. Chem.* **1994**, *19*, 55. (c) Li, Z. Ph. D. Dissertation, Memorial University of Newfoundland, 1996.
18. Bew, P. S.; Sharma, S. *J. Org. Chem.* **2011**, *76*, 7076.

- (b) Morikawa, O.; Nagamastu, Y.; Nishimura, A.; Kobayashi, K.; Konishi, H. *Tetrahedron Lett.* **2006**, *47*, 3991. and references therein.
19. Brotin, T.; Roy, V.; Dutasta, J.-P. *J. Org. Chem.* **2005**, *70*, 6187.
20. Tanaka, N.; Kasai, T. *Bull. Chem. Soc. Jpn.* **1981**, *54*, 3020.
21. (a) Ulmann, F. *Chem. Ber.* **1904**, *37*, 853. (b) Lindley, J. *Tetrahedron* **1984**, *40*, 1433.
22. (a) Merner, B. L.; Dawe, L. N.; Bodwell, G. J. *Angew. Chem. Int. Ed.* **2009**, *48*, 5487.
(b) Vogel, A. I. *Vogel's Textbook of Practical Organic Chemistry* 5th Ed.; Longman; London, 1989.
23. Neudorff, W. D.; Lentz, D.; Anibarro, M.; Schluter, A. D. *Chem. Eur. J.* **2003**, *9*, 2745.
24. Torii, S.; Tanaka, H.; Siroi, T.; Akada, M. *J. Org. Chem.* **1979**, *44*, 3305.
25. (a) Aalten, H. L.; van Koten, G.; Grove, D. M.; Kuilman, T.; Piekstra, O. G.; Hulshof, L. A.; Sheldon, R. A. *Tetrahedron* **1989**, *45*, 5565. (b) Keegstra, M. A.; Peters, T. H. A.; Brandsma, L. *Tetrahedron* **1992**, *48*, 3633.
26. (a) Georghiou, P. E.; Ashram, M.; Li, Z.; Chaulk, S. G. *J. Org. Chem.* **1995**, *60*, 7284. (b) Georghiou, P. E.; Ashram, M.; Clase, H. J.; Bridson, J. N. *J. Org. Chem.* **1998**, *63*, 1819.
27. Falana, O. M.; Al-Farhan, E.; Keehn, P. M.; Stevenson, R. *Tetrahedron Lett.* **1994**, *35*, 65.
28. (a) Snieckus, V. *Chem. Rev.* **1990**, *90*, 879. (b) Biehl, E. R.; Deshmukh, A. R.; Dutta, M. *Synthesis* **1993**, 885.
29. Falana, O. M.; Al-Farhan, E.; Keehen, P. M. *Tetrahedron Lett.* **1994**, *35*, 65.

30. Kornblum, N.; Jones, W. J., Anderson, G. J. *J. Am. Chem. Soc.* **1959**, *81*, 4113.
31. Dawe, L. N. *X-ray Structure Report, TH4-14, August 8, 2011*– Appendix C, Compound **47b**, this Thesis.
32. (a) K. A. Connors, *Binding Constants*, Wiley, New York, 1987. (b) Association constants were calculated using non-linear curve fitting using the program ORIGINPro 7.5 from OriginLab Corporation, or with Excel for simple linear regression analysis.

Chapter 5

Naphthalene ring-based homooxacalix[4]arenes

5.1 Introduction

5.1.1 Heterocalixarenes

Research and development in the chemistry of calixarenes has increased substantially over the past 20 years. Since the seminal work done by Gutsche¹ on the chemistry of the calixarenes which has made calix[*n*]arenes (*n*= 4,6,8) easy to synthesize, many publications have appeared focusing on the development of new methods to synthesize differently-functionalized calixarenes in order to evaluate their properties.

One of the major developments in calixarene synthesis is the construction of "mixed" calixarenes in which one or more of their phenol units have been replaced with other aromatic or heteroaromatic rings, in order to improve their cavity structures and as a result, their molecular recognition properties and selectivities. Interesting heterocalixarenes which have been synthesized and their properties studied include: calixpyrroles² (1), calixfurans³ (2), calixthiophenes⁴ (3), calixpyridines⁵ (4), and calixindoles⁶ (5), each of which consist respectively, of four pyrrole, pyridine, furan, thiophene and indole rings linked via carbon bridges, as shown in Figure 5.1.

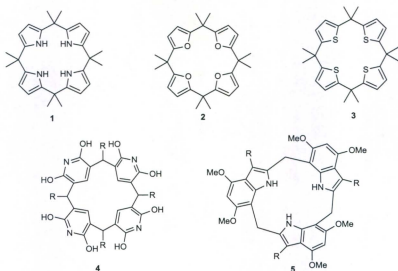


Figure 5.1. Heterocyclic ring-based calixarenes 1-5.

Mixed-heterocalixarenes have also been synthesized using different types of heterocycles, such as: calix[2]bipyrrole[2]thiophene (**6**),⁷ calix[2]bipyrrole[2]furan (**7**),⁷ and the mixed indolecalix[4]arene (**8**),⁸ (Figure 5.2). The synthesis of calix[2]bipyrrole[2]thiophene (**6**) and calix[2]bipyrrole[2]furan (**7**), (Figure 5.2), from the reaction of bipyrrole with thiophene and furan respectively, have been reported by Sessler and co-workers.⁷ ¹H-NMR titration studies revealed that **6** and **7** were able to bind to benzoate and acetate anions strongly and selectively when compared with bromide or chloride anions.

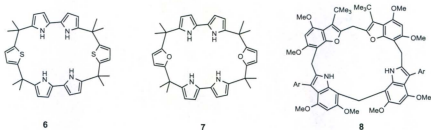


Figure 5.2. Mixed heterocalix[4]arenes **6**, **7** and **8**.

Large mixed heterocalixarene macrocycles such as **9**⁹ and **10**¹⁰ (Figure 5.3), have been synthesized via a convergent approach, starting from *p*-substituted phenols and benzimidazol-2-one units. Both heterocalix[8]arene (**9**) and heterocalix[9]arene (**10**) showed unusual activities as host molecules due to the benzimidazol-2-one unit which has the ability to enhance the formation of more rigid large macrocycles than those formed from anisole units alone, and which also increased the interaction with the guest molecules. Crystallization of **9** from 3-methylpyridine, and **10** from acetone and dichloromethane solutions both afforded single crystals suitable for X-ray crystallographic analysis. The X-ray structure of **9**⁹ revealed the inclusion of 3-methylpyridine and water molecules in a 1:2:1 ratio of host:3-methylpyridine:H₂O. Heterocalix[9]arene (**10**)¹⁰ formed a 1:2:2 complex with acetone and dichloromethane (Figure 5.4).

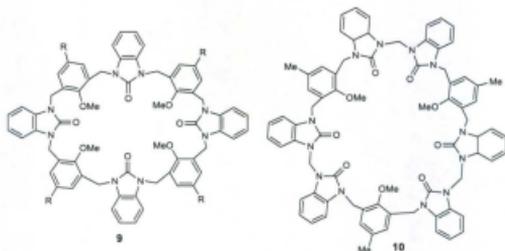


Figure 5.3. Heterocyclic-based calixarenes **9** and **10**.

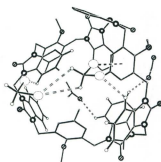
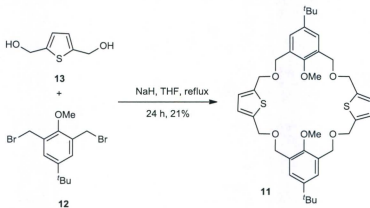


Figure 5.4. X-ray structure showing the inclusion complex of **10** with acetone and dichloromethane.

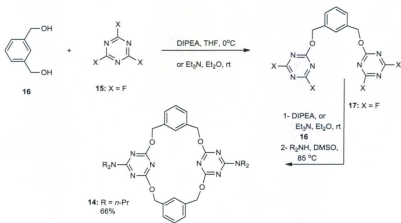
A mixed thiophene-octahomotetraoxacalixarene (**11**) was reported by the Georghiou group¹¹ in 2009. This compound was synthesized via a [2+2] condensation of 2,6-bis(bromomethyl)-4-*tert*-butylanisole (**12**) and 2,5-bis(hydroxymethyl)thiophene (**13**) using sodium hydride in the base-mediated cyclization reaction, (Scheme 5.1). Molecular modeling suggested that it could be a host for C₆₀ or C₇₀ fullerenes. A single crystal X-

ray diffraction analysis revealed the formation of a dimer in the asymmetric unit. Titration experiments using $^1\text{H-NMR}$ with C_{60} and C_{70} in toluene- d_8 , benzene- d_6 or CS_2 , however, failed to show any evidence for complex formation.



Scheme 5.1. Mixed thiophene-octahomotetraoxacalixarene **11**.

In 2010, Mei-Xiang Wang and co-workers¹² reported the synthesis of the homoheterocalix[2]arene[2]triazine (**14**) (Scheme 5.2). The linear trimer precursors were prepared starting from cyanuric halides **15** and 1,3-phenylenedimethanol (**16**) in the presence of base to give the trimers **17** in 87% yield. Coupling of the linear trimers **17** with **14** under basic conditions produced the corresponding macrocycle **14** in 66% yield.



Scheme 5.2. Tetrahomotetraoxacalix[2]arene[2]triazine (**14**).

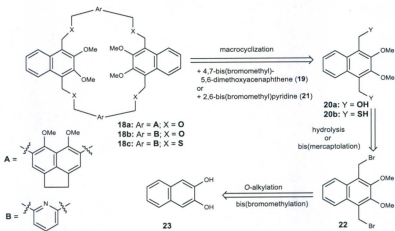
5.2 Synthesis of octahomotetraoxacalix[2]acenaphthene[2]naphthalene (**18a**), octahomotetraoxacalix[2]naphthalene[2]pyridine (**18b**)

5.2.1 Retrosynthetic analysis

The retrosynthetic analysis outlined in Scheme 5.3 suggested that octahomotetraoxacalix[2]naphthalene[2]acenaphthene (**18a**) could be obtained *via* a Williamson ether cross-coupling reaction between 4,7-bis(bromomethyl)-5,6-dimethoxyacenaphthene (**19**) and 1,4-bis(hydroxymethyl)-2,3-dimethoxynaphthalene (**20a**).

Also, the same retrosynthetic analysis indicated that the octahomotetraoxa- (**18b**) and octahomotetraoxacalix[2]naphthalene[2]pyridine (**18c**) could be obtained *via* base-mediated cross-coupling reaction between 1,4-bis(hydroxymethyl)-2,3-dimethoxy

naphthalenes (**20a**) or 1,4-bis(mercaptomethyl)-2,3-dimethoxynaphthalenes (**20b**) with 2,6-bis(bromomethyl)pyridine (**21**). 1,4-Bis(bromomethyl)-2,3-dimethoxy-naphthalene (**22**) could be derived from 2,3-dimethoxynaphthalene (**23**) which in turn, was synthesized from 2,3-dihydroxynaphthalene (**24**).

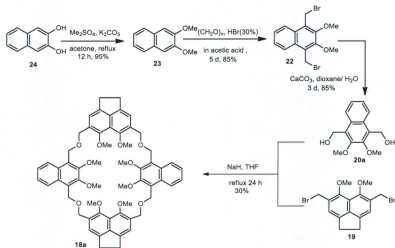


Scheme 5.3. Retrosynthetic analysis of macrocycles **18a-c**.

5.2.2 Results and discussions

The target molecule, octahomotetraoxacalix[2]acenaphthene[2]naphthalene (**18a**), was synthesized from the coupling of two intermediates, 4,7-bis(bromomethyl)-5,6-dimethoxyacenaphthene (**19**) and 1,4-bis(hydroxymethyl)-2,3-dimethoxynaphthalene (**20a**). The synthesis of **19** was previously disclosed in Chapter 4. The other intermediate **20a**, was prepared according to the procedures which were reported by Georghiou and co-workers.¹³ Thus, 2,3-dimethoxynaphthalene (**23**) was synthesized from commercially-

available 2,3-dihydroxynaphthalene (**24**). *O*-Alkylation of **24** with dimethyl sulfate in the presence of K_2CO_3 in acetone heated at reflux for a period of 12 h produced the desired product in 95% yield, after purification by column chromatography. Double bromomethylation of 2,3-dimethoxynaphthalene (**23**), using six equivalents of 30% hydrogen bromide in glacial acetic acid, and six equivalents of paraformaldehyde furnished 1,4-bis(bromomethyl)-2,3-dimethoxynaphthalene (**22**) in 85% yield. Hydrolysis of **24** with $CaCO_3$ in refluxing aqueous dioxane, gave 1,4-bis(hydroxymethyl)-2,3-dimethoxynaphthalene (**20a**). A Williamson cross-coupling reaction between precursors **19** and **20a** produced the desired macrocycle **18a** in 30% yield.



Scheme 5.4. Synthesis of octahomotetraoxacalix[2]acenaphthalene[2]naphthalene (**18a**).

5.2.3 NMR spectra of 18a

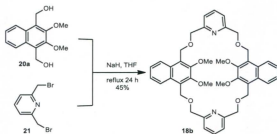
The ^1H - and ^{13}C -NMR spectra of the macrocycle **18a** were very simple and were in agreement with the expected structure. The simplicity of the ^1H - and ^{13}C -NMR spectra confirmed the high symmetry due to rapid interconversion between the different "cone" conformations in which all of the methoxy groups appear as two 12-proton singlets at δ 3.76 and 3.87 ppm. The two sets of methylene protons appear as two sharp singlet signals at δ 4.81 and 5.07 ppm, and there is also one sharp singlet signal at δ 3.21 ppm assigned the ethylene-bridge of acenaphthene rings. One sharp singlet signal appears downfield at δ 7.23 ppm due to the acenaphthyl ring protons and two sets of signals due to the naphthyl ring protons appear as multiplets at δ 7.31-7.33 and at δ 8.03 ppm, as a doublet of doublets with $J = 6.5$ and 3.0 Hz.

The ^{13}C -NMR spectrum is consistent with the assigned structure as a symmetrical macrocycle in an interconverting "cone" conformation in the CDCl_3 solution at room temperature. The ^{13}C -NMR spectrum shows five signals in the upfield region assigned to the two different sets of methoxy groups, the two sets of methylene groups, and one signal for the $-\text{CH}_2\text{CH}_2-$ bridges of the acenaphthyl rings. Eleven signals in the downfield region are related to the corresponding carbons of the aromatic rings.

5.3 Synthesis of octahomotetraoxacalix[2]naphthalene[2]pyridine (**18b**)

5.3.1 Results and discussion

The synthesis of the mixed naphthalene and pyridine ring-containing, octahomotetraoxacalix[2]naphthalene[2]pyridine (**18b**), (Scheme 5.5), was achieved using 2,5-bis(bromomethyl)pyridine (**21**) and 2,3-dihydroxynaphthalene (**24**). As disclosed above, *O*-alkylation of **24** was achieved using dimethyl sulfate in the presence of K_2CO_3 in acetone to produce 2,3-dimethoxynaphthalene (**23**), which is smoothly converted to the 1,4-bis(bromomethyl)-2,3-dimethoxynaphthalene (**22**), upon treatment with paraformaldehyde and 30% hydrogen bromide in glacial acetic acid in 85% yield. Treatment of **22** with $CaCO_3$ in aqueous 50% dioxane gave 1,4-bis(hydroxymethyl)-2,3-dimethoxynaphthalene (**20a**).



Scheme 5.5. Synthesis of octahomotetraoxacalix[2]naphthalene[2]pyridine (**18b**).

A THF solution of the 2,6-bis(bromomethyl)pyridine (**21**) was added slowly to a suspension of NaH and **20a** in anhydrous THF *via* a syringe pump over a 2 h period,

followed by heating the resulting mixture at reflux for 24 h, to produce the octahomotetraoxacalix[2]naphthalene[2]pyridine (**18b**) in 45% yield.

5.3.2 NMR spectra of **18b**

The ambient ^1H - and ^{13}C -NMR spectra of **18b** in CDCl_3 are very simple and show only one set of proton and carbon resonance signals. The simplicity of the ^1H - and ^{13}C -NMR spectra indicates that fast conformational equilibration of the macrocycle has occurred. The ^1H -NMR spectrum shows three sharp singlet signals at δ 3.79, 4.44 and 5.10 ppm, corresponding to the methoxy protons, and the methylene protons of the two bridges, respectively. Also, the ^1H -NMR shows three down-field signals: one appears as a multiplet at δ 7.17–7.20 ppm, corresponding to the naphthyl and pyridine units, the other two signals are at δ 7.47 ppm as a triplet with $J = 7.5$ Hz, and at δ 8.10 ppm, as a doublet of doublets with $J = 6.5$ and 3.0 Hz, corresponding to the pyridine and naphthyl units respectively. The ^{13}C -NMR spectrum shows the chemical shifts for the methylene carbon bridges at δ 61.44 and 62.91 ppm. Both the ^1H - and ^{13}C -NMR spectra therefore are consistent with the macrocycle structure being highly symmetrical and conformationally mobile.

5.3.3 X-Ray crystallography of **18b**

Crystals of macrocycle **18b** were obtained by slow evaporation of the solvent chloroform, or the mixed methanol and dichloromethane solvents used to dissolve the macrocycle. The slow evaporation of the solvent(s) gave colourless crystals which were

suitable for X-ray diffraction analysis. The X-ray structure of the single crystal from CDCl_3 shows that the macrocycle adopted a *1,3-alternate*-type conformation in the solid state with a C_{2v} symmetry (Figure 5.5a). On the other hand, the X-ray structure for the single crystal obtained from the mixed methanol and dichloromethane solvent shows that the macrocycle adopted a *cone*-type conformation (Figure 5.5b). Presumably methanol forms H-bonding with the nitrogen atoms to stabilize the "*cone*" conformer.

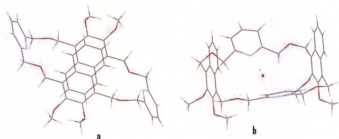


Figure 5.5. The X-ray structures of macrocycle **18b** in (a): a "*1,3-alternate*" (left), and (b): "*cone*" conformation (right).

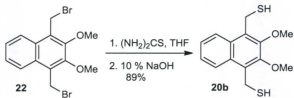
5.4 Attempts at the synthesis of octahomotetrathiacalix[2]naphthalene[2]pyridine (18c)

5.4.1 Results and discussion

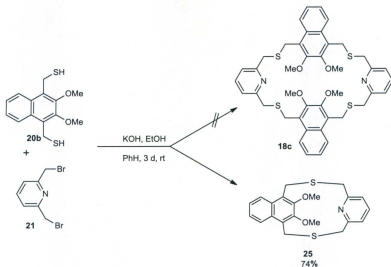
Although an oxygen atom is more electronegative than a sulfur atom, the latter can share non-bonding electrons more easily due to the high polarizability of the sulfur atom. Therefore, it was anticipated that synthesis of homothiacalix[2]naphthalene[2]pyridine

(**18c**) by replacing the $-\text{CH}_2\text{OCH}_2-$ linkages in **18b** with $-\text{CH}_2\text{SCH}_2-$ linkage could produce a new type of calixarene that could have the potential to accommodate different types of electron-deficient guests such as fullerene C_{60} , as well as “soft” cationic guests. 1,4-Bis(bromomethyl)-2,3-dimethoxynaphthalene (**22**)¹³ as disclosed previously, was synthesized from 2,3-dihydroxynaphthalene (**24**) in two steps with an overall yield of 67% (see, Scheme 5.3). 1,4-Bis(mercaptomethyl)-2,3-dimethoxynaphthalene (**20b**),¹⁴ (Scheme 5.6) was prepared by treating compound **22** with thiourea in THF, followed by hydrolysis with NaOH under refluxing conditions to give the desired product in 89% yield.

A coupling reaction between **20b** and **21** took place under basic conditions at room temperature. However, the main product (Scheme 5.7), of this reaction is the dimer product **25**, which was obtained in 73% yield instead of the desired octahomotetraphthalene calix[2]pyridine[2]naphthalene (**18c**).



Scheme 5.6. Synthesis of 1,4-bis(mercaptomethyl)-2,3-dimethoxynaphthalene (**20b**).



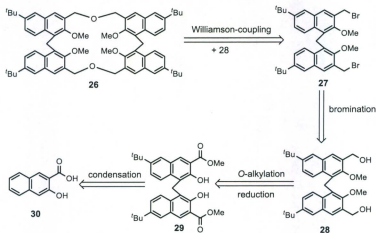
Scheme 5.7. Attempted synthesis of octahomotetrathiacalix[2]naphthalene[2]pyridine (**18c**).

5.5 Synthesis of tetrahomodioxacalix[4]naphthalene (**26**)

5.5.1 Retrosynthetic analysis

The retrosynthetic analysis outlined in Scheme 5.8 suggested that the tetrahomodioxacalix[4]naphthalene (**26**) could be obtained *via* a Williamson ether cross-coupling reaction between bis(3-bromomethyl-7-*tert*-butyl-2-methoxy-1-naphthyl)methane (**27**) and bis(3-hydroxymethyl-7-*tert*-butyl-2-methoxy-1-naphthyl)methane (**28**) precursors. The intermediate **27** was synthesized from bis(methyl-7-*tert*-butyl-2-hydroxy-3-naphthyl)methane (**28**) after protection of the phenolic groups using dimethyl sulfate, and reduction of the ester groups. Also, the intermediate bis(3-bromomethyl-7-*tert*-butyl-2-methoxy-1-naphthyl)methane (**27**) was synthesized from the reaction of intermediate (**28**)

with phosphorus tribromide. The bis(methyl-7-*tert*-butyl-2-hydroxy-3-naphthyl)methane (28), in turn, was derived from reduction of methyl-7-*tert*-butyl-3-hydroxy-2-naphthoate (29) after *O*-alkylation. Friedel-Crafts alkylation of 3-hydroxy-2-naphthoic acid (30) followed by condensation with paraformaldehyde in acidic conditions produced 29.



Scheme 5.8. Retrosynthetic analysis of tetrahomodioxacalix[4]naphthalene (26).

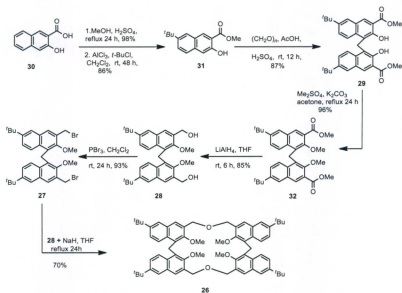
5.5.2 Results and discussion

The strategy required to construct the tetrahomodioxacalix[4]naphthalene (26) again started from the 3-hydroxy-2-naphthoic acid (30) (Scheme 5.9). The key intermediate 29 was synthesized via the reaction sequence as follows: esterification, followed by Friedel-Crafts *tert*-butylation to give 31, and condensation of 31 with paraformaldehyde to give 29 in overall yield of 73% over three steps. Protection of the phenolic groups of 29 was achieved using dimethyl sulfate in the presence of K_2CO_3

followed by reduction of the ester groups using lithium aluminium hydride in anhydrous THF to produce the bis(hydroxymethyl) **28** in 85% yield. Treatment of **28** with phosphorus tribromide afforded bis(bromomethyl) **27** in 93% yield. The coupling reaction between the intermediates **28** and **27** (Scheme 5.9), in the presence of sodium hydride, was conducted as follows: a solution of **27** in THF was added *via* a syringe pump to the THF solution mixture containing **28** and sodium hydride, over two hours under refluxing conditions to furnish tetrahomodioxacalix[4]naphthalene (**26**) in 70% yield. HRMS analysis showed the presence of a potassium adduct of the expected molecular ion peak for **26** at $m/z = 1003.586$ [$M + K$]⁺, (100 %) (calcd. 964.564 for C₆₆H₇₆O₆).

Tetrahomodioxacalix[4]naphthalene (**26**) had simple ¹H- and ¹³C-NMR spectra at ambient-temperature due to its high symmetry. The ¹H-NMR spectra in CDCl₃ indicate rapid interconversion of conformations at room temperature since all of the signals were sharp. Also, the bridging methylene groups and the ether linkage methylene groups appeared as sharp singlets. The ¹H-NMR spectrum shows four sharp singlet signals at δ 1.37, 3.06, 4.65 and 4.74 ppm that are assigned to the *tert*-butyl groups, the methoxy groups, the ether linkage and the methylene bridges, respectively. The spectrum also reveals a doublet, and a doublet of doublets centered at δ 8.02 and 7.46 ppm, with coupling constants of $J = 9.0$ Hz, and $J = 2.0$ Hz. A doublet appears at δ 7.69 ppm has coupling constant $J = 2.0$ Hz, and a sharp singlet at δ 7.77 ppm corresponding to the aromatic regions is also present. The ¹³C-NMR spectrum shows five up-field signals at δ

23.8, 31.2, 34.6, 61.8 and 67.4 ppm and ten down-field signals between δ 123 to 155 ppm.



Scheme 5.9. Synthesis of tetrahomodioxacalix[4]naphthalene (**26**).

5.6 Complexation studies

Due to the important cation- π interactions that exist in biological systems, many research groups have investigated different quaternary ammonium salts as “model” guests in host-guest studies involving e.g. cyclophanes in lipophilic solvents. A vast amount of research has also been devoted to studying the complexation of such ammonium salts and other organic cations with calixarenes. For example, Masci and co-

workers¹⁵ reported the synthesis of a series of homooxacalix[4]arenes and investigated their binding properties with several tetraalkylammonium picrate salts in CDCl_3 . Additionally, the complexation of *p*-substituted calix[4]arenes with tetramethylammonium salts having different counterions such as: chloride, tosylate, acetate, trifluoroacetate and picrate was described by Arduini and co-workers.¹⁶ The Georghiu group¹³ has synthesized homooxacalix[4]naphthalene receptors which have shown an ability to form complexes with tetramethylammonium chloride.

The technique commonly used to study association constants (K_{assoc}) in different solvent is by $^1\text{H-NMR}$ spectroscopy,¹⁷ which has the advantage of using a small amount of the compound under investigation, by titration measuring the chemically-induced chemical shifts (CIS). In practice, a "guest" compound for example tetraalkylammonium halide or tosylate etc. in CDCl_3 is gradually added to a solution of pure macrocycle **18b** in CDCl_3 . A clear change in the chemical shift of the guest signals can be measured after each addition (Figure 5.6).

The K_{assoc} values were calculated from $^1\text{H-NMR}$ titration experiments in CDCl_3 and were based upon measurement of the change in chemical shift ($\Delta\delta$) for the methyl group of the TMAA cation and methyl group of the acetate anion after each addition. The K_{assoc} were calculated using a non-linear regression analysis using the 1:1 binding isotherm according to Connors.¹⁸ Macrocycle **18b** formed 1:1 complexes with TMAA with apparent K_{assoc} values of $134 \pm 19 \text{ M}^{-1}$ and $504 \pm 52 \text{ M}^{-1}$ for the TMAA cation and methyl group of acetate anion respectively (Figures 5.7).

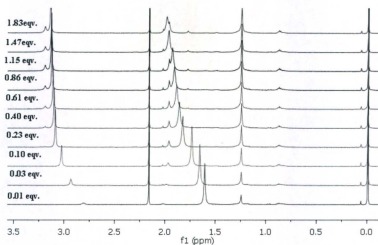


Figure 5.6. Partial ^1H -NMR spectra (500 MHz) of TMAA upon addition to the macrocycle 18b in CDCl_3 solution at 298 K.

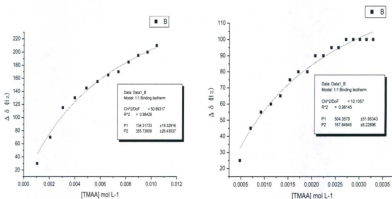


Figure 5.7. ^1H NMR titration curves for TMAA complexation with 18b, titration curves for TMA cation (*left*) and methyl group of acetate anion (*right*).

Wang and co-workers¹⁹ reported that their methylazacalix[4]pyridine macrocycle showed a highly selective recognition towards various diol compounds. Since various diol compounds have biological properties, such as for example, resveratrol and epigallocatechin-3 gallate, which are cancer chemopreventive diol compounds found in grapes and green tea, respectively, the design and synthesis of receptors to detect such compounds are of interest. It was therefore decided to undertake a similar complexation study with **18b**. ¹H-NMR titration of 1,3-dihydroxybenzene and 1,3-dihydroxynaphthalene with macrocycle **18b** showed that the signals of the proton between the two hydroxy groups shifted up-field. Using a nonlinear least-squares fit method based upon Connors,¹⁸ the ¹H-NMR titration revealed that both diol compounds formed 1:1 complexes with **18b**, and with association constant of 260 ± 2 and $509 \pm 4 \text{ M}^{-1}$ respectively, as shown in Figure 5.8.

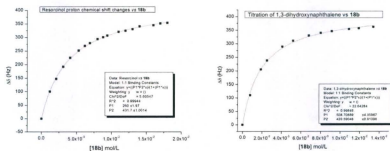


Figure 5.8. ¹H-NMR titration curves for **18b** with 1,3-dihydroxybenzene (*left*), and 1,3-dihydroxynaphthalene (*right*).

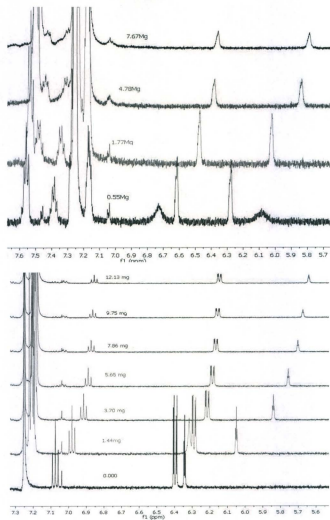


Figure 5.9. Expanded sections of the ¹H-NMR spectra (in 1mL, CDCl₃, 298 K) of 1,3-dihydroxybenzene (*top*) and 1,3-dihydroxynaphthalene (*bottom*) in the presence of increasing amounts of macrocycle **18b**.

5.6.1 Complexation with metal salts

Macrocycle **18b** was expected to show binding properties towards cations due to the presence of the pyridine nitrogen atoms. Lüning and co-workers²⁰ reported using ¹H-NMR spectroscopy to study the ability of macrocycles to extract metal cations from their solid salts. ¹H-NMR spectroscopy was also used in the present study to investigate the potential of the macrocycle **18b** to bind metal cations and to detect their extraction from their solid salts into an organic solvent. A stock solution of the macrocycle was prepared by dissolving macrocycle **18b** (ca. 5.00 mg) in 5.00 mL of CDCl₃ containing 5% DMSO-*d*₆. An excess amount of powdered NaNO₃, KNO₃, LiNO₃ and AgNO₃ salts were prepared in four separate vials. From the stock solution 1.00 mL of the macrocycle **18b** were added to each vial. After stirring at room temperature for 24 h, the solutions were filtered into individual NMR tubes. The ¹H-NMR spectra of these solutions were recorded and analyzed, based on CIS due to the complex formation, with reference to the free macrocycle **18b** (Figure 5.10).

When the ¹H-NMR spectra of the solutions containing NaNO₃, KNO₃, LiNO₃ and AgNO₃ salts were compared, the spectra suggested that macrocycle **18b** has the potential to bind more strongly with AgNO₃ than other metal salts. The ¹H-NMR spectra do not show any changes with NaNO₃, KNO₃, LiNO₃ salts. In the case of AgNO₃ a significant CIS, $\Delta\delta = 0.31$ ppm, of the pyridine protons for the *para*-proton of the pyridine ring and $\Delta\delta = 0.63$ ppm for the *meta*-proton of the pyridine were detected (Figure 5.8, AgNO₃).

This observation is consistent with Lüning's²⁰ observation that the nitrogen atoms in the pyridine rings form strong complexes with silver ions.

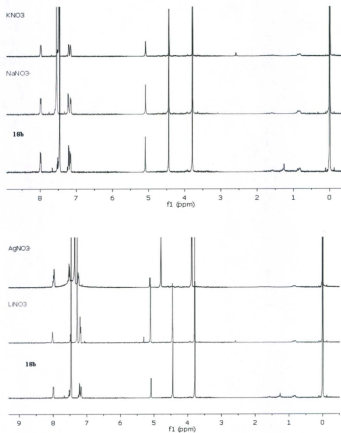


Figure 5.10. Expanded section of the ^1H -NMR spectra ($\text{CDCl}_3/5\% \text{ DMSO-}d_6$, 298 K) of macrocycle **18b** in the presence of different metal nitrate salts.

5.6.2 Protonation of the macrocycle

Protonation of the macrocycle **18b** using different concentrations of $\text{CF}_3\text{CO}_2\text{D}$ was monitored using $^1\text{H-NMR}$ in a study which is similar to that used to investigate the protonation of azacalix[*n*]pyridines by the Wang group.²¹ As expected, the $^1\text{H-NMR}$ titration experiments revealed significant downfield shifts of the pyridine ring protons upon treatment of the macrocycle **18b** with different concentrations of the $\text{CF}_3\text{CO}_2\text{D}$ at room temperature (Figure 5.11). The observed downfield shift or the deshielding effect can be explained by the fact that the protonation is taking place over the two pyridine ring nitrogen atoms.

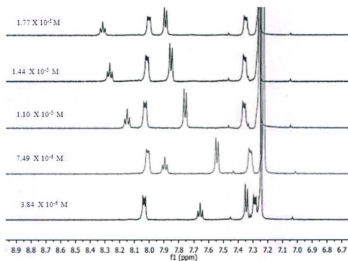


Figure 5.11. Expanded section of $^1\text{H-NMR}$ spectra of macrocycle **18b** in CDCl_3 at 298 K, in the presence of different concentrations of the $\text{CF}_3\text{CO}_2\text{D}$.

5.7 Conclusions

A series of new macrocyclic compounds, namely octahomotetraoxcalix [2]acenaphthene[2]naphthalene (**18a**), octahomotetraoxcalix[2]naphthalene[2]pyridine (**18b**), and tetrahomodioxcalix[4]naphthalene (**26**) have been synthesized and characterized. The complexation properties of **18b** have also been investigated but the complexation properties of the other macrocycles **18c** and **26** have not yet been elucidated. The ^1H - and ^{13}C -NMR spectra of all three macrocycles showed clearly that they were highly symmetrical and conformationally flexible. The X-ray structure of **18b** which crystallized from chloroform-*d*, and from a methanol:dichloromethane solvent revealed that the macrocycle adopted “*1,3-alternate*”- and “*cone*”-type conformations, respectively. The ^1H -NMR titration of **18b** with TMAA revealed formation of a 1:1 host-guest complex. A computer-assisted molecular mechanics modeling study (Figure 5.12),²² and CPK models suggested that macrocycle **18b** had the ability to host C_{60} , but the ^1H -NMR titration experiments did not demonstrate any such binding.



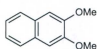
Figure 5.12. A computer-generated model of a 1:1 C_{60} :**18b** complex.²²

5.8 Experimental section

General methods, materials, and instrumentation used are identical to those described in Chapter 2.

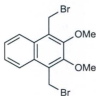
5.8.1 Experimental

2,3-Dimethoxynaphthalene (23).



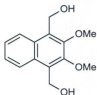
2,3-Dimethoxynaphthalene (**23**) was prepared as previously described by Tran et al.¹³

1,4-Bis(bromomethyl)-2,3-dimethoxynaphthalene (22).



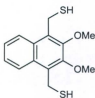
1,4-Bis(bromomethyl)-2,3-dimethoxynaphthalene (**22**) was prepared as previously described by Tran et al.¹³

1,4-Bis(hydroxymethyl)-2,3-dimethoxynaphthalene (20a).



1,4-Bis(hydroxymethyl)-2,3-dimethoxynaphthalene (**20a**) was prepared as previously described by Tran et al.¹³

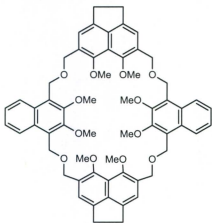
1,4-Bis(mercaptomethyl)-2,3-dimethoxynaphthalene (20b).



1,4-Bis(mercaptomethyl)-2,3-dimethoxynaphthalene (**20b**)

was prepared as previously described by Tran et al.¹⁴

Octahomotetraoxalix[2]acenaphthene[2]naphthalene (18a).

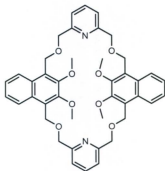


General procedure: To a solution of 1,4-bis(hydroxymethyl)-2,3-dimethoxynaphthalene (**20a**) (0.248 g, 1.00 mmol), in anhydrous THF (150 mL) at room temperature, NaH (0.160 g, 4.00 mmol) was added portion-wise. The mixture was stirred at room temperature for 20 min. 2,6-Bis(bromomethyl)acenaphthene (**19**, 0.400 g, 1.00 mmol) in anhydrous THF (30 mL)

was added to the solution over a period of 2 h using a syringe pump. The reaction mixture was then heated at reflux for 24 h and then cooled to room temperature. The excess sodium hydride was quenched by adding water dropwise, with cooling on an ice-bath. The solvent was then reduced to half of its volume on a rotavap, and the residue was dissolved in CH_2Cl_2 (100 mL). The organic layer was separated and was washed with

aqueous 2 M HCl (10 mL), brine (2 x 20 mL), and then dried over anhydrous sodium sulfate. After the solvent was removed on a rotavap, the product was purified by column chromatography (ethyl acetate:hexanes 15:85) to afford macrocycle **18a** (0.12 g, 25%) as a colourless solid compound, mp 190.3-191.0 °C, (dec.); ¹H-NMR (500 MHz, CDCl₃): δ 3.21 (s, 8H), 3.76 (s, 12H), 3.87 (s, 12H), 4.81 (s, 8H), 5.07 (s, 8H), 7.23 (s, 4H), 7.31-7.33 (m, 4H), 8.03 (dd, *J* = 6.5, 3.0 Hz, 4H); ¹³C-NMR (75.46 MHz, CDCl₃): δ 30.1, 61.8, 63.2, 63.2, 67.6, 119.9, 121.5, 124.8, 125.3, 126.7, 129.6, 130.7, 141.5, 142.6, 150.6, 151.0; (+)-APCI MS *m/z* (relative intensity) 996.2 ([M + Na]⁺, 20)

Octahomotetraoxalix[2]naphthalene[2]pyridine (**18b**).

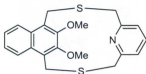


Using the general procedure for compound **18a**:

To solution of 1,4-bis(hydroxymethyl)-2,3-dimethoxynaphthalene (**20a**, 0.248 g, 1.00 mmol) in anhydrous THF (150 mL) at room temperature, NaH (60% in paraffin oil, 0.16 g, 4.0 mmol) was added portion-wise and the mixture stirred at room temperature for 20 minutes. 2,6-Bis(bromomethyl)-pyridine (**21**) (0.264 g, 1.00 mmol) in anhydrous THF (30 mL) was added to the solution using a syringe pump over a period of 2 h, and then the mixture was cooled to room temperature. The reaction mixture was worked-up as in the general procedure to afford a crude product which was purified by column chromatography (ethyl acetate:hexanes 1:9) to afford the macrocycle **18b** (0.12 g, 35%) as a colourless solid: mp 260-261.5 °C; ¹H-

NMR (500 MHz, CDCl₃): δ 3.79 (s, 12H), 4.44(s, 8H), 5.10 (s, 8H), 7.17–7.20 (m, 8H), 7.47 (t, $J = 7.5$ Hz, 2H), 8.10 (dd, $J = 6.5, 3.0$ Hz, 4H); ¹³C-NMR (75.46 MHz, CDCl₃): δ 61.4, 62.9, 119.5, 124.8, 125.2, 125.9, 130.4, 136.5, 151.0, 158.0; HRMS m/z (relative intensity) 725.390 ([M + Na]⁺, 100), 703.399 (M⁺, 12).

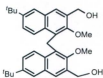
5(1,4)-2,3-Dimethoxynaphthalene-1(2,6)-pyridine-3,7-dithiacyclooctaphane (25).



To solution of KOH (0.336 g, 6.00 mmol) dissolved in ethanol (100 mL) under N₂, was added 1,4-bis(mercaptomethyl)-2,3-dimethoxynaphthalene (**20b**) (0.280 g, 1.00 mmol), and the mixture was stirred at room temperature for 30 min. After that, a solution of 2,6-bis(bromomethyl)pyridine (**21**, 0.265 g, 1.00 mmol) in benzene (20 ml) was added, using a syringe pump, over a period 3 h at room temperature. The reaction mixture was stirred for a further 48 h at room temperature after which solvent was removed on a rotavap. The residue was dissolved in CH₂Cl₂, washed with aqueous 10 % HCl (20 mL), water 30 mL, and the extracted organic layer was dried over anhydrous MgSO₄. After filtration, the solvent was removed on a rotavap and the resulting crude product was purified by column chromatography (ethyl acetate:hexane 1:9) to afford the compound **25** (0.28 g, 74%) as a colourless solid: mp 185.2–185.7 °C; ¹H-NMR (500 MHz, CDCl₃): δ 3.56 (dd, $J = 15.1, 6.2$ Hz, 4H), 4.82 (d, $J = 12.8$ Hz, 2H), 4.93 (d, $J = 12.8$ Hz, 2H), 6.61 (d, $J = 7.6$ Hz, 2H), 6.69 (t, $J = 6.7$ Hz, 1H), 7.18–7.20 (m, 2H), 7.75–7.77 (m, 2H); ¹³C-NMR (75.46 MHz, CDCl₃): δ 25.8,

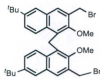
36.3, 60.9, 120.7, 124.3, 124.5, 128.4, 134.5, 151.2, 156.4; GC-MS m/z (relative intensity) 383 (M^+ , 100), 368 (20), 244 (45), 229 (20), 215 (15), 139 (40).

Bis(3-hydroxymethyl-7-*tert*-butyl-2-methoxy-1-naphthyl)methane (28).



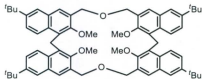
A solution of bis(methyl-7-*tert*-butyl-2-methoxy-3-naphthoyl) methane (**32**) (2.79 g, 0.500 mmol) in THF (40 mL) was added dropwise to a suspension of LiAlH_4 (0.76 g, 20 mmol) in anhydrous THF (30 mL) under Ar at -20°C over a period of 30 min. After the addition was complete, the cooling bath was removed and the reaction mixture was allowed to warm to room temperature. The mixture was stirred for an additional 4 h at room temperature and was then worked-up by adding water dropwise until the excess lithium aluminum hydride decomposed, followed by the addition of 20 mL of aqueous 10% H_2SO_4 . The organic layer was separated and washed with aqueous 5% NaHCO_3 (20 mL), aqueous saturated NaCl (20 mL). After the solution was dried over anhydrous MgSO_4 and filtered, the solvent was removed on a rotavap. The resulting crude product was purified by column chromatography using (ethyl acetate:hexane 30:70) to afford compound **28** (2.2 g, 86%), as a colorless solid: mp 203.5°C ; $^1\text{H-NMR}$ (500 MHz, CDCl_3): δ 1.30 (s, 18H), 3.88 (s, 6H), 4.90 (s, 2H), 4.94 (s, 4H), 7.38 (d, $J = 10.0$ Hz, 2H), 7.62 (s, 2H), 7.69 (s, 2H), 8.09 (d, $J = 10.0$ Hz, 2H); $^{13}\text{C-NMR}$ (75.46 MHz, CDCl_3): δ 22.7, 31.6, 34.5, 62.3, 62.4, 123.4, 124.4, 125.1, 127.2, 128.4, 131.2, 131.4, 133.3, 147.7, 153.5; (-)-APCI MS m/z (relative intensity) 499.4 (M^+ , 42), 481 (45), 212 (82), 124.9 (84).

Bis(3-bromomethyl-7-*tert*-butyl-2-methoxy-1-naphthyl)methane (27).



To a solution of bis(2-methoxy-7-*tert*-butyl-3-(hydroxymethyl)naphthyl)methane (**28**) (0.50 g, 1.3 mmol) in CH_2Cl_2 (30 mL) was added PBr_3 (0.40 mL, 4.1 mmol), dropwise via a syringe over 10 min. The reaction solution was stirred at room temperature for 4 h. The reaction was worked-up by diluting the mixture CH_2Cl_2 (20 mL) and washing with water (3 x 30 mL). After the solution was dried over anhydrous MgSO_4 and filtered, the solvent was removed on a rotavap, and the resulting product purified by column chromatography (ethyl acetate:hexane 30:70) to afford compound **27** (0.49 g, 74%), mp 232.4 °C; $^1\text{H-NMR}$ (500 MHz, CDCl_3): δ 1.29 (s, 18H), 4.04 (s, 6H), 4.83 (s, 4H), 4.90 (s, 2H), 7.38 (dd, $J = 9.0, 2.1$ Hz, 2H), 7.57 (d, $J = 2.0$ Hz, 2H), 7.76 (s, 2H), 8.09 (d, $J = 9.0$ Hz, 2H); $^{13}\text{C-NMR}$ (75.46 MHz, CDCl_3): δ 23.1, 29.7, 31.1, 31.1, 34.6, 62.9, 123.3, 124.6, 125.8, 128.9, 130.5, 130.5, 131.0, 131.0, 132.0, 147.7, 153.2; (-)-APCI MS m/z (relative intensity) 628.3 (M^+ , ^{81}Br , ^{81}Br , 20), 627.2 (M^+ , ^{81}Br , ^{79}Br , 52), 626.2 (M^+ , ^{79}Br , ^{79}Br , 10), 625.2 (22), (45), 212 (82), 124.9 (84).

Tetrahomodioxacalix[4]naphthalene (26).



Using the general procedure for compound **18a**: To a solution of **28** (0.250 g, 0.500 mmol) in anhydrous THF (100 mL) at room temperature was added portion-wise, NaH (0.080 g, 2.0 mmol) and the mixture stirred at room temperature for 20 min. Then **27**

(0.314 g, 0.500 mmol) in anhydrous THF (50 mL) was added to the reaction mixture using a syringe pump over a period of 2 h, and the reaction mixture was heated at reflux for 24 h. After cooling to room temperature, the reaction mixture was worked-up as in the general procedure, to afford a crude product which was purified by column chromatography (ethyl acetate:hexanes 2:8) to afford the macrocycle **26** (0.34 g, 70%) as a colourless solid compound: mp 277.2 °C; ¹H-NMR (500 MHz, CDCl₃): δ 1.37 (s, 36H), 3.06 (s, 12H), 4.65 (s, 8H), 4.74 (s, 4H), 7.46 (dd, *J* = 9.0, 2.0 Hz, 4H), 7.69 (d, *J* = 2.0 Hz, 4H), 7.77 (s, 4H), 8.02 (d, *J* = 9.0 Hz, 4H); ¹³C-NMR (75.46 MHz, CDCl₃): δ 23.8, 31.2, 34.6, 61.8, 67.4, 123.6, 123.6, 125.0, 128.3, 129.2, 130.6, 131.0, 131.4, 146.7, 155.2; HRMS *m/z* (relative intensity) 1003.586 ([M + K]⁺, 100), 987.684 ([M + Na]⁺, 45).

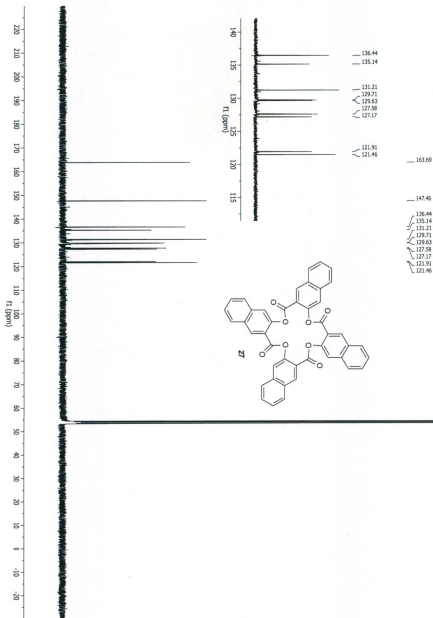
5.9 References

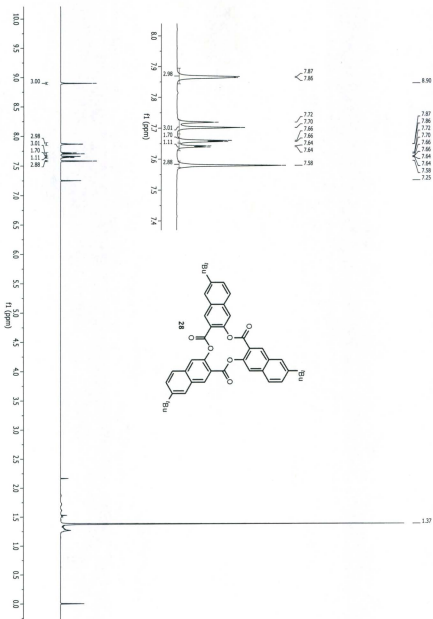
1. Asfari, Z.; Böhmer, V.; Harrowfield, J.; Vicens, J.; Eds., *Calixarenes 2001*, Kluwer Academic Publishers, Dordrecht, The Netherlands 2001, pp 236-248 and the references cited therein.
2. Arumugam, N.; Jang, Y. S.; Lee, C. H. *Org. Lett.* **2000**, *2*, 3115.
3. Ackman, R. G.; Brown, W. H.; Wright, G. F. *J. Org. Chem.* **1955**, *20*, 1147.
4. Ahmed, M.; Meth-Cohn, O. *Tetrahedron Lett.* **1969**, *10*, 1493.
5. Gerkensmeier, T.; Mattay, J.; Näther, C. *Chem. Eur. J.* **2001**, *7*, 465.
6. Black, D. S.; Craig, D. C.; Kumar, N. *Tetrahedron Lett.* **1995**, *36*, 8075.
7. Sessler, J. L.; An, D.; Cho, W. S.; Lynch, V. *J. Am. Chem. Soc.* **2003**, *125*, 13646.
8. Black, D. S.; Craig, D. C.; Rezaie, R. *Chem. Commun.* **2002**, 810.
9. Kravtsov, V. Ch.; Weber, E. Simonov, Yu.; Lipkowski, J.; Trepte, J.; Ganine, E. V. *J. Struct. Chem.* **2005**, *46*, S46.
10. Trepte, J., Czugler, M., Gloea, K., Weber, E. *Chem. Commun.*, **1997**, 1461.
11. Al-Saraierh, H.; Dawe, L. N.; Georghiou, P. E. *Tetrahedron Lett.* **2009**, *50*, 4289.
12. Chen, Y.; Wang, D.-X.; Huang, Z.-H.; Wang, M. *J. Org. Chem.* **2010**, *75*, 3786.
13. Tran, A. H.; Miller, D. O.; Georghiou, P. E. *J. Org. Chem.* **2005**, *70*, 1115.
14. Tran, A. H.; Georghiou, P. E. *New J. Chem.* **2007**, *13*, 921.
15. (a) Masci, B. *Tetrahedron* **1995**, *51*, 5459. (b) Masci, B.; Finelli, M.; Varrone, M. *Chem. Eur. J.* **1998**, *4*, 2018. (c) Masci, B. in *Calixarenes 2001*; Asfair, Z., Bohmer, V.; Harrowfield, J.; Vicens, J.; Eds.; Kluwer Academic Publishers: Dordrecht, The

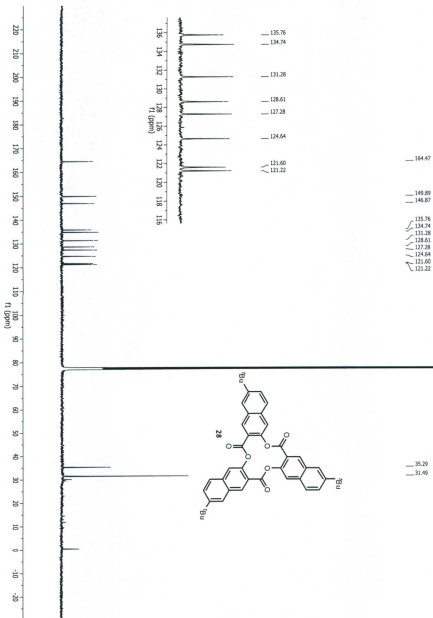
- Netherlands, 2001. (d) Masci, B. *J. Org. Chem.* **2001**, *66*, 1497. (e) Masci, B. *Tetrahedron* **2001**, *57*, 2841.
16. Arduini, A.; Giorgi, G.; Pochini, A.; Secchi, A.; Ugozzoli, F. *J. Org. Chem.* **2001**, *66*, 8302.
17. Fielding, L. *Tetrahedron*, **2000**, *56*, 6151.
18. (a) K. A. Connors, *Binding Constants*, Wiley, New York, 1987. (b) Association constants were calculated using a non-linear curve fitting program with ORIGINPro 7.5 software from OriginLab Corporation.
19. Gong, H.-Y.; Wang, D.-X.; Xiang, J.-F.; Zheng, Q.-Y.; Wang, M.-X. *Chem. Eur. J.* **2007**, *13*, 7791.
20. Eckelmann, J.; Saggiomo, V.; Sonnichsen, F. D.; Lüning, U. *New J. Chem.* **2010**, *34*, 1247.
21. Gong, H.-Y.; Zhang, X.-H.; Wang, D.-X.; Ma, H.-W.; Zheng, Q.-Y.; Wang, M.-X. *Chem. Eur. J.* **2006**, *12*, 9262.
22. Molecular modeling was conducted using the MMFF force field with Spartan'10 software by Wavefunction Inc., Irvine, CA.

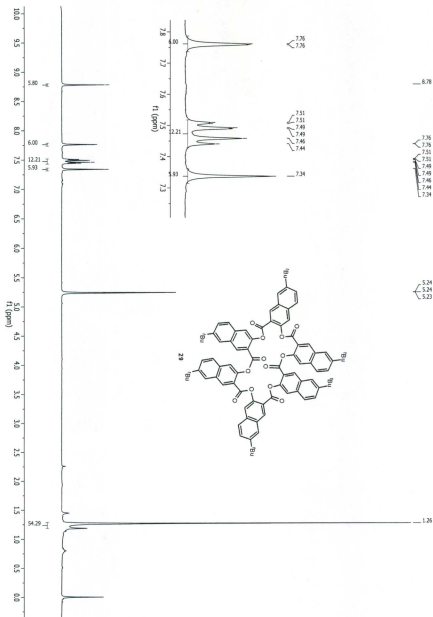
Appendix A

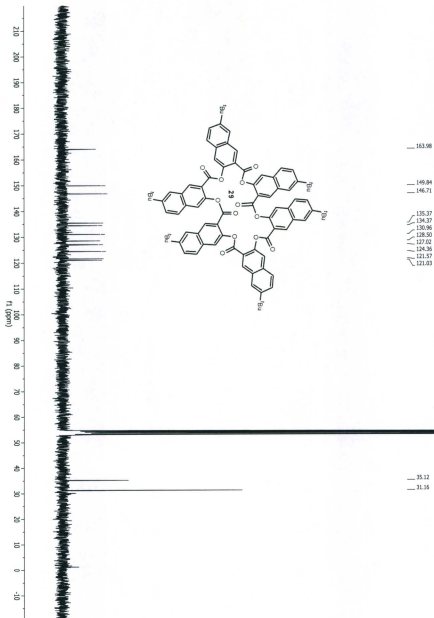
^1H and ^{13}C NMR spectra for compounds described
in Chapter 2

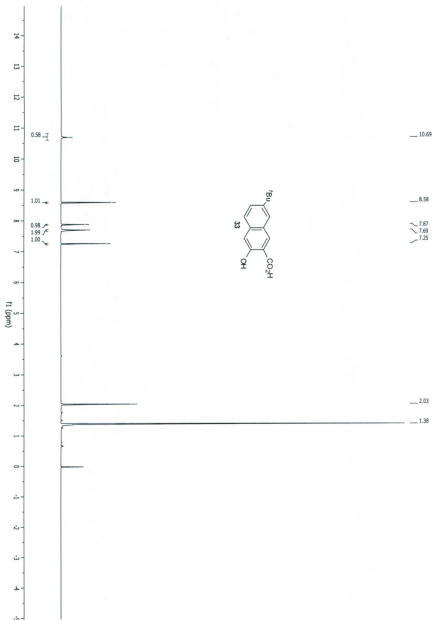


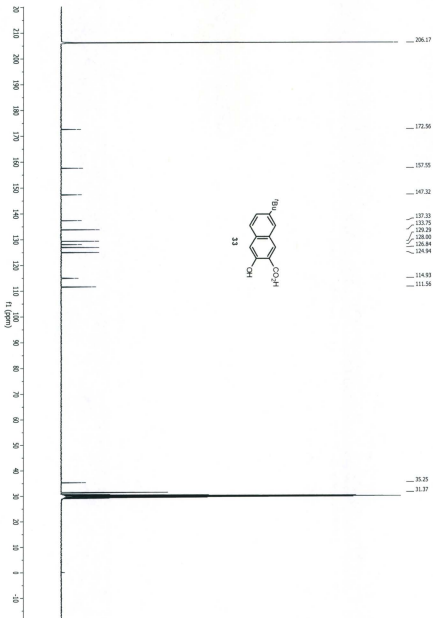






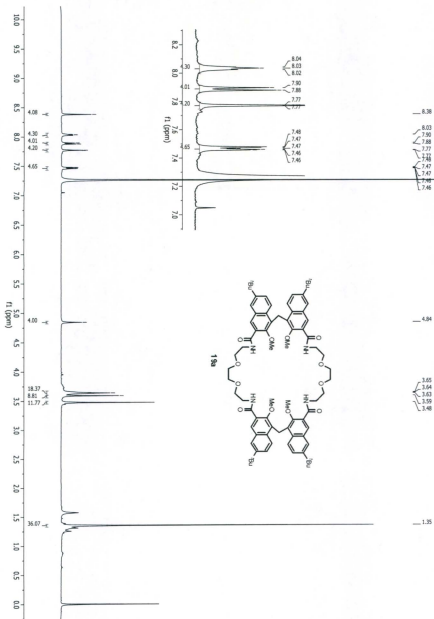


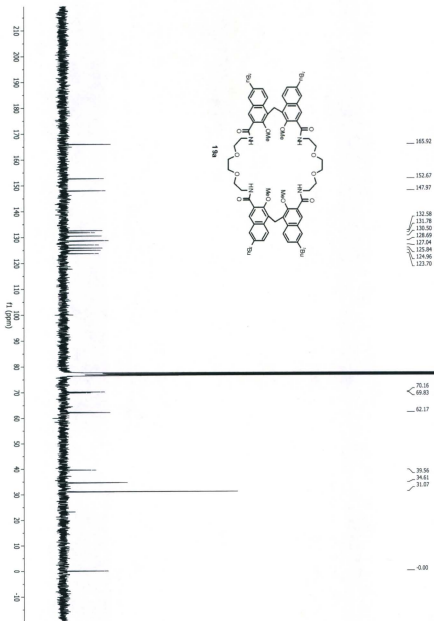


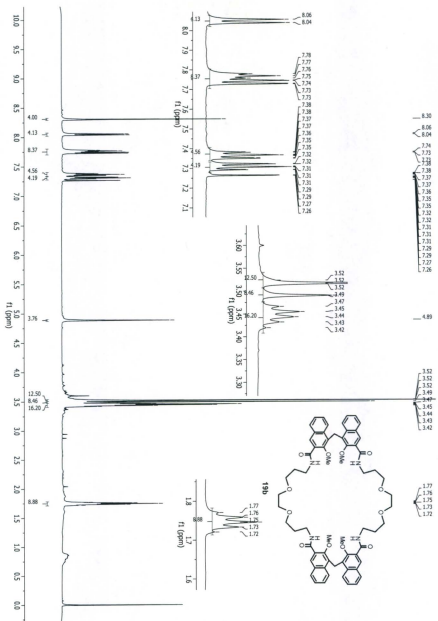


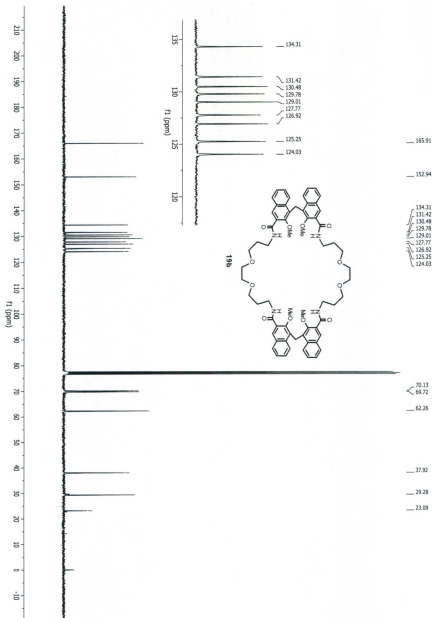
Appendix B

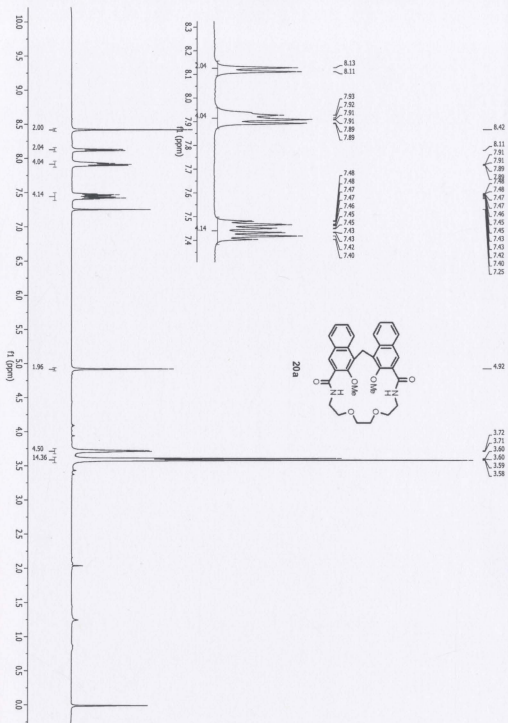
^1H and ^{13}C NMR spectra for compounds described
in Chapter 3

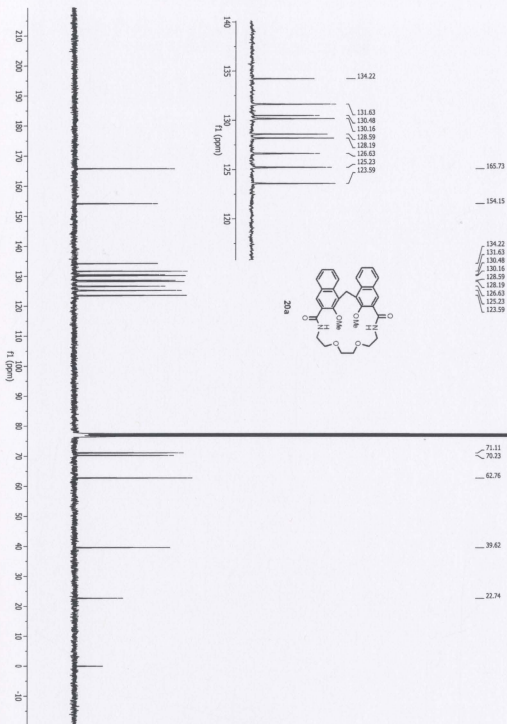


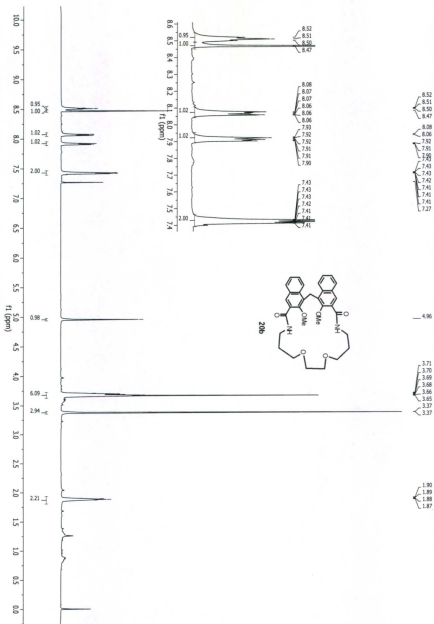


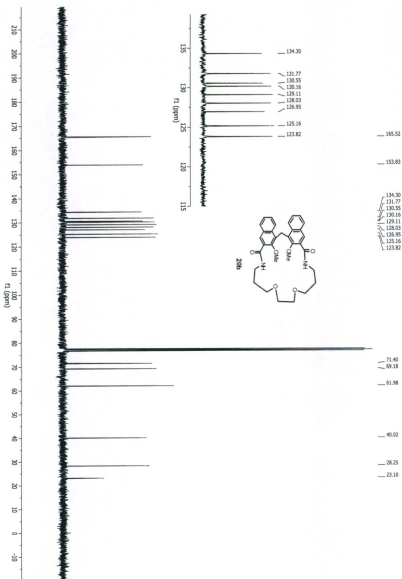


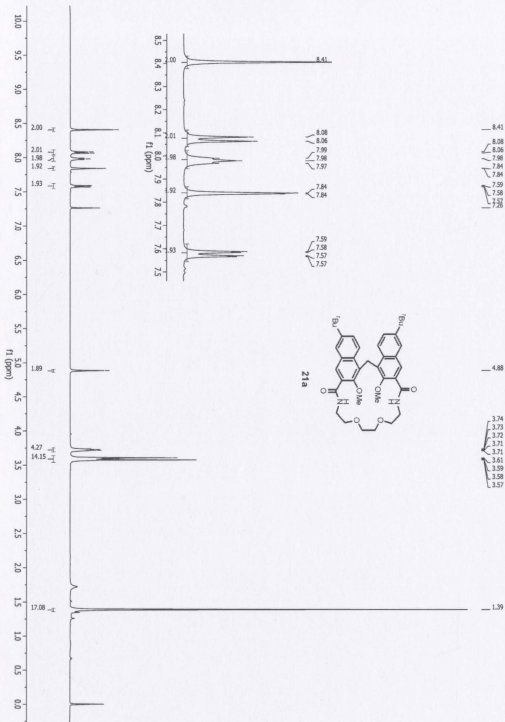


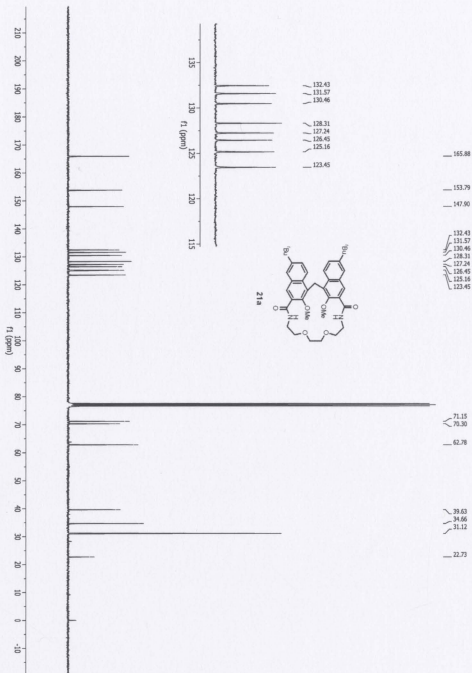


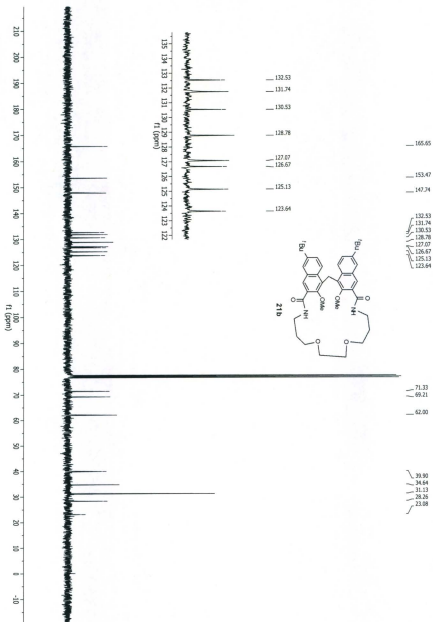


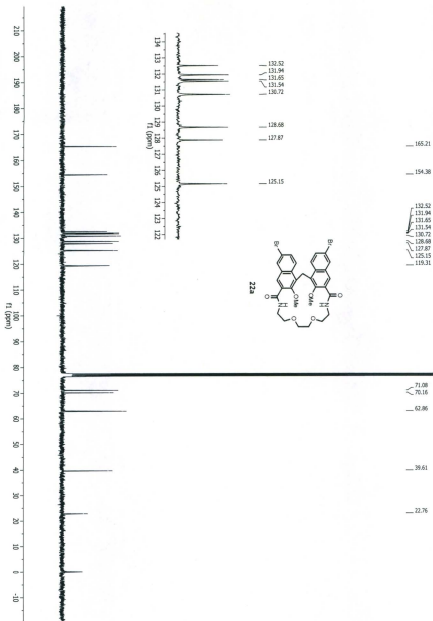


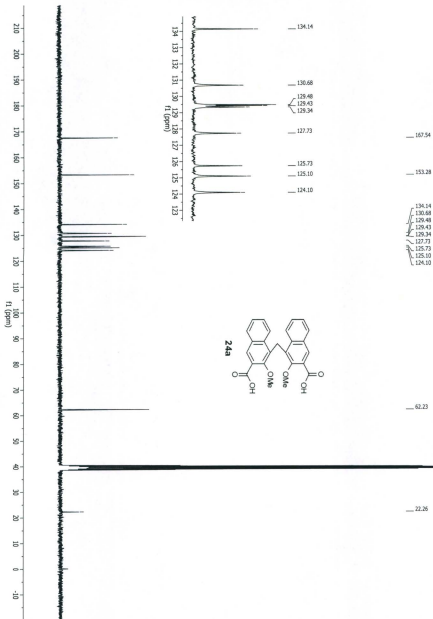


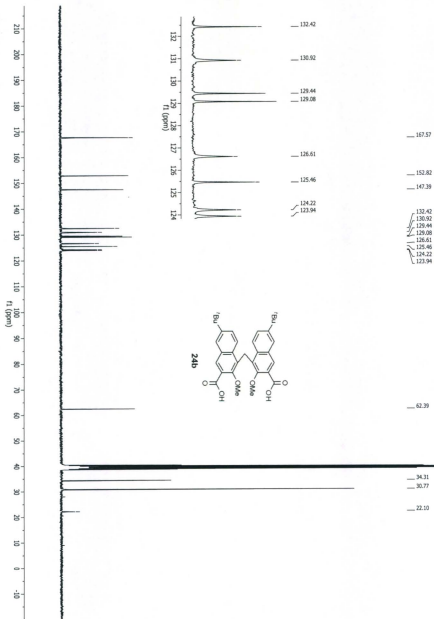


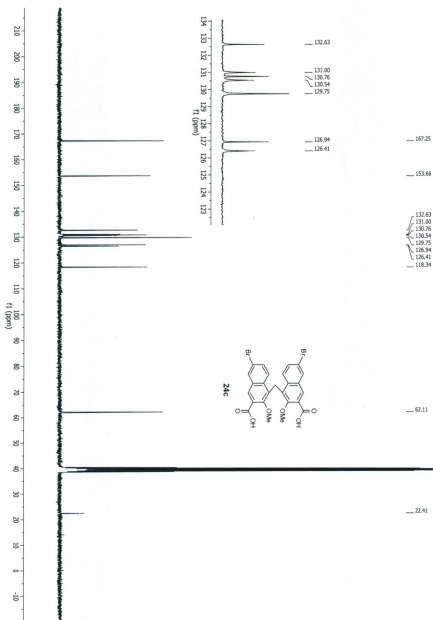


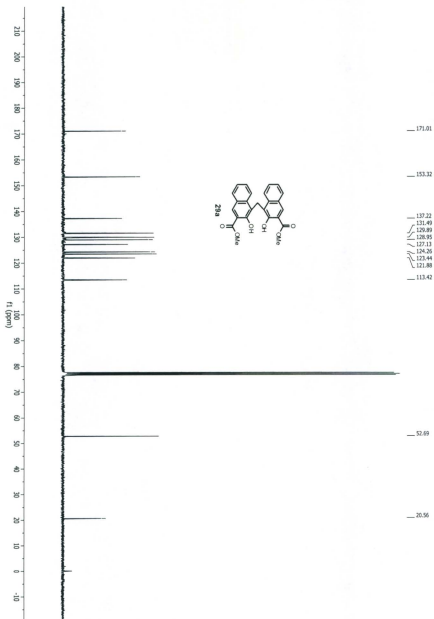


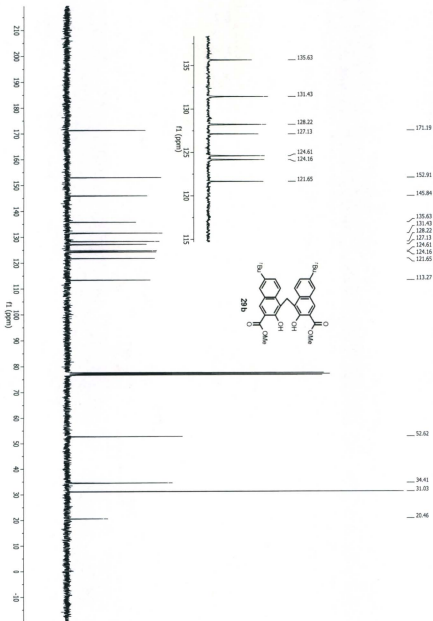


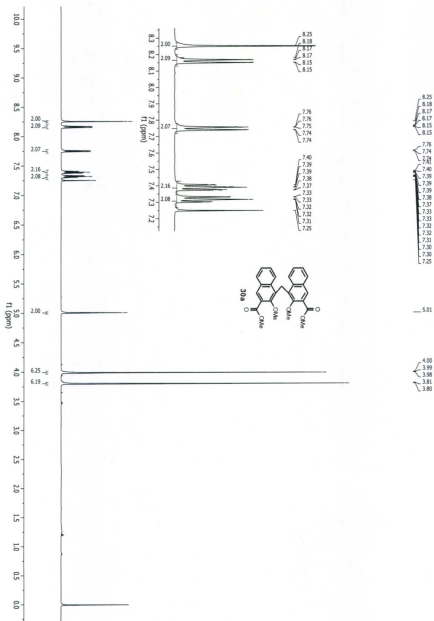


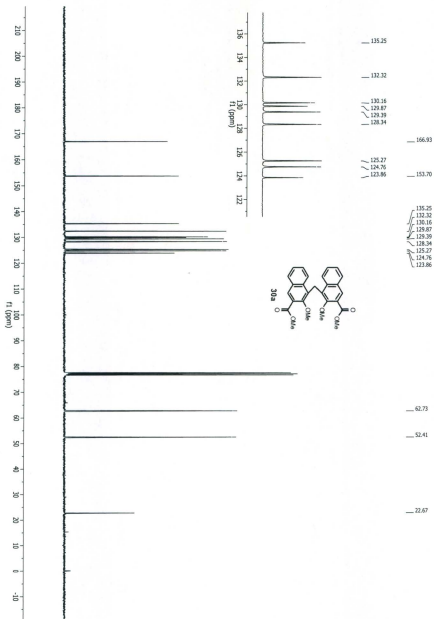


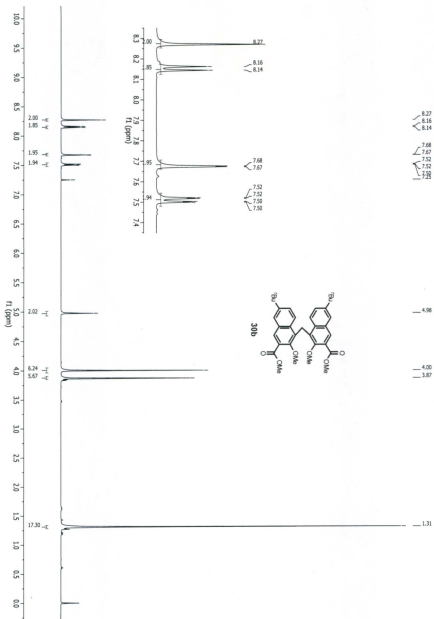


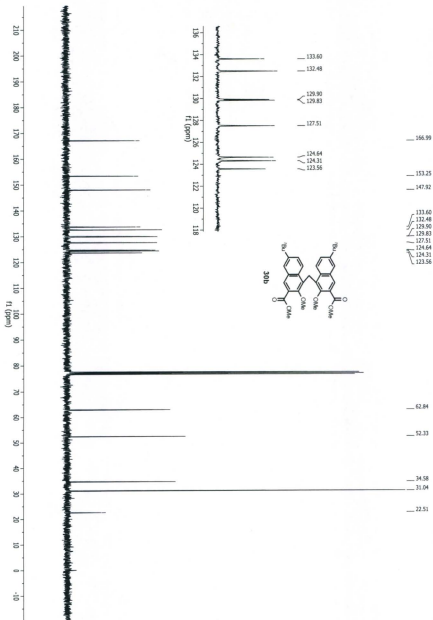


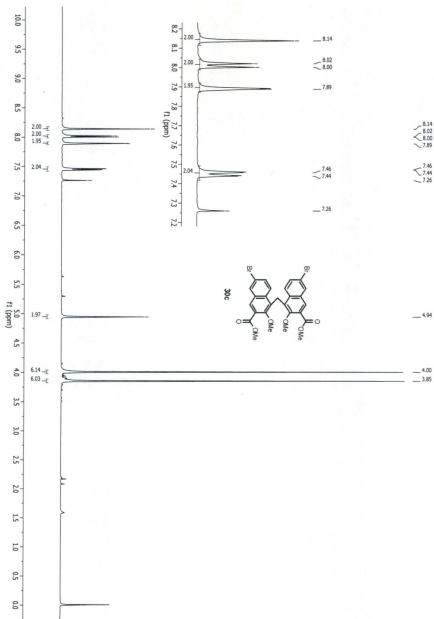


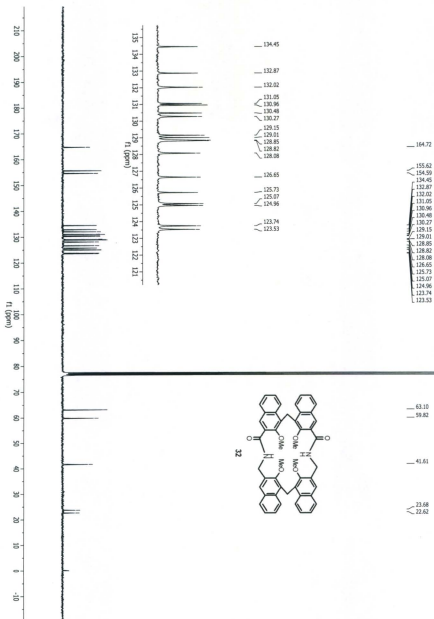


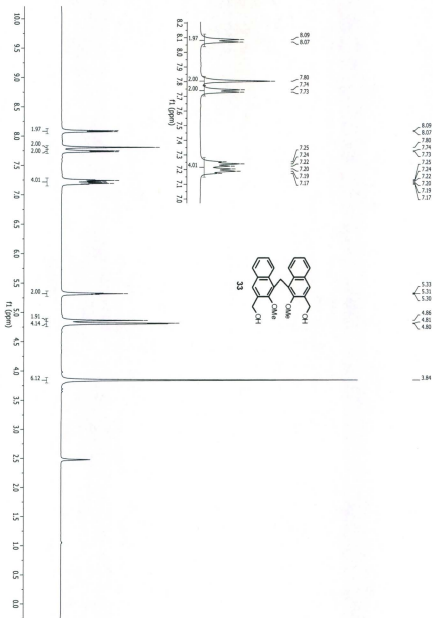


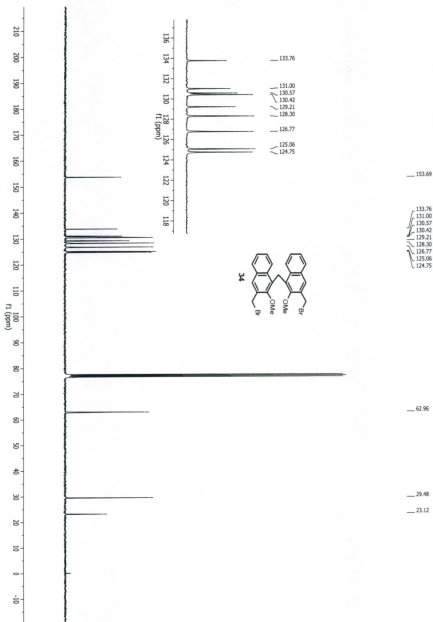


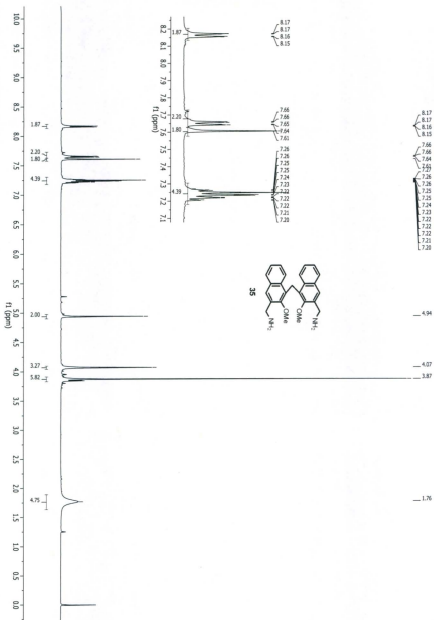


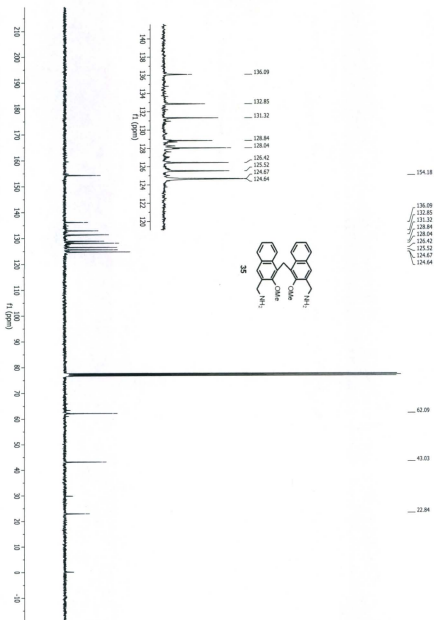


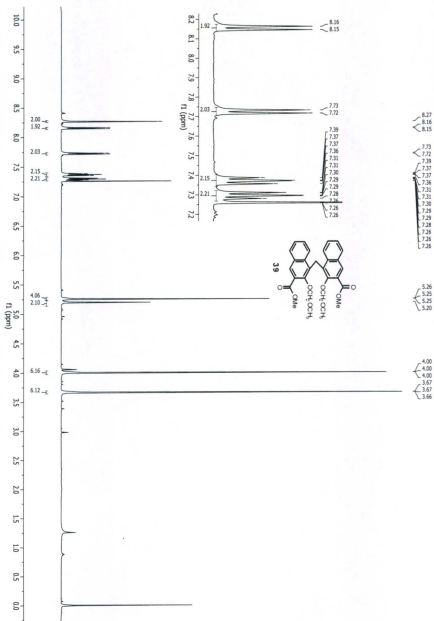


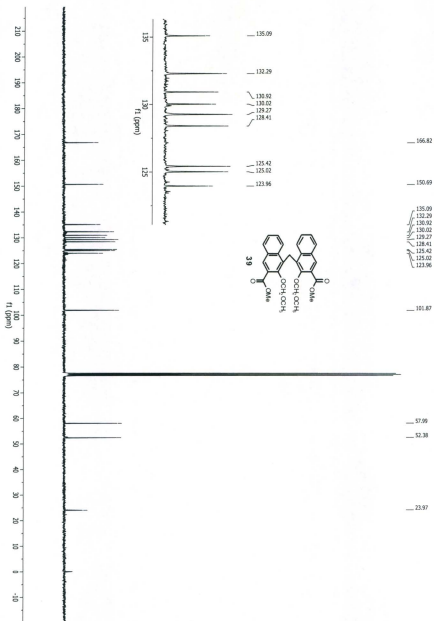


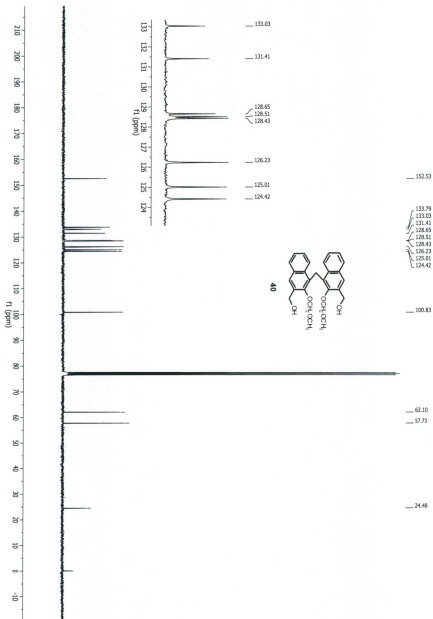


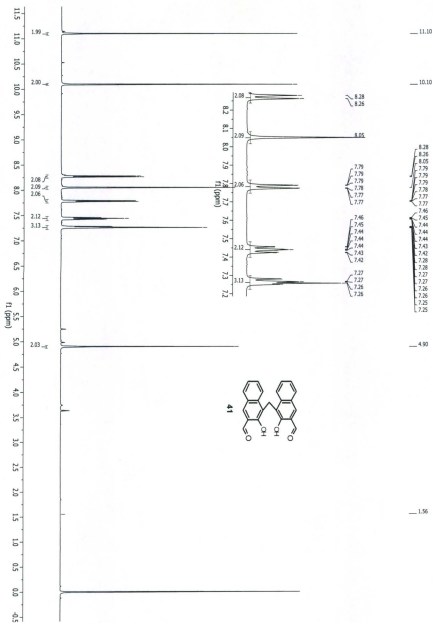


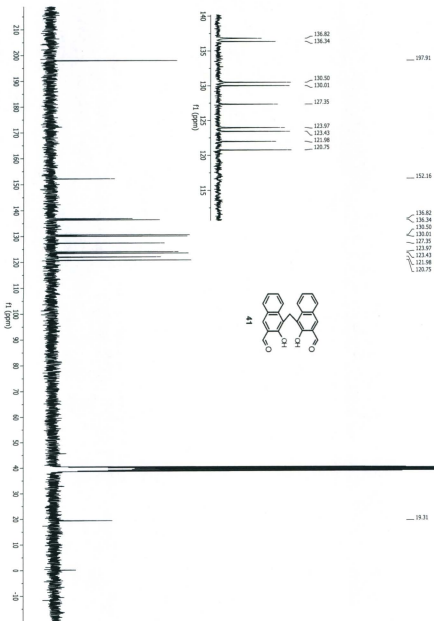










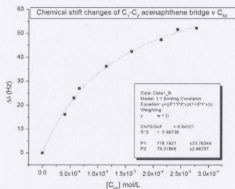
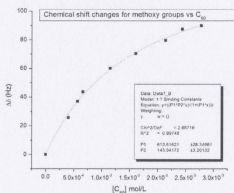


Appendix C

**Complexation data and ^1H and ^{13}C NMR spectra
for compounds described in Chapter 4**

Appendix 4.1 $^1\text{H-NMR}$ titration data of **47b** with C_{60} in toluene- d_8 at 298 K. ($\Delta\delta$ values are absolute values).

Entry	Wt. C_{60} (mg)	$\text{C}_{60} \times 10^6$ mol	$[\text{C}_{60}] \times 10^3 \text{M}$	δ_{Ar} (ppm)	$\Delta\delta_{\text{Ar}}$ (Hz)	$\delta_{-\text{CH}_2\text{CH}_2-}$ (ppm)	$\Delta\delta_{-\text{CH}_2\text{CH}_2-}$ (Hz)	δ_{OCH_3} (ppm)	$\Delta\delta_{\text{OCH}_3}$ (Hz)
1	0	0	0	7.41	0	2.97	0	3.57	0
2	0.29	4.03	4.03	7.39	13.62	3.00	16.1	3.62	25.7
3	0.41	5.69	5.69	7.38	20.12	3.01	23.0	3.64	37.1
4	0.48	6.67	6.67	7.37	23.72	3.02	26.9	3.66	43.7
5	0.83	11.5	11.5	7.35	33.34	3.04	36.2	3.69	60.1
6	1.16	16.1	16.1	7.34	39.49	3.05	42.5	3.71	70.4
7	1.54	21.4	21.4	7.33	44.88	3.06	47.4	3.73	79.5
8	1.76	24.4	24.4	7.32	50.14	3.07	51.6	3.74	87.5
9	2.00	27.8	27.8	7.31	51.94	3.07	52.2	3.75	89.9



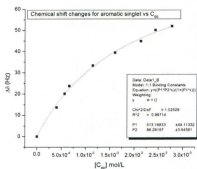


Figure 4.11. 1:1 Binding isotherms for the titration of **47b** with C_{60} : *Top*: Chemical shift changes for the methoxy signal; *Middle*: Chemical shift changes for the $-\text{CH}_2\text{CH}_2-$ bridge signals; and *Bottom*: Chemical shift changes for the aromatic singlet signal.

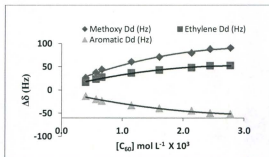
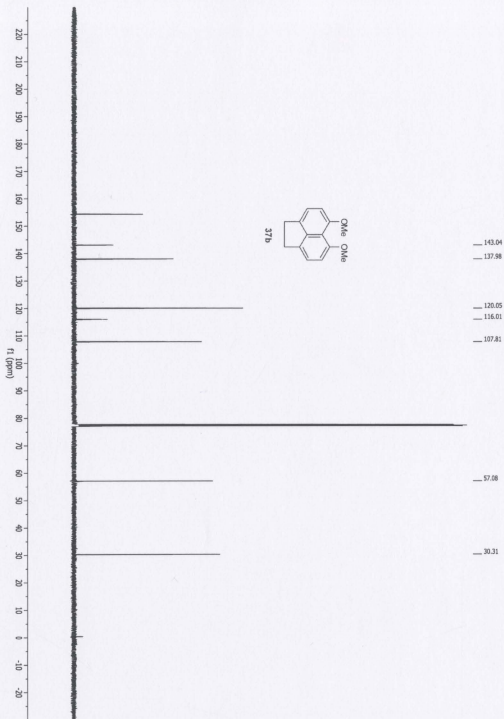
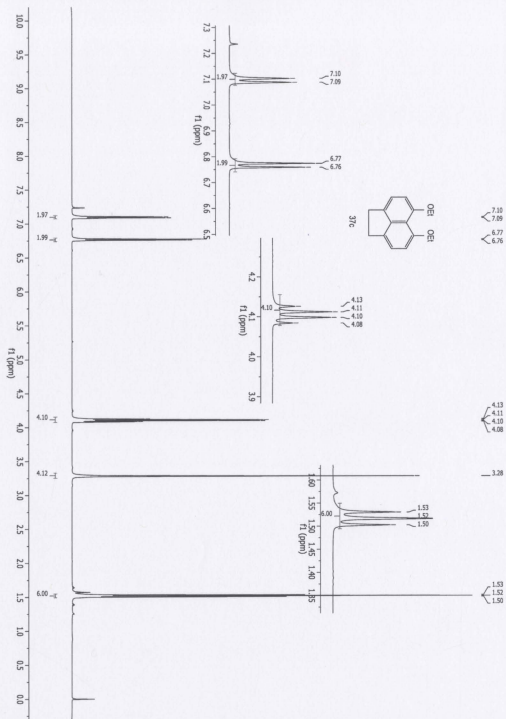
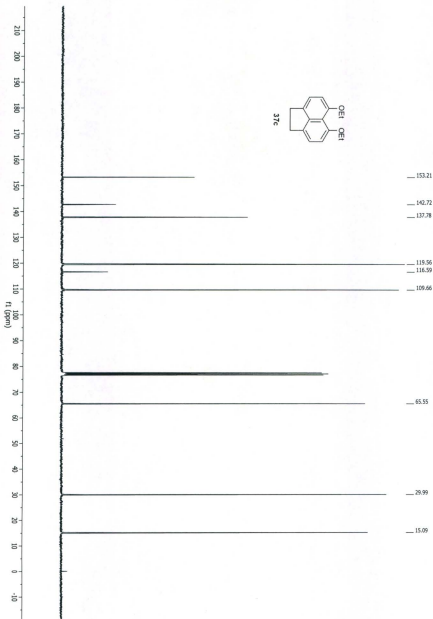
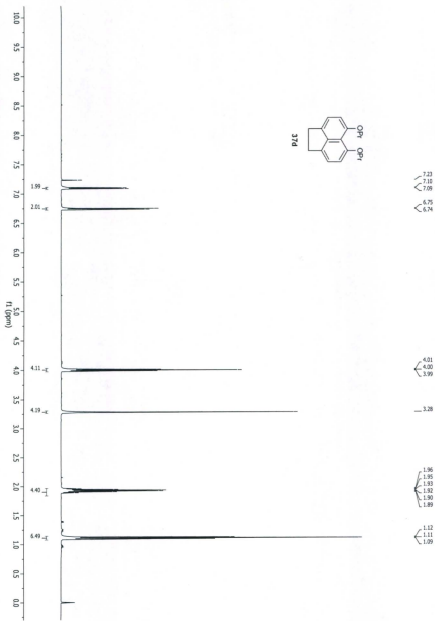


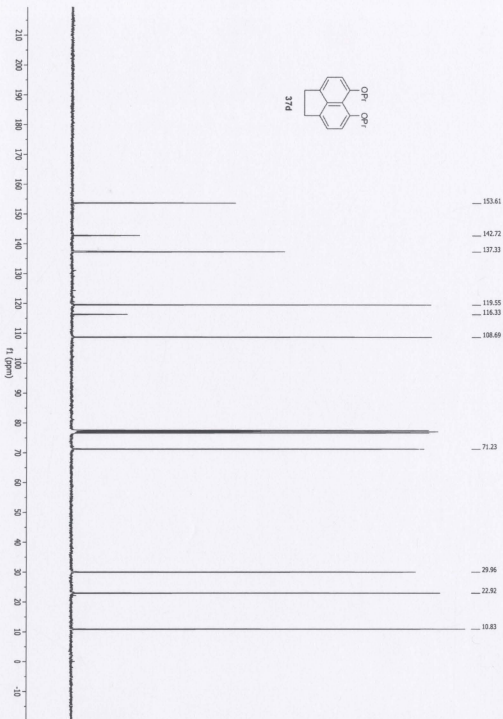
Figure 4.10. Plot of chemical shift changes ($\Delta\delta$) for protons on **47b** in toluene- d_8 solution vs added C_{60} .

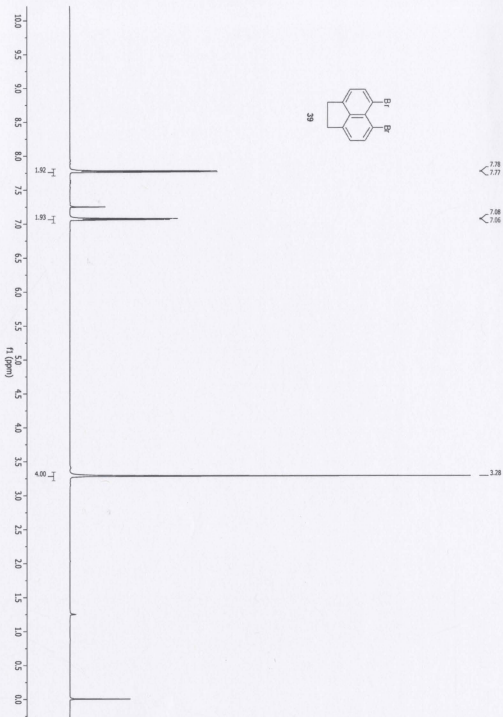


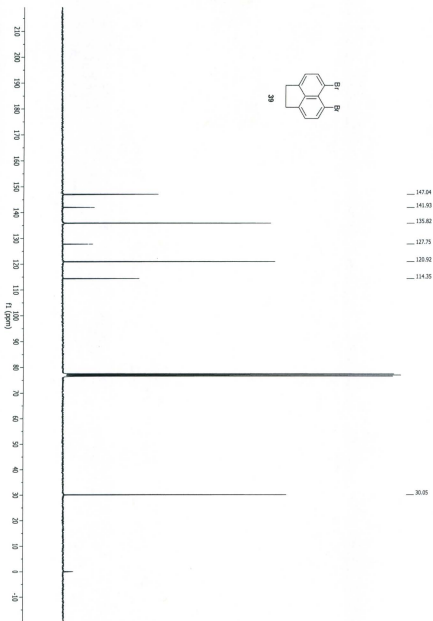


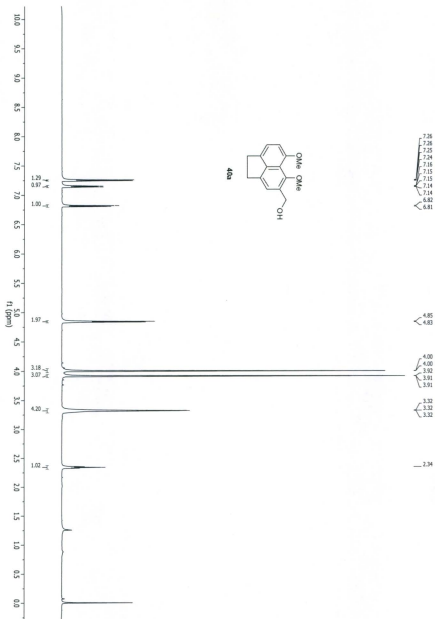


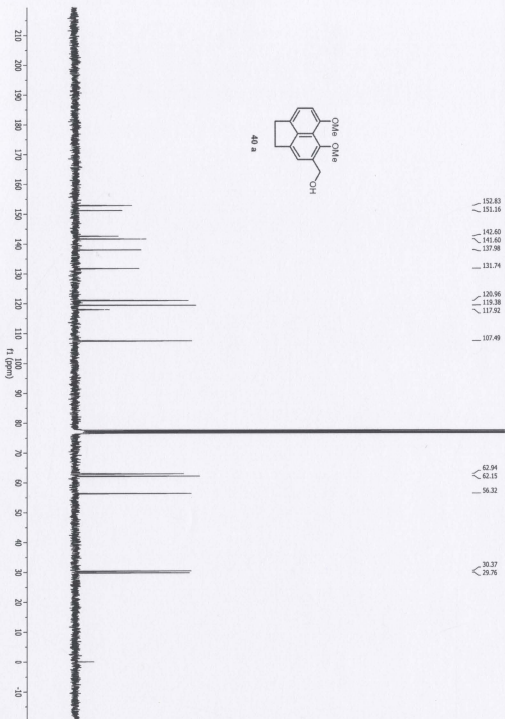


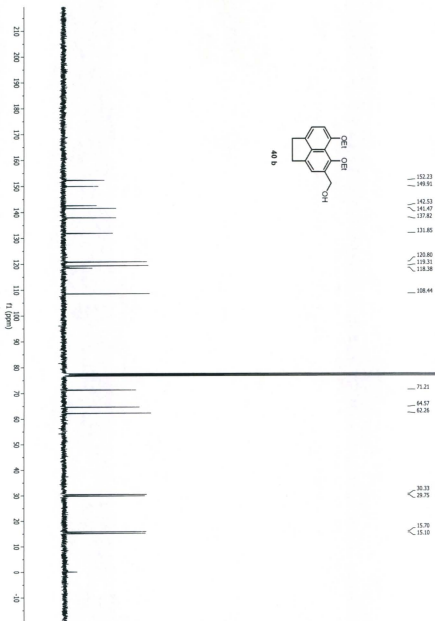


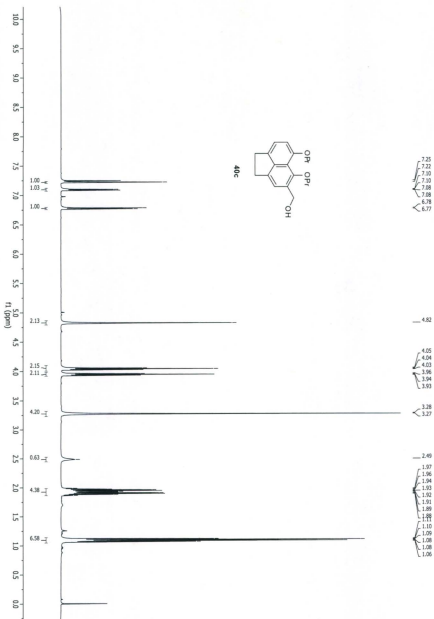


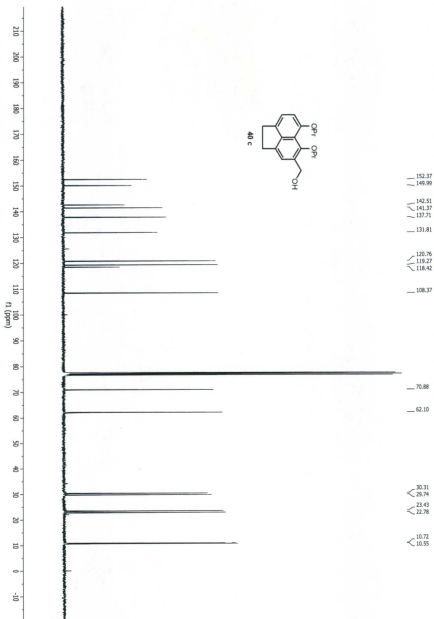


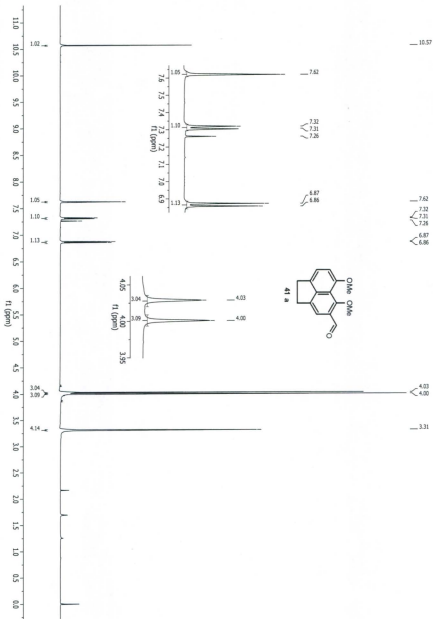


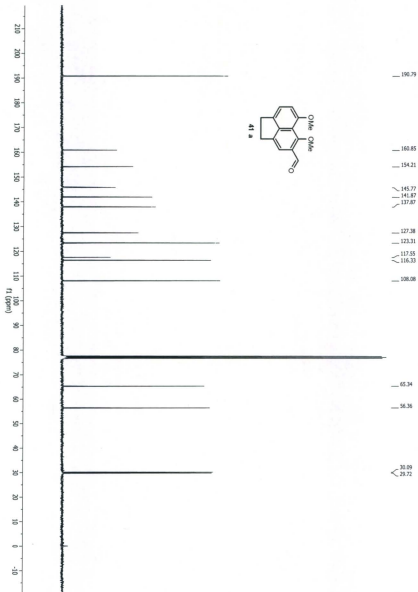


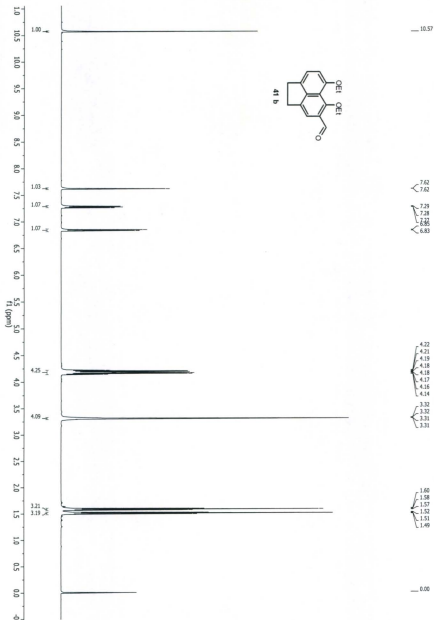


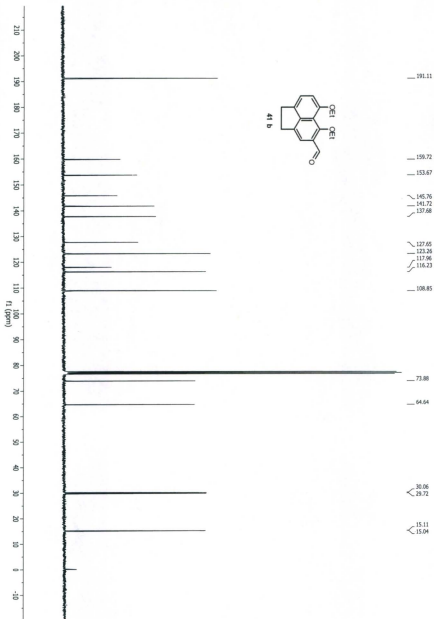


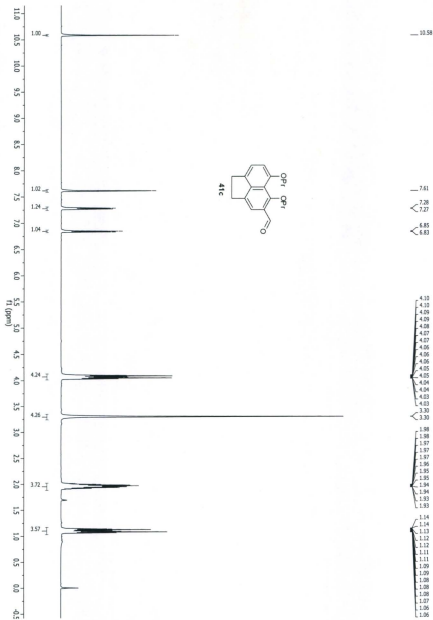


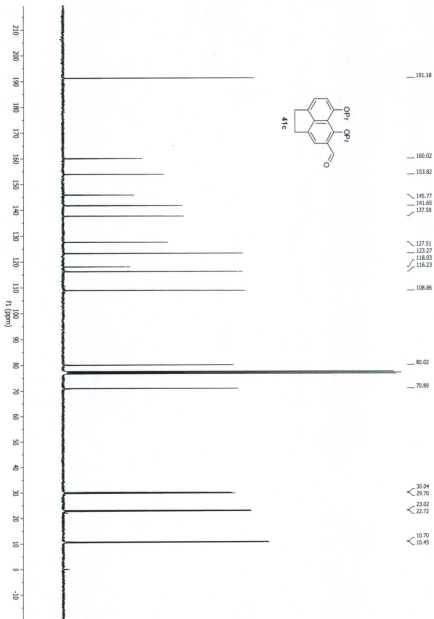


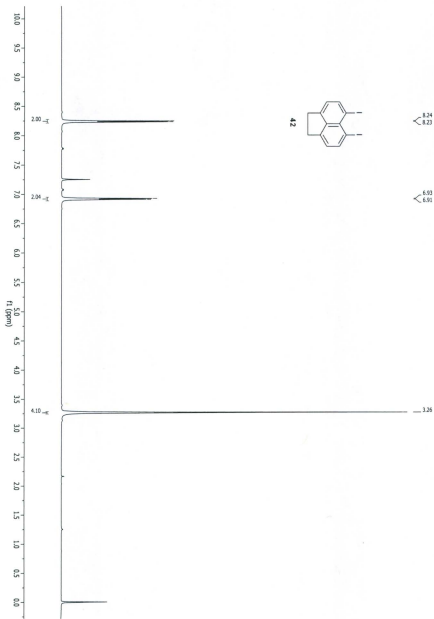


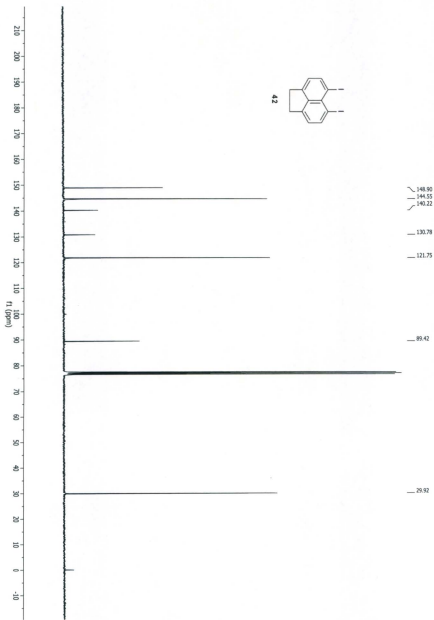


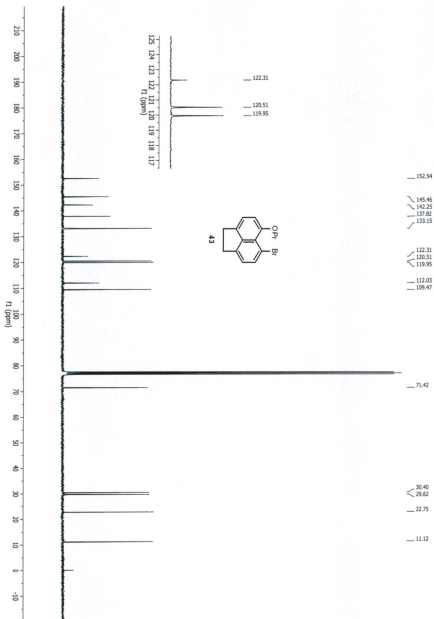


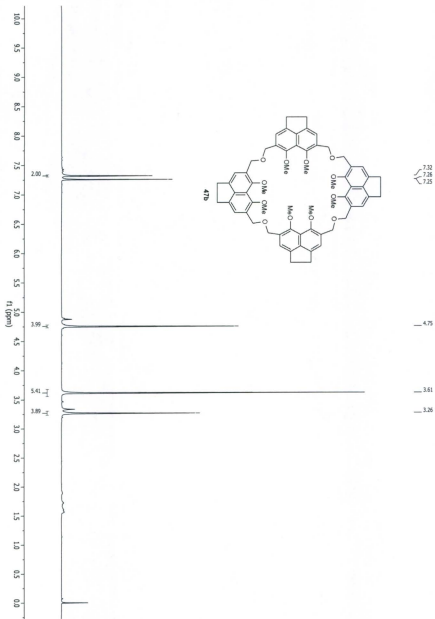


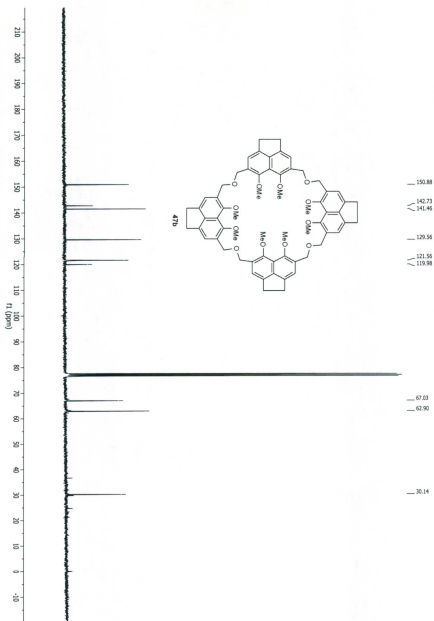


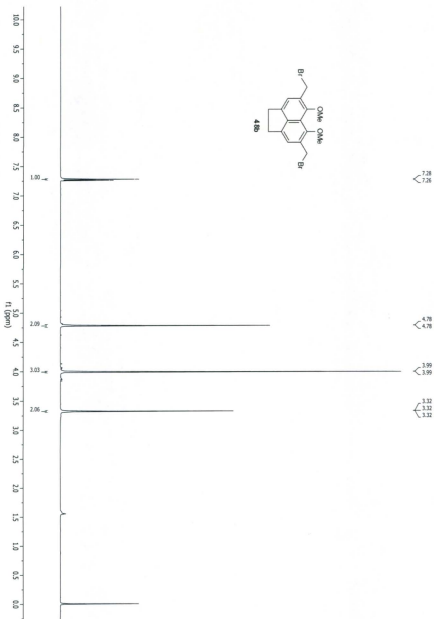


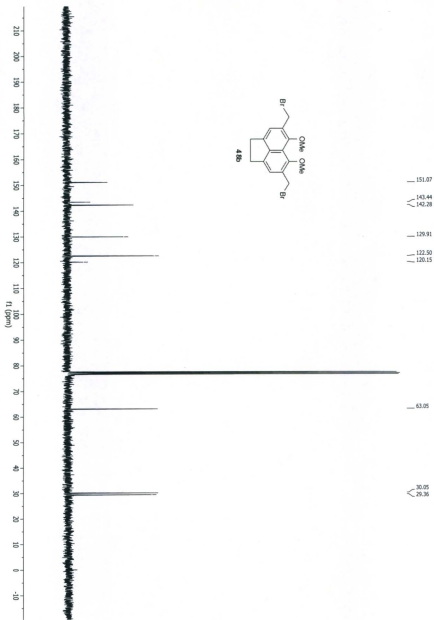


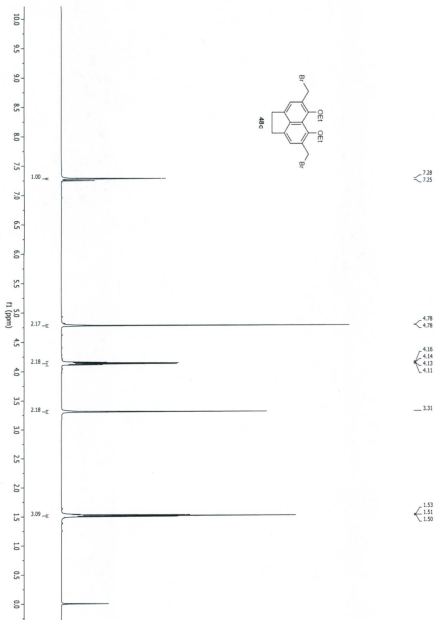


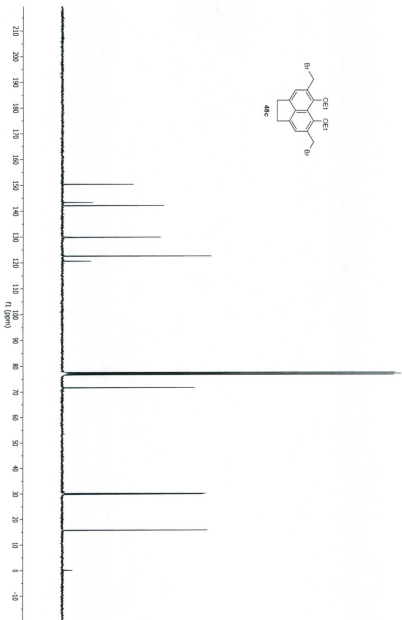
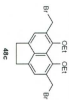


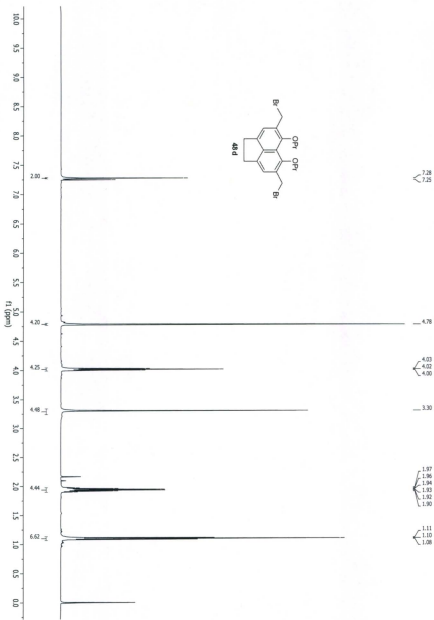


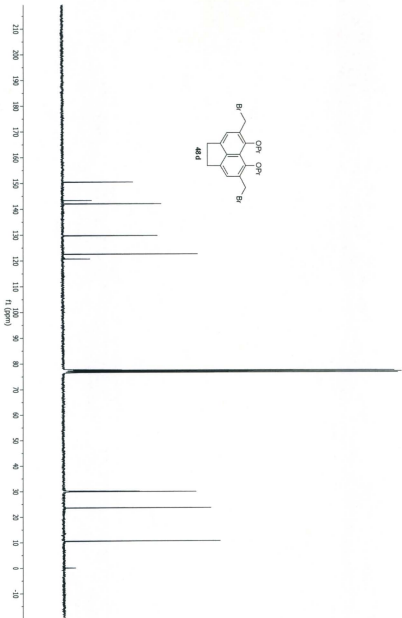


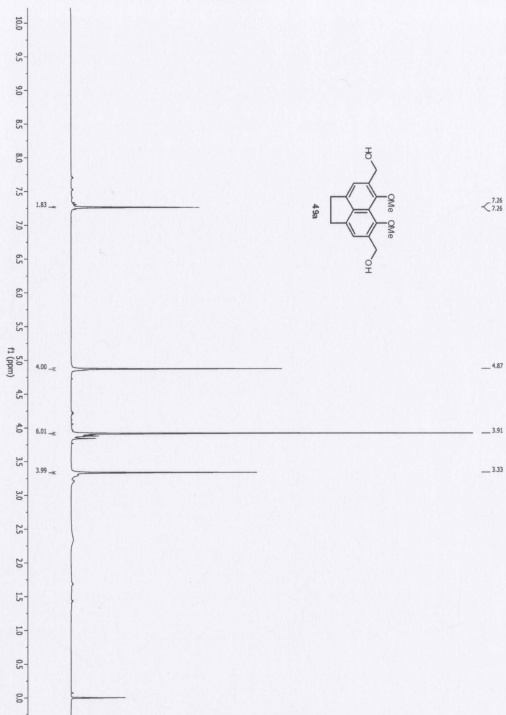


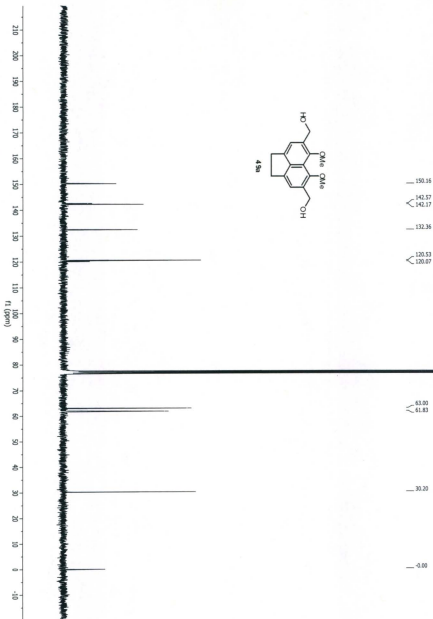


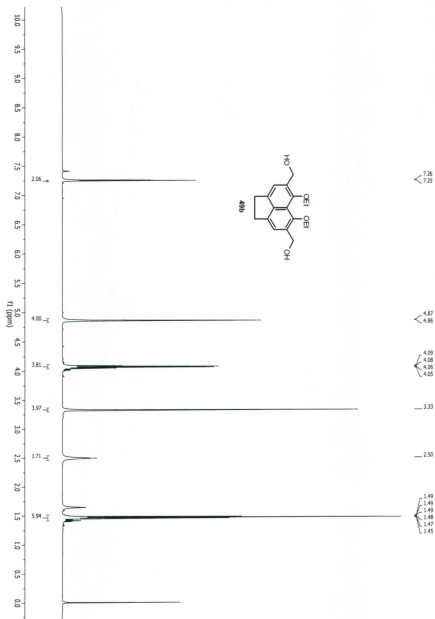


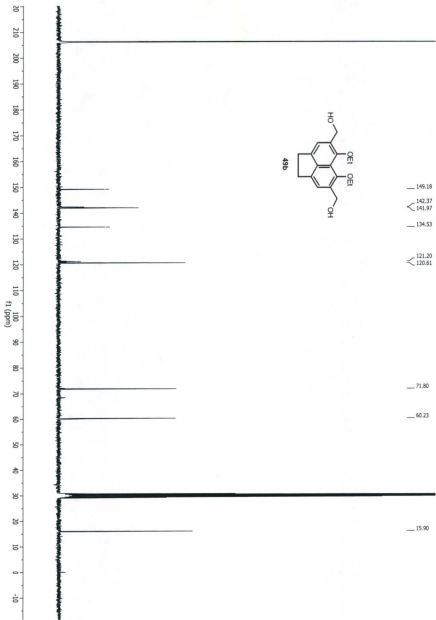


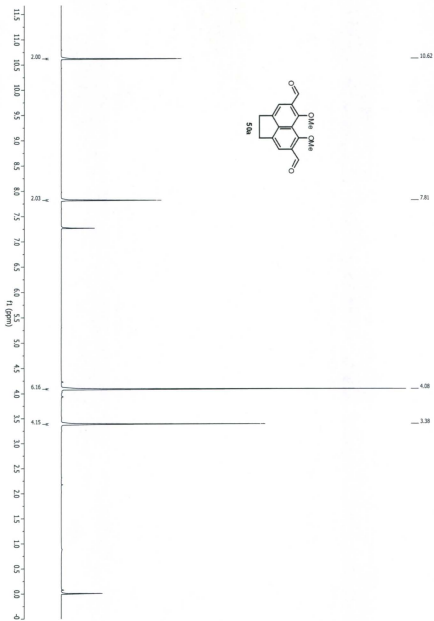


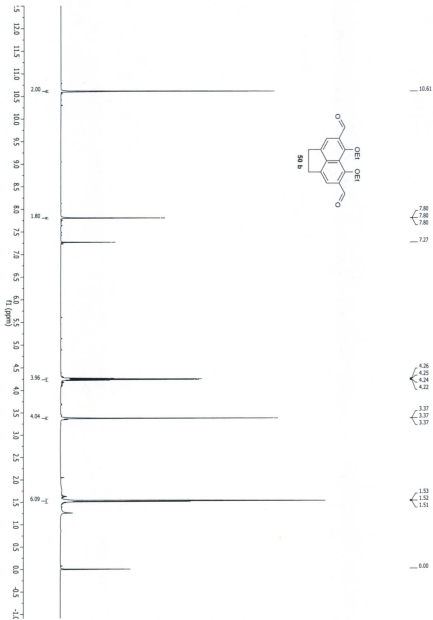


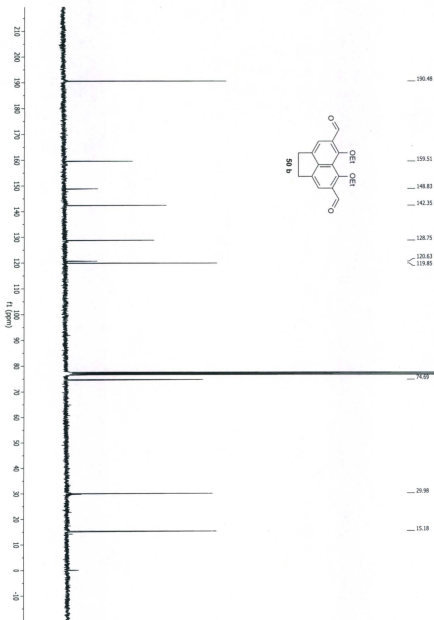


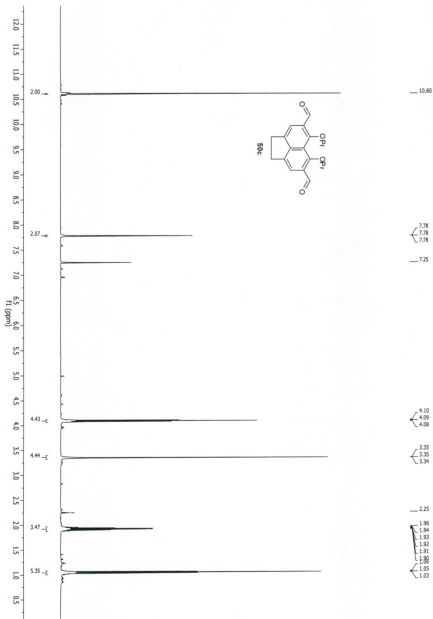


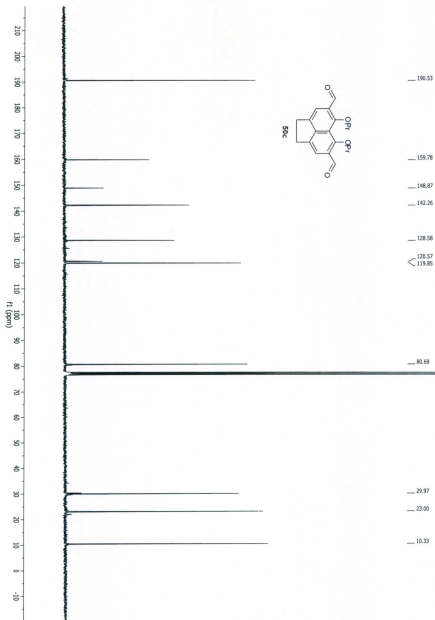












Appendix D

^1H and ^{13}C NMR spectra and complexation data
for compounds described in Chapter 5

Appendix 5.1 Determination of K_{assoc} for **18b**:TMAA complex in CDCl_3 using $^1\text{H-NMR}$ at 298 K. ($\Delta\delta$ values are absolute values)

Entry	Vol. TMAA mL	[TMAA] x 10^3 M	δ_{CH_3} (ppm)	$\Delta\delta_{\text{CH}_3}$ (ppm)	Δ_{CH_3} (Hz)	$\delta_{\text{N}(\text{CH}_3)_4}$ (ppm)	$\Delta\delta_{\text{N}(\text{CH}_3)_4}$ (ppm)	$\Delta\delta_{\text{N}(\text{CH}_3)_4}$ (Hz)
1	10	1.05	2.940	0.0	0.0	1.665	0.050	25.0
2	20	2.06	3.037	0.097	48.50	1.745	0.130	65.0
3	30	3.04	3.099	0.159	79.50	1.836	0.221	110.0
4	40	3.98	3.114	0.174	87.00	1.871	0.256	128.00
5	50	4.88	3.123	0.183	91.50	1.898	0.283	141.5
6	60	5.75	3.136	0.196	98.00	1.922	0.307	153.5
7	70	6.59	3.142	0.202	101.00	1.940	0.325	162.5
8	80	7.40	3.150	0.210	105.00	1.952	0.337	168.5
9	90	8.19	3.155	0.215	107.50	1.979	0.364	182.00
10	100	8.95	3.160	0.220	110.00	1.996	0.381	190.5
11	110	9.68	3.164	0.224	112.00	2.012	0.397	198.5
12	120	10.4	3.168	0.228	114.00	2.027	0.412	206.00

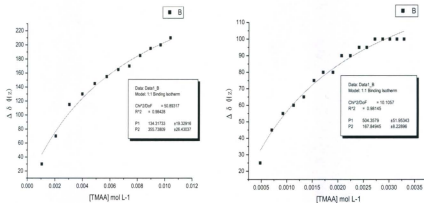


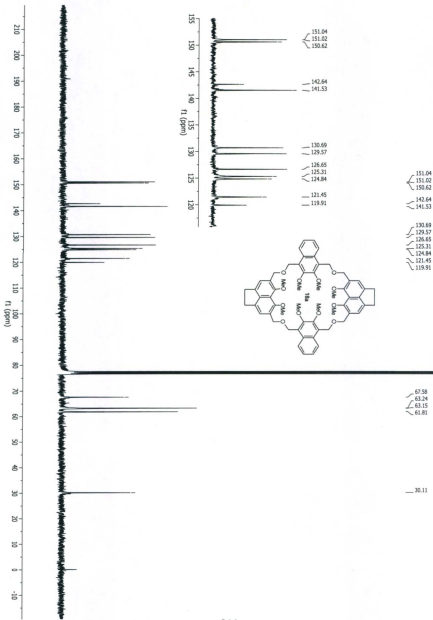
Figure 5.7. $^1\text{H-NMR}$ titration curves for TMAA complexation with **18b**, titration curves for TMA cation (*left*) and methyl group of acetate anion (*right*).

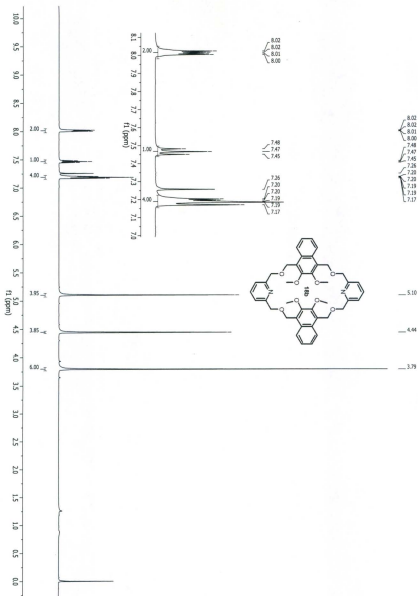
Appendix 5.2 Determination of K_{assoc} for **18b**:1,3-dihydroxybenzene complex in CDCl_3 using $^1\text{H-NMR}$ at 298 K and the concentration of 1,3-dihydroxybenzene 1.61×10^{-3} M.

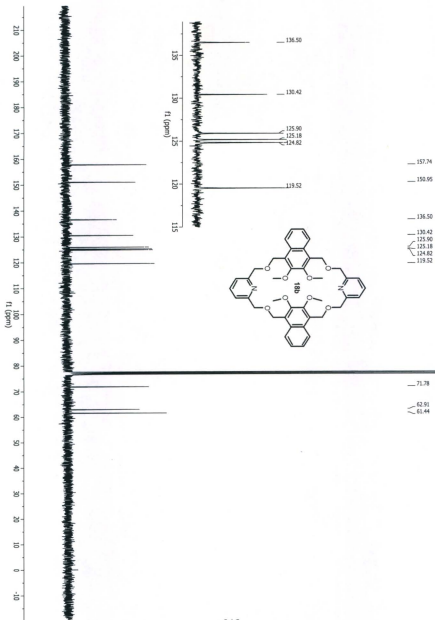
Trial No.	18b Wt(mg)	18b (mole) $\times 10^6$	[18b] $\times 10^3$	18b/guest	Guest/18b	δ (ppm)	$\Delta\delta$ (ppm)	$\Delta\delta$ (Hz)
1	0.00	0.00	0.00	0.00	0.00	6.352	0.00	0.000
2	0.85	1.21	1.21	0.75	1.33	6.153	0.199	99.5
3	1.44	2.05	2.05	1.28	0.78	6.059	0.293	146.5
4	2.20	3.13	3.13	1.95	0.51	5.968	0.384	192
5	2.91	4.15	4.15	2.58	0.39	5.903	0.449	224.5
6	3.7	5.27	5.27	3.28	0.30	5.849	0.503	251.5
7	4.35	6.20	6.20	3.86	0.26	5.814	0.538	269
8	4.85	6.91	6.91	4.30	0.23	5.794	0.558	279
9	5.65	8.05	8.05	5.01	0.20	5.765	0.587	293.5
10	6.18	8.80	8.80	5.48	0.18	5.750	0.602	301
11	6.60	9.40	9.40	5.86	0.17	5.739	0.613	306.5
12	7.86	1.12	1.12	6.97	0.14	5.710	0.642	321
13	8.33	1.19	1.19	7.39	0.14	5.702	0.650	325
14	9.16	1.30	1.30	8.13	0.12	5.690	0.662	331
15	9.75	1.39	1.39	8.65	0.12	5.670	0.682	341
16	10.95	1.56	1.56	9.72	0.10	5.663	0.689	344.5
17	12.13	1.73	1.73	10.76	0.09	5.649	0.703	351.5
18	12.59	1.79	1.79	11.17	0.09	5.645	0.707	353.5

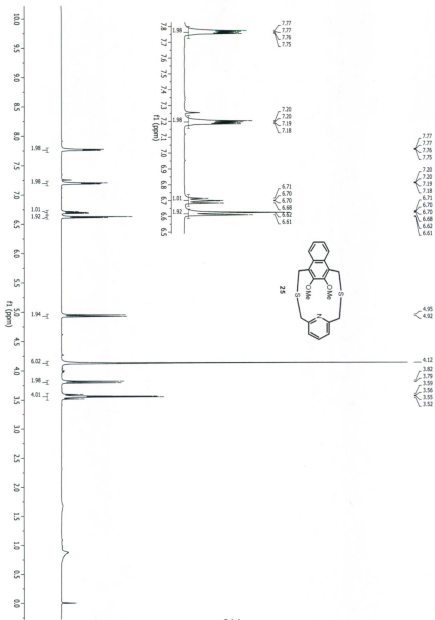
Appendix 5.3 Determination of K_{assoc} for **18b**:1,3-dihydroxynaphthalene complex in CDCl_3 using $^1\text{H-NMR}$ at 298 K and the concentration of 1,3-dihydroxynaphthalene 1.34×10^{-3} M.

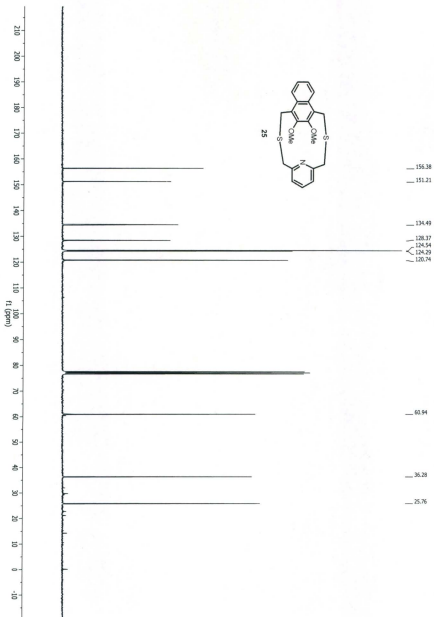
Trial No.	18b Wt(mg)	18b (mole) $\times 10^6$	[18b] $\times 10^3$	Calix/guest	Guest/calix	δ (ppm)	$\Delta\delta$ (ppm)	$\Delta\delta$ (Hz)
1	0.00	0.00	0.00	0.00	0.00	6.507	0.00	0.000
2	0.55	0.78	0.78	0.584	1.713	6.287	0.22	110
3	1.33	1.89	1.89	1.411	0.708	6.098	0.409	204.5
4	1.77	2.52	2.52	1.878	0.532	6.032	0.475	237.5
5	2.87	4.09	4.09	3.046	0.328	5.930	0.577	288.5
6	3.65	5.20	5.20	3.873	0.258	5.885	0.622	311
7	4.78	6.81	6.81	5.073	0.197	5.848	0.659	329.5
8	5.63	8.02	8.02	5.975	0.167	5.828	0.679	339.5
9	6.42	9.15	9.15	6.813	0.147	5.815	0.692	346
10	7.67	10.93	10.93	8.140	0.123	5.800	0.707	353.5
11	8.37	11.92	11.92	8.882	0.113	5.793	0.714	357
12	9.38	13.36	13.36	9.954	0.100	5.784	0.723	361.5

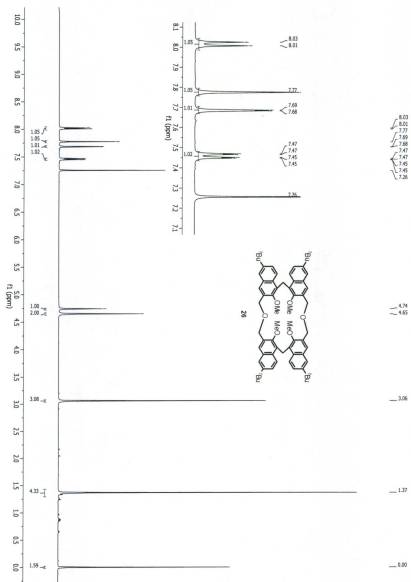


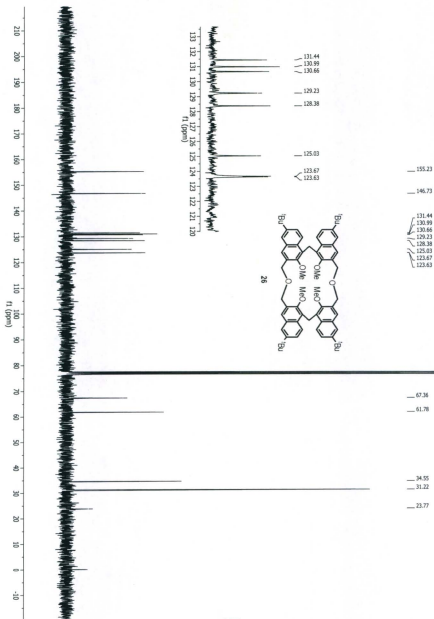


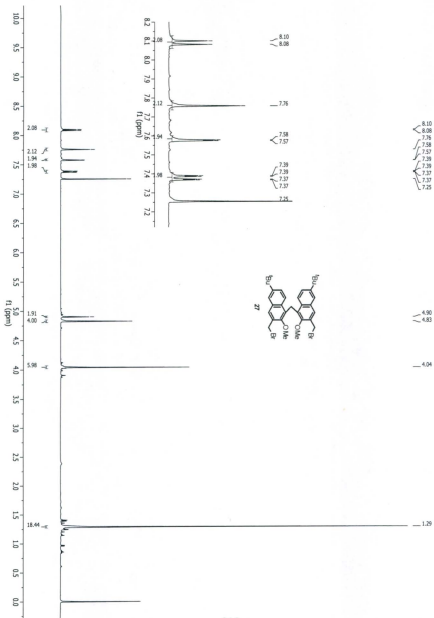


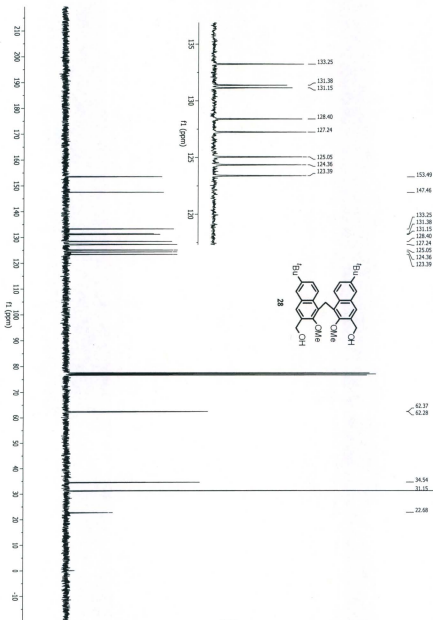












Appendix E

**X-ray crystallographic data reports for compounds
in the order presented in Chapters 2-5**

Appendix 2.1 X-ray crystallographic data for compound **27** (Chapter 2)

(Sample code: th-1-46)

X-ray Structure Report

for

Dr. P. E. Georghiou and T. Al Hujran

prepared by:

Julie L. Collins

February 9, 2009

Introduction

Collection, solution and refinement proceeded normally. All hydrogen atoms were introduced in calculated positions with isotropic thermal parameters set twenty percent greater than those of their bonding partners. They were refined on the riding model, while all other non-hydrogen atoms were refined anisotropically.

Experimental

Data Collection

A colorless prism crystal of $C_{46}H_{28}Cl_4O_8$ having approximate dimensions of 0.23 x 0.08 x 0.08 mm was mounted on a glass fiber. All measurements were made on a Rigaku Saturn CCD area detector with graphite monochromated Mo-K α radiation.

Indexing was performed from 360 images that were exposed for 12.0 seconds. The crystal-to-detector distance was 39.97 mm.

Cell constants and an orientation matrix for data collection corresponded to a C-centered monoclinic cell with dimensions:

$$\begin{aligned} a &= 40.421(12) \text{ \AA} \\ b &= 11.179(3) \text{ \AA} \quad \beta = 95.979(6)^\circ \\ c &= 16.906(5) \text{ \AA} \\ V &= 7598(4) \text{ \AA}^3 \end{aligned}$$

For $Z = 8$ and $F.W. = 850.53$, the calculated density is 1.487 g/cm^3 . Based on the systematic absences of:

$$\begin{aligned} hkl: & h+k \pm 2n \\ h0l: & l \pm 2n \end{aligned}$$

packing considerations, a statistical analysis of intensity distribution, and the successful solution and refinement of the structure, the space group was determined to be:

C2/c (#15)

The data were collected at a temperature of $-150 \pm 1^\circ\text{C}$ to a maximum 2θ value of 62.2° . A total of 1440 oscillation images were collected. A sweep of data was done using ω scans from -75.0 to 105.0° in 0.5° step, at $\chi=45.0^\circ$ and $\phi = 180.0^\circ$. The exposure rate was $24.0 \text{ [sec./}^\circ]$. The detector swing angle was 14.61° . A second sweep was performed using ω scans from -75.0 to 105.0° in 0.5° step, at $\chi=45.0^\circ$ and $\phi = 0.0^\circ$. The exposure rate was $24.0 \text{ [sec./}^\circ]$. The detector swing angle was 14.61° . Another sweep was performed using ω scans from -75.0 to 105.0° in 0.5° step, at $\chi=0.0^\circ$ and $\phi = 180.0^\circ$. The exposure rate was $24.0 \text{ [sec./}^\circ]$. The detector swing angle was 14.61° . Another sweep was performed using ω scans from -75.0 to 105.0° in 0.5° step, at $\chi=45.0^\circ$ and $\phi = 90.0^\circ$. The exposure rate was $24.0 \text{ [sec./}^\circ]$. The detector swing angle was 14.61° . The crystal-to-detector distance was 39.97 mm . Readout was performed in the 0.137 mm pixel mode.

Data Reduction

Of the 62787 reflections that were collected, 7442 were unique ($R_{\text{int}} = 0.057$); equivalent reflections were merged. Data were collected and processed using CrystalClear (Rigaku). Net intensities and sigmas were derived as follows:

$$F^2 = [\Sigma(P_i - mB_{\text{ave}})] \cdot Lp^{-1}$$

where P_i is the value in counts of the i^{th} pixel
 m is the number of pixels in the integration area

B_{ave} is the background average
 L_p is the Lorentz and polarization factor

$$B_{ave} = \Sigma(B_j)/n$$

where n is the number of pixels in the background area
 B_j is the value of the j^{th} pixel in counts

$$\sigma^2(F^2_{hkl}) = [(\Sigma P_i) + m(\Sigma(B_{ave} - B_j)^2)/(n-1))] \cdot L_p \cdot \text{errmul} + (\text{erradd} \cdot F^2)^2$$

where $\text{erradd} = 0.00$
 $\text{errmul} = 1.00$

The linear absorption coefficient, μ , for Mo-K α radiation is 3.699 cm⁻¹. The data were corrected for Lorentz and polarization effects. A numerical absorption correction was applied which resulted in transmission factors ranging from 0.9483 to 0.9858.

Structure Solution and Refinement

The structure was solved by direct methods² and expanded using Fourier techniques³. The non-hydrogen atoms were refined anisotropically. Hydrogen atoms were refined using the riding model. The final cycle of full-matrix least-squares refinement⁴ on F^2 was based on 7442 observed reflections and 524 variable parameters and converged (largest parameter shift was 0.00 times its esd) with unweighted and weighted agreement factors of:

$$R1 = \Sigma ||F_o| - |F_c|| / \Sigma |F_o| = 0.1071$$

$$wR2 = [\Sigma (w (F_o^2 - F_c^2)^2) / \Sigma w (F_o^2)^2]^{1/2} = 0.3185$$

The standard deviation of an observation of unit weight⁵ was 1.17. Unit weights were used. The maximum and minimum peaks on the final difference Fourier map corresponded to 1.89 and -1.00 e⁻/Å³, respectively.

Neutral atom scattering factors were taken from Cromer and Waber⁶. Anomalous dispersion effects were included in F_{calc} ⁷; the values for $\Delta f'$ and $\Delta f''$ were those of Creagh and McAuley⁸. The values for the mass attenuation coefficients are those of Creagh and Hubbell⁹. All calculations were performed using the CrystalStructure^{10,11} crystallographic software package except for refinement, which was performed using SHELXL-97¹².

References

(1) CrystalClear: Rigaku Corporation, 1999. CrystalClear Software User's Guide, Molecular Structure Corporation, (c) 2000. J.W. Pflugrath (1999) Acta Cryst. D55, 1718-1725.

(2) SHELX97: Sheldrick, G.M. (1997).

(3) DIRDIF99: Beurskens, P.T., Admiraal, G., Beurskens, G., Bosman, W.P., de Gelder, R., Israel, R. and Smits, J.M.M. (1999). The DIRDIF-99 program system, Technical Report of the Crystallography Laboratory, University of Nijmegen, The Netherlands.

(4) Least Squares function minimized: (SHELXL97)

$$\sum w(F_o^2 - F_c^2)^2 \quad \text{where } w = \text{Least Squares weights.}$$

(5) Standard deviation of an observation of unit weight:

$$[\sum w(F_o^2 - F_c^2)^2 / (N_o - N_v)]^{1/2}$$

where: N_o = number of observations
 N_v = number of variables

(6) Cromer, D. T. & Waber, J. T.; "International Tables for X-ray Crystallography", Vol. IV, The Kynoch Press, Birmingham, England, Table 2.2 A (1974).

(7) Ibers, J. A. & Hamilton, W. C.; Acta Crystallogr., 17, 781 (1964).

(8) Creagh, D. C. & McAuley, W. J.; "International Tables for Crystallography", Vol C, (A.J.C. Wilson, ed.), Kluwer Academic Publishers, Boston, Table 4.2.6.8, pages 219-222 (1992).

(9) Creagh, D. C. & Hubbell, J.H.; "International Tables for Crystallography", Vol C, (A.J.C. Wilson, ed.), Kluwer Academic Publishers, Boston, Table 4.2.4.3, pages 200-206 (1992).

(10) CrystalStructure 3.7.0: Crystal Structure Analysis Package, Rigaku and Rigaku/MSU (2000-2005). 9009 New Trails Dr. The Woodlands TX 77381 USA.

(11) CRYSTALS Issue 10: Watkin, D.J., Prout, C.K. Carruthers, J.R. & Betteridge, P.W. Chemical Crystallography Laboratory, Oxford, UK. (1996)

(12) SHELX97: Sheldrick, G.M. (1997).

EXPERIMENTAL DETAILS

A. Crystal Data

Empirical Formula	C ₄₆ H ₂₈ Cl ₄ O ₈
Formula Weight	850.53
Crystal Color, Habit	colorless, prism
Crystal Dimensions	0.23 X 0.08 X 0.08 mm
Crystal System	monoclinic
Lattice Type	C-centered
Indexing Images	360 images @ 12.0 seconds
Detector Position	39.97 mm
Pixel Size	0.137 mm
Lattice Parameters	a = 40.421(12) Å b = 11.179(3) Å c = 16.906(5) Å β = 95.979(6)° V = 7598(4) Å ³
Space Group	C2/c (#15)
Z value	8
D _{calc}	1.487 g/cm ³
F ₀₀₀	3488.00
μ(MoKα)	3.699 cm ⁻¹

B. Intensity Measurements

Detector	Rigaku Saturn
Goniometer	Rigaku AFC8
Radiation	MoKα (λ = 0.71075 Å)

	Rigaku SHINE optic
Detector Aperture	70 mm x 70 mm
Data Images	1440 exposures
ω oscillation Range ($\chi=45.0$, $\phi=180.0$)	-75.0 - 105.0 $^{\circ}$
Exposure Rate	24.0 sec./ $^{\circ}$
Detector Swing Angle	14.61 $^{\circ}$
ω oscillation Range ($\chi=45.0$, $\phi=0.0$)	-75.0 - 105.0 $^{\circ}$
Exposure Rate	24.0 sec./ $^{\circ}$
Detector Swing Angle	14.61 $^{\circ}$
ω oscillation Range ($\chi=0.0$, $\phi=180.0$)	-75.0 - 105.0 $^{\circ}$
Exposure Rate	24.0 sec./ $^{\circ}$
Detector Swing Angle	14.61 $^{\circ}$
ω oscillation Range ($\chi=45.0$, $\phi=90.0$)	-75.0 - 105.0 $^{\circ}$
Exposure Rate	24.0 sec./ $^{\circ}$
Detector Swing Angle	14.61 $^{\circ}$
Detector Position	39.97 mm
Pixel Size	0.137 mm
2 θ max	62.2 $^{\circ}$
No. of Reflections Measured	Total: 62787 Unique: 7442 ($R_{\text{int}} = 0.057$)
Corrections	Lorentz-polarization Absorption

Appendix 2.2 X-ray crystallographic data for compound **28** (Chapter 2)

(Sample: TH2-63-2)

X-ray Structure Report

for

Dr. P. E. Georghiou and T. Al Hujran

Prepared by

Louise N. Dawe, PhD

Centre for Chemical Analysis, Research and Training (C-CART)

Department of Chemistry

Memorial University of Newfoundland

St. Johns, NL, A1B 3X7

(709) 737-4556 (X-Ray Laboratory)

May 13, 2010

Introduction

Collection, solution and refinement proceeded normally. H(3) and H(3A) were located in difference map positions and refined on a riding model. All other hydrogen atoms were introduced in calculated positions with isotropic thermal parameters set twenty percent greater than those of their bonding partners and were refined on the riding model. All non-hydrogen atoms were refined anisotropically. The asymmetric unit contains 1/3 of the full molecule, therefore the Z-value was set to 6 in order to reflect the molecular formula:



Experimental

Data Collection

A colorless prism crystal of $C_{45}H_{44}O_7$ having approximate dimensions of 0.46 x 0.42 x 0.24 mm was mounted on a low temperature diffraction loop. All measurements were made on a Rigaku Saturn CCD area detector with a SHINE optic and Mo-K α radiation.

Indexing was performed from 360 images that were exposed for 17 seconds. The crystal-to-detector distance was 40.10 mm.

Cell constants and an orientation matrix for data collection corresponded to a R-centered trigonal cell (laue class: -3) with dimensions:

$$\begin{aligned}a &= 15.849(5) \text{ \AA} \\c &= 26.950(9) \text{ \AA} \\V &= 5863(3) \text{ \AA}^3\end{aligned}$$

For $Z = 6$ and $F.W. = 696.84$, the calculated density is 1.184 g/cm^3 . Based on the systematic absences of:

$$hkil: -h+k+l \pm 3n$$

packing considerations, a statistical analysis of intensity distribution, and the successful solution and refinement of the structure, the space group was determined to be:

R-3 (#148)

The data were collected at a temperature of $-120 \pm 1^\circ\text{C}$ to a maximum 2θ value of 61.8° . A total of 1064 oscillation images were collected. A sweep of data was done using ω scans from -75.0 to 105.0° in 0.5° step, at $\chi=0.0^\circ$ and $\phi = 0.0^\circ$. The exposure rate was $34.0 \text{ [sec./}^\circ\text{]}$. The detector swing angle was 15.06° . A second sweep was performed using ω scans from -75.0 to 105.0° in 0.5° step, at $\chi=45.0^\circ$ and $\phi = 0.0^\circ$. The exposure rate was $34.0 \text{ [sec./}^\circ\text{]}$. The detector swing angle was 15.06° . Another sweep was performed using ω scans from -75.0 to 97.0° in 0.5° step, at $\chi=45.0^\circ$ and $\phi = 180.0^\circ$. The exposure rate was $34.0 \text{ [sec./}^\circ\text{]}$. The detector swing angle was 15.06° . The crystal-to-detector distance was 40.10 mm. Readout was performed in the 0.137 mm pixel mode.

Data Reduction

Of the 25563 reflections that were collected, 2699 were unique ($R_{int} = 0.0307$); equivalent reflections were merged. Data were collected and processed using CrystalClear (Rigaku). Net intensities and sigmas were derived as follows:

$$F^2 = [\Sigma(P_i - mB_{ave})] \cdot L_p^{-1}$$

where P_i is the value in counts of the i^{th} pixel
 m is the number of pixels in the integration area
 B_{ave} is the background average
 L_p is the Lorentz and polarization factor

$$B_{ave} = \Sigma(B_j)/n$$

where n is the number of pixels in the background area
 B_j is the value of the j^{th} pixel in counts

$$\sigma^2(F^2_{hkl}) = [(\Sigma P_i) + m((\Sigma(B_{ave} - B_j)^2)/(n-1))] \cdot L_p \cdot \text{errmul} + (\text{erradd} \cdot F^2)^2$$

where $\text{erradd} = 0.00$
 $\text{errmul} = 1.00$

The linear absorption coefficient, μ , for Mo-K α radiation is 0.79 cm^{-1} . A numerical absorption correction was applied which resulted in transmission factors ranging from 0.9766 to 0.9956. The data were corrected for Lorentz and polarization effects.

Structure Solution and Refinement

The structure was solved by direct methods² and expanded using Fourier techniques³. The non-hydrogen atoms were refined anisotropically. Hydrogen atoms were refined using the riding model. The final cycle of full-matrix least-squares refinement⁴ on F^2 was based on 2699 observed reflections and 158 variable parameters and converged (largest parameter shift was 0.00 times its esd) with unweighted and weighted agreement factors of:

$$R1 = \Sigma ||F_o| - |F_c|| / \Sigma |F_o| = 0.0835$$

$$wR2 = [\Sigma (w (F_o^2 - F_c^2)^2) / \Sigma w(F_o^2)^2]^{1/2} = 0.2405$$

The standard deviation of an observation of unit weight⁵ was 1.13. Unit weights were used. The maximum and minimum peaks on the final difference Fourier map corresponded to 1.13 and -0.27 e⁻/Å³, respectively.

Neutral atom scattering factors were taken from Cromer and Waber⁶. Anomalous dispersion effects were included in F_{calc}⁷; the values for Δf' and Δf'' were those of Creagh and McAuley⁸. The values for the mass attenuation coefficients are those of Creagh and Hubbell⁹. All calculations were performed using the CrystalStructure^{10,11} crystallographic software package except for refinement, which was performed using SHELXL-97¹².

References

- (1) CrystalClear: Rigaku Corporation, 1999. CrystalClear Software User's Guide, Molecular Structure Corporation, (c) 2000. J.W. Pflugrath (1999) Acta Cryst. D55, 1718-1725.
- (2) SHELX97: Sheldrick, G.M. (1997).
- (3) DIRDIF99: Beurskens, P.T., Admiraal, G., Beurskens, G., Bosman, W.P., de Gelder, R., Israel, R. and Smits, J.M.M. (1999). The DIRDIF-99 program system, Technical Report of the Crystallography Laboratory, University of Nijmegen, The Netherlands.
- (4) Least Squares function minimized: (SHELXL97)

$$\sum w(F_o^2 - F_c^2)^2 \quad \text{where } w = \text{Least Squares weights.}$$

- (5) Standard deviation of an observation of unit weight:

$$[\sum w(F_o^2 - F_c^2)^2 / (N_o - N_v)]^{1/2}$$

where: N_o = number of observations
 N_v = number of variables

- (6) Cromer, D. T. & Waber, J. T.; "International Tables for X-ray Crystallography", Vol. IV, The Kynoch Press, Birmingham, England, Table 2.2 A (1974).
- (7) Ibers, J. A. & Hamilton, W. C.; Acta Crystallogr., 17, 781 (1964).
- (8) Creagh, D. C. & McAuley, W. J. ; "International Tables for Crystallography", Vol C, (A.J.C. Wilson, ed.), Kluwer Academic Publishers, Boston, Table 4.2.6.8, pages 219-222 (1992).

(9) Creagh, D. C. & Hubbell, J.H.; "International Tables for Crystallography", Vol C, (A.J.C. Wilson, ed.), Kluwer Academic Publishers, Boston, Table 4.2.4.3, pages 200-206 (1992).

(10) CrystalStructure 3.7.0: Crystal Structure Analysis Package, Rigaku and Rigaku/MSC (2000-2005). 9009 New Trails Dr. The Woodlands TX 77381 USA.

(11) CRYSTALS Issue 10: Watkin, D.J., Prout, C.K. Carruthers, J.R. & Betteridge, P.W. Chemical Crystallography Laboratory, Oxford, UK. (1996)

(12) SHELX97: Sheldrick, G.M. (1997).

EXPERIMENTAL DETAILS

A. Crystal Data

Empirical Formula	C ₄₅ H ₄₄ O ₇
Formula Weight	696.84
Crystal Color, Habit	colorless, prism
Crystal Dimensions	0.46 X 0.42 X 0.24 mm
Crystal System	trigonal
Lattice Type	R-centered
Detector Position	40.10 mm
Pixel Size	0.137 mm
Lattice Parameters	a = 15.849(5) Å c = 26.950(9) Å V = 5863(3) Å ³
Space Group	R-3 (#148)
Z value	6
D _{calc}	1.184 g/cm ³
F000	2220

$\mu(\text{MoK}\alpha)$ 0.79 cm^{-1}

B. Intensity Measurements

Detector Goniometer	Rigaku Saturn Rigaku AFC8
Radiation	MoK α ($\lambda = 0.71075 \text{ \AA}$) graphite monochromated-Rigaku
SHINE	
Detector Aperture	70 mm x 70 mm
Data Images	1064 exposures
ω oscillation Range ($\chi=0.0, \phi=0.0$)	-75.0 - 105.0 $^\circ$
Exposure Rate	34.0 sec./°
Detector Swing Angle	15.06 $^\circ$
ω oscillation Range ($\chi=45.0, \phi=0.0$)	-75.0 - 105.0 $^\circ$
Exposure Rate	34.0 sec./°
Detector Swing Angle	15.06 $^\circ$
ω oscillation Range ($\chi=45.0, \phi=180.0$)	-75.0 - 97.0 $^\circ$
Exposure Rate	34.0 sec./°
Detector Swing Angle	15.06 $^\circ$
Detector Position	40.10 mm
Pixel Size	0.137 mm
$2\theta_{\text{max}}$	61.8 $^\circ$
No. of Reflections Measured	Total: 25563 Unique: 2699 ($R_{\text{int}} = 0.0307$) $I > 2\sigma(I)$: 2677

Corrections

Lorentz-polarization
(trans. factors: 0.9766 - 0.9956)

C. Structure Solution and Refinement

Structure Solution	Direct Methods (SHELX97)
Refinement	Full-matrix least-squares on F^2
Function Minimized	$\sum w (F_o^2 - F_c^2)^2$
Least Squares Weights	$w = 1 / [\sigma^2(F_o^2) + (0.1348 \cdot P)^2 + 12.1828 \cdot P]$ where $P = (\text{Max}(F_o^2, 0) + 2F_c^2)/3$
$2\theta_{\text{max}}$ cutoff	53.0°
Anomalous Dispersion	All non-hydrogen atoms
No. Observations (All reflections)	2699
No. Variables	158
Reflection/Parameter Ratio	17.08
Residuals: R1 ($I > 2.00\sigma(I)$)	0.0835
Residuals: R (All reflections)	0.0839
Residuals: wR2 (All reflections)	0.2405
Goodness of Fit Indicator	1.128
Max Shift/Error in Final Cycle	0.000
Maximum peak in Final Diff. Map	1.13 e ⁻ /Å ³
Minimum peak in Final Diff. Map	-0.27 e ⁻ /Å ³

Appendix 2.3 X-ray crystallographic data for compound **29** (Chapter 2)

(Sample code: TH2-16)

X-ray Structure Report

for

Dr. P. E. Georghiou and T. Al Hujran

Prepared by

Louise N. Dawe, PhD

Centre for Chemical Analysis, Research and Training (C-CART)

Department of Chemistry

Memorial University of Newfoundland

St. Johns, NL, A1B 3X7

(709) 737-4556 (X-Ray Laboratory)

May 14, 2010

Introduction

A report was previously prepared for this data, however, the data was SQUEEZE'd, but the lattice solvent molecules were of interest. This report reflects the full model (though the statistics are significantly higher than the Squeezed solution).

Collection, solution and refinement proceeded normally. All hydrogen atoms were introduced in calculated positions with isotropic thermal parameters set twenty percent greater than those of their bonding partners. They were refined on the riding model. All non-hydrogen atoms were refined anisotropically.

The Z-value was set to 3 to reflect the molecular formula, which is:



Experimental

Data Collection

A colorless prism crystal of $C_{94}H_{88}Cl_{12}O_{12}$ having approximate dimensions of 0.21 x 0.18 x 0.11 mm was mounted on a low temperature diffraction loop. All measurements were made on a Rigaku Saturn CCD area detector equipped with a SHINE optic and Mo-K α radiation.

Indexing was performed from 360 images that were exposed for 30 seconds. The crystal-to-detector distance was 50.09 mm.

Cell constants and an orientation matrix for data collection corresponded to a R-centered trigonal cell (laue class: -3) with dimensions:

$$\begin{aligned}a &= 16.6442(16) \text{ \AA} \\c &= 27.928(3) \text{ \AA} \\V &= 6700.3(12) \text{ \AA}^3\end{aligned}$$

For $Z = 3$ and $F.W. = 1835.04$, the calculated density is 1.364 g/cm^3 . Based on the systematic absences of:

$$hkl: -h+k+l \pm 3n$$

packing considerations, a statistical analysis of intensity distribution, and the successful solution and refinement of the structure, the space group was determined to be:

R-3 (#148)

The data were collected at a temperature of $-120 \pm 1^\circ\text{C}$ to a maximum 2θ value of 59.4° . A total of 1080 oscillation images were collected. A sweep of data was done using ω scans from -70.0 to 110.0° in 0.5° step, at $\chi=45.0^\circ$ and $\phi = 0.0^\circ$. The exposure rate was $60.0 \text{ [sec./}^\circ]$. The detector swing angle was 20.10° . A second sweep was performed using ω scans from -70.0 to 110.0° in 0.5° step, at $\chi=45.0^\circ$ and $\phi = 180.0^\circ$. The exposure rate was $60.0 \text{ [sec./}^\circ]$. The detector swing angle was 20.10° . Another sweep was performed using ω scans from -70.0 to 110.0° in 0.5° step, at $\chi=0.0^\circ$ and $\phi = 180.0^\circ$. The exposure rate was $60.0 \text{ [sec./}^\circ]$. The detector swing angle was 20.10° . The crystal-to-detector distance was 50.09 mm. Readout was performed in the 0.137 mm pixel mode.

Data Reduction

Of the 20958 reflections that were collected, 2622 were unique ($R_{int} = 0.0291$); equivalent reflections were merged. Data were collected and processed using CrystalClear (Rigaku). Net intensities and sigmas were derived as follows:

$$F^2 = [\Sigma(P_i - mB_{ave})] \cdot L_p^{-1}$$

where P_i is the value in counts of the i^{th} pixel
 m is the number of pixels in the integration area
 B_{ave} is the background average
 L_p is the Lorentz and polarization factor

$$B_{ave} = \Sigma(B_j)/n$$

where n is the number of pixels in the background area
 B_j is the value of the j^{th} pixel in counts

$$\sigma^2(F^2_{hkl}) = [(\Sigma P_i) + m(\Sigma(B_{ave} - B_j)^2)/(n-1)] \cdot L_p \cdot \text{errmul} + (\text{erradd} \cdot F^2)^2$$

where $\text{erradd} = 0.00$
 $\text{errmul} = 1.00$

The linear absorption coefficient, μ , for Mo-K α radiation is 4.319 cm⁻¹. A numerical absorption correction was applied which resulted in transmission factors ranging from 0.9497 to 0.9775. The data were corrected for Lorentz and polarization effects.

Structure Solution and Refinement

The structure was solved by direct methods² and expanded using Fourier techniques³. The non-hydrogen atoms were refined anisotropically. Hydrogen atoms were refined using the riding model. The final cycle of full-matrix least-squares refinement⁴ on F^2 was based on 2622 observed reflections and 179 variable parameters and converged (largest parameter shift was 0.00 times its esd) with unweighted and weighted agreement factors of:

$$R1 = \Sigma ||F_o| - |F_c|| / \Sigma |F_o| = 0.1111$$

$$wR2 = [\Sigma (w (F_o^2 - F_c^2)^2) / \Sigma w(F_o^2)^2]^{1/2} = 0.3914$$

The standard deviation of an observation of unit weight⁵ was 1.91. Unit weights were used. The maximum and minimum peaks on the final difference Fourier map corresponded to 0.75 and -0.82 e⁻/Å³, respectively.

Neutral atom scattering factors were taken from Cromer and Waber⁶. Anomalous dispersion effects were included in F_{calc}⁷; the values for Δf' and Δf'' were those of Creagh and McAuley⁸. The values for the mass attenuation coefficients are those of Creagh and Hubbell⁹. All calculations were performed using the CrystalStructure^{10,11} crystallographic software package except for refinement, which was performed using SHELXL-97¹².

References

- (1) CrystalClear: Rigaku Corporation, 1999. CrystalClear Software User's Guide, Molecular Structure Corporation, (c) 2000.J.W.Pflugrath (1999) Acta Cryst. D55, 1718-1725.
- (2) SIR92: Altomare, A., Cascarano, G., Giacovazzo, C., Guagliardi, A., Burla, M., Polidori, G., and Camalli, M. (1994) J. Appl. Cryst., 27, 435.
- (3) DIRDIF99: Beurskens, P.T., Admiraal, G., Beurskens, G., Bosman, W.P., de Gelder, R., Israel, R. and Smits, J.M.M.(1999). The DIRDIF-99 program system, Technical Report of the Crystallography Laboratory, University of Nijmegen, The Netherlands.
- (4) Least Squares function minimized: (SHELXL97)

$$\sum w(F_o^2 - F_c^2)^2 \quad \text{where } w = \text{Least Squares weights.}$$

- (5) Standard deviation of an observation of unit weight:

$$[\sum w(F_o^2 - F_c^2)^2 / (N_o - N_v)]^{1/2}$$

where: N_o = number of observations
 N_v = number of variables

- (6) Cromer, D. T. & Waber, J. T.; "International Tables for X-ray Crystallography", Vol. IV, The Kynoch Press, Birmingham, England, Table 2.2 A (1974).
- (7) Ibers, J. A. & Hamilton, W. C.; Acta Crystallogr., 17, 781 (1964).
- (8) Creagh, D. C. & McAuley, W.J.; "International Tables for Crystallography", Vol C, (A.J.C. Wilson, ed.), Kluwer Academic Publishers, Boston, Table 4.2.6.8, pages 219-222 (1992).

(9) Creagh, D. C. & Hubbell, J.H.: "International Tables for Crystallography", Vol C, (A.J.C. Wilson, ed.), Kluwer Academic Publishers, Boston, Table 4.2.4.3, pages 200-206 (1992).

(10) CrystalStructure 3.7.0: Crystal Structure Analysis Package, Rigaku and Rigaku/MSC (2000-2005). 9009 New Trails Dr. The Woodlands TX 77381 USA.

(11) CRYSTALS Issue 10: Watkin, D.J., Prout, C.K. Carruthers, J.R. & Betteridge, P.W. Chemical Crystallography Laboratory, Oxford, UK. (1996)

(12) SHELX97: Sheldrick, G.M. (1997).

EXPERIMENTAL DETAILS

A. Crystal Data

Empirical Formula	C ₉₄ H ₈₈ Cl ₁₂ O ₁₂
Formula Weight	1835.04
Crystal Color, Habit	colorless, prism
Crystal Dimensions	0.21 X 0.18 X 0.11 mm
Crystal System	trigonal
Lattice Type	R-centered
Detector Position	50.09 mm
Pixel Size	0.137 mm
Lattice Parameters	a = 16.6442(16) Å c = 27.928(3) Å V = 6700.3(12) Å ³
Space Group	R-3 (#148)
Z value	3
D _{calc}	1.364 g/cm ³

F000	2856
$\mu(\text{MoK}\alpha)$	4.32 cm ⁻¹

B. Intensity Measurements

Detector Goniometer	Rigaku Saturn Rigaku AFC8
Radiation	MoK α ($\lambda = 0.71075 \text{ \AA}$) graphite monochromated-Rigaku
SHINE	
Detector Aperture	70 mm x 70 mm
Data Images	1080 exposures
ω oscillation Range ($\chi=45.0, \phi=0.0$)	-70.0 - 110.0 ^o
Exposure Rate	60.0 sec./ ^o
Detector Swing Angle	20.10 ^o
ω oscillation Range ($\chi=45.0, \phi=180.0$)	-70.0 - 110.0 ^o
Exposure Rate	60.0 sec./ ^o
Detector Swing Angle	20.10 ^o
ω oscillation Range ($\chi=0.0, \phi=180.0$)	-70.0 - 110.0 ^o
Exposure Rate	60.0 sec./ ^o
Detector Swing Angle	20.10 ^o
Detector Position	50.09 mm
Pixel Size	0.137 mm
2 θ _{max}	59.4 ^o
No. of Reflections Measured	Total: 20958 Unique: 2622 ($R_{\text{int}} = 0.0291$)

	I>2 σ (I): 2606
Corrections	Lorentz-polarization (trans. factors: 0.9497 - 0.9775)

C. Structure Solution and Refinement

Structure Solution	Direct Methods (SIR92)
Refinement	Full-matrix least-squares on F ²
Function Minimized	$\Sigma w (F_o^2 - F_c^2)^2$
Least Squares Weights	$w = 1 / [\sigma^2(F_o^2) + (0.2000 \cdot P)^2 + 0.0000 \cdot P]$ where $P = (\text{Max}(F_o^2, 0) + 2F_c^2)/3$
2 θ_{max} cutoff	50.0 ^o
Anomalous Dispersion	All non-hydrogen atoms
No. Observations (All reflections)	2622
No. Variables	179
Reflection/Parameter Ratio	14.65
Residuals: R1 (I>2.00 σ (I))	0.1111
Residuals: R (All reflections)	0.1113
Residuals: wR2 (All reflections)	0.3914
Goodness of Fit Indicator	1.908
Max Shift/Error in Final Cycle	0.001
Maximum peak in Final Diff. Map	0.75 e ⁻ /Å ³
Minimum peak in Final Diff. Map	-0.82 e ⁻ /Å ³

Appendix 3.1 X-ray crystallographic data for compound 19b (Chapter 3)

(Sample code: TH3-95AA-T4)

X-ray Structure Report

for

Prof. Paris Georghiou and T. Al Hujran

Prepared by

Louise N. Dawe, PhD

Centre for Chemical Analysis, Research and Training (C-CART)

Department of Chemistry

Memorial University of Newfoundland

St. Johns, NL, A1B 3X7

(709) 864-4556 (X-Ray Laboratory)

(709) 864-8904 (Office)

October 21, 2011

Introduction

All non-hydrogen atoms were refined anisotropically. All C-bound H-atoms were introduced in calculated positions and refined on a riding model. N-H and O-H H-atoms were introduced in difference map positions and were refined positionally with DFIX restraints and riding isotropic displacement parameters (0.88 Å with 1.2Ueq for N-H, and 0.84 Å with 1.5 Ueq for O-H). An angle restraint was introduced for C35-O8-H8A.

Experimental

Data Collection

A colorless prism crystal of $C_{70}H_{88}N_4O_{16}$ having approximate dimensions of 0.29 x 0.23 x 0.09 mm was mounted on a glass fiber. All measurements were made on a Rigaku Saturn70 CCD diffractometer using graphite monochromated Mo-K α radiation, equipped with a SHINE optic.

The crystal-to-detector distance was 50.08 mm.

Cell constants and an orientation matrix for data collection corresponded to a primitive monoclinic cell with dimensions:

$$\begin{aligned} a &= 15.322(7) \text{ \AA} \\ b &= 11.727(5) \text{ \AA} & \beta &= 96.666(5)^\circ \\ c &= 18.013(8) \text{ \AA} \\ V &= 3215(2) \text{ \AA}^3 \end{aligned}$$

For $Z = 2$ and $F.W. = 1241.48$, the calculated density is 1.282 g/cm^3 . The reflection conditions of:

$$\begin{aligned} h0l: l &= 2n \\ 0k0: k &= 2n \end{aligned}$$

uniquely determine the space group to be:

$$P2_1/c \text{ (\#14)}$$

The data were collected at a temperature of $-110 \pm 1^\circ\text{C}$ to a maximum 2θ value of 59.7° . A total of 1064 oscillation images were collected. A sweep of data was done using ω scans from -70.0 to 110.0° in 0.5° step, at $\chi=45.0^\circ$ and $\phi = 90.0^\circ$. The exposure rate was $44.0 \text{ [sec./}^\circ]$. The detector swing angle was 20.12° . A second sweep was performed using ω scans from -70.0 to 110.0° in 0.5° step, at $\chi=45.0^\circ$ and $\phi = 180.0^\circ$. The exposure rate was $44.0 \text{ [sec./}^\circ]$. The detector swing angle was 20.12° . Another sweep was performed using ω scans from -70.0 to 102.0° in 0.5° step, at $\chi=45.0^\circ$ and $\phi = 0.0^\circ$. The exposure rate was $44.0 \text{ [sec./}^\circ]$. The detector swing angle was 20.12° . The crystal-to-detector

distance was 50.08 mm. Readout was performed in the 0.137 mm pixel mode.

Data Reduction

Of the 32798 reflections that were collected, 6650 were unique ($R_{int} = 0.0525$). Data were collected and processed using CrystalClear (Rigaku).

The linear absorption coefficient, μ , for Mo-K α radiation is 0.91 cm⁻¹. An empirical absorption correction was applied which resulted in transmission factors ranging from 0.985 to 0.996. The data were corrected for Lorentz and polarization effects.

Structure Solution and Refinement

The structure was solved by direct methods² and expanded using Fourier techniques. The non-hydrogen atoms were refined anisotropically. Some hydrogen atoms were refined isotropically, some were refined using the riding model, and the rest were included in fixed positions. The final cycle of full-matrix least-squares refinement³ on F^2 was based on 6650 observed reflections and 422 variable parameters and converged (largest parameter shift was 0.00 times its esd) with unweighted and weighted agreement factors of:

$$R1 = \sum ||Fo| - |Fc|| / \sum |Fo| = 0.0747$$

$$wR2 = [\sum (w (Fo^2 - Fc^2)^2) / \sum w(Fo^2)^2]^{1/2} = 0.2137$$

The standard deviation of an observation of unit weight⁴ was 1.10. Unit weights were used. The maximum and minimum peaks on the final difference Fourier map corresponded to 0.53 and -0.61 e-/Å³, respectively.

Neutral atom scattering factors were taken from Cromer and Waber⁵. Anomalous dispersion effects were included in F_{calc} ⁶; the values for $\Delta f'$ and $\Delta f''$ were those of Creagh and McAuley⁷. The values for the mass attenuation coefficients are those of Creagh and Hubbell⁸. All calculations were performed using the CrystalStructure⁹ crystallographic software package except for refinement, which was performed using SHELXL-97².

References

(1) CrystalClear: Rigaku Corporation, 1999. CrystalClear Software User's Guide, Molecular Structure Corporation, (c) 2000. J.W. Pflugrath (1999) Acta Cryst. D55, 1718-1725.

(2) SHELX97: Sheldrick, G.M. Acta Cryst. 2008, A64, 112-122

(3) Least Squares function minimized: (SHELXL97)

$$\sum w(F_o^2 - F_c^2)^2 \quad \text{where } w = \text{Least Squares weights.}$$

(4) Standard deviation of an observation of unit weight:

$$[\sum w(F_o^2 - F_c^2)^2 / (N_o - N_v)]^{1/2}$$

where: N_o = number of observations
 N_v = number of variables

(5) Cromer, D. T. & Waber, J. T.; "International Tables for X-ray Crystallography", Vol. IV, The Kynoch Press, Birmingham, England, Table 2.2 A (1974).

(6) Ibers, J. A. & Hamilton, W. C.; Acta Crystallogr., 17, 781 (1964).

(7) Creagh, D. C. & McAuley, W.J. ; "International Tables for Crystallography", Vol C, (A.J.C. Wilson, ed.), Kluwer Academic Publishers, Boston, Table 4.2.6.8, pages 219-222 (1992).

(8) Creagh, D. C. & Hubbell, J.H.; "International Tables for Crystallography", Vol C, (A.J.C. Wilson, ed.), Kluwer Academic Publishers, Boston, Table 4.2.4.3, pages 200-206 (1992).

(9) CrystalStructure 4.0: Crystal Structure Analysis Package, Rigaku and Rigaku Americas (2000-2010), 9009 New Trails Dr. The Woodlands TX 77381 USA.

EXPERIMENTAL DETAILS

A. Crystal Data

Empirical Formula	C ₇₀ H ₈₈ N ₄ O ₁₆
Formula Weight	1241.48
Crystal Color, Habit	colorless, prism
Crystal Dimensions	0.29 X 0.23 X 0.09 mm
Crystal System	monoclinic
Lattice Type	Primitive
Lattice Parameters	a = 15.322(7) Å b = 11.727(5) Å c = 18.013(8) Å β = 96.666(5) ° V = 3215(2) Å ³
Space Group	P2 ₁ /c (#14)
Z value	2
D _{calc}	1.282 g/cm ³
F ₀₀₀	1328
μ(MoKα)	0.91 cm ⁻¹

B. Intensity Measurements

Diffractometer	Rigaku Saturn70 CCD
Radiation	MoKα (λ = 0.71075 Å) graphite monochromated-Rigaku
SHINE	
Voltage, Current	50kV, 30mA

Temperature	-110.0°C
Detector Aperture	70 x 70 mm
Data Images	1064 exposures
ω oscillation Range ($\chi=45.0$, $\phi=90.0$)	-70.0 - 110.0°
Exposure Rate	44.0 sec./°
Detector Swing Angle	20.12°
ω oscillation Range ($\chi=45.0$, $\phi=180.0$)	-70.0 - 110.0°
Exposure Rate	44.0 sec./°
Detector Swing Angle	20.12°
ω oscillation Range ($\chi=45.0$, $\phi=0.0$)	-70.0 - 102.0°
Exposure Rate	44.0 sec./°
Detector Swing Angle	20.12°
Detector Position	50.08 mm
Pixel Size	0.137 mm
$2\theta_{\max}$	59.7°
No. of Reflections Measured	Total: 32798 Unique: 6650 ($R_{\text{int}} = 0.0525$) $I > 2\sigma(I)$: 5521
Corrections	Lorentz-polarization (trans. factors: 0.985 - 0.996)

C. Structure Solution and Refinement

Structure Solution	Direct Methods
Refinement	Full-matrix least-squares on F^2
Function Minimized	$\sum w (F_o^2 - F_c^2)^2$
Least Squares Weights	$w = 1 / [\sigma^2(F_o^2) + (0.1034 \cdot P)^2 + 1.7136 \cdot P]$ where $P = (\text{Max}(F_o^2, 0) + 2F_c^2)/3$
$2\theta_{\text{max}}$ cutoff	53.0°
Anomalous Dispersion	All non-hydrogen atoms
No. Observations (All reflections)	6650
No. Variables	422
Reflection/Parameter Ratio	15.76
Residuals: R1 ($I > 2.00\sigma(I)$)	0.0747
Residuals: R (All reflections)	0.0890
Residuals: wR2 (All reflections)	0.2137
Goodness of Fit Indicator	1.103
Max Shift/Error in Final Cycle	0.000
Maximum peak in Final Diff. Map	0.53 e ⁻ /Å ³
Minimum peak in Final Diff. Map	-0.61 e ⁻ /Å ³

Appendix 3.2 X-ray crystallographic data for compound **20a** (Chapter 3)

(Sample: TH3-29A1)

X-ray Structure Report

for

Prof. Paris Georghiou and T. Al Hujran

Prepared by

Louise N. Dawe, PhD

Centre for Chemical Analysis, Research and Training (C-CART)

Department of Chemistry

Memorial University of Newfoundland

St. Johns, NL, A1B 3X7

(709) 864-4556 (X-Ray Laboratory)

January 12, 2011

Introduction

Collection, solution and refinement proceeded normally. H1, H2 and H7A were introduced in difference map positions, and refined positionally, with fixed displacement ellipsoids. All other hydrogen atoms were introduced in calculated positions and refined on a riding model. All non-hydrogen atoms were refined anisotropically.

Experimental

Data Collection

A colorless prism crystal of $C_{32}H_{36}N_2O_7$ having approximate dimensions of 0.30 x 0.27 x 0.10 mm was mounted on a low temperature diffraction loop. All measurements were made on a Rigaku Saturn70 CCD diffractometer using graphite monochromated Mo-K α radiation, equipped with a SHINE optic.

The crystal-to-detector distance was 50.17 mm.

Cell constants and an orientation matrix for data collection corresponded to a primitive triclinic cell with dimensions:

$$\begin{aligned} a &= 11.077(9) \text{ \AA} & \alpha &= 101.180(13)^\circ \\ b &= 11.101(9) \text{ \AA} & \beta &= 95.953(6)^\circ \\ c &= 12.5856(10) \text{ \AA} & \gamma &= 108.874(9)^\circ \\ V &= 1413.3(16) \text{ \AA}^3 \end{aligned}$$

For $Z = 2$ and $F.W. = 560.65$, the calculated density is 1.317 g/cm^3 . Based on a statistical analysis of intensity distribution, and the successful solution and refinement of the structure, the space group was determined to be:

P-1 (#2)

The data were collected at a temperature of $-110 \pm 1^\circ\text{C}$ to a maximum 2θ value of 59.4° . A total of 850 oscillation images were collected. A sweep of data was done using ω scans from -70.0 to 110.0° in 0.5° step, at $\chi=45.0^\circ$ and $\phi = 180.0^\circ$. The exposure rate was $16.0 \text{ [sec./}^\circ]$. The detector swing angle was 20.09° . A second sweep was performed using ω scans from -70.0 to 110.0° in 0.5° step, at $\chi=45.0^\circ$ and $\phi = 0.0^\circ$. The exposure rate was $16.0 \text{ [sec./}^\circ]$. The detector swing angle was 20.09° . Another sweep was performed using ω scans from -10.0 to 55.0° in 0.5° step, at $\chi=0.0^\circ$ and $\phi = 90.0^\circ$. The exposure rate was $16.0 \text{ [sec./}^\circ]$. The detector swing angle was 20.09° . The crystal-to-detector distance was 50.17 mm. Readout was performed in the 0.137 mm pixel mode.

Data Reduction

Of the 11795 reflections that were collected, 5787 were unique ($R_{int} = 0.0328$). Data were collected and processed using CrystalClear (Rigaku).

The linear absorption coefficient, μ , for Mo-K α radiation is 0.93 cm^{-1} . An empirical absorption correction was applied which resulted in transmission factors ranging from 0.979 to 0.995. The data were corrected for Lorentz and polarization effects.

Structure Solution and Refinement

The structure was solved by direct methods² and expanded using Fourier techniques. The non-hydrogen atoms were refined anisotropically. Some hydrogen atoms were refined isotropically, some were refined using the riding model, and the rest were included in fixed positions. The final cycle of full-matrix least-squares refinement³ on F^2 was based on 5787 observed reflections and 382 variable parameters and converged (largest parameter shift was 0.00 times its esd) with unweighted and weighted agreement factors of:

$$R1 = \sum ||F_o| - |F_c|| / \sum |F_o| = 0.0541$$

$$wR2 = [\sum (w (F_o^2 - F_c^2)^2) / \sum w(F_o^2)^2]^{1/2} = 0.1453$$

The standard deviation of an observation of unit weight⁴ was 1.06. Unit weights were used. The maximum and minimum peaks on the final difference Fourier map corresponded to 0.30 and $-0.26 \text{ e}^-/\text{\AA}^3$, respectively.

Neutral atom scattering factors were taken from Cromer and Waber⁵. Anomalous dispersion effects were included in Fcalc⁶; the values for $\Delta f'$ and $\Delta f''$ were those of Creagh and McAuley⁷. The values for the mass attenuation coefficients are those of Creagh and Hubbell⁸. All calculations were performed using the CrystalStructure⁹ crystallographic software package except for refinement, which was performed using SHELXL-97².

References

(1) CrystalClear: Rigaku Corporation, 1999. CrystalClear Software User's Guide, Molecular Structure Corporation, (c) 2000. J.W. Pflugrath (1999) Acta Cryst. D55, 1718-1725.

(2) SHELX97: Sheldrick, G.M. Acta Cryst. 2008, A64, 112-122.

(3) Least Squares function minimized: (SHELXL97)

$$\sum w(F_o^2 - F_c^2)^2 \quad \text{where } w = \text{Least Squares weights.}$$

(4) Standard deviation of an observation of unit weight:

$$[\sum w(F_o^2 - F_c^2)^2 / (N_o - N_v)]^{1/2}$$

where: N_o = number of observations
 N_v = number of variables

(5) Cromer, D. T. & Waber, J. T.; "International Tables for X-ray Crystallography", Vol. IV, The Kynoch Press, Birmingham, England, Table 2.2 A (1974).

(6) Ibers, J. A. & Hamilton, W. C.; Acta Crystallogr., 17, 781 (1964).

(7) Creagh, D. C. & McAuley, W. J. ; "International Tables for Crystallography", Vol C, (A.J.C. Wilson, ed.), Kluwer Academic Publishers, Boston, Table 4.2.6.8, pages 219-222 (1992).

(8) Creagh, D. C. & Hubbell, J.H.; "International Tables for Crystallography", Vol C, (A.J.C. Wilson, ed.), Kluwer Academic Publishers, Boston, Table 4.2.4.3, pages 200-206 (1992).

(9) CrystalStructure 4.0: Crystal Structure Analysis Package, Rigaku and Rigaku Americas (2000-2010). 9009 New Trails Dr. The Woodlands TX 77381 USA.

EXPERIMENTAL DETAILS

A. Crystal Data

Empirical Formula	$C_{32}H_{36}N_2O_7$
Formula Weight	560.65
Crystal Color, Habit	colorless, prism
Crystal Dimensions	0.30 X 0.27 X 0.10 mm
Crystal System	triclinic
Lattice Type	Primitive
Lattice Parameters	$a = 11.077(9) \text{ \AA}$ $b = 11.101(9) \text{ \AA}$ $c = 12.5856(10) \text{ \AA}$ $\alpha = 101.180(13)^\circ$ $\beta = 95.953(6)^\circ$ $\gamma = 108.874(9)^\circ$ $V = 1413.3(16) \text{ \AA}^3$
Space Group	P-1 (#2)
Z value	2
D_{calc}	1.317 g/cm^3
F_{000}	596
$\mu(\text{MoK}\alpha)$	0.93 cm^{-1}

B. Intensity Measurements

Diffractometer	Rigaku Saturn70 CCD
Radiation	MoK α ($\lambda = 0.71075 \text{ \AA}$) graphite monochromated-Rigaku
SHINE	

Voltage, Current	50kV, 30mA
Temperature	-110.0°C
Detector Aperture	70 x 70 mm
Data Images	850 exposures
ω oscillation Range ($\chi=45.0$, $\phi=180.0$)	-70.0 - 110.0°
Exposure Rate	16.0 sec./°
Detector Swing Angle	20.09°
ω oscillation Range ($\chi=45.0$, $\phi=0.0$)	-70.0 - 110.0°
Exposure Rate	16.0 sec./°
Detector Swing Angle	20.09°
ω oscillation Range ($\chi=0.0$, $\phi=90.0$)	-10.0 - 55.0°
Exposure Rate	16.0 sec./°
Detector Swing Angle	20.09°
Detector Position	50.17 mm
Pixel Size	0.137 mm
$2\theta_{\max}$	59.4°
No. of Reflections Measured	Total: 11795 Unique: 5787 ($R_{\text{int}} = 0.0328$) $I > 2\sigma(I)$: 4709
Corrections	Lorentz-polarization (trans. factors: 0.979 - 0.995)

C. Structure Solution and Refinement

Structure Solution	Direct Methods
Refinement	Full-matrix least-squares on F^2
Function Minimized	$\sum w (F_o^2 - F_c^2)^2$
Least Squares Weights	$w = 1 / [\sigma^2(F_o^2) + (0.0656 \cdot P)^2 + 0.5120 \cdot P]$ where $P = (\text{Max}(F_o^2, 0) + 2F_c^2)/3$
$2\theta_{\text{max}}$ cutoff	53.0°
Anomalous Dispersion	All non-hydrogen atoms
No. Observations (All reflections)	5787
No. Variables	382
Reflection/Parameter Ratio	15.15
Residuals: R1 ($I > 2.00\sigma(I)$)	0.0541
Residuals: R (All reflections)	0.0659
Residuals: wR2 (All reflections)	0.1453
Goodness of Fit Indicator	1.057
Max Shift/Error in Final Cycle	0.001
Maximum peak in Final Diff. Map	0.30 e-/Å ³
Minimum peak in Final Diff. Map	-0.26 e-/Å ³

Appendix 3.3 X-ray crystallographic data for compound **21a** (Chapter 3)

(Sample code: TH3-82)

X-ray Structure Report

for

Prof. Paris Georghiou and T. Al Hujran

Prepared by

Louise N. Dawe, PhD

Centre for Chemical Analysis, Research and Training (C-CART)

Department of Chemistry

Memorial University of Newfoundland

St. Johns, NL, A1B 3X7

(709) 864-4556 (X-Ray Laboratory)

(709) 864-8904 (Office)

April 1, 2011

Introduction

Collection, solution and refinement proceeded normally. H1 and H2 were introduced in difference map positions, and refined positionally, with fixed displacement ellipsoids. All other hydrogen atoms were introduced in calculated positions and refined on a riding model. All non-hydrogen atoms were refined anisotropically.

Experimental

Data Collection

A colorless prism crystal of $C_{39.50}H_{50}N_2O_{6.50}$ having approximate dimensions of 0.27 x 0.05 x 0.04 mm was mounted on a low temperature diffraction loop. All measurements were made on a Rigaku Saturn70 CCD diffractometer using graphite monochromated Mo-K α radiation, equipped with a SHINE optic.

The crystal-to-detector distance was 50.06 mm.

Cell constants and an orientation matrix for data collection corresponded to a primitive triclinic cell with dimensions:

$$\begin{aligned} a &= 10.982(6) \text{ \AA} & \alpha &= 75.471(17)^\circ \\ b &= 12.108(6) \text{ \AA} & \beta &= 81.794(16)^\circ \\ c &= 14.903(7) \text{ \AA} & \gamma &= 79.266(15)^\circ \\ V &= 1875.1(16) \text{ \AA}^3 \end{aligned}$$

For $Z = 2$ and $F.W. = 656.84$, the calculated density is 1.163 g/cm^3 . Based on a statistical analysis of intensity distribution, and the successful solution and refinement of the structure, the space group was determined to be:

P-1 (#2)

The data were collected at a temperature of $-110 \pm 1^\circ\text{C}$ to a maximum 2θ value of 59.7° . A total of 840 oscillation images were collected. A sweep of data was done using ω scans from -70.0 to 110.0° in 0.5° step, at $\chi=45.0^\circ$ and $\phi = 180.0^\circ$. The exposure rate was $80.0 \text{ [sec./}^\circ]$. The detector swing angle was 20.07° . A second sweep was performed using ω scans from -70.0 to 110.0° in 0.5° step, at $\chi=45.0^\circ$ and $\phi = 0.0^\circ$. The exposure rate was $80.0 \text{ [sec./}^\circ]$. The detector swing angle was 20.07° . Another sweep was performed using ω scans from -55.0 to 5.0° in 0.5° step, at $\chi=0.0^\circ$ and $\phi = 0.0^\circ$. The exposure rate was $80.0 \text{ [sec./}^\circ]$. The detector swing angle was 20.07° . The crystal-to-detector distance was 50.06 mm. Readout was performed in the 0.137 mm pixel mode.

Data Reduction

Of the 14387 reflections that were collected, 6894 were unique ($R_{\text{int}} = 0.0573$). Data were collected and processed using CrystalClear (Rigaku).

The linear absorption coefficient, μ , for Mo-K α radiation is 0.78 cm^{-1} . An empirical absorption correction was applied which resulted in transmission factors ranging from 0.988 to 0.998. The data were corrected for Lorentz and polarization effects.

Structure Solution and Refinement

The structure was solved by direct methods² and expanded using Fourier techniques. The non-hydrogen atoms were refined anisotropically. Hydrogen atoms were refined using the riding model. The final cycle of full-matrix least-squares refinement³ on F^2 was based on 6894 observed reflections and 458 variable parameters and converged (largest parameter shift was 0.00 times its esd) with unweighted and weighted agreement factors of:

$$R1 = \sum ||F_o| - |F_c|| / \sum |F_o| = 0.1189$$

$$wR2 = [\sum (w (F_o^2 - F_c^2)^2) / \sum w(F_o^2)^2]^{1/2} = 0.3918$$

The standard deviation of an observation of unit weight⁴ was 1.32. Unit weights were used. The maximum and minimum peaks on the final difference Fourier map corresponded to 1.19 and $-0.47 \text{ e}^{-}/\text{Å}^3$, respectively.

Neutral atom scattering factors were taken from Cromer and Waber⁵. Anomalous dispersion effects were included in F_{calc} ⁶; the values for $\Delta f'$ and $\Delta f''$ were those of Creagh and McAuley⁷. The values for the mass attenuation coefficients are those of Creagh and Hubbell⁸. All calculations were performed using the CrystalStructure⁹ crystallographic software package except for refinement, which was performed using SHELXL-97².

References

(1) CrystalClear: Rigaku Corporation, 1999. CrystalClear Software User's Guide, Molecular Structure Corporation, (c) 2000. J.W. Pflugrath (1999) Acta Cryst. D55, 1718-1725.

(2) SHELX97: Sheldrick, G.M. Acta Cryst. 2008, A64, 112-122.

(3) Least Squares function minimized: (SHELXL97)

$$\sum w(F_o^2 - F_c^2)^2 \quad \text{where } w = \text{Least Squares weights.}$$

(4) Standard deviation of an observation of unit weight:

$$[\sum w(F_o^2 - F_c^2)^2 / (N_o - N_v)]^{1/2}$$

where: N_o = number of observations
 N_v = number of variables

(5) Cromer, D. T. & Waber, J. T.; "International Tables for X-ray Crystallography", Vol. IV, The Kynoch Press, Birmingham, England, Table 2.2 A (1974).

(6) Ibers, J. A. & Hamilton, W. C.; Acta Crystallogr., 17, 781 (1964).

(7) Creagh, D. C. & McAuley, W. J. ; "International Tables for Crystallography", Vol C, (A.J.C. Wilson, ed.), Kluwer Academic Publishers, Boston, Table 4.2.6.8, pages 219-222 (1992).

(8) Creagh, D. C. & Hubbell, J.H.; "International Tables for Crystallography", Vol C, (A.J.C. Wilson, ed.), Kluwer Academic Publishers, Boston, Table 4.2.4.3, pages 200-206 (1992).

(9) CrystalStructure 4.0: Crystal Structure Analysis Package, Rigaku and Rigaku Americas (2000-2010). 9009 New Trails Dr. The Woodlands TX 77381 USA.

EXPERIMENTAL DETAILS

A. Crystal Data

Empirical Formula	$C_{39.50}H_{50}N_2O_{6.50}$
Formula Weight	656.84
Crystal Color, Habit	colorless, prism
Crystal Dimensions	0.27 X 0.05 X 0.04 mm
Crystal System	triclinic
Lattice Type	Primitive
Lattice Parameters	$a = 10.982(6) \text{ \AA}$ $b = 12.108(6) \text{ \AA}$ $c = 14.903(7) \text{ \AA}$ $\alpha = 75.471(17)^\circ$ $\beta = 81.794(16)^\circ$ $\gamma = 79.266(15)^\circ$ $V = 1875.1(16) \text{ \AA}^3$
Space Group	P-1 (#2)
Z value	2
D_{calc}	1.163 g/cm^3
F_{000}	706
$\mu(\text{MoK}\alpha)$	0.78 cm^{-1}

B. Intensity Measurements

Diffractometer	Rigaku Saturn70 CCD
Radiation	MoK α ($\lambda = 0.71075 \text{ \AA}$) graphite monochromated-Rigaku

SHINE

Voltage, Current	50kV, 30mA
Temperature	-110.0°C
Detector Aperture	70 x 70 mm
Data Images	840 exposures
ω oscillation Range ($\chi=45.0$, $\phi=180.0$)	-70.0 - 110.0°
Exposure Rate	80.0 sec./°
Detector Swing Angle	20.07°
ω oscillation Range ($\chi=45.0$, $\phi=0.0$)	-70.0 - 110.0°
Exposure Rate	80.0 sec./°
Detector Swing Angle	20.07°
ω oscillation Range ($\chi=0.0$, $\phi=0.0$)	-55.0 - 5.0°
Exposure Rate	80.0 sec./°
Detector Swing Angle	20.07°
Detector Position	50.06 mm
Pixel Size	0.137 mm
$2\theta_{max}$	59.7°
No. of Reflections Measured	Total: 14387 Unique: 6894 ($R_{int} = 0.0573$) $I > 2\sigma(I)$: 4407
Corrections	Lorentz-polarization (trans. factors: 0.988 - 0.998)

C. Structure Solution and Refinement

Structure Solution	Direct Methods
Refinement	Full-matrix least-squares on F^2
Function Minimized	$\sum w (F_o^2 - F_c^2)^2$
Least Squares Weights	$w = 1 / [\sigma^2(F_o^2) + (0.2000 \cdot P)^2 + 0.0000 \cdot P]$ where $P = (\text{Max}(F_o^2, 0) + 2F_c^2)/3$
$2\theta_{\text{max}}$ cutoff	51.0°
Anomalous Dispersion	All non-hydrogen atoms
No. Observations (All reflections)	6894
No. Variables	458
Reflection/Parameter Ratio	15.05
Residuals: R1 ($I > 2.00\sigma(I)$)	0.1189
Residuals: R (All reflections)	0.1639
Residuals: wR2 (All reflections)	0.3918
Goodness of Fit Indicator	1.323
Max Shift/Error in Final Cycle	0.000
Maximum peak in Final Diff. Map	1.19 e ⁻ /Å ³
Minimum peak in Final Diff. Map	-0.47 e ⁻ /Å ³

Appendix 3.4 X-ray crystallographic data for compound **22a** (Chapter 3)

(Sample code: TH3-39-A1)

X-ray Structure Report

for

Prof. Paris Georghiou and T. Al Hujran

Prepared by

Louise N. Dawe, PhD

Centre for Chemical Analysis, Research and Training (C-CART)

Department of Chemistry

Memorial University of Newfoundland

St. Johns, NL, A1B 3X7

(709) 864-4556 (X-Ray Laboratory)

January 12, 2011

Introduction

Collection, solution and refinement proceeded normally. H1 and H2 were introduced in difference map positions, and refined positionally, with fixed displacement ellipsoids. All other hydrogen atoms were introduced in calculated positions and refined on a riding model. All non-hydrogen atoms were refined anisotropically.

Experimental

Data Collection

A colorless prism crystal of $C_{31}H_{30}Br_2N_2O_6$ having approximate dimensions of 0.18 x 0.17 x 0.16 mm was mounted on a low temperature diffraction loop. All measurements were made on a Rigaku Saturn70 CCD diffractometer using graphite monochromated Mo-K α radiation, equipped with a SHINE optic.

The crystal-to-detector distance was 40.05 mm.

Cell constants and an orientation matrix for data collection corresponded to a primitive triclinic cell with dimensions:

$$\begin{aligned} a &= 10.614(3) \text{ \AA} & \alpha &= 64.615(14)^\circ \\ b &= 12.465(3) \text{ \AA} & \beta &= 75.96(2)^\circ \\ c &= 12.520(3) \text{ \AA} & \gamma &= 82.36(2)^\circ \\ V &= 1451.1(7) \text{ \AA}^3 \end{aligned}$$

For $Z = 2$ and $F.W. = 686.40$, the calculated density is 1.571 g/cm^3 . Based on a statistical analysis of intensity distribution, and the successful solution and refinement of the structure, the space group was determined to be:

P-1 (#2)

The data were collected at a temperature of $-109 \pm 1^\circ\text{C}$ to a maximum 2θ value of 61.5° . A total of 786 oscillation images were collected. A sweep of data was done using ω scans from -75.0 to 105.0° in 0.5° step, at $\chi=45.0^\circ$ and $\phi = 180.0^\circ$. The exposure rate was $40.0 \text{ [sec./}^\circ]$. The detector swing angle was 15.10° . A second sweep was performed using ω scans from -75.0 to 105.0° in 0.5° step, at $\chi=45.0^\circ$ and $\phi = 0.0^\circ$. The exposure rate was $40.0 \text{ [sec./}^\circ]$. The detector swing angle was 15.10° . Another sweep was performed using ω scans from -75.0 to -42.0° in 0.5° step, at $\chi=0.0^\circ$ and $\phi = 0.0^\circ$. The exposure rate was $40.0 \text{ [sec./}^\circ]$. The detector swing angle was 15.10° . The crystal-to-detector distance was 40.05 mm. Readout was performed in the 0.137 mm pixel mode.

Data Reduction

Of the 13922 reflections that were collected, 5976 were unique ($R_{\text{int}} = 0.0317$). Data were collected and processed using CrystalClear (Rigaku).

The linear absorption coefficient, μ , for Mo-K α radiation is 28.40 cm $^{-1}$. An empirical absorption correction was applied which resulted in transmission factors ranging from 0.6837 to 0.8561. The data were corrected for Lorentz and polarization effects.

Structure Solution and Refinement

The structure was solved by direct methods² and expanded using Fourier techniques. The non-hydrogen atoms were refined anisotropically. Some hydrogen atoms were refined isotropically, some were refined using the riding model, and the rest were included in fixed positions. The final cycle of full-matrix least-squares refinement³ on F^2 was based on 5976 observed reflections and 378 variable parameters and converged (largest parameter shift was 0.00 times its esd) with unweighted and weighted agreement factors of:

$$R1 = \Sigma ||F_o| - |F_c|| / \Sigma |F_o| = 0.0651$$

$$wR2 = [\Sigma (w (F_o^2 - F_c^2)^2) / \Sigma w(F_o^2)^2]^{1/2} = 0.1743$$

The standard deviation of an observation of unit weight⁴ was 1.05. Unit weights were used. The maximum and minimum peaks on the final difference Fourier map corresponded to 2.61 and -1.49 e $^{-}/\text{\AA}^3$, respectively.

Neutral atom scattering factors were taken from Cromer and Waber⁵. Anomalous dispersion effects were included in Fcalc⁶; the values for $\Delta f'$ and $\Delta f''$ were those of Creagh and McAuley⁷. The values for the mass attenuation coefficients are those of Creagh and Hubbell⁸. All calculations were performed using the CrystalStructure⁹ crystallographic software package except for refinement, which was performed using SHELXL-97².

References

- (4) CrystalClear: Rigaku Corporation, 1999. CrystalClear Software User's Guide, Molecular Structure Corporation, I 2000.J.W.Pflugrath (1999) Acta Cryst. D55, 1718-1725.
- (2) SHELX97: Sheldrick, G.M. Acta Cryst. 2008, A64, 112-122.
- (3) Least Squares function minimized: (SHELXL97)
- $$\sum w(F_o^2 - F_c^2)^2 \quad \text{where } w = \text{Least Squares weights.}$$
- (4) Standard deviation of an observation of unit weight:
- $$[\sum w(F_o^2 - F_c^2)^2 / (N_o - N_v)]^{1/2}$$
- where: N_o = number of observations
 N_v = number of variables
- (5) Cromer, D. T. & Waber, J. T.; "International Tables for X-ray Crystallography", Vol. IV, The Kynoch Press, Birmingham, England, Table 2.2 A (1974).
- (6) Ibers, J. A. & Hamilton, W. C.; Acta Crystallogr., 17, 781 (1964).
- (7) Creagh, D. C. & McAuley, W.J. ; "International Tables for Crystallography", Vol C, (A.J.C. Wilson, ed.), Kluwer Academic Publishers, Boston, Table 4.2.6.8, pages 219-222 (1992).
- (8) Creagh, D. C. & Hubbell, J.H.; "International Tables for Crystallography", Vol C, (A.J.C. Wilson, ed.), Kluwer Academic Publishers, Boston, Table 4.2.4.3, pages 200-206 (1992).
- (9) CrystalStructure 4.0: Crystal Structure Analysis Package, Rigaku and Rigaku Americas (2000-2010). 9009 New Trails Dr. The Woodlands TX 77381 USA.

EXPERIMENTAL DETAILS

4. Crystal Data

Empirical Formula	$C_{31}H_{30}Br_2N_2O_6$
Formula Weight	686.40
Crystal Color, Habit	colorless, prism
Crystal Dimensions	0.18 X 0.17 X 0.16 mm
Crystal System	triclinic
Lattice Type	Primitive
Lattice Parameters	$a = 10.614(3) \text{ \AA}$ $b = 12.465(3) \text{ \AA}$ $c = 12.520(3) \text{ \AA}$ $\alpha = 64.615(14)^\circ$ $\beta = 75.96(2)^\circ$ $\gamma = 82.36(2)^\circ$ $V = 1451.1(7) \text{ \AA}^3$
Space Group	P-1 (#2)
Z value	2
D_{calc}	1.571 g/cm ³
F_{000}	696
$\mu(\text{MoK}\alpha)$	28.40 cm ⁻¹

B. Intensity Measurements

Diffractometer	Rigaku Saturn70 CCD
Radiation	MoK α ($\lambda = 0.71075 \text{ \AA}$) graphite monochromated-Rigaku
SHINE	

Voltage, Current	50kV, 30mA
Temperature	-109.8°C
Detector Aperture	70 x 70 mm
Data Images	786 exposures
ω oscillation Range ($\chi=45.0$, $\phi=180.0$)	-75.0 – 105.0°
Exposure Rate	40.0 sec./°
Detector Swing Angle	15.10°
ω oscillation Range ($\chi=45.0$, $\phi=0.0$)	-75.0 – 105.0°
Exposure Rate	40.0 sec./°
Detector Swing Angle	15.10°
ω oscillation Range ($\chi=0.0$, $\phi=0.0$)	-75.0 - -42.0°
Exposure Rate	40.0 sec./°
Detector Swing Angle	15.10°
Detector Position	40.05 mm
Pixel Size	0.137 mm
$2\theta_{\max}$	61.5°
No. of Reflections Measured	Total: 13922 Unique: 5976 ($R_{\text{int}} = 0.0317$) $I > 2\sigma(I)$: 5279
Corrections	Lorentz-polarization (trans. Factors: 0.6837 – 0.8561)

C. Structure Solution and Refinement

Structure Solution	Direct Methods
Refinement	Full-matrix least-squares on F^2
Function Minimized	$\sum w (F_o^2 - F_c^2)^2$
Least Squares Weights	$w = 1 / [\sigma^2(F_o^2) + (0.0840 \cdot P)^2 + 5.1221 \cdot P]$ where $P = (\text{Max}(F_o^2, 0) + 2F_c^2)/3$
$2\theta_{\text{max}}$ cutoff	53.0°
Anomalous Dispersion	All non-hydrogen atoms
No. Observations (All reflections)	5976
No. Variables	378
Reflection/Parameter Ratio	15.81
Residuals: R1 ($I > 2.00\sigma(I)$)	0.0651
Residuals: R (All reflections)	0.0717
Residuals: wR2 (All reflections)	0.1743
Goodness of Fit Indicator	1.050
Max Shift/Error in Final Cycle	0.002
Maximum peak in Final Diff. Map	2.61 e-/Å ³
Minimum peak in Final Diff. Map	-1.49 e-/Å ³

Appendix 4.1 X-ray crystallographic data for compound **48b** (Chapter 4)

(Sample code: th1-16-7)

X-ray Structure Report

for
Prof. Paris Georghiou and T. Al Hujran

Prepared by
Julie L. Collins

January 31, 2008

Introduction

Collection, solution and refinement all proceeded normally. Hydrogen atoms were included in calculated or difference map positions with isotropic parameters set twenty percent greater than those of their bonding partners.

Experimental

Data Collection

A colorless prism crystal of $C_{16}H_{16}Br_2O_2$ having approximate dimensions of 0.20 x 0.20 x 0.20 mm was mounted on a glass fiber. All measurements were made on a Rigaku Saturn CCD area detector with graphite monochromated Mo-K α radiation.

Indexing was performed from 360 images that were exposed for 8.0 seconds. The crystal-to-detector distance was 40.04 mm.

Cell constants and an orientation matrix for data collection corresponded to a primitive triclinic cell with dimensions:

$$\begin{aligned}
 a &= 7.946(2) \text{ \AA} & \alpha &= 91.288(6)^\circ \\
 b &= 9.482(3) \text{ \AA} & \beta &= 97.874(7)^\circ \\
 c &= 9.955(3) \text{ \AA} & \gamma &= 96.912(5)^\circ \\
 V &= 737.0(4) \text{ \AA}^3
 \end{aligned}$$

For $Z = 2$ and $F.W. = 400.11$, the calculated density is 1.803 g/cm^3 . Based on a statistical analysis of intensity distribution, and the successful solution and refinement of the structure, the space group was determined to be:

P-1 (#2)

The data were collected at a temperature of $-160 \pm 1^\circ\text{C}$ to a maximum 2θ value of 61.6° . A total of 684 oscillation images were collected. A sweep of data was done using ω scans from -25.0 to 5.0° in 0.5° step, at $\chi=0.0^\circ$ and $\phi=0.0^\circ$. The exposure rate was $16.0 \text{ [sec./}^\circ]$. The detector swing angle was 15.11° . A second sweep was performed using ω scans from -75.0 to 105.0° in 0.5° step, at $\chi=54.0^\circ$ and $\phi=0.0^\circ$. The exposure rate was $16.0 \text{ [sec./}^\circ]$. The detector swing angle was 15.11° . Another sweep was performed using ω scans from -75.0 to 57.0° in 0.5° step, at $\chi=54.0^\circ$ and $\phi=90.0^\circ$. The exposure rate was $16.0 \text{ [sec./}^\circ]$. The detector swing angle was 15.11° . The crystal-to-detector distance was 40.04 mm . Readout was performed in the 0.137 mm pixel mode.

Data Reduction

Of the 6186 reflections that were collected, 3012 were unique ($R_{\text{int}} = 0.016$); equivalent reflections were merged. Data were collected and processed using CrystalClear (Rigaku). Net intensities and sigmas were derived as follows:

$$F^2 = [\Sigma(P_i - mB_{\text{ave}})] \cdot L_p^{-1}$$

where P_i is the value in counts of the i^{th} pixel
 m is the number of pixels in the integration area
 B_{ave} is the background average
 L_p is the Lorentz and polarization factor

$$B_{\text{ave}} = \Sigma(B_j)/n$$

where n is the number of pixels in the background area
 B_j is the value of the j^{th} pixel in counts

$$\sigma^2(F^2_{hkl}) = [(\sum P_i) + m((\sum(B_{ave} - B_j)^2)/(n-1))] \cdot L_p \cdot \text{errmul} + (\text{erradd} \cdot F^2)^2$$

$$\begin{aligned} \text{where erradd} &= 0.00 \\ \text{errmul} &= 1.00 \end{aligned}$$

The linear absorption coefficient, μ , for Mo-K α radiation is 55.141 cm⁻¹. A numerical absorption correction was applied which resulted in transmission factors ranging from 0.1974 to 0.3596. The data were corrected for Lorentz and polarization effects. A correction for secondary extinction² was applied (coefficient = 0.012040).

Structure Solution and Refinement

The structure was solved by direct methods³ and expanded using Fourier techniques⁴. The non-hydrogen atoms were refined anisotropically. Hydrogen atoms were refined using the riding model. The final cycle of full-matrix least-squares refinement⁵ on F^2 was based on 3012 observed reflections and 183 variable parameters and converged (largest parameter shift was 0.00 times its esd) with unweighted and weighted agreement factors of:

$$R1 = \sum ||F_o| - |F_c|| / \sum |F_o| = 0.0257$$

$$wR2 = [\sum (w (F_o^2 - F_c^2)^2) / \sum w(F_o^2)^2]^{1/2} = 0.0625$$

The standard deviation of an observation of unit weight⁶ was 1.10. Unit weights were used. The maximum and minimum peaks on the final difference Fourier map corresponded to 0.45 and -0.69 e⁻/Å³, respectively.

Neutral atom scattering factors were taken from Cromer and Waber⁷. Anomalous dispersion effects were included in F_{calc} ⁸; the values for $\Delta f'$ and $\Delta f''$ were those of Creagh and McAuley⁹. The values for the mass attenuation coefficients are those of Creagh and Hubbell¹⁰. All calculations were performed using the CrystalStructure^{11,12} crystallographic software package except for refinement, which was performed using SHELXL-97¹³.

References

- (1) CrystalClear: Rigaku Corporation, 1999. CrystalClear Software User's Guide, Molecular Structure Corporation, (c) 2000. J.W. Pflugrath (1999) Acta Cryst. D55, 1718-

1725.

(2) Larson, A.C. (1970), *Crystallographic Computing*, 291-294. F.R. Ahmed, ed. Munksgaard, Copenhagen (equation 22, with V replaced by the cell volume).

(3) SHELX97: Sheldrick, G.M. (1997).

(4) DIRDIF99: Beurskens, P.T., Admiraal, G., Beurskens, G., Bosman, W.P., de Gelder, R., Israel, R. and Smits, J.M.M.(1999). The DIRDIF-99 program system, Technical Report of the Crystallography Laboratory, University of Nijmegen, The Netherlands.

(5) Least Squares function minimized: (SHELXL97)

$$\sum w(F_o^2 - F_c^2)^2 \quad \text{where } w = \text{Least Squares weights.}$$

(6) Standard deviation of an observation of unit weight:

$$[\sum w(F_o^2 - F_c^2)^2 / (N_o - N_v)]^{1/2}$$

where: N_o = number of observations
 N_v = number of variables

(7) Cromer, D. T. & Waber, J. T.; "International Tables for X-ray Crystallography", Vol. IV, The Kynoch Press, Birmingham, England, Table 2.2 A (1974).

(8) Ibers, J. A. & Hamilton, W. C.; *Acta Crystallogr.*, 17, 781 (1964).

(9) Creagh, D. C. & McAuley, W. J. ; "International Tables for Crystallography", Vol C, (A.J.C. Wilson, ed.), Kluwer Academic Publishers, Boston, Table 4.2.6.8, pages 219-222 (1992).

(10) Creagh, D. C. & Hubbell, J.H.; "International Tables for Crystallography", Vol C, (A.J.C. Wilson, ed.), Kluwer Academic Publishers, Boston, Table 4.2.4.3, pages 200-206 (1992).

(11) CrystalStructure 3.7.0: Crystal Structure Analysis Package, Rigaku and Rigaku/MSC (2000-2005). 9009 New Trails Dr. The Woodlands TX 77381 USA.

(12) CRYSTALS Issue 10: Watkin, D.J., Prout, C.K. Carruthers, J.R. & Betteridge, P.W. Chemical Crystallography Laboratory, Oxford, UK. (1996)

(13) SHELX97: Sheldrick, G.M. (1997).

EXPERIMENTAL DETAILS

A. Crystal Data

Empirical Formula	C ₁₆ H ₁₆ Br ₂ O ₂
Formula Weight	400.11
Crystal Color, Habit	colorless, prism
Crystal Dimensions	0.20 X 0.20 X 0.20 mm
Crystal System	triclinic
Lattice Type	Primitive
Indexing Images	360 images @ 8.0 seconds
Detector Position	40.04 mm
Pixel Size	0.137 mm
Lattice Parameters	a = 7.946(2) Å b = 9.482(3) Å c = 9.955(3) Å α = 91.288(6) ° β = 97.874(7) ° γ = 96.912(5) ° V = 737.0(4) Å ³
Space Group	P-1 (#2)
Z value	2
D _{calc}	1.803 g/cm ³
F ₀₀₀	396.00
μ(MoKα)	55.141 cm ⁻¹

B. Intensity Measurements

Detector	Rigaku Saturn
Goniometer	Rigaku AFC8
Radiation	MoK α ($\lambda = 0.71070 \text{ \AA}$) graphite monochromated
Detector Aperture	70 mm x 70 mm
Data Images	684 exposures
ω oscillation Range ($\chi=0.0, \phi=0.0$)	-25.0 - 5.0 $^\circ$
Exposure Rate	16.0 sec./ $^\circ$
Detector Swing Angle	15.11 $^\circ$
ω oscillation Range ($\chi=54.0, \phi=0.0$)	-75.0 - 105.0 $^\circ$
Exposure Rate	16.0 sec./ $^\circ$
Detector Swing Angle	15.11 $^\circ$
ω oscillation Range ($\chi=54.0, \phi=90.0$)	-75.0 - 57.0 $^\circ$
Exposure Rate	16.0 sec./ $^\circ$
Detector Swing Angle	15.11 $^\circ$
Detector Position	40.04 mm
Pixel Size	0.137 mm
$2\theta_{\text{max}}$	61.6 $^\circ$
No. of Reflections Measured	Total: 6186 Unique: 3012 ($R_{\text{int}} = 0.016$)
Corrections	Absorption (trans factors: 0.1974 - 0.3596) Lorentz-polarization Secondary Extinction (coefficient: 1.20400e-002)

C. Structure Solution and Refinement

Structure Solution	Direct Methods (SIR92)
Refinement	Full-matrix least-squares on F ²
Function Minimized	$\Sigma w (F_o^2 - F_c^2)^2$
Least Squares Weights	$w = 1 / [\sigma^2(F_o^2) + (0.0268 \cdot P)^2 + 0.8454 \cdot P]$ where $P = (\text{Max}(F_o^2, 0) + 2F_c^2)/3$
2 θ _{max} cutoff	53.0°
Anomalous Dispersion	All non-hydrogen atoms
No. Observations (All reflections)	3012
No. Variables	183
Reflection/Parameter Ratio	16.46
Residuals: R1 ($I > 2.00\sigma(I)$)	0.0257
Residuals: R (All reflections)	0.0271
Residuals: wR2 (All reflections)	0.0625
Goodness of Fit Indicator	1.099
Max Shift/Error in Final Cycle	0.001
Maximum peak in Final Diff. Map	0.45 e ⁻ /Å ³
Minimum peak in Final Diff. Map	-0.69 e ⁻ /Å ³

Appendix 4.2 X-ray crystallographic data for compound **47b** (Chapter 4)

(Sample code: TH4-14)

X-ray Structure Report

for

Prof. Paris Georghiou and T. Al Hujran

Prepared by

Louise N. Dawe, PhD

Centre for Chemical Analysis, Research and Training (C-CART)
Department of Chemistry
Memorial University of Newfoundland
St. Johns, NL, A1B 3X7
(709) 864-4556 (X-Ray Laboratory)
(709) 864-8904 (Office)

August 8, 2011

Introduction

All non-hydrogen atoms were refined anisotropically. All hydrogen atoms were introduced in calculated positions and refined on a riding model.

The Platon¹⁰ Squeeze procedure was applied to recover 228 electrons per unit cell in four voids that were sufficiently large to contain a small molecule (total volume 5143 Å³); with $Z = 16$, that is 14.25 electrons per formula unit. Discrete lattice solvent could not be located from difference maps, however, each void electron count (57 electrons) is consistent with the presence of one hexane molecule (50 electrons). The formula was therefore adjusted by 0.25 hexane to reflect this electron contribution to the calculation of the intensive properties.

Experimental

Data Collection

A colorless prism crystal of $C_{65.50}H_{67.50}O_{12}$ having approximate dimensions of 0.14 x 0.14 x 0.14 mm was mounted on a glass fiber. All measurements were made on a Rigaku Saturn70 CCD diffractometer using graphite monochromated Mo-K α radiation, equipped with a SHINE optic.

The crystal-to-detector distance was 50.08 mm.

Cell constants and an orientation matrix for data collection corresponded to an I-centered tetragonal cell (laue class: 4/mmm) with dimensions:

$$\begin{aligned}a &= 27.6050(9) \text{ \AA} \\c &= 32.4280(13) \text{ \AA} \\V &= 24711.3(15) \text{ \AA}^3\end{aligned}$$

For $Z = 16$ and $F.W. = 1046.75$, the calculated density is 1.125 g/cm³. The reflection conditions of:

$$\begin{aligned}hkl: h+k+l &= 2n \\0kl: l &= 2n \\hk0: h &= 2n \\hhl: 2h+1 &= 4n\end{aligned}$$

uniquely determine the space group to be:

$$I4_1/acd \text{ (#142)}$$

The data were collected at a temperature of $22 \pm 1^\circ\text{C}$ to a maximum 2θ value of 59.8° . A total of 360 oscillation images were collected. A sweep of data was done using ω scans from -70.0 to 110.0° in 0.5° step, at $\chi=45.0^\circ$ and $\phi = 90.0^\circ$. The exposure rate was 100.0 [sec./ $^\circ$]. The detector swing angle was 20.10° . The crystal-to-detector distance was 50.08 mm. Readout was performed in the 0.137 mm pixel mode.

Data Reduction

Of the 5752 reflections that were collected, 5752 were unique ($R_{int} = 0.0000$). Data were collected and processed using CrystalClear (Rigaku).

The linear absorption coefficient, μ , for Mo-K α radiation is 0.77 cm^{-1} . An empirical absorption correction was applied which resulted in transmission factors ranging from 0.991 to 0.995. The data were corrected for Lorentz and polarization effects.

Structure Solution and Refinement

The structure was solved by direct methods² and expanded using Fourier techniques. The non-hydrogen atoms were refined anisotropically. Hydrogen atoms were refined using the riding model. The final cycle of full-matrix least-squares refinement³ on F^2 was based on 5752 observed reflections and 347 variable parameters and converged (largest parameter shift was 0.00 times its esd) with unweighted and weighted agreement factors of:

$$R1 = \sum ||F_o| - |F_c|| / \sum |F_o| = 0.0904$$

$$wR2 = [\sum (w (F_o^2 - F_c^2)^2) / \sum w(F_o^2)^2]^{1/2} = 0.2371$$

The standard deviation of an observation of unit weight⁴ was 1.16. Unit weights were used. The maximum and minimum peaks on the final difference Fourier map corresponded to 0.20 and -0.20 $e^{-}/\text{\AA}^3$, respectively.

Neutral atom scattering factors were taken from Cromer and Waber⁵. Anomalous dispersion effects were included in F_{calc} ⁶; the values for $\Delta f'$ and $\Delta f''$ were those of Creagh and McAuley⁷. The values for the mass attenuation coefficients are those of Creagh and Hubbell⁸. All calculations were performed using the CrystalStructure⁹ crystallographic software package except for refinement, which was performed using SHELXL-97².

References

(1) CrystalClear: Rigaku Corporation, 1999. CrystalClear Software User's Guide, Molecular Structure Corporation, (c) 2000. J.W. Pflugrath (1999) Acta Cryst. D55, 1718-1725.

(2) SHELXL97: Sheldrick, G.M. Acta Cryst. 2008, A64, 112-122

(3) Least Squares function minimized: (SHELXL97)

$$\sum w(F_o^2 - F_c^2)^2 \quad \text{where } w = \text{Least Squares weights.}$$

(4) Standard deviation of an observation of unit weight:

$$[\sum w(F_o^2 - F_c^2)^2 / (N_o - N_v)]^{1/2}$$

where: N_o = number of observations
 N_v = number of variables

(5) Cromer, D. T. & Waber, J. T.; "International Tables for X-ray Crystallography", Vol. IV, The Kynoch Press, Birmingham, England, Table 2.2 A (1974).

(6) Ibers, J. A. & Hamilton, W. C.; Acta Crystallogr., 17, 781 (1964).

(7) Creagh, D. C. & McAuley, W.J.; "International Tables for Crystallography", Vol C, (A.J.C. Wilson, ed.), Kluwer Academic Publishers, Boston, Table 4.2.6.8, pages 219-222 (1992).

(8) Creagh, D. C. & Hubbell, J.H.; "International Tables for Crystallography", Vol C, (A.J.C. Wilson, ed.), Kluwer Academic Publishers, Boston, Table 4.2.4.3, pages 200-206 (1992).

(9) CrystalStructure 4.0: Crystal Structure Analysis Package, Rigaku and Rigaku Americas (2000-2010). 9009 New Trails Dr. The Woodlands TX 77381 USA.

(10) Spek, A.L. (2003), J.Appl.Cryst. 36, 7-13.

EXPERIMENTAL DETAILS

A. Crystal Data

Empirical Formula	C _{65.50} H _{67.50} O ₁₂
Formula Weight	1046.75
Crystal Color, Habit	colorless, prism
Crystal Dimensions	0.14 X 0.14 X 0.14 mm
Crystal System	tetragonal
Lattice Type	I-centered
Lattice Parameters	a = 27.6050(9) Å c = 32.4280(13) Å V = 24711.3(15) Å ³
Space Group	I4 ₁ /acd (#142)
Z value	16
D _{calc}	1.125 g/cm ³
F ₀₀₀	8904
μ(MoKα)	0.77 cm ⁻¹

B. Intensity Measurements

Diffractometer	Rigaku Saturn70 CCD
Radiation	MoKα (λ = 0.71075 Å) graphite monochromated-Rigaku
SHINE	
Voltage, Current	50kV, 40mA

Temperature	22.0°C
Detector Aperture	70 x 70 mm
Data Images	360 exposures
ω oscillation Range ($\chi=45.0$, $\phi=90.0$)	-70.0 - 110.0°
Exposure Rate	100.0 sec./°
Detector Swing Angle	20.10°
Detector Position	50.08 mm
Pixel Size	0.137 mm
$2\theta_{\max}$	59.8°
No. of Reflections Measured	Total: 5752 Unique: 5752 ($R_{\text{int}} = 0.000$) $I > 2\sigma(I)$: 4008
Corrections	Lorentz-polarization (trans. factors: 0.991 - 0.995)

C. Structure Solution and Refinement

Structure Solution	Direct Methods
Refinement	Full-matrix least-squares on F^2
Function Minimized	$\sum w (F_o^2 - F_c^2)^2$
Least Squares Weights	$w = 1 / [\sigma^2(F_o^2) + (0.0900 \cdot P)^2 + 18.1340 \cdot P]$ where $P = (\text{Max}(F_o^2, 0) + 2F_c^2)/3$
$2\theta_{\max}$ cutoff	51.0°

Anomalous Dispersion	All non-hydrogen atoms
No. Observations (All reflections)	5752
No. Variables	347
Reflection/Parameter Ratio	16.58
Residuals: R1 ($I > 2.00\sigma(I)$)	0.0904
Residuals: R (All reflections)	0.1274
Residuals: wR2 (All reflections)	0.2371
Goodness of Fit Indicator	1.160
Max Shift/Error in Final Cycle	0.000
Maximum peak in Final Diff. Map	0.20 e ⁻ /Å ³
Minimum peak in Final Diff. Map	-0.20 e ⁻ /Å ³

Appendix 5.1 X-ray crystallographic data for compound **18b** (Chapter 5)

(Sample code: TH4-2)

X-ray Structure Report

for

Prof. Paris Georghiou and T. Al Hujran

Prepared by

Louise N. Dawe, PhD

Centre for Chemical Analysis, Research and Training (C-CART)
Department of Chemistry
Memorial University of Newfoundland
St. Johns, NL, A1B 3X7
(709) 864-4556 (X-Ray Laboratory)
(709) 864-8904 (Office)

July 8, 2011

Introduction

Collection, solution and refinement proceeded normally. All hydrogen atoms were introduced in calculated positions and refined on a riding model. All non-hydrogen atoms were refined anisotropically.

Intramolecular π - π contacts exist between the plane made by C1-C10 and its symmetry equivalent plane generated by $[-x, 1-y, 1-z]$. The centroid-centroid distance is 3.9203(11) Å, while the plane separation is 3.4778(13) Å, shifted by 1.8093(16) Å.

Experimental

Data Collection

A colorless prism crystal of $C_{42}H_{42}N_2O_8$ having approximate dimensions of 0.22 x 0.21 x 0.12 mm was mounted on a low temperature diffraction loop. All measurements were made on a Rigaku Saturn70 CCD diffractometer using graphite monochromated Mo-K α radiation, equipped with a SHINE optic.

The crystal-to-detector distance was 50.00 mm.

Cell constants and an orientation matrix for data collection corresponded to a primitive triclinic cell with dimensions:

$$\begin{array}{ll} a = 9.5757(13) \text{ \AA} & \alpha = 103.810(7)^\circ \\ b = 9.7504(13) \text{ \AA} & \beta = 92.027(7)^\circ \\ c = 10.5487(14) \text{ \AA} & \gamma = 115.519(8)^\circ \\ V = 852.3(2) \text{ \AA}^3 & \end{array}$$

For $Z = 1$ and F.W. = 702.80, the calculated density is 1.369 g/cm³. Based on a statistical analysis of intensity distribution, and the successful solution and refinement of the structure, the space group was determined to be:

P-1 (#2)

The data were collected at a temperature of $-110 \pm 1^\circ\text{C}$ to a maximum 2θ value of 54.9° . A total of 882 oscillation images were collected. A sweep of data was done using ω scans from -70.0 to 110.0° in 0.5° step, at $\chi=45.0^\circ$ and $\phi = 0.0^\circ$. The exposure rate was 30.0 [sec./ $^\circ$]. The detector swing angle was 20.00° . A second sweep was performed using ω scans from -70.0 to 93.0° in 0.5° step, at $\chi=45.0^\circ$ and $\phi = 90.0^\circ$. The exposure rate was 30.0 [sec./ $^\circ$]. The detector swing angle was 20.00° . Another sweep was performed using ω scans from -70.0 to -2.0° in 0.5° step, at $\chi=45.0^\circ$ and $\phi = 180.0^\circ$. The exposure rate was 30.0 [sec./ $^\circ$]. The detector swing angle was 20.00° . Another sweep was performed using ω scans from 40.0 to 70.0° in 0.5° step, at $\chi=0.0^\circ$ and $\phi = 90.0^\circ$. The exposure rate was 30.0 [sec./ $^\circ$]. The detector swing angle was 20.00° . The crystal-to-detector distance was 50.00 mm. Readout was performed in the 0.137 mm pixel mode.

Data Reduction

Of the 7232 reflections that were collected, 3500 were unique ($R_{int} = 0.0500$); equivalent reflections were merged. Data were collected and processed using CrystalClear (Rigaku).

The linear absorption coefficient, μ , for Mo-K α radiation is 0.95 cm^{-1} . An empirical absorption correction was applied which resulted in transmission factors ranging from 0.574 to 0.989. The data were corrected for Lorentz and polarization effects.

Structure Solution and Refinement

The structure was solved by direct methods² and expanded using Fourier techniques. The non-hydrogen atoms were refined anisotropically. Hydrogen atoms were refined using the riding model. The final cycle of full-matrix least-squares refinement³ on F^2 was based on 3500 observed reflections and 237 variable parameters and converged (largest parameter shift was 0.00 times its esd) with unweighted and weighted agreement factors of:

$$R1 = \sum ||F_o| - |F_c|| / \sum |F_o| = 0.0587$$

$$wR2 = [\sum (w (F_o^2 - F_c^2)^2) / \sum w(F_o^2)^2]^{1/2} = 0.1738$$

The standard deviation of an observation of unit weight⁴ was 1.10. Unit weights were used. The maximum and minimum peaks on the final difference Fourier map corresponded to 0.27 and -0.32 $e^{-}/\text{Å}^3$, respectively.

Neutral atom scattering factors were taken from Cromer and Waber⁵. Anomalous dispersion effects were included in F_{calc} ⁶; the values for $\Delta f'$ and $\Delta f''$ were those of Creagh and McAuley⁷. The values for the mass attenuation coefficients are those of Creagh and Hubbell⁸. All calculations were performed using the CrystalStructure⁹ crystallographic software package except for refinement, which was performed using SHELXL-97².

References

(1) CrystalClear: Rigaku Corporation, 1999. CrystalClear Software User's Guide, Molecular Structure Corporation, (c) 2000. J.W. Pflugrath (1999) Acta Cryst. D55, 1718-1725.

(2) SHELX97: Sheldrick, G.M. Acta Cryst. 2008, A64, 112-122.

(3) Least Squares function minimized: (SHELXL97)

$$\sum w(F_o^2 - F_c^2)^2 \quad \text{where } w = \text{Least Squares weights.}$$

(4) Standard deviation of an observation of unit weight:

$$[\sum w(F_o^2 - F_c^2)^2 / (N_o - N_v)]^{1/2}$$

where: N_o = number of observations
 N_v = number of variables

(5) Cromer, D. T. & Waber, J. T.; "International Tables for X-ray Crystallography", Vol. IV, The Kynoch Press, Birmingham, England, Table 2.2 A (1974).

(6) Ibers, J. A. & Hamilton, W. C.; Acta Crystallogr., 17, 781 (1964).

(7) Creagh, D. C. & McAuley, W.J. ; "International Tables for Crystallography", Vol C, (A.J.C. Wilson, ed.), Kluwer Academic Publishers, Boston, Table 4.2.6.8, pages 219-222 (1992).

(8) Creagh, D. C. & Hubbell, J.H.; "International Tables for Crystallography", Vol C, (A.J.C. Wilson, ed.), Kluwer Academic Publishers, Boston, Table 4.2.4.3, pages 200-206 (1992).

(9) CrystalStructure 4.0: Crystal Structure Analysis Package, Rigaku and Rigaku Americas (2000-2010). 9009 New Trails Dr. The Woodlands TX 77381 USA.

EXPERIMENTAL DETAILS

A. Crystal Data

Empirical Formula	C ₄₂ H ₄₂ N ₂ O ₈
Formula Weight	702.80
Crystal Color, Habit	colorless, prism
Crystal Dimensions	0.22 X 0.21 X 0.12 mm
Crystal System	triclinic
Lattice Type	Primitive
Lattice Parameters	a = 9.5757(13) Å b = 9.7504(13) Å c = 10.5487(14) Å α = 103.810(7) ° β = 92.027(7) ° γ = 115.519(8) ° V = 852.3(2) Å ³
Space Group	P-1 (#2)
Z value	1
D _{calc}	1.369 g/cm ³
F ₀₀₀	372
μ(MoKα)	0.95 cm ⁻¹

B. Intensity Measurements

Diffractometer	Rigaku Saturn70 CCD
Radiation	MoKα (λ = 0.71075 Å) graphite monochromated-Rigaku
SHINE	
Voltage, Current	50kV, 30mA

Temperature	-110.0°C
Detector Aperture	70 x 70 mm
Data Images	882 exposures
ω oscillation Range ($\chi=45.0$, $\phi=0.0$)	-70.0 - 110.0°
Exposure Rate	30.0 sec./°
Detector Swing Angle	20.00°
ω oscillation Range ($\chi=45.0$, $\phi=90.0$)	-70.0 - 93.0°
Exposure Rate	30.0 sec./°
Detector Swing Angle	20.00°
ω oscillation Range ($\chi=45.0$, $\phi=180.0$)	-70.0 - -2.0°
Exposure Rate	30.0 sec./°
Detector Swing Angle	20.00°
ω oscillation Range ($\chi=0.0$, $\phi=90.0$)	40.0 - 70.0°
Exposure Rate	30.0 sec./°
Detector Swing Angle	20.00°
Detector Position	50.00 mm
Pixel Size	0.137 mm
$2\theta_{\max}$	54.9°
No. of Reflections Measured	Total: 7232 Unique: 3500 ($R_{\text{int}} = 0.0500$) $I > 2\sigma(I)$: 2825
Corrections	Lorentz-polarization (trans. factors: 0.574 - 0.989)

C. Structure Solution and Refinement

Structure Solution	Direct Methods
Refinement	Full-matrix least-squares on F^2
Function Minimized	$\Sigma w (Fo^2 - Fc^2)^2$
Least Squares Weights	$w = 1 / [\sigma^2(Fo^2) + (0.1121 \cdot P)^2 + 0.0000 \cdot P]$ where $P = (\text{Max}(Fo^2, 0) + 2Fc^2)/3$
$2\theta_{\text{max}}$ cutoff	53.0°
Anomalous Dispersion	All non-hydrogen atoms
No. Observations (All reflections)	3500
No. Variables	237
Reflection/Parameter Ratio	14.77
Residuals: R1 ($I > 2.00\sigma(I)$)	0.0587
Residuals: R (All reflections)	0.0670
Residuals: wR2 (All reflections)	0.1738
Goodness of Fit Indicator	1.097
Max Shift/Error in Final Cycle	0.000
Maximum peak in Final Diff. Map	0.27 e ⁻ /Å ³
Minimum peak in Final Diff. Map	-0.32 e ⁻ /Å ³



